Chemical and pharmacological characterization of terpenoids from *Hericium* species and other Basidiomycota as neuroregenerative compounds

Von der Fakultät für Lebenswissenschaften

der Technischen Universität Carolo-Wilhelmina zu Braunschweig

zur Erlangung des Grades einer

Doktorin der Naturwissenschaften

(Dr. rer. nat.)

genehmigte

D i s s e r t a t i o n

von Monique Rascher

aus Wolmirstedt

1. Referent: Professor Dr. Marc Stadler
2. Referent: Professor Dr. Reinhard Köster
eingereicht am: 24.04.2020
mündliche Prüfung (Disputation) am: 24.06.2020

Druckjahr 2020

Vorveröffentlichungen der Dissertation

Teilergebnisse aus dieser Arbeit wurden mit Genehmigung der Fakultät für Lebenswissenschaften, vertreten durch den Mentor der Arbeit, in folgenden Beiträgen vorab veröffentlicht:

Wittstein K and **Rascher M**, Rupcic Z, Löwen E, Winter B, Köster RW, Stadler M. corallocins A-C, Nerve Growth and Brain-Derived Neurotrophic Factor Inducing Metabolites from the Mushroom *Hericium coralloides*. J Nat Prod.; 79(9):2264-9 (2016)

Rupcic Z and **Rascher M**, Kanaki S, Köster RW, Stadler M and Wittstein K. Two New Cyathane Diterpenoids from Mycelial Cultures of the Medicinal Mushroom *Hericium erinaceus* and the Rare Species, *Hericium flagellum*. Int. J. Mol. Sci.,19 (2018)

Rascher M, Wittstein K, Winter B, Wolf-Asseburg A, Stadler M and Köster RW. erinacine C activates ETS signal transduction in astrocytes independent of NGF induction. *Submitted* (2020)

Tagungsbeiträge

Rupcic Z, Wittstein K, **Rascher M**, Köster RW, Stadler M. Nerve growth- and brain-derived neurotrophic factor inducing metabolites from *Hericium* spp. International Conference of the DGfM. Bernried, Germany (2016).

Wittstein K, Rupcic Z, **Rascher M**, Löwen E, Winter B, Köster RW, Stadler M. Novel antimicrobial and neurotrophic compounds from basidiomycetes. Fungal Biodiversity and Biotechnology symposium. Mae Fah Luand Univrsity, Chiang Rai, Thailand (2016).

Wittstein K, Rupcic Z, **Rascher M**, Löwen E, Winter B, Köster RW, Stadler M. Novel antimicrobial and neurotrophic compounds from basidiomycetes. CBS Spring Symposium "Fungi and Global Challenges". Amsterdam, Netherlands (2016).

Wittstein K. Fungi make the world go round (08/2017 Symposium "Famous fungi", Westerdijk Fungal Biodiversity Institute, Utrecht, Niederlande)

Rascher M. Chemical and pharmacological characterization of terpenoids from *Hericium* species and other Basidiomycota as neuroregenerative compounds. HZI PhD Retreat (2018)

Rascher M. Glia cell culture as approach for neurotrophic compound analysis in zebrafish. 3rd Brainswick Symposium Braunschweig (2018)

Rupcic Z, Wittstein K, **Rascher M**, Kanaki S, Köster RW, Bunjes H, Stadler M. Neuroprotective metabolites from *Hericium*. 11th International Mycological Congress. San Juan, Puerto Rico (2018).

Rascher M. Chemical and pharmacological characterization of terpenoids from *Hericium* species and other Basidiomycota as neuroregenerative compounds. HZI PhD Retreat (2019)

Posterbeiträge

Wittstein K, **Rascher M**, Mudalungu CM, Helaly S, Richter C, Rupcic Z, Löwen E, Winter B, Süssmuth R, Köster RW and Stadler M. Novel Antimicrobial and Neurotrophin-inducing Compounds from Basidiomycetes (12/2016 Konferenz “Drug Innovation in Academia" DKFZ Heidelberg)

Rupcic Z, Wittstein K, **Rascher M**, Löwen E, Winter B, Köster RW, Stadler M. Neuroprotective and antimicrobial metabolites from *Hericium* species. RGJ-Ph.D. Congress. Pattaya, Thailand (2016).

Wittstein K, **Rascher M**, Mudalungu CM, Helaly S, Richter C, Rupcic Z, Löwen E, Winter B, Thongbai B, Hyde KD, Matasyoh JC, Süssmuth R, Köster RW, Stadler M. New bioactive metabolites from cultures and fruiting bodies of basidiomycetes. PERCH-CIC Congress IX: 2016 "Chemistry in ASEAN Economic Community and Beyond", Pattaya, Thailand (2016).

Rascher M, Köster RW and Stadler M. Chemical and pharmacological characterization of terpenoids from *Hericium* species and other Basidiomycota as anti-inflammatory and neurodegenerative compounds. HZI PhD Retreat (2017)

Rascher M, Köster RW and Stadler M. Chemical and pharmacological characterization of terpenoids from *Hericium* species and other Basidiomycota as anti-inflammatory and neurodegenerative compounds. 2nd Brainswick Symposium Braunschweig (2017)

Rascher M, Wittstein K, Rupcic Z, Köster RW and Stadler M. Chemical and pharmacological characterization of terpenoids from *Hericium* species and other Basidiomycota as neuroregenerative compounds. HZI PhD Symposium (2017)

Rupcic Z, Wittstein K, **Rascher M**, Köster RW, Bunjes H, Stadler M. Production and processing of anti-infectives from microbial sources. SPhERe-Symposium on Pharmaceutical Engineering Research. Braunschweig, Germany (2017).

Rascher M, Wittstein K, Rupcic Z, Stadler M and Köster RW. Chemical and pharmacological characterization of terpenoids from *Hericium* species and other Basidiomycota as neuroregenerative compounds. FishMed Conference Warsaw (2018)

Rascher M, Wittstein K, Rupcic Z, Stadler M and Köster RW. Chemical and pharmacological characterization of terpenoids from *Hericium* species and other Basidiomycota as neuroregenerative compounds. HZI PhD Symposium (2018)

Wittstein K, **Rascher M**, Rupcic Z, Mitschke N, Löwen E, Kellner H, Winter B, Köster RW and Stadler M. Neurotrophin inducing terpenoids from basidiomycetes of the family Hericiaceae (02/2018 30. Irseer Naturstofftage, Irsee)

Rupcic Z, Wittstein K, **Rascher M**, Kanaki S, Köster RW, Bunjes H, Stadler M. Neuroprotective metabolites from *Hericium*. 11th International Mycological Congress. San Juan, Puerto Rico (2018).

Table of Contents

Acknowledgment

Die Doktorarbeit war ein interessanter und abenteuerlicher Weg, der ohne die Unterstützung der Leute, die ich nun erwähnen werde, nicht möglich gewesen wäre. Diesen Leuten gebührt meine ganze Wertschätzung dafür, dass sie diese Erfahrung für mich unvergesslich und einzigartig gemacht haben. Jeder, der in der Wissenschaft gearbeitet hat, weiß, wie anstrengend und frustrierend dieser Job sein kann. Wenn es jedoch jemanden gibt, der an dich glaubt, ist es viel einfacher, in einer schwierigen Zeit die Motivation zu finden.

Zunächst möchte ich mich bei meinen Mentoren und Thesis Prüfern, Prof. Dr. Marc Stadler und Prof. Dr. Reinhard W. Köster, bedanken. Ich werde immer dankbar darüber sein, dass ich die Chance bekommen habe, dieses Thema bearbeiten zu dürfen. Aber auch für die vielen aufbauenden Worte und auch die interessanten Diskussionen. Am wichtigsten jedoch ist, die Unterstützung, während der Bearbeitung des Themas! Ich erhielt einmalige Möglichkeiten und die Zeit, die ich brauchte, um mich wissenschaftlich entwickeln zu können und neue Herausforderungen meistern zu können. Das war alles außergewöhnlich für mich.

Ich möchte mich auch bei Prof. Dr. Ingo Schmitz bedanken, für die Teilnahme an meinen Thesis Committees und die interessante Unterstützung und Ideen für das Voranschreiten meiner Arbeit.

Weiterhin möchte ich bei meiner Betreuerin, Dr. Barbara Winter bedanken, dafür, dass sie immer da war und für Ihren kritischen Blick auf meine Arbeit.

Eine große Unterstützung während meiner Doktorandenzeit und auch während des Schreibens meiner Arbeit war Dr. Sol Pose-Méndez: Gracias, Sol, por estar siempre ahí para mí y siempre escuchando. ¡Te has convertido en un buen amigo para mí! ¡Espero que en el futuro consigas todo lo que deseas y sueñas!

Ich möchte mich auch bei Dr. Kathrin Wittstein bedanken, für die große Unterstützung während der Bearbeitung der chemischen Fragen und für die vielen Erklärungen und die viele Zeit, die du für mich hattest. Weiterhin bin ich sehr froh, dass du mich auch bei der Ausführung der Experimente unterstützt hast.

Ich möchte auch bei Dr. Astrid Buchberger-Seidel und Dr. Ulrike Theisen danken, für ihre wertvolle wissenschaftliche Hilfe in diesen Jahren und vor allem für die sehr produktiven

Gespräche und Ideen und das offene Ohr, wenn ich gerade einmal Unterstützung brauchte. Auch möchte ich mich bei Alexandra Wolf-Asseburg bedanken. Danke! Manchmal sind kleine Probleme riesig groß und es hilft, darüber einmal reden zu können. Weiterhin möchte ich mich bei Dr. Zeljka Rupcic und Verena Ledwig für die Unterstützung bei meinen Experimenten bedanken. Auch bei Timo Fritsch möchte ich mich bedanken, für die große Unterstützung und Ausrechterhaltung unseres Fischraums.

Ein Dank gilt auch den Studenten, Larissa, Franziska und Sonja, die ich während meiner Doktorandenzeit betreut habe und die mir gezeigt haben, wie gerne ich jemanden etwas beibringe.

Ich möchte mich weiterhin auch bei allen Kollegen der Arbeitsgruppen ZMN und MWIS bedanken, dafür dass wir alle fröhlichen und schwierigen Momente geteilt haben.

Es gibt Leute, die oftmals die emotionalen Tiefen meiner Arbeit mitbekommen haben und mich immer unterstützt haben. Dazu zählen zuallererst meine Eltern. Danke, dass ihr so seid, wie ihr seid. Ihr habt mich immer unterstützt, egal wie merkwürdig meine Ideen für meine Zukunft erschienen. Ihr habt mich immer ermutigt, weiter zu machen, auch wenn es für mich eher ausweglos erschien. Ihr hattet immer ein offenes Ohr und manchmal musste mir auch der Kopf geradegerückt werden. Danke auch meiner Familie, ihr habt mir immer Beständigkeit und Freude in den manchmal traurigen Zeiten gegeben.

Ich widme meinem Opa, Uwe Müller, diese Arbeit. Gerne würde ich jetzt dein Gesicht sehen…

الشيء الأكثر أهمية بالنسبة لي هو حبيبي .بفضله أكتملت سعادتي وتمكنت من إتمام عملي على أكمل وجه .حيث قام بدعمي عندما كنت بحاجة إلى دعم وأستمع لمشاكلي عندما كنت بحاجة للبوح بها. شاركني بفرحي وحزني.

Summary

With an aging population, neurodegenerative diseases are getting a severe problem. A big disadvantage by that is, that medications are poorly discovered. Common in many neurodegenerative diseases is the death of neurons. Neurotrophins, like nerve growth factor (NGF) and brain-derived neurotrophic factor (BDNF), are involved in the central and peripheral nervous system in regulation of survival and regeneration of neurons. These factors have been the focus of much research attention as potential therapies for severe neurodegenerative disease. However, the problem in using neurotrophins is their high molecular weight which prevents them from passing through the blood-brain barrier (BBB). To circumvent these limitations, much effort is currently focused on searching for small molecules, small enough to pass the BBB and that exhibit either intrinsic neurotrophic activity or stimulatory effects on neurotrophic factors. Several secondary metabolites from species of the medicinal mushroom genus *Hericium* have already been purified and were found to have a neurotrophic effect. In this thesis different substances isolated from *Hericium* sp. were characterized regarding their neurotrophin stimulating ability. Corallocins, unknown structures isolated from the fruiting body of *H. coralloides* were able to stimulate NGF and BDNF. The same was shown for erinacines (metabolites from mycelia cultures of *H. erinaceus*). One important member of the erinacines is erinacine C. Using a small library of transcriptional activation reporters, different activation, and inactivation of signaling cascades were analyzed. Treatment of astrocytoma cells with erinacine C causes a profound change in their transcriptional activity. Transcriptional activation was seen for E26 transformation specific (ETS), glioma -associated oncogene (Gli1), signal transducer and activator of transcript (STAT3), ETS like protein (Elk1) and Polyomavirus enhancer activator (Pea3B) transcription factor. Since several times, the conserved sequence of ETS is highly activated upon erinacine C treatment (in ETS, Elk1, Pea3B), the ETS-mediated signaling cascades were analyzed. It was demonstrated that the activation of ETS acted in parallel and independent of neurotrophin induction. Another approach was the analysis of erinacine C dependent activation of a putative *Tetraodon* enhancer region of the *ngf* gene. It was proven, that this 2.1kb large enhancer region was activated in the presence of erinacine C as well as with the activation and repression of ETS signaling. Erinacine C is a molecule having a smaller molecular weight, suggesting, that it can cross the BBB. In this thesis the ability to cross the BBB was shown by using an *in vitro* approach of mimicking the BBB as well as by using an *in vivo* vertebrate model system, the zebrafish. To analyze the effect of these compounds *in vivo* it was clarified in this thesis where *ngf* or its receptor *trkA* are expressed. It

is also essential to show their effect *in vivo* using zebrafish as model organism. Therefore, a reporter line was established, expressing mClover in *trkA* expressing cells, which are the trigeminal neurons and motor neurons, but also in sensory neurons of the central nervous system. Using this transgenic line different regeneration models were established. This finding provides access to explain the functions of *Hericium* derived cyathane diterpenoids, like erinacine C. These studies offer first genetic ability to the function of cyathane diterpenoids, secondary metabolites isolated from *Hericium* sp., in astrocytic cells and improves the mechanistically understanding of the action of cyathanes in glial cells. On the other hand, different model system for analyzing the neurotrophin stimulating effects *in vivo* were established. This study allows to characterized other signaling cascades being activated by cyathanes as well as studying the effect *in vivo* in future.

Zusammenfassung

Mit einer alternden Bevölkerung werden neurodegenerative Erkrankungen zu einem ernsten Problem. Ein großer Nachteil dabei ist, dass mit Medikamenten meist nur die Symptome behandelt werden. Bei vielen neurodegenerativen Erkrankungen ist der Tod von Neuronen charakterisierend. Neurotrophine sind, wie der Nervenwachstumsfaktor (NGF) und der brain-derived-neurotrophic-factor (BDNF), im zentralen und peripheren Nervensystem an der Regulation des Überlebens und der Regeneration von Neuronen beteiligt. Diese Faktoren stehen im Mittelpunkt vieler Forschungsarbeiten als potenzielle Therapien für schwere neurodegenerative Erkrankungen. Das Problem bei der Verwendung von Neurotrophinen ist jedoch ihr hohes Molekulargewicht, das verhindert, dass sie die Blut-Hirn-Schranke (BBB) passieren. Um diese Einschränkungen zu umgehen, werden derzeit große Anstrengungen unternommen, um nach kleinen Molekülen zu suchen, die klein genug sind, um die BHS zu passieren, und die entweder eine intrinsische neurotrophe Aktivität oder stimulierende Wirkungen auf neurotrophe Faktoren aufweisen. Viele Sekundärmetaboliten wurden bereits aus Heilpilzgattungen wie *Hericium* aufgereinigt und es wurde gezeigt, dass sie eine neurotrophe Wirkung zeigen. In dieser Arbeit wurden verschiedene aus *Hericium* sp. isolierte Metabolite hinsichtlich ihrer Neurotrophin-stimulierenden Fähigkeit charakterisiert. Corallocine, unbekannte Strukturen, die aus dem Fruchtkörper von *H. coralloides* isoliert wurden, sind in der Lage NGF und auch BDNF stimulieren. Gleiches wurde für Erinacine (Metaboliten aus Myzel Kulturen von *H. erinaceus*) gezeigt. Ein wichtiges Mitglied der Erinacine ist Erinacin C. Unter Verwendung einer kleinen Bibliothek von Transkriptionsaktivierungsreportern wurden verschiedene Aktivierungen und Inaktivierungen von Signalkaskaden analysiert. Die Behandlung von Astrozytom-Zellen mit Erinacin C führt zu einer tiefgreifenden Veränderung ihrer Transkriptionsaktivität. Die Transkriptionsaktivierung wurde für den E26-transformationsspezifischen (ETS), Gliom-assoziierten Onkogen (Gli1), transducer and activator of transcript (STAT3), ETS-ähnliches Protein (Elk1) und den Transkriptionsfaktor des Polyomavirus-Enhancer-Aktivators (Pea3B) beobachtet. Da die konservierte Sequenz von ETS bei Behandlung mit Erinacin C (in ETS, Elk1, Pea3B) mehrmals stark aktiviert wurde, wurden im Weiteren die ETS-vermittelten Signalkaskaden analysiert. Es wurde gezeigt, dass die Aktivierung von ETS parallel und unabhängig von der Neurotrophin-Induktion erfolgt. Ein anderer Ansatz war die Analyse der Erinacin C-abhängigen Aktivierung einer mutmaßlichen *Tetraodon*-Enhancer-Region des *ngf*-Gens. Es wurde nachgewiesen, dass diese 2,1 kb große Enhancer-Region in Gegenwart von

Erinacin C sowie bei Aktivierung und Unterdrückung der ETS-Signalübertragung aktiviert wurde. Erinacin C ist ein Molekül mit einem geringeren Molekulargewicht, was darauf hindeutet, dass es die BHS überqueren kann. In dieser Arbeit wurde die Fähigkeit zur Überwindung der BHS unter Verwendung eines *In-vitro*-Ansatzes zur Nachahmung der BHS sowie unter Verwendung eines *In-vivo*-Wirbeltiermodellsystems, des Zebrafisches, gezeigt. Um die Wirkung dieser Verbindungen *in vivo* zu analysieren, wurde in dieser Arbeit geklärt, wo *ngf* oder sein Rezeptor *trkA* exprimiert werden. Es ist auch wichtig, ihre Wirkung *in vivo* unter Verwendung von Zebrafischen als Modellorganismus zu zeigen. Daher wurde eine Reporterlinie hergestellt, die mClover in *trkA*-exprimierenden Zellen markiert. Diese zeigt Expression in Trigeminus- und Motorneuronen, aber auch in sensorischen Neuronen des Zentralnervensystems. Unter Verwendung dieser transgenen Linie wurden verschiedene Regenerationsmodelle etabliert. Dieser Befund bietet Zugang zur Erklärung der Funktionen von aus *Hericium* stammenden Cyathan diterpenoiden wie Erinacin C. Diese Studien bieten erste genetische Möglichkeiten zur Analyse der Funktion von Cyathan diterpenoiden, aus *Hericium* sp. isolierten Sekundärmetaboliten, in Astrozytenzellen und verbessern das mechanistische Verständnis der Wirkung von Cyathanen in Gliazellen. Andererseits wurden verschiedene Modellsysteme zur Analyse der Neurotrophin-stimulierenden Wirkungen *in vivo* etabliert. Diese Studie ermöglicht es, andere Signalkaskaden zu charakterisieren, die von Cyathanen aktiviert werden, und den Effekt in Zukunft *in vivo* zu untersuchen.

1. **Introduction**

Caused by an aging population, neurodegeneration in the brain during lifetime could lead to severe problems. Unfortunately, no medication is found until now to heal neurodegenerative diseases. It is only possible to treat their symptoms. In this aspect, small secreted polypeptides called neurotrophins, could serve for possible medications (Hefti, 1994). Neurotrophins can influence the degeneration, maturation, maintenance and regeneration of neurons, which are mostly affected during the development of neurodegenerative diseases (Xiao and Le, 2016). However, neurotrophins have relatively high molecular weights, which prevent them to cross the blood-brain barrier (BBB) (Pardridge, 2002b). Instead, small molecular weight metabolites that can cross the BBB are suspected to influence the expression of neurotrophins (Pardridge, 2002a). It is unknown until now, how such small metabolites work and influence the neurotrophin expression. This thesis focuses on pure compounds that are isolated from an edible fungus and characterizes its suspected effect to stimulate neurotrophin expression.

1.1 With an aging population, neurodegenerative diseases lead to severe problems.

Neurodegenerative disease is a collective term for several diseases that affect neurons in the nervous system. Neurons are differentiated cells that do not divide (Yang *et al*., 2014) and are important components of the nervous system. Damaged or dead neurons, caused by traumata or neurodegenerative disease, cannot be replaced. The most prominent neurodegenerative diseases are Parkinson's, Alzheimer's and Huntington's disease. These diseases are not curable. The progressive death of neuronal cells results in problems with mental abilities (dementia) or leads to impaired abilities in the movement coordination (ataxia). Here, neurotrophins could serve as possible medications.

1.2 Neurotrophins can serve as possible medication.

The term “neurotrophin” was introduced by Viktor Hamburger and Rita Levi-Montalcini earning the Nobel prize for that discovery (Levi-Montalcini and Cohen, Nobel prize 1986). Neurotrophins are the body's own signaling substances that guide targeted connections between neuronal cells (Loughlin and Fallon, 1993) and ensure the maintenance of neuronal connections. Neurotrophins are small proteins with a molecular mass of approximately 13 kDa. These molecules are secreted proteins, produced by a target tissue in small quantities. It is assumed that immature neurons compete for limited trophic factors. Only those neurons that

successfully establish synaptic connections get enough trophic factors to survive (Huang and Reichardt, 2001). Neurons that do not receive enough trophic factors are removed by apoptosis (Dekkers *et al*., 2013). If neurotrophins are present, they bind to cell surface receptors of the Trk family (tropomyosin receptor kinase) (Huang and Reichardt, 2001). Then, a cascade of kinases become triggered and target proteins can suppress apoptosis (Lu and Xu, 2006; Pearson *et al*., 2001).

Different neurotrophins have been identified up to now: nerve growth factor (NGF; Franck *et al*., 1983, Weis, 1972), brain-derived neurotrophic factor (BDNF; Leibrock *et al*., 1989) and five more neurotrophins, called NT3 (neurotrophin 3; Maisonpierre *et al*., 1990), NT4 (neurotrophin 4; Hallbrook *et al*., 1991), NT5 (neurotrophin 5; Berkemeier *et al*., 1992, Berkemeier *et al*., 1991), NT6 (neurotrophin 6; Götz *et al*., 1994) and NT7 (neurotrophin 7; Nilsson *et al*., 1998). It was shown before, that neurotrophins can work as chemotactic and as chemorepulsive factors (Paves and Saarma, 1997), but they can also act as survival factors.

Neurotrophins are a group of proteins, which are encoded by genes that show a similar structure (Figure 1). The coding gene has one larger exon of approximately 1kb (Berkemeier *et al*., 1992; Ebendal *et al*., 1986; Ip *et al*., 1992; Leingartner and Lindholm, 1994), which codes the neurotrophin precursor. A smaller exon is located upstream of the large exon which codes for the neurotrophin precursor (Edwards *et al*., 1986; Salin *et al*., 1997; Sekimoto *et al*., 1998). The neurotrophin precursor element contains the signal sequence, the pro-peptide and the mature neurotrophin (Francke *et al*., 1983; Meier *et al*., 1986). Six cysteine residues form disulfide bridges that generate a specific tertiary structure called cysteine knots (Server *et a*l., 1976). Therefore, these cysteines are important for the folding and the maintenance of a stable tertiary structure. Neurotrophins build dimers (Arakawa *et al*., 1994).

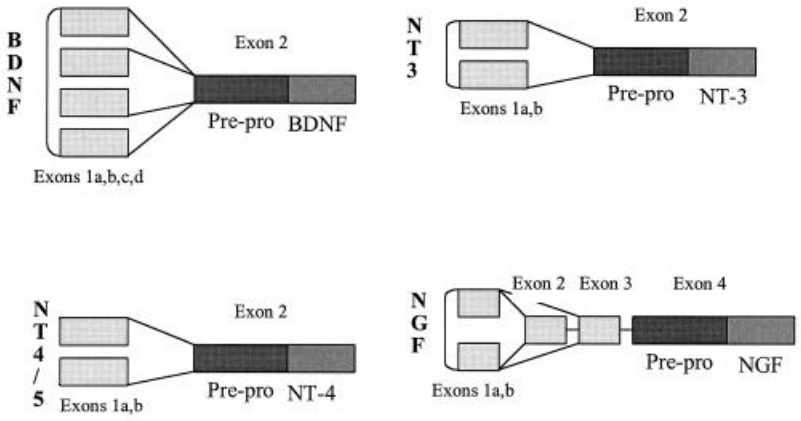

Figure 1: Exon/ intron organization of selected neurotrophin genes. Exons are represented by boxes and lines represent introns and alternative splicing. (taken from Heinrich and Lum, 2000)

Neurotrophins have multiple functions. The best-studied role in mammals is their control of apoptosis, the mechanism of programmed cell death. During development, neurons and glial cells are initially overproduced and then selectively eliminated by programmed cell death. This is regulated by neurotrophic factors during target innervations (Lotto *et al*., 2001). Two major members of the neurotrophins are nerve growth factor (NGF) and brain-derived neurotrophic factor (BDNF).

1.2.1 Nerve growth factor (NGF)

NGF belongs to the group of neurotrophic factors. It was first discovered in the snake venom and the salivary gland of a male mouse (Franck *et al*., 1983; Weis, 1972). It is involved in the migration, differentiation, and maturation of sensory and sympathetic neurons in the developing and the adult peripheral nervous system (Levi-Montalcini and Hamburger, 1951; Johnson and Gorin, 1980; Levi-Montalcini, 1987; Longo *et al*., 1992). Further findings show that NGF is involved in regeneration, physiology, and survival of retinal ganglion cells (Turner *et al*., 1987). In general, NGF has powerful biological activities, such as the promotion of neurite outgrowth and the prevention of neuronal death. NGF is also crucial to maintain and coordinate the neuronal functionality (Obara and Nakahata, 2002).

1.2.2 Brain-derived neurotrophic factor (BDNF)

The growth factor BDNF is another protein from the group of neurotrophins and is closely related to the nerve growth factor (Binder and Scharfmann, 2004). BDNF affects various

neuronal cell types in the central and peripheral nervous system. It helps to protect existing neurons and synapses and promotes the growth of new ones (Acheson *et al.*, 1995; Huang and Reichardt, 2001). BDNF is active in brain areas that are essential for memory and abstract thinking, such as the hippocampus, the cerebral cortex and the forebrain (Yamada and Nabeshima, 2003). BDNF also plays a major role in long-term memory (Bekinschtein *et al*., 2008). It is one of the most active neurotrophins in adult neurogenesis (Barde *et al*., 1982). By that BDNF is involved in supporting survival of present neurons and it also provides growth and differentiation of new neurons and synapses via axonal and dendritic outgrowth. The high affinity receptor of BDNF is TrkB.

1.2.3 The family of tropomyosin receptor kinases

Tropomyosin-related receptors kinases (Trks) play an important role in the development and function of the vertebrate nervous system. Three distinct members are identified in mammals: TrkA (Klein *et al*., 1991), TrkB (Klein *et al*., 1990) and TrkC (Lamballe *et al*., 1991). Trks control the survival of neurons (Klein, 1994; Barbacid, 1994). They have an impact on the function of synapses (Lindholm *et al*., 1994), the maturation of synapses (Wang *et al*., 1995) and contribute to the neuronal response of injury (Persson and Ibanez, 1993). TrkA is one member of the tropomyosin-related kinase receptor family, which is characterized by a fusion of tropomyosin with an unknown tyrosine kinase (Heinrich and Lum, 2000). The intracellular domain of the tyrosine kinase is related to the FGF/ EGF/ PDGF/ insulin receptor family. The kinase domain is highly conserved.

All immature neurotrophins, called precursor peptides, can bind the low affinity neurotrophin receptor p75 NTR (Binder and Scharfman, 2004). P75 NTR is related to proteins of the tumor necrosis factor (TNFR) superfamily (Binder and Scharfman, 2004). It has a glycosylated extracellular region that is involved in the binding of ligands, a transmembrane region, and a short cytoplasmic sequence, which lacks an intrinsic catalytic activity (Chao and Hempstead, 1995; Dechant and Barde, 2002). The binding of neurotrophins to p75 activates various intracellular signal transduction pathways (Dechant and Barde, 2002). P75 signaling provides biologic actions distinct from those of the Trk receptors, in patricular the initiation of programmed cell death (apoptosis) (Casaccia-Bonnefil *et al*., 1996; Dechant and Barde, 2002).

p75NTR binds all five neurotrophins, but the affinity is low. On the other hand, the receptors of the Trk family are more affine and can specifically bind certain neurotrophins: TrkA can bind NGF, TrkB can bind BDNF, NT4 and NT5 and TrkC can bind NT3. The binding of

neurotrophins to p75NTR lead to programmed cell death (apoptosis) of the cell. In contrast, the binding to receptors of the Trk family, triggers a cascade of kinases with anti-apoptotic effects.

1.2.4 NGF-TrkA-Signaling

NGF is released by target cells and activates the high affinity receptor TrkA (Klein *et al.*, 1991) (Figure 2). NGF binding to TrkA initiates dimerization, followed by an autophosphorylation of the tyrosine residue and activation of the intracellular signaling cascade (Kaplan *et al.*, 1991; Jing *et al.*, 1992). The neurotrophin signaling is transmitted via the activation of the tropomyosin-related kinase (Cordon-Cardo *et al.*, 1991; Loeb *et al.*, 1991; Zhou *et al.*, 1994) and affects a variety of downstream signal cascades involved in cell survival, axon and dendritic growth and the specification and synapse formation of sympathetic and sensory neurons (Harrington and Ginty, 2013). The different downstream signaling cascades become activated after autophosphorylation of the TrkA receptor, which has ten conserved tyrosine residues in the cytoplasmic domain. Phosphorylation of the tyrosines Y670, Y674 and Y675 enhance the kinase activity (Cunningham and Greene, 1998; Stephens *et al.*, 1994). Phosphorylation of the tyrosine Y490 activates binding of an adaptor called proteins of the Src homology and Collagen family (Shc) or Fibroblast growth factor receptor substrate 2 (Frs2), which activates Mitogen-activated protein kinases (MAPK) and Phosphoinositid-3-Kinases (PI3K) signaling. On the other hand, phosphorylation of Y785 activates Phosphoinositid-Phospholipase C (PLC_γ) (Obermeier *et al.*, 1993; Stephens *et al.*, 1994). Activated MAPKs target the Extracellular-signal Regulated Kinases (Erk1/2) pathways, which are able to signal through cAMP response element-binding protein (CREB), ETS Like protein 1 (Elk1) and myocyte enhancer factor-2 (MEF2) to regulate target gene expression, which influence neuronal differentiation and survival (Pearson *et al.*, 2001; Riccio *et al.*, 1999). On the other hand, activation of PI3K is important for cell survival via signal transduction through the serine/threonine kinase 1 (Akt) and phosphorylation of apoptosis-enhancing proteins, like the BCL2 associated agonist of cell death (Bad) and the glycogen synthase kinase

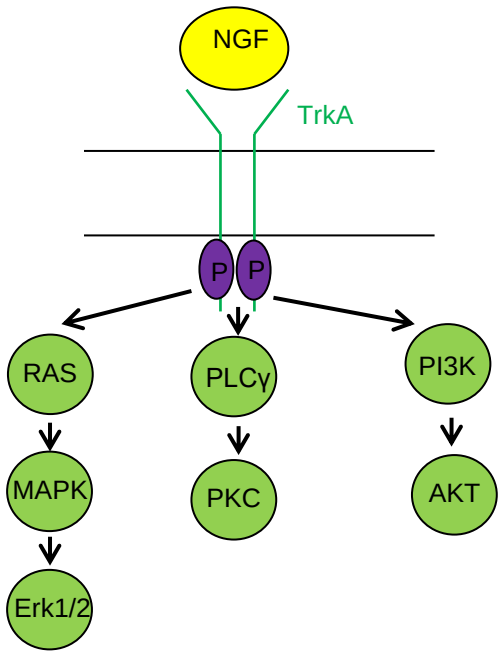

Figure 2: Schematic drawing of the NGF/TrkA signaling cascade. Binding of NGF to its high affinity receptor TrkA leads to dimerization and autophosphorylation of the cytosolic region of TrkA and the activation of the kinase region. This activation is causing the initiation of several downstream cascades, including MAPK, PLC_γ and PI3K.

3 (GSK3β) (Datta *et al*., 1999; Hetman *et al*., 2000). Another downstream pathway of NGF/TrkA signaling is mediated by PLC_{γ}, which leads to the production of inositol trisphosphate (IP3) and dystroglycan (DAG). This promotes Ca^{2+} mobilization and an activation of different protein kinases C (Kaplan and Miller, 2000).

Neurotrophins could serve as possible activator of regeneration by activating several downstream signaling cascades. But the high molecular mass disables them to cross the BBB. Lower molecular weight metabolites are getting more and more into the focus of research. These lower molecular weight metabolites were isolated as secondary metabolites from fungi (as natural products), like the family of fungi *Hericium*, which were known from Chinese medicine as medication against nervous system disorders, cancer, and weak immune system. But it could also be shown that secondary metabolites isolated from fungi and plants are able to stimulate neurotrophins (La *et al*., 2013; Naidu *et al*., 2007).

1.3 Secondary metabolites isolated from an edible fungus could overcome the BBB problems.

Since neurotrophins are not able to pass the blood-brain barrier, they cannot be used for external treatment (Pardridge, 2002). Therefore, molecules of small molecular weights are needed that can induce the expression of neurotrophic signaling molecules.

Medicinal mushrooms have been characterized for potential neurotrophic metabolites for about 25 years, and in particular, the genus *Hericium erinaceus* has raised major attention as food supplements and alternative medicine (Thongbai *et al*., 2015). But not only the mushroom *H. erinaceus*, was studied intensively, also other medical mushrooms, like *Antrodia camphorate*, *Ganoderma* spp., *Lignosus rhinocerotis* and *Pleurotus giganteus*, were characterized extensively. But most of the potential neuroactive compounds, which could serve as possible medication against neurodegenerative disease, have been reported from *H. erinaceus*. *Hericium* species are basidiomycota which belongs to the family Hericiaceae. It was demonstrated that extracts from both, basidiomes and mycelial cultures of *Hericium erinaceus*, are able to induce expression of neurotrophins in astrocytic cells. Two major substance classes can be isolated from *H. erinaceus*: hericenones and erinacines. A recent publication reveals that isolated cyathane diterpenoid compounds of *Hericium erinaceus* extracts are able to mediate neurotrophin-inducing activities (Wang *et al*., 2019). Other publications in regard to secondary metabolites of this edible mushroom report various biological properties, such as antibacterial,

cytotoxic and neuritogenic effects (Kawagishi *et al*., 1990; Kawagishi *et al*., 1994; Kawagishi *et al*., 2006; Ma *et al*., 2010; Kim *et al*., 2012).

Different other substances are in focus for medical treatment options and discussed in this thesis. Corallocins, for example, are isolated from *Hericium coralloides*. These fungi have fruiting bodies which looks like a white coral. There are only a few reports of the metabolite production of *H. coralloides* (Kim *et al*., 2018; Saito *et al*., 1998; McCracken and Dodd, 1971; Zou *et al*., 2012). The second group of compounds that will be characterized in this thesis are the erinacines. Erinacines are cyathane diterpenoids, which were only produced in the cultures and can be isolated from mycelial cultures *H. erinaceus* and *H. flagellum*, the most famous representatives of this genus. It has been used in traditional Chinese medicine for a long time and is processed into food supplements and alternative medicines (Ying *et al*., 1987; Thongbai *et al*., 2015). It could be shown that erinacine S and erinacine A, which was isolated from the mycelial ethanol extract of *H. erinaceus*, are able to significantly increase the level of insulin-degrading enzyme (IDE) in cerebral cortex and by that reduce the AB10-stained plaques (Chen *et al*., 2016). But substances isolated from other medical mushrooms were reported, to influence neurotrophin production (Eik *et al*., 2012; Seow *et al*., 2013; Phan *et al*., 2012; Mitschke 2017; Bai *et al*., 2015; Cao *et al*., 2018). On the other hand, the mode of action remains to be clarified.

So, it is known that extracts isolated from *Hericium erinaceus* are able to induce neurotrophins, but how they are able to induce the expression of neurotrophin and what is the direct signaling answer is unknown. This important question will be investigated in this thesis.

1.4 Signaling cascades

In biochemistry and physiology, processes are referred to signal transduction or signaling cascades, when cells have to react, for example, to external stimuli, convert them, transmit them as a signal into the cell interior and lead to a cellular effect via a signal cascade. A large number of enzymes and secondary messengers (second messengers) are often involved in these processes, in one level or on several successive levels (signal cascade). The original signal can be amplified considerably under certain circumstances (signal amplification). Signals from different signal paths are often related to and integrated by “crosstalk” in the cytoplasm or in the cell nucleus (Alberts *et al*., 2001).

The start of a signal transduction process is initiated or triggered by an intracellular or extracellular stimulus. Extracellular stimuli can be substances such as hormones, growth

factors, extracellular matrix, cytokines, chemokines, neurotransmitters and neurotrophins. However, nothing is said about the molecular nature of these substances and the signaling molecules can be whole proteins, steroids or small organic molecules such as serotonin. In addition, environmental stimuli can also trigger signal transduction. Intracellular stimuli, such as calcium ions (Ca^{2+}), are often themselves part of signal transduction cascades (Alberts *et al*., 2001).

With the help of proteins in the cell membrane and inside the cell (receptors), the extracellular signals are recorded and processed inside the cell. These receptors can be differentiated according to their location, structure and function: Cytosolic receptors, such as steroid receptors, retinoid receptors and soluble guanylyl cyclase, are the primary targets for steroids, retinoids and small, soluble gases such as nitrogen monoxide (NO) and carbon monoxide (CO), which can pass through the cell membrane due to their lipophilicity or small molecular size. Activation of steroid receptors leads, for example, to the formation of receptor dimers which, after binding to a response element, e.g. B. Sterol Response Element (SRE) act on the DNA itself as transcription factors. Membrane-based receptors are proteins, such as transmembrane proteins, which are located in the membrane and have both an outside and an inside domain. This enables them to bind signal molecules outside the cell and to trigger a signal inside the cell due to the change in conformation. The signal molecule does not cross the membrane, but binds to the extracellular domain, which leads to biochemical changes in the receptor molecule that also have an intracellular effect. The next family are the ion channels. Ion channels are voltage-, light- and ligand-dependent channels. These are transmembrane proteins that are either activated or deactivated as a result of the binding of a ligand as a signal substance, which increases or decreases the permeability of the membrane for certain ions. This is particularly important when transmitting electrical nerve signals to chemical synapses. The next family are the G-protein coupled receptors. The signaling pathways via G-proteins are among the best investigated signaling pathways. They are involved in many sensory physiological processes, such as visual recognition (via phototransduction), smelling and tasting, as well as the effects of numerous hormones and neurotransmitters. The last group of receptors are the enzyme-linked receptors. Enzyme-linked receptors are the third important group of cell surface receptors. To this group the receptor tyrosine kinases belong, which can activate, for example, the MAP kinase pathway and the PI3 kinase signaling pathway. TrkA and TrkB are prominent members of this class (Knippers, 2006).

The aim of the signal transduction process is the activation of effector proteins that trigger a specific cellular response. Effector proteins are, for example, transcription factors that activate the transcription of certain genes. Transcription factors are proteins, being able to bind to specific sequences in the DNA, which are normally located in front of the promotor of a gene. After binding these factors enhance or inhibit the expression of this gene.

1.5 ETS signaling

In the field of molecular biology, the ETS family (E26 transformation-specific (Nunn *et al*., 1983) or E-26 (Leprince *et al*., 1983)) belongs to the largest family of transcription factors. The ETS gene family is named after the first gene that was identified from the leukemia virus E26 and plays an important role in the development of various tissues. All proteins of the ETS family consist of a highly conserved DNA binding domain, the ETS domain, which is a winged helix-turn-helix structure (Papas et al., 1989; Wasylyk et al., 1993; Werner et al., 1995), which is able to bind to DNA sites with a central DNA sequence of GGA (A / T). In addition to the DNA binding function, the ETS domain is responsible for protein-protein interactions. However, ETS proteins differ significantly in the sequences that flanks the core motif.

The ETS protein family is implicated in a variety of functions including regulation of cell differentiation, cell cycle control, cell migration, cell proliferation, apoptosis (programmed cell death) and angiogenesis. Two major groups within the ETS family have been described: the ETS group, including Ets1, Ets2 and Pointed, and the ternary complex factors (TCFs), which include Elk1, Sap1a, Sap1b, Fli1 and Net. Ets1, Ets2 and Pointed (Pt2). Each of this contains a C-terminal conserved DNA binding domain and an N-terminal domain, which is described as a pointed domain. This group of members of the ETS family has a single MAPK phosphorylation site near the pointed domain (Brunner *et al*., 1994; Wasylyk *et al*., 1997). TCFs, on the other hand, contain a transactivation domain, which can be phosphorylated on several serine and threonine residues (Hipskind *et al*., 1994; Treisman, 1994). In addition, in vertebrates, Pea3 is an essential player in the differentiation of dopaminergic neurons in both *C. elegans* and in olfactory bulbs of mice (Flames and Hobert, 2009).

ETS1 is a prominent member of the ETS family. ChIP-Seq studies have shown that ETS1 can bind to both, AGGAAG and CGGAAG, motifs (Cauchy *et al*., 2016). ETS1 binds to DNA as a homodimer or heterodimer (Samorodnitsky *et al*., 2015). The phosphorylation of serine residues of the C-terminal domain makes ETS1 inactive, known as autoinhibition (Besnard *et a*l., 2011). There are several ways to activate ETS1. First, ETS1 can become dephosphorylated

(Cowley and Graves, 2000). Second, two ETS1 can be activated when two ETS molecules homodimerize. Homodimerization occurs, when the DNA binding sites are in a correct orientation and have the right distance. Thus, the specific location of the binding sites within an enhancer or promoter segment can have a strong impact on whether ETS1 can bind or not (Hollenhorst *et al*., 2017). Third, ETS1 proteins can be activated by Erk2 and Ras at threonine Thr38. Many Ras-responsive genes contain combinatorial ETS/AP1 recognition motifs by which ETS1 and AP1 synergistically activate the transcription after the stimulation of Ras (Wasylyk *et al.,* 1998). ETS1 interacts directly with various transcription factors. Their interaction leads to the formation of multiprotein complexes. When ETS1 interacts with other transcription factors (like Runx1, Pax5, TFE3 or USF1), its final impact on transcription depends on whether its C-terminal domain is phosphorylated. The acetyl transferases CBP and the p300 protein bind to the transactivation domain. AP1, STAT5 and VDR bind to the C-terminal domain.

Cumulative data have shown that ETS proteins are considered to be subordinated to the Ras-MAPK signaling cascade (Wasylyk *et al*., 1998). The phosphorylation of ETS factors by MAPKs controls their downstream activity, but also the protein partnerships, target specificity or transactivation.

1.6 *Danio rerio* as model organism

Thinking about the importance to study the effect of compounds being able to induce neurotrophins and other cascades during neurodegeneration and neuroregeneration, a model system is needed. *Danio rerio* is a perfect model when thinking about screening compounds and is also a vertebrate model, which apart from that surprisingly show neuroregeneration until the juvenile age. In this thesis the zebrafish was used for initial quantification of substances isolated from the medical mushroom *Hericium*.

The zebrafish (*Danio rerio*) is a freshwater fish from the family of carps (*Cyprinidae*) and is resident in the rivers of the Indian subcontinent. It is a prominent model organism in the research of vertebrates. The research of genetic mechanisms elucidating the morphogenesis of vertebrates has been pioneered especially by the work of George Streisinger and later by Christiane Nüsslein-Volhard (Streisinger *et al*., 1981; Nüsslein-Volhard, 1995). Pharmacological studies, toxicological material classifications and many other essential applications in the field of genetics have used zebrafish as model systems (Janning and Knust, 2008).

The zebrafish is easy to maintain due to its small size (3-4 cm) and produces a high number of offspring within a short time. A female is able to lay up to 200 eggs at least two times per week. The zebrafish is very suitable for genetic experiments, because it has a short maturation time of three to four months to reach sexual maturity.

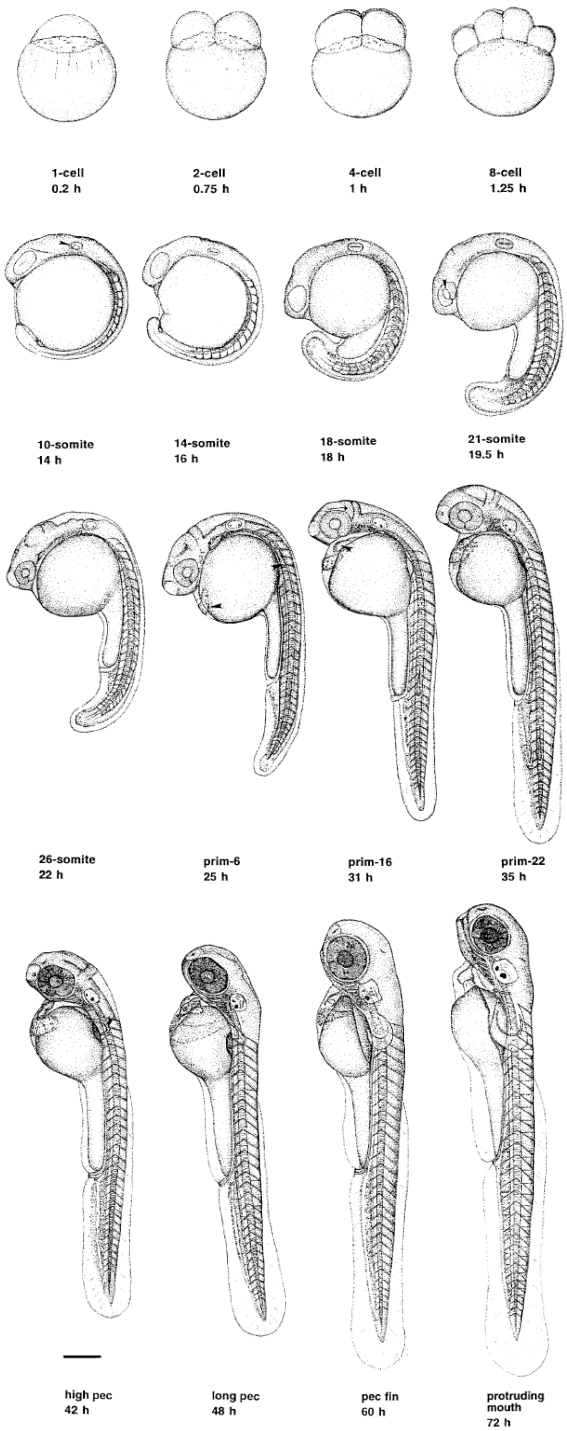

Figure 3: Development of the Zebrafish during the first 72h post fertilization. (Kimmel *et al.*, 1995)

The fertilization and the embryonic development occur outside of the mother and the embryo is transparent. This allows a detailed analysis of embryonic development starting with a fertilized oocyte to developed larvae within 72 hours (Figure 3). The role of genes and cells during organogenesis cab be analyzed in detail by the use of time-lapse microscopy (William *et al*., 2009).

The genome of the zebrafish (1700 Mbp) is completely sequenced and available in public databases. Even though the fish is genetically further distant to mammals, it is nevertheless suitable as a model for mammalian development. As a vertebrate, the zebrafish shares a high

degree of conserved genes and protein functions and signaling cascades. The zebrafish brain is highly conserved to the brain of mammalians (Bandmann and Burton, 2010; Panula *et al*., 2010).

Many methods of reverse and forward genetics are well established in zebrafish research. Due to the transparency of the embryo, phenotypes can easily be analyzed. In the zebrafish field many transgenic lines and mutants are available or can be generated with ease (Howe *et al*., 2013).

In addition, fish are able to generate new neurons in all stages of life. This can help to understand the role of neurotrophic factors, their receptors and signaling cascades in detail during the lifetime. Furthermore, many compounds can be added to the water and analyzed for their pharmacological benefits, making the zebrafish an ideal organism to study the stimulating effect of neurotrophic factors.

The similarity of neuronal death in fish and higher vertebrates, as well as the conserved neurotrophic factors and their receptors, suggest equally prominent regulators of neuronal apoptosis in fish (Heinrich and Lum, 2000). One neuronal population that performs programmed cell death in fish are the Rohon Beard neurons. They are primary sensory cells, known as first established neurons that are located in the dorso-lateral spinal cord. When they die, they become replaced by sensory neurons in the dorsal root ganglia (Metcalfe et al., 1990). Depending on their peripheral targets, Rohon Beard neurons either die or migrate from the spinal cord (Weis, 1968). Cell death is also visible in all three layers of the embryonic retina (Hoke and Fernald, 1998). New cells are continually generated in the marginal zone of the retina in adult and growing fish. Even the cerebellum shows an active adult neurogenesis (Soutschek and Zupanc, 1996). The proliferation and maturation of neurons in the developing and adult fish is accompanied and balanced by a regulated neuronal death.

In addition, NGF and BDNF signaling is found in the adult brain of adult teleost fish near neurogenic niches, suggesting a potential a role in adult neurogenesis in the vertebrate brain (Cacialli and Lucini, 2019).

It is known, that extracts isolated from *Hericium* species are able to influence neurotrophin production, but until now only one neurotrophin was characterized, NGF. In this thesis another neurotrophin will be characterized, whether it is upregulated upon addition of pure substances. Also, the different direct cellular answers after addition are not characterized yet. This thesis

will give the first insights into characterization of signaling response upon compound treatment *in vitro*.

Apart from that, *in vivo* models to characterize compound dependent neurotrophin upregulation are missing. The zebrafish is, as shown before, a perfect model for compound screening. A model for quantifying NGF mediated influence on degeneration and regeneration will be established in this thesis.

2. Material and Methods

2.1 Materials

Table 1: List of Primer

Primer name	Sequence 5'-3'
mGAPDH up	ACCACAGTCCATGCCATCAC
mGAPDH low	TCCACCACCCTGTTGCTGTA
hNGF sense	CCAAGGGAGCAGTTTCTATCCTGG
hNGF antisense	GGCAGTTGTCAAGGGAATGCTGAAGTT
hBDNF sense	TAACGGCGGCAGACAAAAAGA
hBDNF antisense	GAAGTATTGCTTCAGTTGGCCT
ETS sense	TATATCGATACCACCATGAAGGCGGCCGTCGA TCTCAAGCCGA
ETS antisense	CCAACAAAGTCTGGGGCCAGCTCGAGAAAGC AGTCTTTAC

Table 2: List of used Plasmids

Plasmid name	Discription
pCS-rat dnTrkA-CitrineERex	N-terminus of rat TrkA until Serine 477 fused to mCitrine connected with an Endoplasmic reticulum export signal
pBSII-Tol2-4xNFkb-EIb-Luc2	4x NFkappaB binding sites (GGGAATTCCC) followed by E1b-luciferase2-pA
pTol2-4xGli-EIb-Luc2	4x GLi1 binding sites (GACCACCCA) followed by E1b-luciverse2-pA
pTol2-4xRBP-EIb-Luc2	4x RBPJ bindings sites (CGTGGGAA) followed by E1b-luciferase2-pA
pTol2-4xDyrk1A-EIb-Luc2	4x Dyrk1A binding sites (TCTCGCGAGA) followed by E1b-luciferase2-pA
pTol2-4xPea3b(ETS)-EIb-Luc2	4x Pea3b (ETS) binding sites (GGAAATTCCTTTCC) followed by E1b-luciferase2-pA
pTol2-4xCREB-EIb-Luc2	4x CREB binding sites (CTGACGTCA) followed by E1b-luciferse2-pA
pTol2-4xTCF/LEF-E1b-Luc2	4x TCF/LEF binding sites (AGATCAAAGGG) followed by E1b-luciferase2-pA
pTol2-4xLhx2/Sox2-EIb-Luc2	4x Lhx2-Sox2 bindings sites (CTAATTAAAGAACAAAG) followed by E1b-luciferase2-pA
pTol2-4xSBE-Eib-Luc2	4x TGFbeta SBE binding sites (AG(C/A)CAGACA) followed by E1b-luciferase2-pA
pTol2-4xHIF1-EIb-Luc2	4x HIF1 binding sites (TGTGTACGTGCTG) followed by E1b-luciferase2-pA
pTol2-4xNBRE-EIb-Luc2	4x NBRE binding sites (AAAAGGTCA) followed by E1b-luciferase2-pA
pTol2-4xSF1-E1b-Luc2	4x SF1 binding sites (TCAAGGTCA) followed by E1b-luciferase2-pA
pTol2-4xSRF-EIb-Luc2	4x SRF binding sites (CCATA T/A AAGG) followed by E1b-luciferse2-pA

pTol2-4xHSE-E1b-Luc2	4x HSF1 binding sites (HSE sites AGAACGTTCTAGAAC) followed by E1b-luciferase2-pA
pTol2-4xUAS-E1b-Luc2	4x Gal4 binding sites (UAS CGGAGTACTGTCCTCCG) followed by E1b-luciferase2-pA
pTol2-4xSTAT3-E1b-Luc2	4x STAT3 binding sites (ATTTCCCGGAAAT) followed by E1b-luciferase2-pA
pTol2-4xARE-E1b-Luc2	4x ARE binding sites (GGAAATGACATTGCTAATGGTGACAAAGCAACTTT) followed by E1b-luciferase2-pA
pTol2-4xELK1-E1b-Luc2	4x ELK1 bindings sites (G/A ACCGGAAGT) followed by E1b-luciferase2-pA
pTol2-4xNFY-E1b-Luc2	4x NFY bindings sites (AGCCAATCGG) followed by E1b-luciferase2-pA
pTol2-4xKLF-E1b-Luc2	4x ETS bindings sites for SP1-KLF (GGCCCCGCCCCC) followed by E1b-luciferase2-pA
pTol2-4xNRF-E1b-Luc2	4x NRF bindings sites for ROS-signaling (CTGCGCATGCGC) followed by E1b-luciferase2-pA
pTol2-4xE2F-E1b-Luc2	4x E2F bindings sites for E2F-signaling (CTGGCGGGAA) followed by E1b-luciferase2-pA
pTol2-4xbHLH-E1b-Luc2	4x bHLH bindings sites for bHLH-signaling (AAACAGCTGT) followed by E1b-luciferase2-pA
pTol2-4xbzip-E1b-Luc2	4x bzip bindings sites for bZIP-signaling (AAACAGCTGT) followed by E1b-luciferase2-pA
pTol2-4xSoxPou-E1b-Luc2	4x Sox-Pou bindings sites for bZIP-signaling (CATTGACATGCTAAT) followed by E1b-luciferase2-pA
pTol2-4xKLF5-E1b-Luc2	4x KLF5 bindings sites for KLF5-signaling (AGGGTGTGGC) followed by E1b-luciferase2-pA
pTol2-4xETS-E1b-Luc2	4x ETS bindings sites for ETS-signaling (CACTTCCGGT) followed by E1b-luciferase2-pA
pTol2-4xNARE-E1b-Luc2	4x NARE bindings sites for Egr1-signaling (CTCCCCCCAC/CGCCCCCGC) followed by E1b-luciferase2-pA
pTol2-4xNFAT/AP-E1b-Luc2	4x NFAT/AP bindings sites for NFAT-signaling (TGGAAAATTTGACTCATAG) followed by E1b-luciferase2-pA
pTol2-4xERE-E1b-Luc2	4x ERE binding sites for Estrogenreceptor-signaling (GGTCACAGTGACC) followed by E1b-luciferase2-pA
pTol2-4xRunt-E1b-Luc2	4x Runt binding sites for Runx-signaling (CTGTGGTTT) followed by E1b-luciferase2-pA
pTol2-4xFez-E1b-Luc2	4x Fexf2 binding sites for Fez-signaling (CAGCAACC) followed by E1b-luciferase2-pA
pTol2-4xlexA-E1b-Luc2	4x lexA binding sites for Runx-signaling (CTGTACATCCATACAG) followed by E1b-luciferase2-pA
pTol2-4xNFAT-E1b-Luc2	4x NFAT binding sites for NFAT-signaling (GGATTTTCCA) followed by E1b-luciferase2-pA
pTol2-4xSim2-E1b-Luc2	4x Sim2 binding sites for Sim2-signaling (TTGTTATGCAAA) followed by E1b-luciferase2-pA
pTol2-4xTbox-E1b-Luc2	4x T-box binding sites for T-box-signaling (TCACACCT) followed by E1b-luciferase2-pA

pTol2-4xFOXO-E1b-Luc2	4x FOXO binding sites for FOXO-signaling (TCCTGTTTACCA) followed by E1b-luciferase2-pA
pTol2-4xBRE-E1b-Luc2	4x BRE bindings sites for BMP-signaling (CTGG(C/A)GCC) followed by E1b-luciferase2-pA
pTol2-4xTAED-E1b-Luc2	4x TAED bindings sites for YAP-TAZ-signaling (ACATTCCAC) followed by E1b-luciferase2-pA
pTol2-4xa1ACT-E1b-Luc2	4x a1ACT binding site ATTATAAGATG followed by E1b-luciferase2-pA
pTol2-2xUAS-E1b-Luc2	2x Gal4 binding sites (CGGAGTACTGTCCTCCG) followed by E1b-luciferase2-pA
pTol2-6xUAS-E1b-Luc2	6x Gal4 binding sites (CGGAGTACTGTCCTCCG) followed by E1b-luciferase2-pA
pTol2-8xUAS-E1b-Luc2	8x Gal4 binding sites (CGGAGTACTGTCCTCCG) followed by E1b-luciferase2-pA
pTol2-2xETS-E1b-Luc2	2x ETS binding site CACTTCCGGT followed by E1b-luciferase2-pA
pTol2-6xETS-E1b-Luc2	6x ETS binding sites (CACTTCCGGT) followed by E1b-luciferase2-pA
pTol2-8xETS-E1b-Luc2	8x ETS binding sites (CACTTCCGGT) followed by E1b-luciferase2-pA
pCS-NLS-ETS(DB)-TA4	NLS-DNA-binding domain of human ETS1 fused to TA4
pCS-NLS-ETS(DB)-TA2	NLS-DNA-binding domain of human ETS1 fused to TA2
pCS-NLS-ETS(DB)-KRAB	NLS-DNA-binding domain of human ETS1 fused to KRAB repressor domain
p-Tngf-Luc2	*Tetraodon nigorividis* 2.1kb upstream sequence of ngf-b drving Luciferase 2 expression
p-Tngf(1500)-Luc2	*Tetraodon nigorividis* 1.5kb upstream sequence of ngf-b driving Luciferase 2 expression
p-Tngf(1000)-Luc2	*Tetraodon nigorividis* 1.0kb upstream sequence of ngf-b driving Luciferase 2 expression
p-Tngf(500)-Luc2	*Tetraodon nigorividis* 500bp upstream sequence of ngf-b driving Luciferase 2 expression
pTol2-Tngf500-E1B-Luc2	*Tetraodon* ngfb enhancer (-2.000-1.500)-E1b-Luciferase2
pTol2-Tngf1000-E1B-Luc2	*Tetraodon* ngfb enhancer (-2.000-1.000)-E1b-Luciferase2
pTol2-Tngf1500-E1B-Luc2	*Tetraodon* ngfb enhancer (-2.000-500)-E1b-Luciferase2

2.2 Cell culture methods

2.2.1 Cultivation of PC12 cells

PC12 is a cell line, which was derived from a tumor of the adrenal medulla (pheochromocytoma) in rats (Greence and Tischler, 1976). Pheochromocytoma has an embryonic origin from neural crest, which is represented by a mixture of neuroblastic and eosinophilic cells. PC12 cells are widely used as a model system for neuronal cells with a variety of neuronal processes, such as neurite outgrowth, which can by studied. Under normal

cell culture conditions, these cells have mostly no extensions. Through addition of nerve growth factor (NGF), neuronal differentiation can be initiated, which leads directly to a change in the actin cytoskeleton and within a few hours to a plating and the outgrowth of several long neurite-like extensions. Differentiated PC12 cells with extensions are postmitotic and produce neurotransmitters (noradrenalin) and neuronal marker proteins, such as *gap-43*.

PC12 cell culture medium

5 ml Fetal calf serum (Capricorn Scientific)
10 ml Horse serum (Capricorn Scientific)
1 ml Penicillin-streptomycin solution (Gibco^{TM}; 100x)
1 ml Glutamine (Gibco^{TM}; 100x)
add RPMI-1640 (Gibco^{TM})medium to 100 ml.

At the beginning of the experimental phase, cells are taken from a stock culture (stored at -196°C) and transferred to a collagen-coated collagen cell culture dish for propagation for at least 7 days before starting an assay. About $1x10^7$ cells are added to 10 ml PC12 cell culture medium in a cell culture plate. Cells are incubated at 37°C and 5% CO_2 concentration in an incubator. The medium is changed every two days and cells are splitted if necessary.

2.2.2 Cultivation of 1321N1 astrocytoma cells

1321N1 are human astrocytoma cells, which were isolated in 1972 as a subclone of another cell line called 1181N1 which was derived from malignant gliomas by Pontén (Pontén *et al*., 1968).

1321N1 cell culture medium

10ml Fetal calf serum (Capricorn Scientific)
1ml Penicillin-streptomycin solution (Gibco^{TM} ; 100x)
1ml Glutamine (Gibco^{TM} ; 100x)
Add DMEM (Gibco^{TM}) medium to 100ml.

To start the cultivation of 1321N1 cells, cells are taken from a stock culture which are stored at -196°C and transferred to a 10 cm dish for propagation for at least 7 days before starting an assay. On a 10 cm dish around $1x10^6$ cells are added in 10 ml cell culture medium. Cells are incubated at 37°C and 5% CO_2 concentration in an incubator. The medium are changed every two days and the cells had to be splitted if about 80-90% confluence was visible.

2.2.3 Collagen-coating of cell culture plates for PC12 cell cultivation

Cells isolated from animals as primary cells as well as cell lines may not easily be attached to plastic. Cell culture dishes are therefore normally positively charged to enable cells to attach to the ground by the negatively charged proteins. Especially, primary cells or cells which are grown in suspension, which are normally cell isolated from cancerous origin, have problem to attach without any structural proteins. Especially, primary cells or cells which are grown in suspension, which are usually derived from cancers, need supplementation by structural proteins, such as collagen.

Since PC12 cells are derived from a pheochromocytoma these cells are not able to attach to normal treated cell culture dishes. Collagen is used to pretreat the cell culture plate before PC12 cells are added. A suspension of 10µg/ml Collagen (Roche) is produced following the protocol of the costumers. This suspension is added on the required cell culture dish an incubated for 4h at 37°C. After 4h the suspension is removed and can be reused again. The cell culture dishes are dried at room temperature overnight under the clean bench and disinfected with UV light. After that PC12 cells was added directly.

2.2.4 Pretreatment of cover slips for cell cultivation

Adherent cells normally cannot attach to glass surfaces. And the second problem when cultivating cells on glass cover slips is that they need to be washed and sterilized before introducing them in culture. That is why glass cover slips need to be cleaned, washed and sterilized before.

To rinse them glass slides are incubated for 10 min in 0.1% HCl at room temperature (RT). This step is followed by an intense step of washing with PBS. To sterilize the glass slide they are stored in 70% EtOH until usage. For experiments slides are transferred to 24 well plate. To make it possible that cells attach to the ground, the surface needed to be coated. In this thesis a 10 µg/ml collagen (Roche) solution is used. The surface is coated as explained before.

2.2.5 Determination of cell number using a Neubauer's counting chamber

The total number of grown cells is determined with a small volume of cell suspension and a Neubauer's counting chamber. A cover slip is moistened and pressed on the counting chamber and it should be secure and may no longer be possible to move. This is usually the case when Newton's rings get visible. A small volume of cell suspension is pipetted beneath the cover slip

placed, so that the drop can flow under the cover slip. The net quantity of the Neubauer's chamber is determined by exactly 1 µl. On the chamber itself, a grid of 16 small and in total 4 large squares is recorded. To determine the cell number, cells of all 4 large squares were counted under a light microscope. The total number in suspension is determined by applying the following formula:

$$total\ cell\ number = \left(\left(\frac{counted\ cell\ number}{4}\right) \cdot 10^4\right) \cdot dilution$$

2.2.6 Cytotoxicity measurement of pure compounds – MTT Assay

The cytotoxicity of the test compounds needed to be determined prior to the neurotrophin studies.

Cells are incubated with the required cell number in a 96 well plate and incubated with the for the cell type specific media for 24h. After the attachment of the cells, the different treatments are added and incubated for 24 – 48h. After that, the toxicity measurements, using CK04 – Cell Counting Kit 8 (Dojindo Molecular Technologies), is performed.

The assay is performed according to the manufacturer information. On 100µl media 10µl CCK8 is added and incubated for 1 – 4h in the cell culture incubator. For PC12 cells an incubation time for 3h is sufficient, whereas 1321N1 astrocytoma cells needed only 2h of treatment. During this time an orange color is developed, and the absorbance was measured using a microplate reader (Tecan) with a wavelength of 450 nm. The value of cells incubated with normal media is set to 100% survival.

Compounds are tested with increasing concentration and with the solvent control in addition. The highest nontoxic concentration is used for further experiments.

2.2.7 Assay for analysis of direct PC12 cell differentiation

PC12 cells undergo the extension of neurites, when nerve growth factor (NGF) is added to the medium This was published before (Greence and Tischler, 1976). This experiment is used for analyzing potential neurotrophic activity of substances. If Hericium compounds have direct neurotrophic activity (Mori et al., 2008), there should be a neurite outgrowth of PC12 cells.

For preparation, 24 well plates are coated with 10µg/ml collagen as descripted before. After that, 3x104 cells in 1ml Medium were plated in each well and incubated overnight at 37°C, 5% CO2 in an incubator. On the next day, Hericium probes and NGF (human ß-NGF, Sigma, SRP3015) with a concentration of 200ng/ml are dissolved in 1ml serum-reduced medium and added to cells. Then, cells are incubated at 37°C with 5% CO2 and documented after 48 hours with a bright field microscope.

2.2.8 Assay for analysis of indirect stimulation of PC12 cell differentiation with conditioned media

The experiment is used to analyze the neurotrophin inducing capacity of different isolated Hericium compounds. If these substances are able to induce neurotrophin production, like NGF, these polypeptides are secreted into the media. Then the so-called conditioned media is added on PC12 cells, these cells should differentiate afterwards (Mori *et al*., 2008).

1321N1 astrocytoma cells are seeded with a density of 5x105 cells per well on a 6-well plate an incubated for 24h to leave the cells to attach to the surface. After 24h incubation medium was replaced to serum-reduced media and incubated for another 24h. Then the different Hericium compounds are added in their highest non-toxic concentration in serum-reduced media to the 1321N1 in the 6well plate. These cells were incubated for 48h. PC12 cells were plated on a 24well with a density of 3x104 cells per well plate 24h before the conditioned media, produced by the astrocytoma cells incubated for 48h with the different *Hericium* substances, were added. After 48h of incubation to produce the so-called conditioned media this media is added on the PC12 cells. These cells were incubated for another 48h and afterwards documented with a bright field microscope. The amount of differentiated cells as well as the neurite length is analyzed using FIJI. A differentiated cell is defined by neurites longer than the cells diameter. For the amount of differentiated cell, the number of differentiated cells in percent is calculated from each picture contain around 100 cells. The neurite length is quantified by measuring of 10 neurites of each picture. The ANOVA test was done using GraphPad Prism.

Serum-reduced medium

1ml Fetal calf serum (Capricorn Scientific)

1ml Penicillin-streptomycin solution (Gibco™; 100x)

1ml Glutamine (Gibco™; 100x)

Add DMEM (Gibco™) medium to 100ml.

2.2.9 Reverse Transfection of PC12 cells using Fugene® HD (Promega)

Transfection is the introduction of DNA or RNA into cells. There are different chemical ways to transfect cells: with Calcium-Phosphate-Precipitation, where a mixture of calcium chloride and sodium phosphate leads to the binding of the precipitating calcium phosphate, which then is added on the cell. Cationic polymers can be also used to introduce DNA into a cell, where positively charged, highly branched polymers can build complexes to the plasmid DNA, which is then taken up by the cells. In this thesis lipofection was used, where the genetic material can be introduced into the cell by liposomes, which are vesicles being able to bind to cells membranes.

The transfection is done referring to the user guide (Promega) in the following order:

	Per well in 96 well	**Per well in 24 well**
Opti-MEM™ (Thermo Fisher Scientific)	7.75 µl	38.75 µl
DNA (0.1 µg/ml)	2µl	10 µl
Fugene® HD (Promega)	0.25 µl	1.25 µl
	Mix serval times by pipetting up and down	

The mixture is incubated for 10-15 min at RT. Afterwards, the DNA-Fugene® HD complex is added into the appropriated well.

In the next step cells are seeded with a density of $1x10^4$/well (96 well) or $6x10^4$/well (24 well) an incubated for 48h in the transfection mixture in an incubator at 37°C with 5% CO_2.

2.2.10 Reverse transfection of 1321N1 cells using Lipofectamine® 3000 (Thermo Fisher Scientific)

The transfection is done referring to the user guide (Invitrogen) in the following order:

	Per well in 96 well	Per well in 24 well
Opti-MEM™ (Thermo Fisher Scientific)	3.8 µl	19 µl
DNA (0.1 µg/ml)	1µl	5 µl
P3000 (Thermo Fisher Scientific)	0.2 µl	1 µl
	Mix serval times by pipetting up and down	
Opti-MEM™ (Thermo Fisher Scientific)	4.75 µl	23.75 µl
Lipofectamine® 3000 Reagent (Thermo Fisher Scientific)	0.25 µl	1.25 µl
	Mix serval times by pipetting up and down	

DNA solution and the Lipofectamine® solution had to be mixed in the following step by pipetting up and down. This mixture is incubated for 10-15 min at RT. Afterwards, the DNA-Lipofectamine® complex is added into the appropriated well.

In the next step cells are seeded with a density of $2x10^4$/well (96 well) or $1x10^5$/well (24 well) an incubated for 48h in the transfection mixture in an incubator at 37°C with 5% CO_2.

2.1.11Transfection of cells using electroporation

Since with other transfections methods only a small number of cells (20-30%) are transfected, a different transfection method was used. Electroporation is a method of making cell membranes temporarily permeable in order to introduce DNA into cells. An electrical field, which is usually generated as a short pulse by the discharge current of a capacitor, permeabilizes the cell membrane of cells in the capacitor due to various effects.

To electroporate cells, the cells are diluted in PBS with a cells number of $2x10^6$ cells/ml. Afterwards, $1x10^6$ cells are transfected in a 4mm electroporation cuvette with 10 µg DNA with a specific voltage and capacitance shown in the table underneath (Table 3). To the approximated transfection volume of 500µl another 500µl normal cell culture media is added after transfection. The required amount of cells are plated in the needed size of cell culture plate. The cells are incubated at 37°C with 5% CO_2 in an incubator and after 24h the media should be exchanged to wanted cell culture media.

Table 3: Electroporation conditions.

Name	Voltage [V]	Capacitance [µF]
PC12	250	950
1321N1	300	1000

2.2.12 Analysis of PC12 cells differentiation using different inhibitors

Pharmacological inhibitors are factors which can prevent a substance to bind to the target protein. Most of the inhibitor reactions are reversible. Two types of inhibitions are known: The competitive inhibition is when the inhibitor competes with the substrate. The second one is the allosterically inhibition where the inhibitor changes the molecular structure of the protein, so that the substrate can no longer be bound. Signal transduction inhibitors are inhibitors which are able to interfere with or inhibit important cellular signal transduction pathways. Signal transduction refers to the biochemical transfer of information or information from the cell membrane into the cell interior, or from one cell compartment to another. Different inhibitors for signaling cascades were analyzed in this thesis (Table 4).

Table 4: Used inhibitors.

Inhibitor name	Target	Concentration	Producer
PD98059	MAPK	40 mM in DMSO	Sigma
U0126	Erk1/2	50 µM in DMSO	Sigma
LY294002	PI3K	50 mM in DMSO	Sigma
k252a	TrkA	50 µM in DMSO	Sigma
Bisindolylmaleimide I	PLCγ	2.4 mM in DMSO	Merck

PC12 cells are seeded at the appropriated density and incubated for 24h at 37°C with 5% CO_2 to plate the cells. 1h before NGF or the conditioned media is added they are preincubated with the described concentration. NGF or the conditioned media is added with the addition of the different inhibitors. Cells are incubated for 48h and afterwards documented with a bright field microscope. The amount of differentiated cells as well as the neurite length is analyzed using FIJI. A differentiated cell is defined by neurites longer than the cells diameter. For the amount of differentiated cells, the number of differentiated cells in percent is calculated from each picture contain around 100 cells. The neurite length is quantified by measuring of 10 neurites of each picture. The ANOVA test is done using GraphPad Prism.

2.2.13 Experiment to analyze different signaling cascades

Signaling cascades are processes which is coupled normally with multiple different transcription factors which are activating or downregulating the activity. Substances which are presented to the cells are activating or inactivating different signaling cascades. To analyze the effect, an assay to quantify the activity of different signaling cascades have to be established.

Therefore, 1321N1 astrocytoma cells are reverse transfected with Lipofectamine®. The transfection mix will be shown in the following:

Opti-MEM™	49.4 µl
P3000	0.2 µl
Renilla Standard [0.1 µg/ml]	3.9 µl
Firefly construct [0.1 µg/ml]	9.1 µl

The DNA dilution is mixed with the Lipofectamine® dilution:

Opti-MEM™	61.75 µl
Lipofectamine®	3.25 µl

The mixture is afterwards given in 96 well plate with 10µl each on 12 wells.

To analyzed different signaling cascades a standard transfection with a standard renilla luciferase cotransfected with a standard firefly luciferase had to be done every assay, to get a standard for all independent experiments. The standard is set for each experiment to 1. All different transfections (for the standard or for the different signaling cascades) are incubated after transfection for 48h for another 24h with serum-reduced media (control) or with ethanol

(0.5%) or erinacine C (5µg/ml; 0.5% ethanol) in addition. After the 24h of incubation the luciferase activity is measured.

For the cotransfection experiments the firefly luciferase construct is used with only 1:2 or 1:5 amount and filled up for normal incubation with a vehicle plasmid or with the different ETS variant constructs.

2.2.14 Measurement of the luciferase activity

Luciferases are structurally different enzymes, through the catalytic activity of which luciferins react with oxygen to form high-energy, unstable dioxetanes or dioxetanones. The decomposition of these substances leads to bioluminescence and can be measured.

To analyze the activity of luciferase the PJK System is used. After the incubation time, the cells are lysated with 25µl of a passive lysis puffer, which has to be diluted firstly 1:1 with water. The cells are incubated with lysis buffer for 15 min. After the cells are detached, which can be improved by freezing at -20°C for 5-10 min. During this time the Beetle Juice® which was prepared regarding the constructor protocol and the Renilla juice® which was also prepared by that, with additionally set the buffer pH to 5.0, are heated up to 37°C. The lysate is afterwards transferred to a white 96 well plate (Tecan). With the Beetle juice® the firefly luciferase is measured and with the Renilla juice® the renilla luciferase can be analyzed. When the juices are heated up, 50µl first of the Beetle juice® and after measurement from the Renilla juice® is added and mixed to the lysate in the 96 well plate.

2.2.15 Calculation for the results from the luciferase assay

The standard, which is performed in all experiments, was set to 1, to standardize every experiment. The background level is characterized by two different firefly constructs, the Gal4 construct and the LexA construct. The Gal4 level is for every experiment subtracted from the measured luciferase activity from the different signaling cascades.

For the cotransfection experiments the Gal4 background is also cotransfected with the different ETS variants as the same values and each was subtracted from the respected firefly luciferase activity of the signaling cascades.

2.2.16 *In vitro* model of the blood-brain barrier

The blood-brain barrier consists of three different cell types: pericytes, astrocytes and endothelial cells. To build a strong blood-brain barrier in vitro, the different cell types have to be co-cultivated in the right order.

The complete experiment is done by Verena Ledwig in the institute of pharmaceutical technology of the Technical University of Braunschweig under the control of Prof. Dr. Stephan Reichl. To establish the co-culture the different cell types are isolated from porcine primary cell culture and cultivated to get purity. The purity is checked with specific markers for the different cell types: Endothelial cells are marked with the Van-Willebrand-factor. Pericytes can be specifically marked with alpha-smooth muscle actin and the astrocytes can be analyzed with GFAP (glial fibrillary acid protein).

For the triple culture the different nearly pure cell types are co-cultivated on 12 well inserts, as shown in Figure 4. The cells are incubated in a culture media (developed by Verena Ledwig) at 37°C with 5%CO_2 for three days. After that the permeabilization is performed. Before the permeabilization is done, the media above and underneath the border is exchanged by Krebs-Ringer Buffer (KRB). The cells are incubated for another 30 min at 37°C with 5% CO_2. After that, the permeabilization is done. Therefore, the KRB solution above and underneath the border is removed. Firstly, 1500 µl of the acceptor solution is added underneath the border, followed by addition of 500 µl of the donator solution containing 10µg/ml erinacine C in DMSO is added above. This is done for analysis of the apical to basolateral diffusion. For the basolateral to apical diffusion the experimental design was done by adding, firstly, the donor solution containing erinacine C underneath and afterwards addition of the donor solution above. The cells are incubated at 37°C with 5% CO_2. After 30, 90, 150, 210, 270 and 330 minutes of incubation 500µl of the acceptor solution is removed and the amount of erinacine C is measured using HPLC. The removed media is displaced by new 500 µl of the KRB solution.

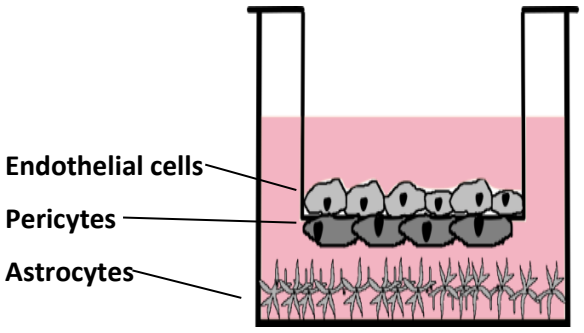

Figure 4: Schematic drawing of the triple culture for analysis of the ability to cross the blood-brain barrier *in vitro*.

Krebs-Ringer Buffer

NaCl	6.8 g
NaH_2PO_4 x H_2O	0.14 g
$NaHCO_3$	2.1 g
D-Glucosemonohydrate	1.1 g
$CaCl_2$ x $6H_2O$	0.26 g
HEPES	3.575 g
KCl	0.4 g
$MgSO_4$ x $7H_2O$	0.2 g

fill up with ddH_2O to 1000 ml.

For the analysis of the P-gp efflux transporter the inhibitor, Verapamil (Sigma; 200µM), is added 30 min before starting the permeabilization experiment.

2.3 Molecular biological methods

2.3.1 RNA Isolation from 1321N1 cells using peqGOLD RNAPure

Obtaining high-quality RNA is the first and the most critical step in performing many molecular techniques such as reverse transcription PCR, transcriptome analysis using next-generation sequencing, array analysis and cDNA library construction. Most RNA isolation procedures take place in the presence of RNase inhibitory agents. During this process, the sample is homogenized in a phenol-containing solution and separated after centrifugation step into three phases: a lower organic phase, a middle phase containing denatured proteins and genomic DNA, and an upper aqueous phase that contains RNA. The upper aqueous phase is recovered, and RNA is collected by alcohol precipitation and rehydration.

For isolation of total mRNA from astrocytoma cells incubated with the different substances 1321N1 cells are seeded at a density of $1x10^5$ cells / 3.5 cm cell culture dish and incubated for 24h at 37°C with 5% CO_2 in an incubator. After that cells are incubated for another 24h in serum-reduced media following by the incubation for the estimated time with the different compound.

For 3.5 cm dish 1 ml peqGOLD RNAPure is used. peqGOLD RNAPure is a reagent required for extraction of total RNA. By pipetting up and down the cells were homogenized in the reagent and then incubated for 5 minutes at room temperature. In the following step 200 µl of

chloroform is added to separate the phases and the solution is mixed vigorously. After this step the samples are incubated for 10 minutes on ice and centrifuged for 5 minutes at 12,000 rpm. Three phases were visible: The interphase and the lower phenol phase contain proteins and genomic DNA. The isolated RNA was present in the upper aqueous phase. This phase is transferred into a new reaction tube by using a pipette. The RNA is precipitated by adding the same volume of isopropanol and the mixture is incubated for 15 minutes at 4°C. Subsequently, the suspension is centrifuged at 4°C for 15 minutes at 12,000 rpm. Then the precipitate is washed twice with 1 ml 70% ethanol (trough centrifugation 10 min at 12,000 rpm). The last step involved drying of the RNA pellet at RT for 5 minutes and dissolving in 50 µl RNase-free water. The concentration is measured photometrically and the quality is analyzed by gelelectrophoresis.

2.3.2 Photometric determination of DNA/RNA concentration

To determine the concentration of recovered or purified DNA/RNA the corresponding sample is measured using an UV photometer. Usually 1:50 or 1:100 dilutions of nucleic acids are measured using the photometer at wavelengths of 230 nm, 260 nm and 280 nm. DNA absorbs light of a wavelength of 260 nm, the other two values determine protein impurities (280 nm) or RNA contaminations (230 nm).

$$DNA\ \left[\frac{\mu g}{\mu l}\right] = \frac{OD260 \cdot delution\ factor\ \cdot\ \vartheta}{1000\ \mu l}$$

ϑ – Conversion factor (DNA: 50; RNA: 40)

The purity of DNA/RNA was calculated from the ration of OD260 and OD280, wherein the value of 1.8 indicates a pure DNA (Sambrook and Russell, 2001).

$$Purity = \frac{OD260}{OD280}$$

2.3.3 Electrophoretic separation of DNA/ RNA fragments in agarose gels

To analyze DNA, newly synthesized RNA by size or to determine the concentration of DNA/RNA the horizontal gel electrophoresis is used. Principle of the method is a separation of DNA/RNA in an electrical field based on their size. DNA/RNA is separated by moving through

an immobilized matrix (agarose) with certain pore size by reason of their negatively charge in an electric field. DNA or RNA samples in *GelLoading Dye Purple (6x)* are placed in the loading wells of the agarose gel. Then the fragments are separated according to their size, with smaller fragments running faster than larger. The separation of the fragments is adjusted to the concentration of the agarose gel. Normally 1% agarose is used for analyzing DNA/RNA with a size of 500 bp to 6 kbp. After electrophoretic separation the agarose gel is placed in an ethidium bromide bath (0.05%) and incubated for 15 min. Ethidium bromide is intercalating between bases of nucleic acids and allows detection of nucleic acids under UV light.

2.3.4 Synthesis of cDNA using AMV reverse transcriptase

For preparation of cDNA, the isolated RNA is transcribed with viral reverse transcriptase to produce a double stranded DNA. Oligo dT primer, which hybridize to the poly A tail of RNA is used to start the transcription reaction.

The following solutions were mixed for the reaction:

1 µl	Oligo dT primer [50 µM]
2 µg	Total RNA
x µl	RNase-free water
10 µl	∑

The mixture is incubated for 5 minutes at 70°C to split the double strands and secondary structures and in the following incubated for 10 minutes on ice to allow the attachment of the primer to the RNA.

The following substances are added to the premix:

5 µl	AMV reaction Buffer (5x)
2 µl	dNTP mix [10 mM]
1 µl	RNase inhibitor *Ribolock* [40 U/µl]
1 µl	DTT [100 mM]
4 µl	RNase-free water
1 µl	*AMV Reverse Transcriptase* [10 U/µl]
25 µl	∑

The entire reaction mix is incubated for 1 hour at 42°C in a water bath and then an aliquot is analyzed on a 1% agarose gel. The successful cDNA synthesis is reviewed by a polymerase

chain reaction (PCR) for detecting β-actin to analyze the cDNA synthesis efficiency, and to adjust the concentration of different synthesis reaction. GAPDH is an ubiquitous expressed gene and therefore can be used to compare the concentration. The cDNA is stored at -20°C. After this procedure, the cDNA is used for a semi-quantitative PCR reaction.

2.3.5 Control of cDNA synthesis by a *gapdh* PCR reaction

The semi-quantitative *gapdh* PCR is used to compare the concentration of different samples. Specific primers for *gapdh* are used for the PCR to hybridize complementary cDNA. The quality and efficiency of the reverse transcription can be determined with this method.

The following substances are mixed for this reaction:

2 µl	cDNA
0.1 µl	Primer I (mGAPDH up; [100 µM])
0.1 µl	Primer II (mGAPDH low; [100 µM])
0.5 µl	dNTP mix [10 mM]
5 µl	Go Taq Buffer (5x)
1 µl	cDNA
0.2 µl	Go Taq polymerase [100 U/µl]
17.1 µl	RNase-free water
25 µl	∑

Substances are mixed in a PCR tube and amplified in a *Thermocycler* by using the following program:

PCR program

95°C	2 min	
95°C	30 sec	⎫
60°C	30 sec	⎬ 20 cycles
72°C	45 sec	⎭
72°C	5 min	
16°C	∞	

After the amplification, the synthesized product is analyzed on a 1% agarose gel. The expected PCR product had a size of 451 bp.

2.3.6 Reverse Transcriptase PCR for *ngf, bdnf* and *ets1*

Substances isolated from medical fungi are suspected to alter neurotrophin production. Two of these neurotrophins are analyzed in this thesis (NGF and BDNF). To quantify the mRNA level of *ngf* and *bdnf,* a PCR for this mRNA should be done, using specific primer, as well as for *ets1* mRNA

The following substances are mixed for this reaction:

2 µl	cDNA
0.1 µl	Primer I (hNGF sense/ hBDNF sense/ ETS sense; [100 µM])
0.1 µl	Primer II (hNGF antisense/ hBDNF antisense/ ETS antisense; [100 µM])
0.5 µl	dNTP mix [10 mM]
5 µl	Go Taq Buffer (5x)
1 µl	cDNA
0.2 µl	Go Taq polymerase [100 U/µl]
17.1 µl	RNase-free water
25 µl	∑

Substances are mixed in a PCR tube and amplified in a Thermocycler by using the following program:

PCR program for *ngf*

95°C	2 min	
95°C	30 sec	⎫
61°C	30 sec	⎬ 30 cycles
72°C	30 sec	⎭
72°C	5 min	
16°C	∞	

PCR program for *bdnf*

95°C	2 min	
95°C	30 sec	30 cycles
58°C	30 sec	
72°C	30 sec	
72°C	5 min	
16°C	∞	

PCR program for *ets1*

95°C	2 min	
95°C	30 sec	30 cycles
58°C	30 sec	
72°C	30 sec	
72°C	5 min	
16°C	∞	

After the amplification, the synthesized product is analyzed on a 2% agarose gel. The expected PCR product for *ngf* had a size of 189 bp and for *bdnf* 101 bp and for *ets1* 370 bp.

2.4 Zebrafish methods

2.4.1 Maintenance and crossing of zebrafish

The breeding and maintenance of zebrafish took place in an approved fish room where the temperature in the chamber is adapted to the ambient temperature of the natural habitat of Danio rerio and is obtained at constantly 28°C. Also, a day-night-cycle is generated by a time-controlled room lighting. For production of embryos, a couple of wild type fish (Brass, AB or TLF) or transgenic lines (*trkA*:mClover, *ca8*:RFP) is placed in crossing tanks. At the beginning, they are isolated by gender using a separation slide in the middle. Furthermore, a mesh-like ground is used to separate eggs from the parents, so that the parental fishes cannot eat them up. The date of ovulation is timed precisely by removing the separation slide. During the next half hour, eggs are laid and can be collected with a sieve. Eggs are cleaned with special water and transferred into petri dishes containing 30% Danieau. Embryos are incubated for several hours

or up to the required days in an incubator. To protect from pigmentation fishes can be treated with 0.03% phenylthiourea (PTU) in 30% Danieau (Westerfield, 1993) starting at 24 hpf.

30% Danieau

300% Danieau 100ml
fill up to 1000 ml with deionized H_2O

300% Danieau

2.9 M NaCl	60 mL
70 mM KCl	30 mL
40 mM $MgSO_4$	30 mL
60 mM $Ca(NO3)_2$	30 mL
0.5 M HEPES (pH 7.2)	30 mL

fill up to 1000 ml with deionized H_2O

0.03% PTU in 30% Danieau

PTU 3g
add 1 l 30% Danieau.

2.4.2 *In vivo* blood-brain barrier model

After crossing of wildtype zebrafish (Brass), zebrafish larvae are maintained and grown up until the required developmental stages (4dpf, 7dpf, 10dpf) is reached. After the time point is attained the fishes are incubated with erinacine C with a concentration of 5µg/ml in 0.5% ethanol, or with 0.5% ethanol alone. The media is renewed every day. The fishes are feeded every day starting at 7dpf with *Paramecium*. After 24h, 48h or 72h of incubation at least 50 fishes are cooled down in ice for 10min and afterwards washed ten times with ice cooled Washing media. The first and last Washing Media is kept for further analysis after washing. After the last washing step, the fishes are transferred into 4%PFA/PBST in a 3 cm petri dish and incubated for 10 min at room temperature. After incubation the brains are isolated under a dissection microscope with e dissection pin and forceps. The isolated brains are transferred into a 2 ml Eppendorf tube and together with the Washing media stored at -80°C until transportation to the Helmholtz Centre of Infection research, where the following steps are done by Dr. Kathrin Wittstein.

The aqueous solutions of the Washing Media samples are concentrated at 39° C in a stream of nitrogen. Thereafter, the residues of the washing samples and the selected brains are taken up in 1 ml of methanol and extracted for 35 minutes in an ultrasonic bath. After centrifuging the samples (5 min, 10,000 rpm), the supernatants are removed, and the solvent evaporated at 39 ° C in a stream of nitrogen. The residues thus obtained are dissolved in 70 µl of methanol and analyzed by HPLC-UV / Vis and HPLC-ESI-MS.

The content determinations are carried out by HPLC-UV / Vis on an Agilent 1260 Infinity System with diode array detector and a Waters Acquity UPLC BEH C18 column (2.1 × 50 mm, 1.7 µm). Eluent A: H_2O + 0.1% formic acid, eluent B: acetonitrile + 0.1% formic acid; Gradient 1: 5% B for 0.5 min, increasing to 100% B in 19.5 min, isocratic 100% B for 5 min; Gradient 2: 40% B for 4 min, increasing to 60% B in 16 min, increasing to 100% B in 5 min, isocratic 100% B for 5 min; Flow rate = 0.6 mL min-1, UV detection at 200-600 nm. For the HPLC-ESI-MS data, a Dionex Ultimate 3000 system with coupled ion trap mass spectrometer amaZon speed from Bruker is used. The same running conditions and analytical column as on the Agilent 1260 Infinity System are chosen. The ESI-MS spectra are recorded alternately in positive and negative ionization. The chemicals and solvents used are obtained from AppliChem GmbH, Avantor Performance Materials, Carl Roth GmbH & Co. KG and Merck KGaA in analytical and HPLC purity grade.

Washing media

Methanol 10%
in 30% Danieau.
keep on ice until usage.

4% PFA/PBST

Paraformaldahyde	40 g
10 x PBS	100 ml
Tween20	100 ml

fill up with ddH_2O to 1000 ml.

Paraformaldehyde and water are mixed at max. 60°C, additionally 4M NaOH (sodium hydroxide) can be added, to clear the solution. The solution was filtered afterwards. Set the pH to 7 – 7.5. If the pH was too low, it can be set by using H_3PO_4 (phosphoric acid). Afterwards add PBS and Tween20. Aliquots can be maintained at -20°C.

10 x PBS

Potassium chloride	0.2 g
Potassium dihydrogen phosphate	0.2 g
Sodium chloride	8 g
Sodium hydrogen phosphate	1.15 g

add ddH2O to 1 l

autoclave

2.4.3 Isolation and Fixation of an adult zebrafish brain

Adult zebrafish are maintained as described before in a special room at 28.5°C. To isolate the brain, the fishes are anesthetized with Tricaine and cooled down on ice and afterwards decapitated. To isolate the brain the tissue from the bottom, like the gills, had to be removed. Afterwards, the bone over the brain would be broken by two forceps taking care, to not destroy the brain. Following, the brain could take out easily by careful pulling at the nerve of the eyes. The eyes are removed afterwards, and the brain was transferred into ice cold 4%PFA/PBS and incubated over night at 4°C.

2.4.4 Sectioning of the adult zebrafish brain with a vibratome

After fixation the brains are washed several times with PBS on a shaker. To remove the water one brain is transferred into a 2ml Eppendorf tube with 1% low melting agarose (Pronadisa) in PBS and incubated at 37°C for 30min. Afterwards, the brain are transferred in a special embedding mold and the low melting agarose is removed and directly exchanged by 3% Agarose in PBS. The orientation has to be directly after adding of the 3% agarose since it colds down very fast and by that it gets hard. After alignment of the brain, the agarose block had to be cold down completely at room temperature and afterwards for at least 5 min at 4°C.

At the same time, the vibratome (Leica VT1000S vibratome) is prepared. The object box is filled with PBS and the blade is installed. The brain in the agarose block is orientated to cut from the anterior to posterior in sagittal orientation. Section of 50µm are done and dried on a superfrost slide at 40°C.

4%PFA/PBS

Paraformaldahyde 40 g
10 x PBS 100 ml
fill up with ddH_2O to 1000 ml.

Paraformaldehyde and water are mixed at max. 60°C, additionally 4M NaOH (sodium hydroxide) was added, to clear the solution. The solution is filtered afterwards. Set the pH to 7 – 7.5. If the pH was too low, it can be set by using H_3PO_4 (phosphoric acid). Afterwards PBS is added. Aliquots was maintained at -20°C.

10 x PBS

Potassium chloride	0.2 g
Potassium dihydrogen phosphate	0.2 g
Sodium chloride	8 g
Sodium hydrogen phosphate	1.15 g

add dH2O to 1 l
autoclave

PBS

10 x PBS 100 ml
add dH2O to 1 l

2.4.5 Fluorescence *in situ* hybridization of vibratome slides

After vibratome sectioning the sagittal sections are transferred in a chamber full with PBS and was maintained for several days at 4°C.

Day 1

The sections are washed at least 10 min with PBST at room temperature. Afterwards, the slides are laid horizontal with the section on the top and incubated for 35 min in 6% H_2O_2 in PBST with a parafilm on the top. To remove the H_2O_2 the slides are washed in a chamber for 10 min with PBST. The permeabilize section the slides are treated for 10min 0.5% TritonX100/PBST (parafilm) and followed by a washing step for 10 min with PBST (chamber). The block unspecific RNA bindings the sections were prehybridize with Prehybridization buffer 68°C in

an oven for at least 1h (Parafilm). The hybridization is done with 100ng/ml RNA probe for NGF or TrkA in Hybridization buffer ON 68°C (Parafilm).

Day 2

The parafilm is removed and the slides were washed for 15 min in prewarmed 2 x SSC pH 4.5 at 68°C (chamber) followed by two times washing for 30min in prewarmed 0,2 x SSC pH 4.5 at 68°C (chamber). Afterwards, the slides are cooled down to room temperature.

The sections are washed for 10 min in PBST (chamber) and equilibrated for 10min Maleic acid buffer (chamber). To block unspecific bindings the sections are incubated in 1xBM blocking reagent/Maleic acid buffer at least for 1h (Parafilm). The antibody reaction is done with anti Dig-POD at a concentration of 1:300 in 1 x BM blocking reagent/Maleic acid buffer (Parafilm) at 4°C overnight.

Day 3

The unbound antibody is washed away by washing 6 times for 20min with PBST (chamber). The first fluorescence reaction is done in the following mixture:

FITC-tyramide	5 µl
0.3% H_2O_2	10 µl
50% dextran sulfate/H_2O	40 µl
PBST	945 µl

Add the reaction mix to the slides (1ml per sample) and incubate for 30–40min in the dark without agitation. Protect the FITC fluorophore from light during and after the reaction. Afterwards, the leftover of the reaction mix is washed away by washing two times with PBST for 5min (chamber) and 3 times for 20min (chamber).With this fluorescence reaction a green fluorescence can be created another mixture has to be used, when the fluorescence should be red:

TAMRA-tyramide	4 µl
0.3% H_2O_2	10 µl
50% dextran sulfate/H_2O	40 µl
PBST	946 µl

The samples should be protected from light. An antibody reaction or DAPI staining can be done afterwards.

PBST

20% Tween20	1 ml

add 1 x PBS to 200 ml

20%Tween20

100%Tween20	10 ml

add sterile dH_2O to 50 ml

keep in the dark

6% H_2O_2 in PBST

30% H_2O_2	2 ml

add PBST to 10 ml

keep in the dark

0.5% TritonX100/PBST

10% TritonX100	500 µl

add PBST to 10ml

10%TritonX100

100%TritonX100	5 ml

add sterile ddH_2O to 50ml

keep in the dark

Prehybridization buffer

Formamide	25ml
20X SSC pH 4.5	12.5ml
1M citric acid	640µl
50mg/ml heparin	50µl
yeast tRNA	500µl
20%Tween 20	250µl

Fill up with dH2O to 50ml. The solution can be kept at -20°C for several month.

20 x SSC pH 4.5

Sodium chloride	175.3 g
Sodium citrate	88.2 g

set the pH to 4.5 with 1 M Citric acid

add dH2O to 1 l

autoclave

1M citric acid

Citric acid	105.07 g

add dH2O to 500 ml

50mg/ml heparin

50 mg dissolved in 1 ml DEPC water.

yeast tRNA

50 mg dissolved in 1 ml DEPC water.

Hybridization buffer

Formamide	25ml
SSC 20 x pH 4.5	12.5ml
50% dextran sulfate/H_2O	2.5ml
1M citric acid	640µl
50mg/ml heparin	50 µl
yeast tRNA	500µl
10%Tween 20	250 µl

Fill up with ddH2O to 50ml. The solution can be kept at -20°C for several month.

50% dextran sulfate/H_2O

Dextran sulfate	5 g
dd H_2O	10ml

Dissolve the dextran sulfate in H_2O overnight on a shaker at room temperature and store afterwards at 4°C.

2 x SSC pH 4.5

20 x SSC (4.5) 50 ml
add dH2O to 500 ml

0,2 x SSC pH 4.5

20 x SSC (4.5) 5 ml
add dH2O to 500 ml

Maleic acid buffer

Maleic acid 116.07 g
NaCl 87.66 g
Adjust to 1000ml with ddH_2O.

Dissolve the maleic acid and NaCl in 800ml of ddH2O. Afterwards add solid NaOH tablets to increase the pH. Autoclave stock solution and store at room temperature.

1 x BM blocking reagent/Maleic acid buffer

10 x BM blocking reagent 1ml
add Maleic acid buffer to 10ml.

10 x BM blocking reagent

BM blocking reagent 10 g
add Maleic acid buffer to 100ml. Autoclave and aliquot. The aliquots can be stored at -20°C.

0.3% H_2O_2

30% H_2O_2 100 µl
add dH_2O to 10 ml. Store in the dark.

2.4.6 Tyramide synthesis from protocol of Dr. Jakob von Trotha

The fluorophore esters 5-carboxyfluorescein succinimidyl ester (FITC; Thermo Scientific 46410) and 5-(and-6)-Carboxytetramethylrhodamine (TAMRA; Thermo Scientific C1171) are conjugated to tyramine hydrochloride (Sigma-Aldrich T2879) in a 1.1 times equimolar reaction (see below and Hopman et al.,1998; Lauter et al., 2011). The esters are very unstable and should

be protected from light, or better, dissolve them directly in Dimethylformamide (DMF; Sigma-Aldrich D4551) and use at once.

FITC–tyramide synthesis (adapted from L. Davidson)

FITC-DMF – Solution A:

FITC ester [10mg/ml]	100mg
Dimethylformamide (DMF)	10ml

DMF–TEA – Solution B

DMF	6ml
Triethylamine (TEA)	60 µl

Tyramine DMF–TEA – Solution C

Tyramine hydrochloride [10mg/ml]	50mg
DMF–TEA (Solution B)	5ml

End reaction

FITC-DMF (Solution A)	8ml
Tyramide DMF–TEA (Solution C)	2.74ml

The solution A and C should be mixed and incubated for 2 h in the dark at room temperature. Afterwards, 9.2 ml of absolute ethanol should be added to the synthesized tyramide–FITC conjugates to obtain 20ml of stock solution. The solution can be maintained as aliquots at -20°C. For reaction the mixture should be diluted 1 : 200.

TAMRA–tyramide synthesis (adapted from Lauter *et al*. (2011) and P.Affaticati)

TAMRA-DMF – Solution A3

TAMRA ester [10mg/ml]	25mg
Dimethylformamide (DMF)	2.5ml

DMF–TEA – Solution B

DMF	6ml
Triethylamine (TEA)	60 µl

Tyramine DMF–TEA – Solution C

Tyramine hydrochloride [10mg/ml]	50mg
DMF–TEA (Solution B)	5ml

End reaction

TAMRA-DMF (Solution A)	2.5ml
Tyramine DMF–TEA (Solution C)	762 µl

The solution A and C should be mixed and incubated for 2 h in the dark at room temperature. Afterwards, 21 ml of absolute ethanol should be added to the synthesized tyramide– TAMRA conjugates to obtain 24ml of stock solution. The solution can be maintained as aliquots at -20°C. For reaction the mixture should be diluted 1 : 250.

3. Results

With an aging population, neurodegenerative diseases, like Alzheimer's or Parkinson's diseases are getting more and more a severe problem. And a big problem for diseases like this is that there is no medication for them. In most cases only the symptoms can be treated but not the cause of the disease itself. Common in many neurodegenerative diseases is the death of neurons. Keeping in mind that small secreted polypeptides, called neurotrophins, was a possible medication, neurotrophins are known to have an influence on the survival and regeneration of neurons in the nervous system. By that they are important key regulator of the of the maintenance of this system. Unfortunately, the high molecular weight of this peptides does not enable them to cross the blood-brain barrier (BBB), a barrier to separate the blood system from the central nervous system. Smaller molecular weight molecules, which are able to cross the BBB and can have an influence on neurotrophins are getting more and more in the focus of research.

3.1 Secondary metabolites isolated from *Hericium* are able to induce PC12 cell differentiation

Medical mushrooms from the genus *Hericium*, which were known from traditional Chinese medicine as medication against gastric and respiratory problems, nervous disorders, high cholesterol, cancer and a weak immune system, are discussed frequently in research (Thongbai *et al*., 2015). Recent publications show that compounds isolated from different *Hericium* species contain highly bioactive compounds that could work as antibiotics, but also as stimulators of neurotrophin expression (Wang *et al*., 2019).

The present thesis was aimed at the isolation and characterization of new metabolites from both cultures and basidiomes of *Hericium* species. The first study deals with some new meroterenoids that were obtained from *H. coralloides.* The second study characterize cyathane diterpoids, called erinacines, isolated from cultures of the rare and unstudied species *H. alpestre* and *H. erinaceus*.

3.1.1 Corallocines are able to induce PC12 differentiation by stimulation of neurotrophin production in astrocytes

Corallocins are substances isolated from the fruiting body of *Hericium coralloides*. *H. coralloides* obtained its name from the coral-like shape of its fruiting body and this mushroom belongs to the family *Hericiaceae*. Three previously undescribed meroterpenoids were isolated

and purified from *H. coralloides* by Dr. Zeljka Rupcic and were further analyzed in this thesis. corallocin A has a benzofuranone structure, whereas corallocin B and C are isoindolinone derivatives (Fig. 5).

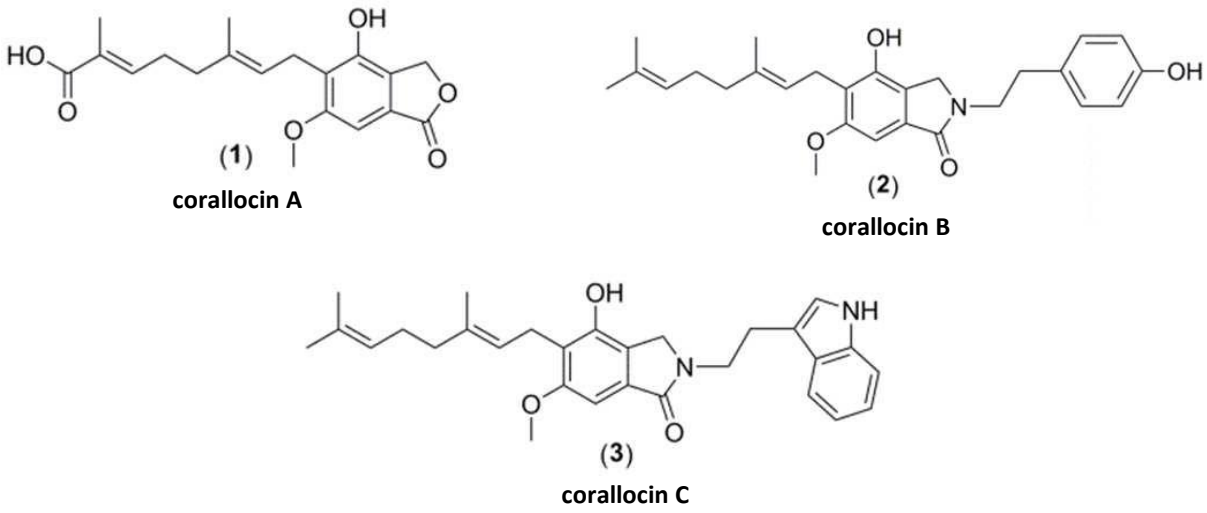

Figure 5: Structure of the isolated corallocins. The substances corallocin A-C were isolated from Hericium coralloides. By analysis with spectral methods the structure was characterized. (1) corallocin A shows a benzofuranone arrangement, whereas (2) corallocin B and (3) corallocin C can be classified as isoindolinone derivates.

Secondary metabolites isolated from different medicinal mushrooms are suggested to have an influence on the nervous system. In the nervous system neurotrophins, like NGF, have a major impact on neuronal survival as well as on neuroregeneration (Hennigan *et al*., 2007). To test if the isolated fungal metabolites exert a neurotrophin-like function in the nervous system directly on neuronal cells, pheochromocytoma derived from rat adrenal medulla (PC12) cells were used. PC12 cells are obtained from a rat adrenal medullary tumor. This cell type normally has a rounded shape but when NGF is contained in the media the cells produce neurites, which is a sign for differentiation of PC12 cells into neuron-like cells (Green and Tischler, 1976; Arsenijevic and Weiss, 1998; Sucher et al., 1993; Sugita et al., 1999; Tyson et al., 2003). The three pure substances isolated from *Hericium coralloides* were tested directly on PC12 cells to analyze if these compounds have a neurotrophin-like function on these cells (Figure 6). Before, the highest non-toxic concentration was characterized. Therefore, PC12 cells were seeded on a collagen-coated platen and incubated with increasing concentrations of the different substances and incubated for 48h. Dying cells normally detach and start to float in the middle of the plate. By that, the highest non-toxic concentration showing no floating cells was characterized. To analyze now if the compounds have direct neurotrophic function, the different substances were added in the highest not lethal concentration of 20 µg/ml for corallocin A, 30 µg/ml for corallocin B and 9 µg/ml for corallocin C, to the PC12 cells in serum-reduced media. Since serum contains normally growth factors, the amount of these factors should be as low as

possible causing the usage of serum-reduced media, containing only 1% fetal calf serum (FCS). The cells were incubated with the compounds for 48h, and after the incubation period the amount of differentiated cells and the neurite length was examined by brightfield microscopy. In Figure 6 the control, which was incubated with serum-reduced media, shows the normal rounded shape of PC12 cells (Figure 6, black arrow). When incubated with nerve growth factor (NGF) in the media the cells start to develop extensions called neurites (Figure 6, white arrow). Compared to the cell morphology of differentiation when incubated with NGF, none of the substances were able to induce neurite outgrowth directly from PC12 cells. This led to the conclusion that none of the tested corallocins are able to induce PC12 cell differentiation directly.

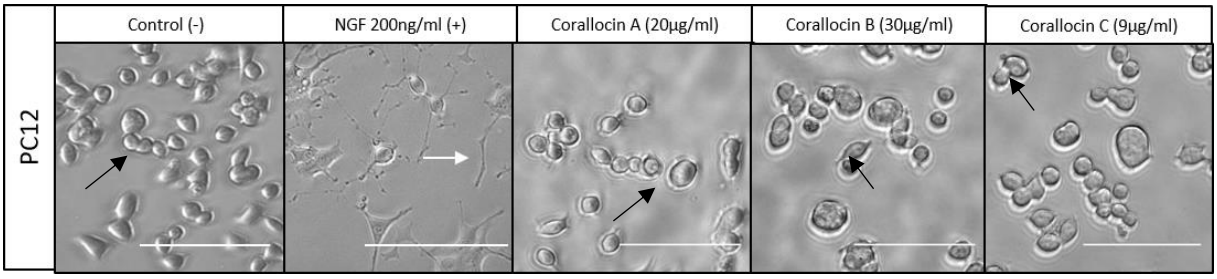

Figure 6: Differentiation of PC12 cells incubated directly with the different corallocins. (−) DMSO: negative control with DMSO; (+) NGF: positive control with 200 ng/ml human NGF. A nondifferentiated cell is marked with a black arrow, whereas a differentiated cell is marked with a white arrow. Scale bar 100 µm.

Since PC12 cells do not produce neurotrophins on their own, the next step was to characterize, if corallocins are able to induce neurotrophin expression in other cells of the nervous system. To evaluate this, a second cell line derived from a glial tumor was used as an astrocytic cell line to produce conditioned media. It was decided to use a glial cell line since in the brain glial cells support neurons. A human astrocytoma cell line was employed. After clarifying the not toxic concentration using astrocytic cell line, the media of these cells was supplemented with corallocins at the highest not toxic concentration solved in DMSO in serum-reduced media and the cells were allowed to condition the media for 48h. These conditioned supernatants were added to PC12 cells which were incubated for another 48h in these media. The results were shown in Figure 7. The control, which are PC12 cells incubated with normal serum-reduced media, showed the normal rounded silhouette of PC12 cells. When NGF is added to the serum-reduced media, the cells acquired long protrusions, called neurites. Neurites are also visible, when the media of corallocin A and C conditioned 1321N1 astrocytoma cells were used. Only corallocin B was not able to induce the production of neurites from PC12 cells. In conclusion, it was shown that two of three corallocins (A and C) are able to induce the differentiation of PC12 cells in the context of astroglial conditioned media (Figure 7).

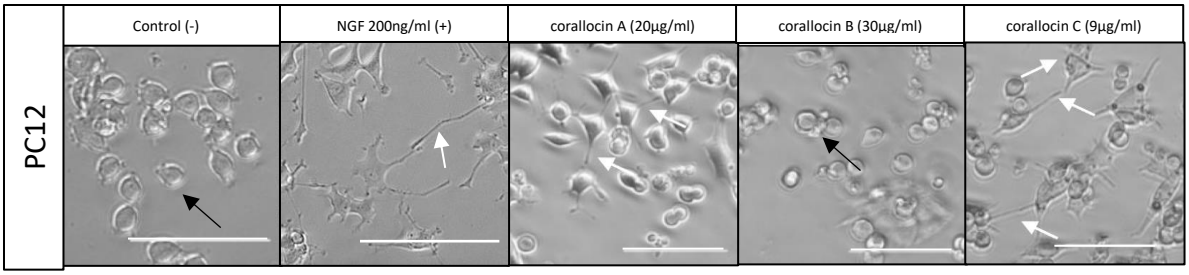

Figure 7: Differentiation of PC12 cells incubated with conditioned astroglial media incubated with the different corallocins. (−) DMSO: negative control conditioned media produced by 1321N1 incubated with DMSO; (+) NGF: positive control with 200 ng/ml human NGF. A nondifferentiated cell is marked with a black arrow, whereas a differentiated cell is marked with a white arrow. Scale bar 100 µm.

To quantify the obtained results, the amounts of differentiated cells and the neurite lengths were analyzed (Figure 8). Two negative controls were obtained: conditioned media from 1321N1 cells incubated with no additives and conditioned media from 1321N1 cells incubated with 1% DMSO. Both controls showed only a low number of differentiated cells of 1.2 ±0.1% and 2.1 ± 0.2% cells bearing neurites and an average neurite length of 10.2 ± 2.5 µm and 11.7 ± 2.7 µm was visible. In comparison to that is the positive control: human NGF (200 ng/ml). The number of differentiated cells of 35.2 ±2.5% as well as the neurite length with 71.2 ± 1.7 µm was significantly increased compared to the controls. The supernatant, of corallocin A and C treated 1321N1 astrocytoma cells, was also able to significantly increase the number of differentiated cells (to 23.2 ±5% and 30.7 ±4.8%) as well as the neurite length, to a length of 45.7 ± 2.3 µm and 51.3 ±2.5 µm. These values are weaker than the positive control, but clearly show a significant induction of differentiation and neurite outgrowth over non-treated controls. Only corallocin B conditioned astroglial media was not able to induce PC12 cell differentiation, which was visible in the number of differentiated cells (1.1 ±0.1%) as well as in the neurite length (11.9 ±2.2 µm; Figure 8).

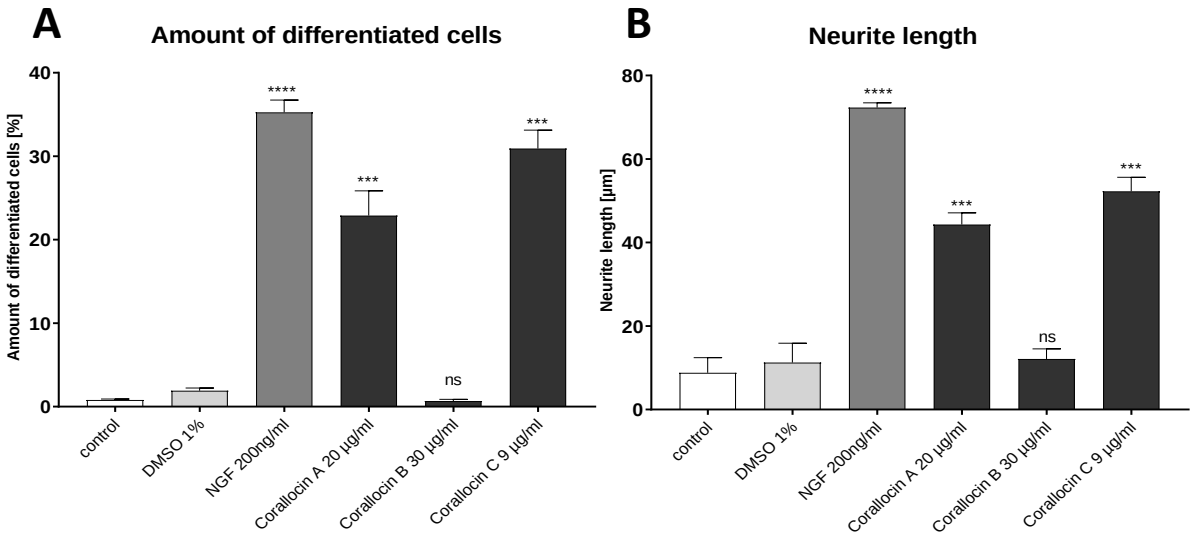

Figure 8: Quantification of the level of differentiation when incubated with conditioned media of the corallocins. A) Quantification was done by counting the amount of differentiated cells and is shown as a percentage. B) Quantification was done by analyzing neurite length and is given in µm. Control: conditioned media produced by 1321N1 without any additives. DMSO: conditioned media produced by 1321N1 incubated with 1% DMSO (solvent control). NGF: direct incubation of PC12 cells with human NGF (200 ng/ml). corallocin A-C: conditioned media produced by 1321N1 incubated with the different corallocins. (n = 4; ± SEM; One-way-Anova: *** $p \leq 0.001$; **** $p \leq 0.0001$)

It was shown that corallocin conditioned astrocytoma cell supernatants were able to stimulate PC12 cell differentiation. Nevertheless, so far, it is not known what is causing this differentiation. Yet, *Hericium* extracts are known to induce neurotrophin expression (Wang *et al*., 2019) and PC12 cells respond to the neurotrophin NGF with differentiation. Therefore, whole mRNA of astrocytes incubated for 6h with the different corallocins was isolated and a semi quantitative RT-PCR for *ngf* and *bdnf* expression was performed (Figure 9). Figure 9A shows the pictures of the agarose gel after RT-PCR against *gapdh*, *ngf* and *bdnf* was done. Expression of *gapdh* (Glyceraldehyde 3-phosphate dehydrogenase) was analyzed as a loading control, because this gene is a housekeeping gene being an enzyme involved in the catalyzation of glycolysis, expressed in equal amounts. Analyzing the results from *ngf* PCR in the control showing 1321N1 astrocytoma cells incubated for 6h with serum-reduced media, the amount of *ngf* mRNA is relatively low. When these cells were incubated with 1% DMSO in the serum-reduced media the expression of *ngf* mRNA was slightly increased. When incubated with the different corallocins the highest increase was visible for corallocin C, followed by corallocin A. corallocin B was also able to increase the amount of the *ngf* mRNA. Characterizing the results for *bdnf* mRNA, the control, as well as the DMSO treated cells, and the corallocin A treated cells show a similar amount of *bdnf* expression. Corallocin B and C were able to cause the increase of the *bdnf* mRNA. Again, corallocin C was the strongest inducer, increasing the amount of *bdnf* by about 4-fold compared to the other corallocins and about 40-fold over non-treated control. The results were quantified shown in Figure 9B and C. As demonstrated before

in Figure 9A the control shows a basal level of *ngf* mRNA, and this value was set to 1 ±0. The other results were shown as fold induction over control value. When the 1321N1 astrocytoma cells were incubated with DMSO the level of *ngf* expression increases up to 2.4 ±0.6 times compared to non-treated 1321N1 cells. When incubated with the different corallocins, all of them were able to significantly increase the *ngf* mRNA level. The highest inducer of *ngf* mRNA is corallocin C with an increase of 20.1 ± 3.7-fold, followed by corallocin A with an increase of 10.6 ±2.6 fold and corallocin B with 7.5 ±0.7. The *bdnf* level in the control cells are relatively low and was set to 1 ±0. When incubated with DMSO the amount of *bdnf* mRNA was increased until 2.6 ±0.6. Incubation with the different corallocins: corallocin A and B increased the amount of *bdnf* mRNA up to 10.2 ±2.7 and 12.4 ±1.5, respectively but this increase was statistically not significant. Strikingly, corallocin C is able to significantly increase the *bdnf* mRNA on the value of 41.3 ±8.9 on the transcriptional level. The results lead to the conclusion, that corallocin A and B are able to induce NGF expression. corallocin B is surprisingly able to induce NGF production, but despite the fact that *ngf* level PC12 cells did not show signs of differentiation, this suggest that there is a threshold of NGF, which needs to be overcome in order to trigger differentiation of PC12 cells, like it was suggested also by Mori and colleagues (2008). Corallocin C is able to induce transcriptional both neurotrophins, NGF and BDNF. In the PC12 cell differentiation assay the BDNF activity could not be analyzed, since PC12 cells do not express the responding receptor, TrkB (Squinto *et al*., 1991), which represents the high affinity receptor of BDNF.

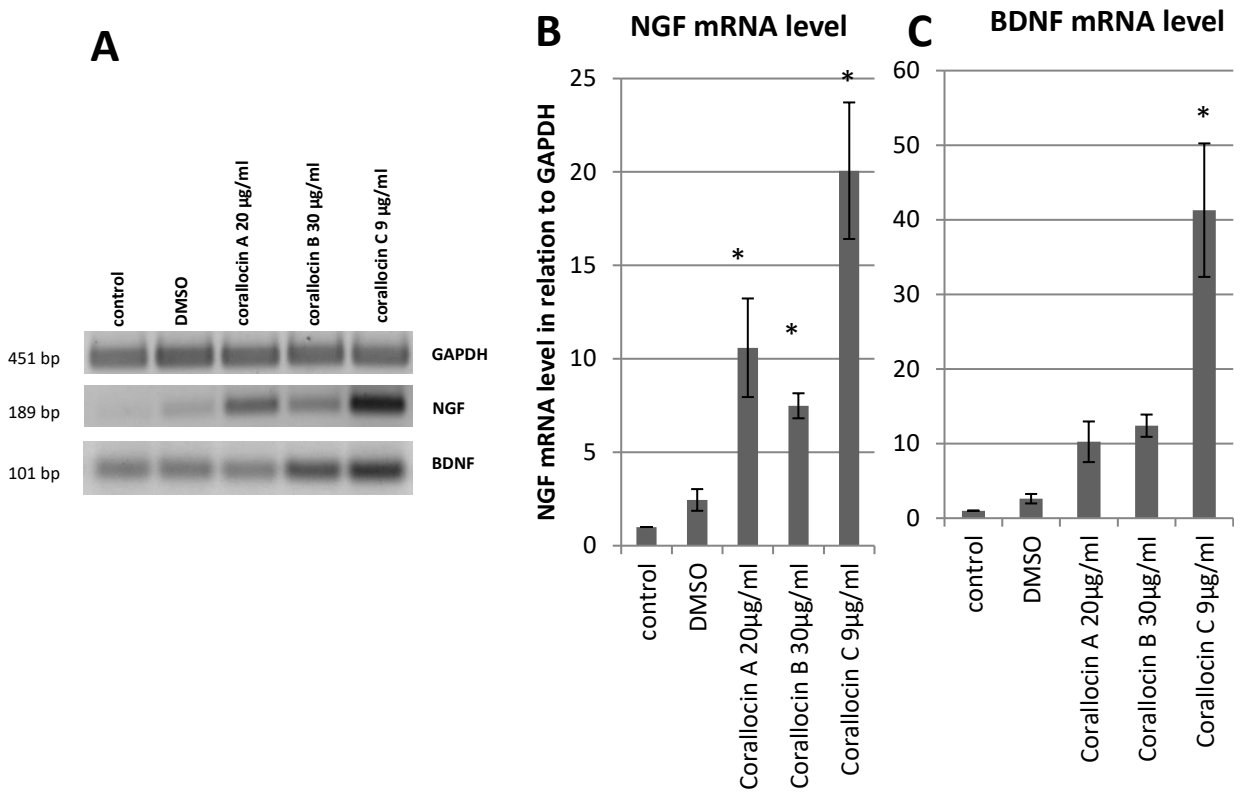

Figure 9: Analysis of the mRNA levels in astrocytes, when incubated with corallocins. A) Representative agarose gel picture of the semi quantitative RT-PCR. Control means astrocytoma cells incubated without any additive; DMSO – 1321N1 incubated with 1% DMSO; corallocin A-C – astrocytoma cells incubated with the different corallocins. *gapdh* was used as a loading control and to induce *ngf* and *bdnf* mRNA levels. The lower bands show the *ngf* and *bdnf* pattern, when astrocytes were incubated with the different additives. A quantification is shown in B) and C). (n = 3; ±SEM; t Test * $p \leq 0.05$)

Summarizing the results above, the corallocins are not able to induce PC12 cell differentiation directly. Yet, it was shown that two of these three compounds are able to induce differentiation after incubating 1321N1 astrocytoma cells with these cells allowing them to condition their media and subsequently adding their supernatant to PC12 cells. This shows that corallocins induce neurotrophin expression in glial but not in neural cells. corallocin A and C are able to induce differentiation of PC12 cells by inducing *ngf* expression. Also, corallocin B is able to induce NGF production, but it is unable to overcome the NGF threshold needed for initiating significant PC12 cell differentiation. In addition, corallocin C is able to induce BDNF production.

3.1.2 Erinacines are able to induce PC12 differentiation by stimulation of neurotrophin production in astrocytes

erinacines were isolated from the mycelia of *Hericium erinaceus* and *Hericium flagellum* by Dr. Kathrin Wittstein and Dr. Zeljka Rupcic. Structurally the erinacines belong to the group of cyathane diterpenoids. In this work seven pure of such cyathanes were analyzed and two of them were found to be new derivates (Figure 10, 1 and 2).

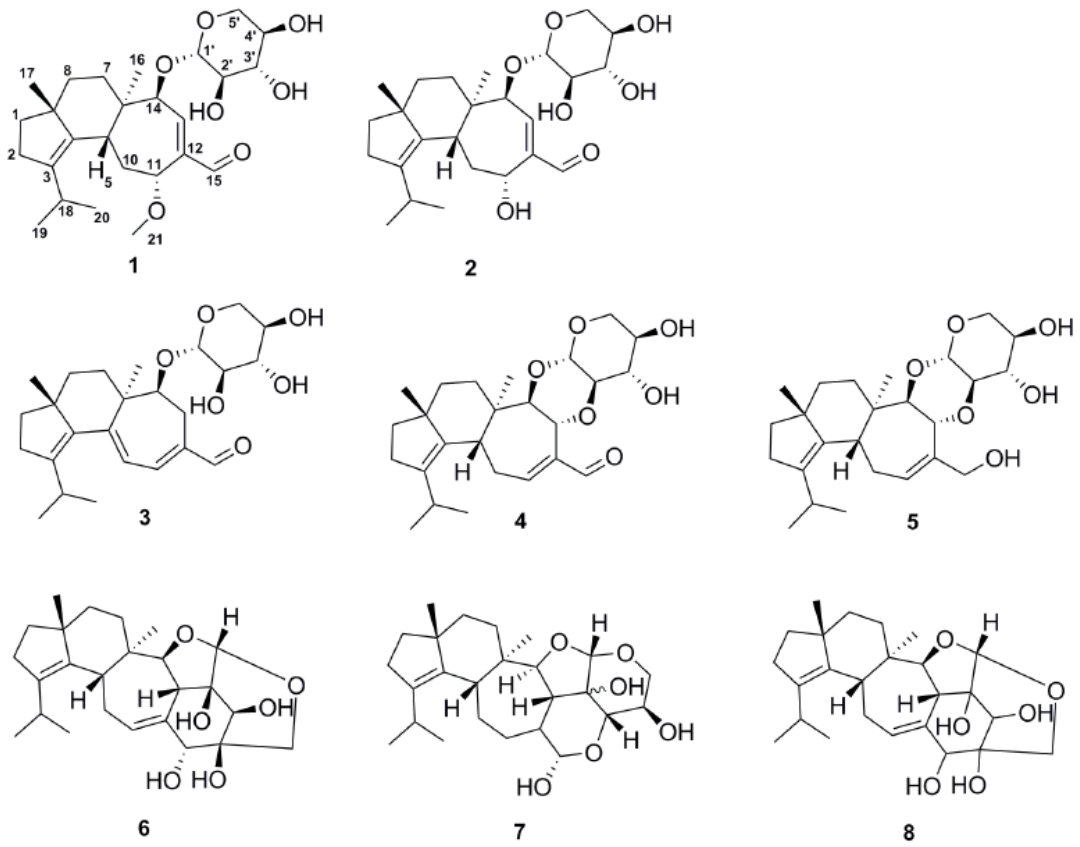

Figure 10: Structure of the isolated erinacines. (1) erinacine Z1; (2) erinacine Z2; (3) erinacine A; (4) erinacine B; (5) erinacine C; (6) erinacine E; (7) CJ14.258; (8) erinacine F. Erinacin Z1 can be only isolated from *Hericium erinaceus*, erinacine Z2, CJ14.258 and erinacine F can be only isolated from *Hericium flagellum* and erinacine A, B, C and E can be found in both *Hericium* species. All substances have the characteristics of diterpenoids.

These isolated erinacines were first analyzed for their direct neurotrophin-like effect on PC12 cells. Before starting the experiments, the highest non-toxic concentration was measured as described before. The different erinacines were added directly on PC12 cells with increasing concentration. When cells start to float the toxic concentration was reached and the highest non-toxic concentration was analyzed. To characterize if the erinacines had direct neurotrophic activity, the different erinacines were added in their highest nontoxic concentration (erinacine A 12 µg/ml, B 0.8 µg/ml, C 5 µg/ml, CJ14.258 1 µg/ml, erinacine E 10 µg/ml, Z1 1µg/ml and Z2 3 µg/ml) directly in serum-reduced media on PC12 cells and incubated for 48h. After the incubation time, the control cells, which were incubated in serum-reduced media showed a rounded shape (Figure 11) characteristic for undifferentiated PC12 cells, whereas the positive control, which were cells incubated with NGF (200 ng/ml) in the media, showed many membrane protrusions characterized as neurites – a typical sign for PC12 cell differentiation. As it was observed for the corallocins, all of the tested erinacines showed no neurite outgrowth effect on PC12 cells, suggesting that the erinacines have no direct differentiation effect on PC12 cells.

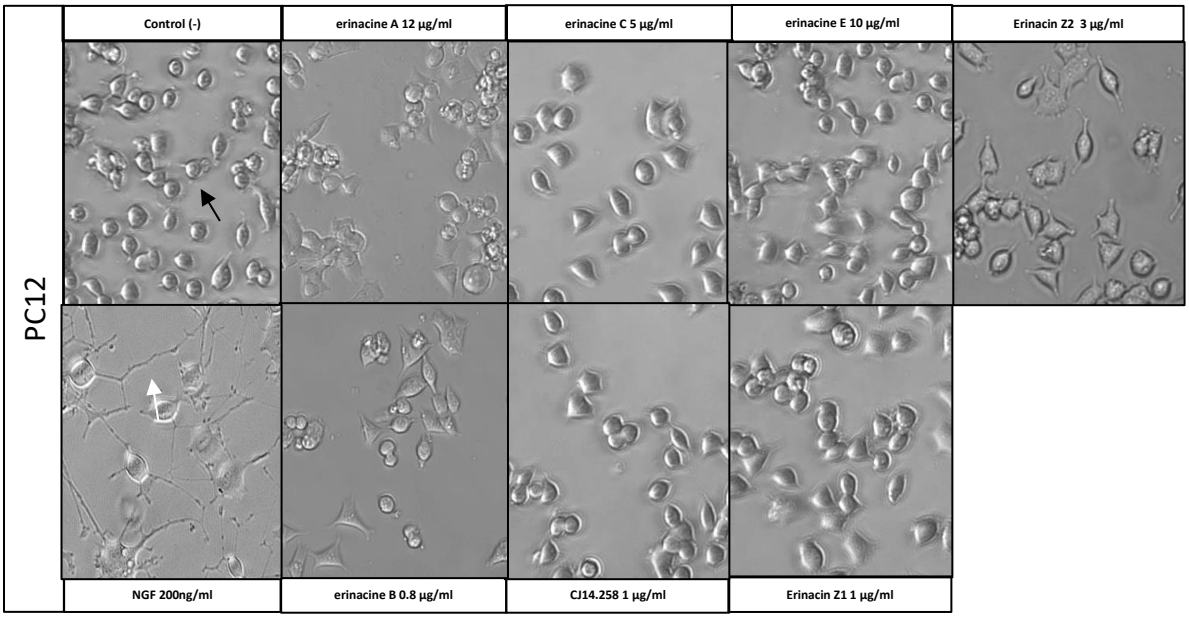

Figure 11: Differentiation of PC12 cells incubated with the different erinacines. (−) Ethanol: negative control with 0.5 %Ethanol; (+) NGF: positive control with 200 ng/ml human NGF. A nondifferentiated cell is marked with a black arrow and a differentiated cell with a white arrow.

Consequently, the erinacines were also tested for their neurotrophin producing effect using 1321N1 astrocytoma cells. Therefore, the astrocytoma cells were incubated with the different erinacines with their highest non-toxic concentration (measured before using the 1321N1 astrocytoma cell line and performed as described before) in serum-reduced media and incubated for 48h to condition the medium. The media conditioned by 1321N1 astrocytoma cells was added afterwards to PC12 cells. These cells were incubated for another 48h. After the incubation time, the control cells incubated with serum-reduced media with 0.5% ethanol as solvent control showed a rounded shape, which is characteristic for undifferentiated PC12 cells (Figure 12, black arrow). All tested erinacines at different concentrations showed the effect with the media conditioned by astroglial cells on PC12 cells to induce membrane protrusions, which were called neurites, implying that they are able to induce neurotrophin production and thereby the differentiation of PC12 cells.

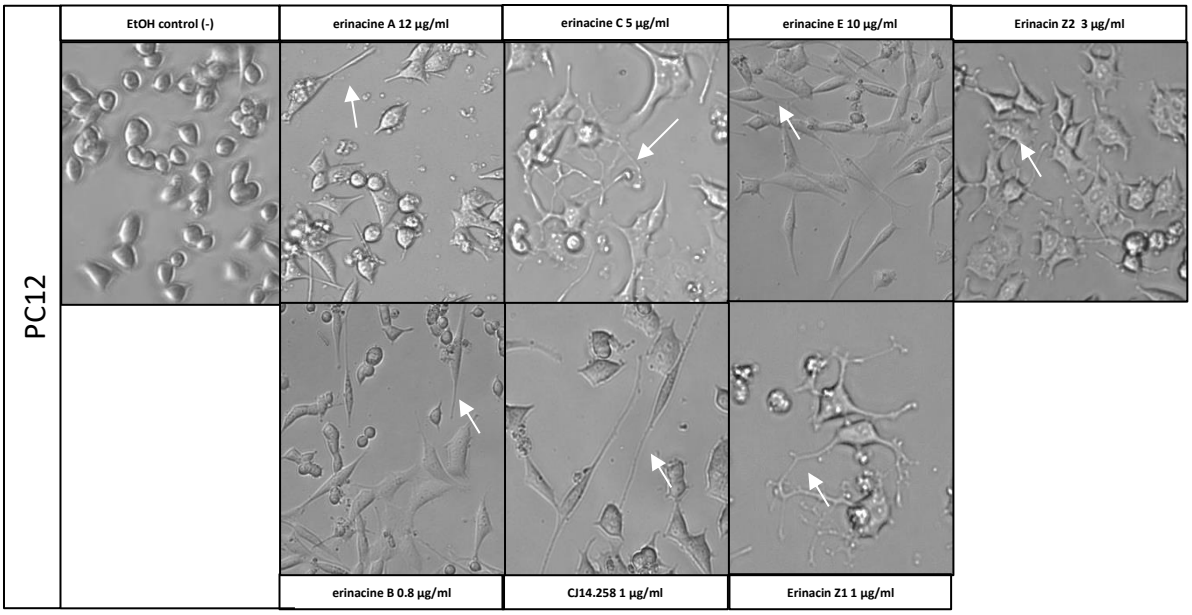

Figure 12: Differentiation of PC12 cells incubated with media conditioned by 1321N1 astrocytoma cells incubated with the different erinacines. (−) Ethanol: negative control conditioned media produced by 1321N1 incubated with Ethanol; (+) NGF: positive control with 200 ng/ml human NGF. A differentiated cell is marked with a white arrow. Scale bar 100 µm.

To quantify these results, the number of differentiated cells containing neurites and the average length of the neurites were measured (Figure 13). Compared to the negative controls, which showed only a small amount of differentiated cells of 1.2 ±0.1% (serum-reduced media) and 5.2 ±1.1% (0.5% ethanol) with short neurites having an average length of 10.2 ±2.5 µm (serum-reduced media) and 10.5 ± 3.1 µm (0.5% ethanol), all erinacines as well as the positive control (NGF) were able to significantly induce PC12 cell differentiation shown by the amount of differentiated cells as well as by the average length of neurite extensions that they induced. The NGF positive control induced differentiation of 35.2 ±2.5% of the cells and these cells were extending neurites with an average length of 71.2 ± 1.7 µm. The strongest differentiation-inducing supernatant conditioned by astroglial cells was erinacine A with 39.5 ±5.7% differentiated cells which had neurites with an average length of 57.2 ±5.9 µm. This was followed by the weaker inducing erinacine B (37.2 ±10.7%; 51.9 ±3.2 µm), erinacine C (39.2 ± 3.2%; 50.8 ±2.8 µm), CJ14.258 (36.7 ± 10.2%; 48.2 ±3.1 µm), erinacine E (31.8 ±3.1%; 48.1 ±2.8 µm), erinacine Z1 (18.2 ±3.3%; 18.7 ±2.8 µm) and erinacine Z2 (17.5 ±3.3%; 19.2 ±2.7 µm). So, it was shown that the already known structures erinacine A, B, C, E and CJ14.258 are able to induce differentiation equivalent to the positive control. Both, erinacine Z1 and Z2 are weaker in the induction of PC12 differentiation compared to the positive control or the already known erinacines.

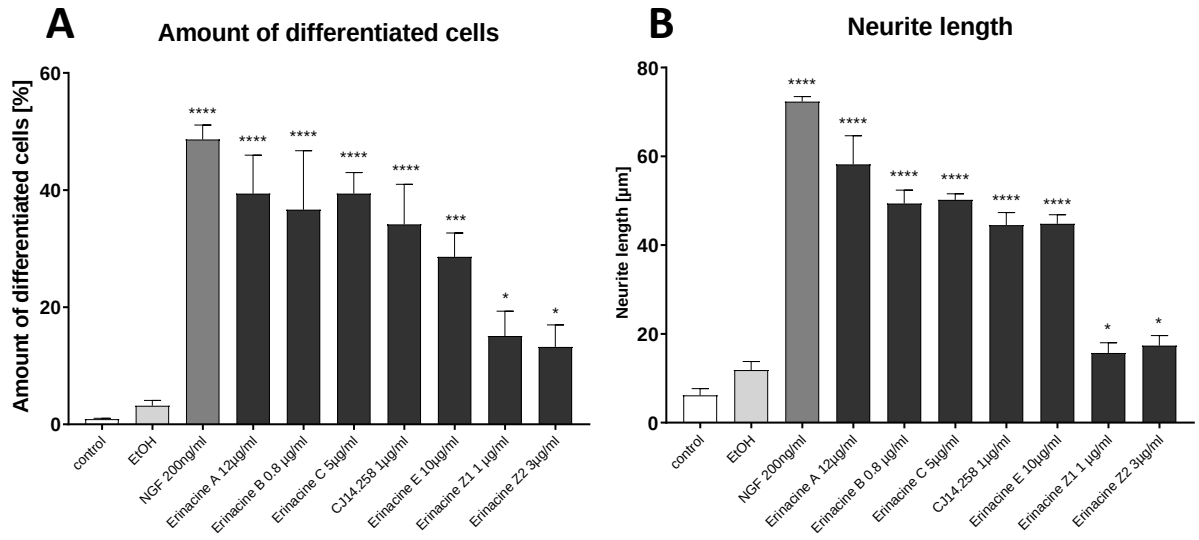

Figure 13: Quantification of the level of differentiation of PC12 cells when incubated with media conditioned by 1321N1 astrocytoma cells incubated with different erinacines. A) Quantification was performed by counting the amount of differentiated cells shown as percentage. B) Quantification was performed by analyzing neurite length which is given as average value in µm. Control: conditioned media produced by 1321N1 without any additives. EtOH: conditioned media produced by 1321N1 incubated with 0.5% Ethanol alone (solvent control). NGF: direct incubation of PC12 cells with human NGF (200 ng/ml). The grade of differentiation of PC12 cells is shown when these were incubated with conditioned media produced by 1321N1 incubated with the different erinacines. (n = 4; ± SEM; One-way-Anova: * $p \leq 0.05$; *** $p \leq 0.001$; **** $p \leq 0.0001$)

The next step was to explore if erinacines caused differentiation of PC12 cells by media conditioned by erinacine-treated 1321N1 astrocytoma cells. This differentiation is potentially triggered through stimulation of neurotrophin expression and secretion by these astrocytic cells. Consequently, 1321N1 astrocytoma cells were incubated with the various erinacines for 6h in serum-reduced media. After the incubation time the RNA was isolated, reverse transcribed to cDNA which was further analyzed by semi-quantitative RT-PCR against *gapdh*, *ngf* and *bdnf* mRNA level was evaluated (Figure 14). Figure 14A shows the RT-PCR results of the *gapdh*, *ngf* and *bdnf* mRNAs, no clear difference of the *ngf* level and *bdnf* level was visible compared to the controls. Therefore, a quantification of three independent experiments was done, shown in Figure 14 B and C. The ubiquitously expressed *gapdh* is used as a loading control. The amount of *ngf* and *bdnf* mRNA isolated from the control cells being incubated with serum-reduced media with ethanol as solvent control was set to a value of 1, the following results are shown as x times to the control. Surprisingly, not all of the erinacines were able to increase the *ngf* mRNA level. The strongest inducer of *ngf* expression is erinacine C with a value of 2.5 ±0.2, followed by erinacine A with a value of 2.1 ±0.04. Additionally, erinacine B was able to induce NGF production by a 2.03 ±0.1fold upregulation, followed by erinacine E with a value of 2 ±0.1. All of these upregulations were statistically significant. Furthermore, the new structure erinacine Z2 was able to induce *ngf* expression by 1.4 ±0.2, but this increase was not significant. Also, CJ14.258 (0.8 ±0.2) and erinacine Z1 (0.9 ±0.1) were not able to induce *ngf*

expression. In addition to the fact that only one erinacine was able to significantly increase *bdnf* mRNA levels and this was erinacine C with a value of 2.5 ±0.2. All of the other erinacines were not able to significantly induce the *bdnf* expression, exemplified by the values for erinacine A (1.1 ±0.1), erinacine B (1.2 ±0.03), CJ14.258 (1.3 ±0.1), erinacine E (1.2 ±0.1), erinacine Z1 (1.1 ±0.02) and erinacine Z2 (1.2 ±0.1). This leads to the conclusion that only erinacine A, B, C and E are able to induce significantly expression of *ngf* in astrocytic 1321N1 cells. All erinacines are able to induce with the conditioned media of incubated astrocytoma cells the PC12 cells. erinacine C is in addition to the influence on the expression of *ngf* also able to significantly stimulate the *bdnf* mRNA production, which cannot be analyzed by the PC12 cell-based differentiation due to the lack of TrkB receptor expression. The other erinacines were not able to increase *bdnf* expression.

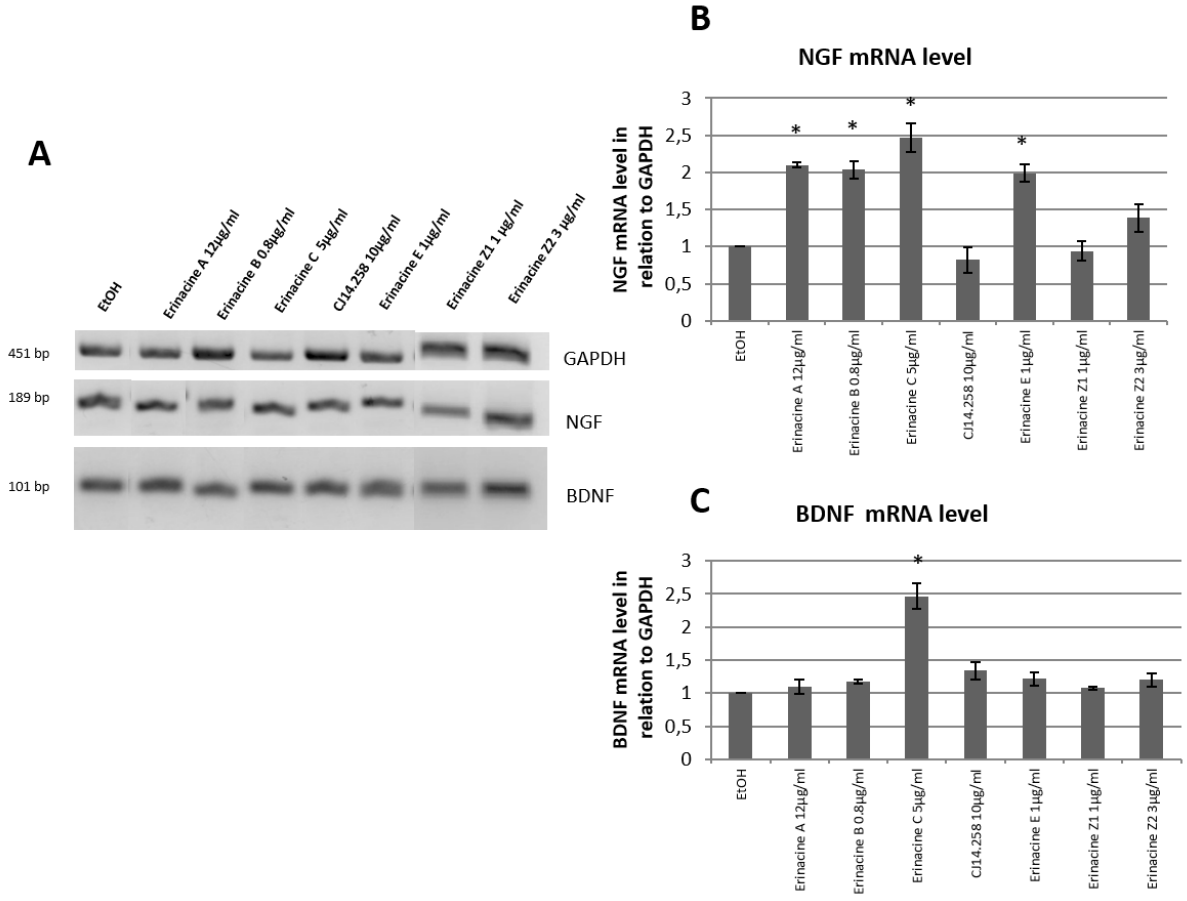

Figure 14: Analysis of the mRNA level of neurotrophin expression on 1321N1 cells, when incubated with erinacines. A) Representative agarose gel picture of a semi quantitative RT-PCR analysis. EtOH – 1321N1 cells incubated with 1% Ethanol followed by astrocytoma cells incubated with the different erinacines. *gapdh* was used as a loading control. The lower bands show the *ngf* and *bdnf* expression pattern, when astrocytes were incubated with the different additives. A quantification is shown in B) and C). (n = 3; ±SEM; t Test * $p \leq 0.05$)

Over all these findings confirm that erinacines and corallocins are not able to induce PC12 cell differentiation directly, but after the media was conditioned by astrocytoma cells treated with

these erinacines. Besides, neurotrophins such as NGF and BDNF are stimulated in their expression. For further analysis the signaling cascade by which PC12 cell differentiation is initiated, the most prominent member, erinacine C, which is able to cause the activation of NGF and also BDNF expression should be further analyzed.

3.1.3 Analysis of signaling cascades involved in the induction of PC12 cell differentiation by erinacine C-conditioned medium.

It was shown before that PC12 cells differentiate when the conditioned media of erinacine C incubated 1321N1 astrocytoma cells is added onto PC12 cells. In this work the signaling cascades, which mediate this differentiation, are evaluated.

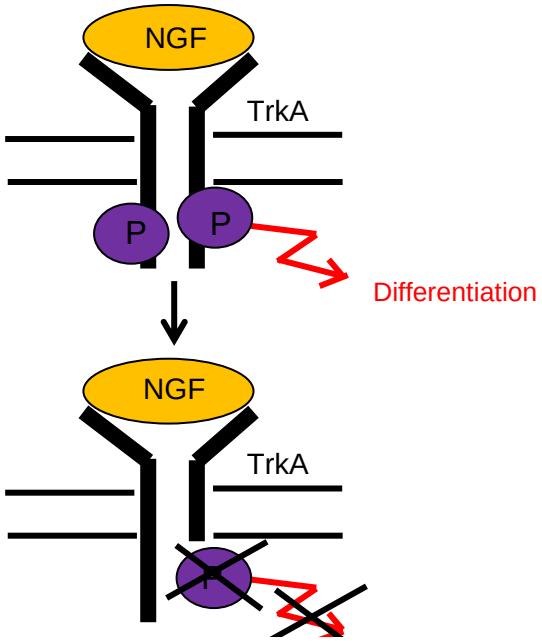

Figure 15: Scheme of how the dnTrkA System works. Normally, when NGF binds to its high affinity receptor TrkA this binding leads to an autophosphorylation of the transmembrane receptor (TrkA) shown in the upper picture. This phosphorylation activated several signaling cascades, which causes in PC12 cells the production of neurites and differentiation. In the dnTrkA variant (lower picture) the kinase region is exchanged by a citrine to mark all cells expressing the variant. When the kinase region is not part of the transmembrane receptor the autophosphorylation cannot take place, so the signaling cascades cannot be activated and the PC12 cells should not be able to differentiate NGF/TrkA dependent.

As erinacine C induces *ngf* expression in astrocytic cells and PC12 cells are known to differentiate upon NGF signaling, the signal transduction cascade downstream of NGF was evaluated. NGF binds to its high affinity receptor, called tropomyosin receptor kinase A (TrkA). Upon ligand binding this receptor forms a homodimer. TrkA is a transmembrane rector kinase and ligand binding results in cross-autophosphorylation of its own cytosolic domain. Due to this autophosphorylation the intracellular kinase is activated and causes the activation of different downstream signaling cascades, like Phosphoinositid-Phospholipase C γ (PLCγ), Phosphoinositid-3-Kinase (PI3K), Mitogen-activated protein kinase (MAPK) which activates the extracellular signal–regulated kinases 1/2 (Erk1/2) further downstream (Obermeier *et al.*, 1993; Stephens *et al.*, 1994; Pearson *et al.*, 2001; Riccio *et al.*, 1999; Datta *et al.*, 1999; Hetman *et al.*, 2000; Kaplan and Miller, 2000). Using the known autophosphorylation properties a dominant negative (dn) variant of TrkA can be established (Figure 15), like it was shown for the FGF receptor (Amaya *et al.*, 1991). The dominant negative variant (Figure 16) is represented by a truncated TrkA receptor, which lacks the intracellular

kinase domain. When this truncated variant is overexpressed, it forms heterodimers with the endogenous TrkA upon ligand binding. This heterodimer cannot cross-phosphorylate each other because the kinase domain and the target domain is missing. Therefore, ligand binding does not activate TrkA downstream signaling. To monitor the expression of the dominant negative TrkA variant, the domain was replaced by the fluorescent protein mCitrine, which contains an ER exit sequence (FCYENEV) at its C-terminus to promote incorporation into the cytoplasmic membrane.

Figure 16: Construct of rat dnTrkA for PC12 cells transfection. The Plasmid consists of a pCS backbone where the N-terminus of the rat TrkA receptor is cloned fused to a mCitrine, which is connected to an Endoplasmic reticulum export signal (ERex).

The above described construct was used to analyze, if the differentiation caused by conditioned media of erinacine C treated 1321N1 astrocytoma cells is triggered by NGF/TrkA signaling. Therefore, 1321N1 cells were incubated with erinacine C (5 µg/ml) for 48h. During this time PC12 cells were transfected and incubated for 48h with the expression construct to overexpress the dominant negative TrkA receptor. These PC12 cells were exposed to the conditioned supernatant of the 1321N1 cells. In addition, transfected cells were also incubated with NGF as positive control. The cells were cultured for another 48h, afterwards the cells were analyzed for differentiation by neurite outgrowth. Transfected cells demonstrated a green fluorescence in the membrane, not transfected cells did not display fluorescence (Figure 17). Cells incubated with only serum-reduced media and 0.5% ethanol as solvent control showed the rounded shape of normal PC12 cells, both transfected and non-transfected cells. After incubation with NGF at a concentration of 200 ng/ml the non-transfected cells indicated the generation of neurites (Figure 17, second picture, black arrow), but the transfected green cells did not extend such membrane protrusions (Figure 17, white arrow). When the PC12 cells were treated with the conditioned media of erinacine C incubated astrocytoma cells the non-transfected cells exhibited neurites (Figure 17, third picture, black arrow), whereas in the transfected green fluorescent cells no neurites were visible (Figure 17, white arrow). The weakly expressing PC12 cells confirmed elongations, but shorter than the non-transfected cells (Figure 17, red arrow). This confirms that dnTrkA expressing cells indicated no differentiation, when human NGF was added to these cells, whereas the non-transfected cells indicated differentiation. The same applied for the conditioned media, of note some transfected cells with weak expression also displayed a weak differentiation profile.

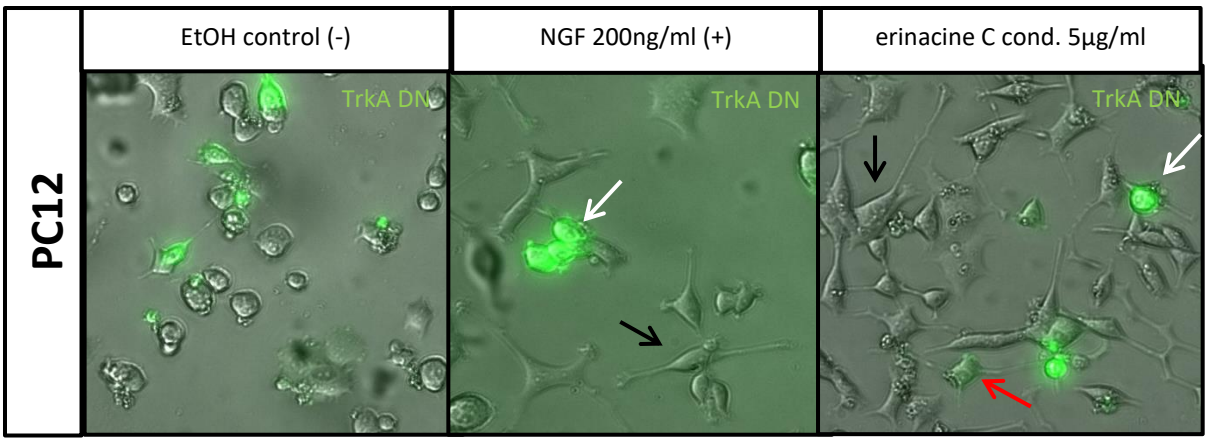

Figure 17: Effect of NGF or erinacine C conditioned media on dnTrkA transfected PC12 cells. Figure shows transfected PC12 cells with the before explained dnTrkA construct. A heterogeneous cell population is visible. Green fluorescent cells represent transfected PC12 cells expressing the dominant negative variant of the TrkA receptor. EtOH control (-) shows PC12 cells incubated with normal media with 1% Ethanol as solvent control. NGF shows transfected PC12 cells incubated with NGF in normal media. Non-transfected cells, marked with a black arrow, show differentiation, whereas transfected cells, marked with a white arrow, are not differentiated. The picture erinacine C show transfected PC12 cells, which were incubated with conditioned media of Erinacin C. Non-transfected cells (black arrow) are differentiated. Some transfected cells with green fluorescence show no differentiation (white arrow), whereas other show weak differentiation (red arrow).

The results were quantified regarding the amount of differentiated cells and the neurite length (Figure 18). The control where PC12 cells were only treated with serum-reduced media or with 0.5% ethanol in addition demonstrate only a small number of differentiated cells of 4.3 ±0.5% with short neurites having an average length of 12.3 ±1.2 µm. When the PC12 cells were incubated with NGF the quantity of differentiated cells and the neurite length were significantly increased with an average value of 36.3 ±4.2% and 72 ±2.7 µm, the same was seen for the conditioned media treated PC12 cells. 23.2 ±4.3% PC12 cells were differentiated and had neurites with an average length of 57.2 ±2.3 µm. When the PC12 cells were transfected with the construct of the dnTrkA and treated after transfection with NGF or the conditioned media, the amount of differentiated cells was significantly decreased with an average value of 12.5 ±3.9% and 11.9 ±3.8% differentiated cells a nearly 4-fold decrease compared to the non-transfected cells. These cells had neurites with an average length of 18.2 ±1.3 µm and 21.8 ± 1.5 µm, respectively (Figure 18).

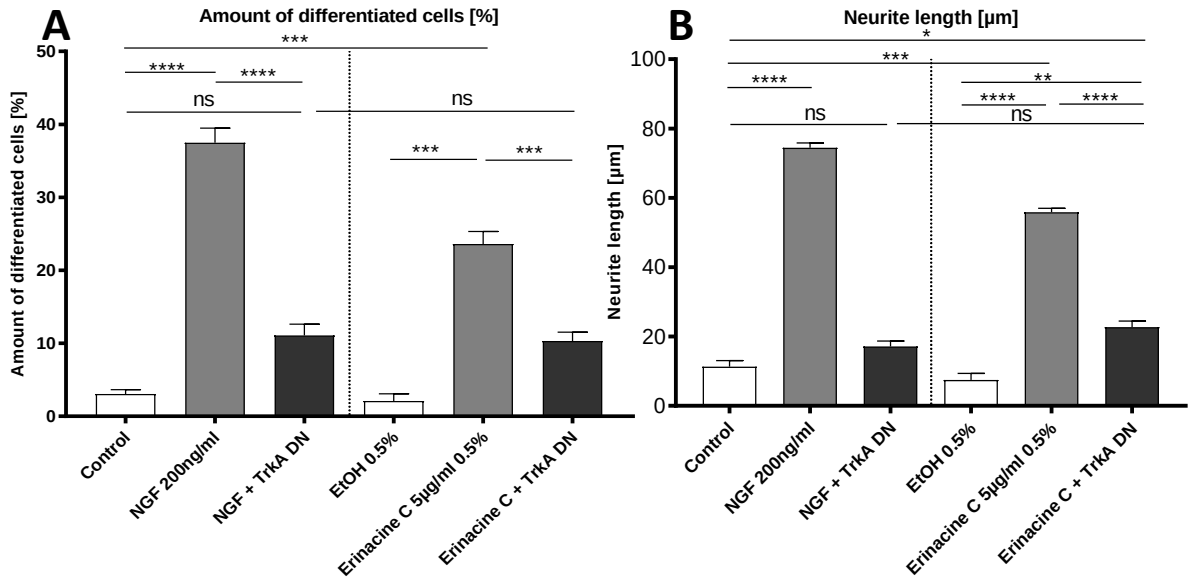

Figure 18: Quantification of the percentage of differentiated cells when PC12 cells were transfected with dnTrkA and treated with neurotrophin. Quantification was performed by counting the amount of differentiated cells compared to all cells shown as percentage. B) Quantification was done by analyzing neurite length which is given in µm. Control: conditioned media produced by 1321N1 without any additives. NGF: direct incubation of PC12 cells with human NGF (200 ng/ml). NGF + TrkA DN means PC12 cells, which where transfected with the dominant negative TrkA variant and incubated with NGF in the media. The same was performed with conditioned media using erinacine C (erinacine C + TrkA DN). EtOH: conditioned media produced by 1321N1 incubated with 1% Ethanol (solvent control). erinacine C stands for PC12 cells which were incubated with conditioned media of Erinacin C. (n = 4; ± SEM; One-way-Anova: * $p \leq 0.05$; ** $p \leq 0.001$; *** $p \leq 0.001$; **** $p \leq 0.0001$)

These results confirmed that using a construct to repress NGF/TrkA signaling the differentiation of PC12 cells is decreased. This confirms that the differentiated PC12 cells is triggered by the NGF-TrkA signaling pathway. As similar results were obtained for erinacine C cultured astrocytic media it is plausible that this conditioned media introduced PC12 cell differentiation via TrkA receptor. Because transfection only effects 20-30% of the cells non-transfected cells serves as direct control, it was decided to utilize also a pharmacological approach by using an inhibitor to analyze the dependence of the differentiation to the NGF/TrkA signaling. An inhibitor directly for the kinase activity of TrkA was used (K252a): K252a is an alkaloid isolated from *Nocardiopsis bacteria* and is a potent cell permeable inhibitor of kinases and phosphorylase kinase, as well as for serine/threonine protein kinases (Figure 19). Apart from that, NGF/TrkA signaling activates different downstream cascades, which are involved in initiating the differentiation of PC12 cells (Figure 19). Different inhibitors for the downstream

cascades were used to characterize the effect on the different downstream pathways (shown also in Table 5): Phosphoinositid-3-Kinase (PI3K; LY294002), Phosphoinositid-Phospholipase C γ (PLCγ; Bisindolylmaleimide I), Mitogen-activated protein kinase (MAPK; PD98059), extracellular signal–regulated kinases 1/2 (Erk1/2; U0126) (Obermeier *et al*., 1993; Stephens *et al*., 1994; Pearson *et al*., 2001; Riccio *et al*., 1999; Datta *et al*., 1999; Hetman *et al*., 2000; Kaplan and Miller, 2000). LY294002 (PI3K) is a potent, cell permeable inhibitor of phosphatidylinositol 3-kinase (PI3K) that functions at the ATP binding site of the enzyme. Bisindolylmaleimide I (PLCγ) enables the binding of ATP to PKC and by that it enables the activity of PLCγ. PD98059 (MAPK) is a potent and selective inhibitor of MAP kinase kinases (MAPKK – MAPK kinase). It binds to the inactive form of MAPKK and inhibits activation by upstream activators such as c-Raf. U0126 (Erk1/2) inhibits activation of MAPK (ERK 1/2) by preventing the kinase activity of MAP Kinase Kinase (MAPKK or MEK 1/2).

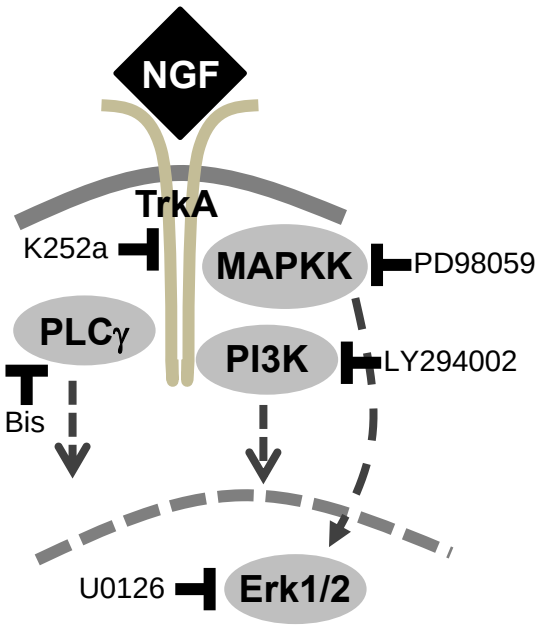

Figure 19: Illustration of the different downstream signaling cascades being activated by NGF/TrkA signaling causing the differentiation of PC12 cells. The different inhibitors are acting on different downstream cascades of TrkA. K252a is an inhibitor for different kinases, which inhibits the autophosphorylation of the TrkA kinase region. Three main cascades are activated in PC12 cells that are involved in differentiation: MAPK/Erk1/2 signaling, PLCγ and PI3K. To inactivate MAPK/Erk1/2 signaling two different inhibitors were used: for MAPK (PD98059) and for Erk1/2 (U0126). The PLCγ signaling was impaired with Bisindolylmaleimide I and PI3K with LY294002.

Table 5: List of different used inhibitors.

Name	Inhibition of	Function
K252a	TrkA	inhibits the kinase region of TrkA where the autophosphorylation takes place
Bisindolylmaleimide I	PLCγ	enables the binding of ATP to PKC enables the activity of PLCγ
LY294002	PI3K	acts on the ATP binding site of phosphatidylinositol 3-kinase (PI3K)
PD98059	MAPK	binds to the inactive form of MAPKK prevents activation by upstream activators
U0126	Erk1/2	inhibiting the kinase activity of MAP Kinase Kinase

Astrocytoma cells were treated with erinacine C for 48h and the conditioned media was added afterwards onto PC12 cells. 1h before these PC12 cells had been treated with the different inhibitors, while the supernatant in addition to the different inhibitors was added 1h later. The cells were treated for another 48h to allow differentiation in the presents of different inhibitors and analyzed afterwards. After this incubation time the amount of differentiated cells was quantified (Figure 20). The cells processed as the control were incubated in serum-reduced media with 0.5% ethanol and 1% DMSO. These showed a low amount of differentiated cells of 0.8 ± 0.01%, with short neurites (average length of 5.2 ±0.1 µm). When PC12 cells were incubated with NGF or with the erinacine C conditioned media the amount of differentiated cells ranged around a value of 35.2 ± 5.2% and 23.7 ±5.7% respectively, as well as the neurite length (65.7 ±5.1 µm and 48.7 ±5.2 µm), increased significantly. In comparison to that, the amount of differentiated cells, as well as the average neurite length, were significantly reduced when the different inhibitors were added. The inhibitor for TrkA is able to significantly decrease the neurite length (for NGF treatment 42.7 ±3.5 µm and for conditioned media 32.8 ± 4.2 µm) and the amount of differentiated cells (12.7 ±5.4% and 9.8 ±3.7%), comparable to the findings of the dnTrkA expression in PC12 cells. The other inhibitors for MAPK, Erk1/2, PLC_{γ} and PI3K were also able to significantly reduce the differentiation amount of the NGF treated cells, as well as of PC12 cell incubated in the erinacine C conditioned media, compared to the positive controls. Regarding MAPK inhibition (PD98059), the amount of differentiated cells was decreased down to 8.7 ±0.01% and 7.9 ±2.3% and these cells had neurites with an average length of 30.7 ±7.3 µm and 32.7 ±5.8 µm respectively. Inhibition of Erk1/2 (U0126) lead to a decrease of the amount of differentiated cells to 7.8 ±2.5% and 8.1 ±1.5% and the neurites had an average length of 33.8 ±6.8 µm and 32.9 ± 4.7 µm respectively. When PLC_{γ} (Bisindolylmaleimide I) was inhibited the differentiation of the PC12 cells incubated with NGF or the conditioned media was also significantly decreased to values of 2.5 ±1.2% and 11.1 ± 5.2% of differentiated cells respectively, and these cells had neurites with an average length of 5.2 ±2.5 µm and 32.5 ±5.5 µm. The last used inhibitor for preventing downstream signaling cascades was LY294002 to inhibit PI3K, the amount of differentiated cells was decreased down to 18.7 ±1.2% for NGF incubation and 5.7 ±1.5% for supernatant from erinacine C treated astroglial cells. These cells had neurites with an average length of 55.2 ±1.5 µm for NGF and 31.2 ±1.5 µm. Summarizing these results, all used inhibitors were able to significantly decrease the amount of differentiation of PC12 cells incubated with NGF or the supernatant of erinacine C treated 1321N1 astrocytoma cells. Not all inhibitors showed the same efficiency, a stronger inhibitor is Bisindolylmaleimide I and a weaker inhibitor is LY294002.

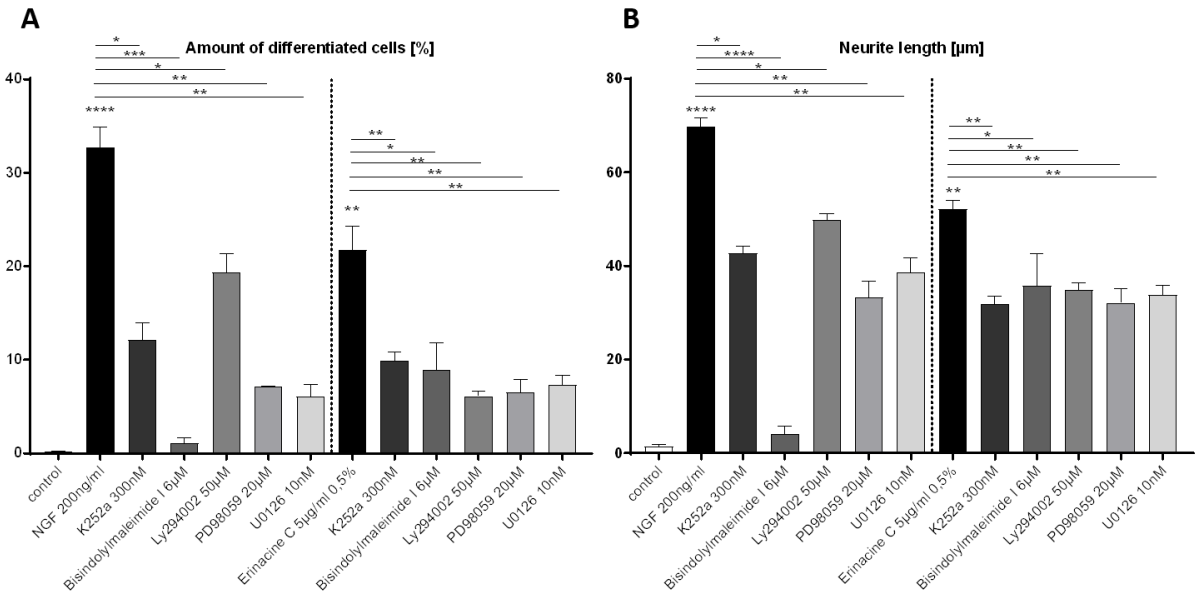

Figure 20: erinacine C conditioned astrocytic media mediates PC12 differentiation via TrkA signaling. Quantification was performed by counting the amount of differentiated cells compared to undifferentiated cells shown as percentage. B) Quantification was performed by analyzing the average neurite length which is given in µm. Control: media produced by 1321N1 without any additives. NGF: direct incubation of PC12 cells with human NGF (200 ng/ml). Followed by incubation of different inhibitors together with NGF, a strong decrease in the amount of differentiated cells is visible for PD98059, U0126 and Bisindolylmaleimide and a weaker decrease for LY294002 and K252a is visible. The neurite length is strongly reduced for Bisindolylmaleimide and weaker decreased for the other inhibitors. erinacine C: incubation of PC12 cells with the conditioned media of erinacine C treated 1321N1 cells. This media was used alone or was supplemented with the different inhibitors. A strong decrease in the amount of differentiated cells is visible for all inhibitors and also the average neurite length is reduced but weaker compared to pure NGF. (n = 4; ± SEM; One-way-Anova: * $p \leq 0.05$; ** $p \leq 0.001$; *** $p \leq 0.001$; **** $p \leq 0.0001$)

The demonstrated results lead to the suggestion that the differentiation caused by the media of erinacine C treated 1321N1 cells occurred by NGF/TrkA mediated signaling. Regarding the efficiency of the induction of differentiation there is a clear difference between pure NGF and erinacine C conditioned media. The differentiation mediated by NGF can be reduced by the different inhibitors but compared to the differentiation caused by the erinacine C-conditioned media, the reduction is stronger. However, with the dn TrkA experiment, a comparable reduction of the differentiation for NGF incubated PC12 cells as well as with the conditioned media of erinacine C treated astrocytic cells was demonstrated.

This shows that erinacine C conditioned media of astrocytic cells induces PC12 differentiation via TrkA signaling and further downstream through the activation of PLC_{γ}, PI3K and MAPK signaling. This suggests that there is a connection between the erinacine C incubation and induction of NGF production. The next step will be to analyze the direct effect of erinacine C on 1321N1 astrocytoma cells.

3.2 Analysis of the response of astrocytoma cells to erinacine C

3.2.1 Analysis of different signaling cascades in astrocytoma cells treated with erinacine C

Signal transduction combines several biochemical and physiological processes, for example cells respond to external stimuli, transform them, pass them as signal into the cell interior and lead through a biochemical signal chain to a cellular response. In this thesis the activation of different signaling cascades upon the exposure of astrocytic cells to erinacine C as analyzed. This was shown by binding of transcription factors to the DNA and activating the expression of target genes. DNA binding sites for different transcription factors have been described, like NFkappaB sites or SBE for TGFβ signaling and are listed in openly available databases (Kuri *et al*., 2017; Dennler *et al*., 1998).

Activity analysis can be easily performed by using a luciferase expression approach followed by quantifying luciferase enzyme activity via generating a bioluminescent product. Quantification of photon yield directly relates to expression strength. Therefore, four times repeat of different already known DNA binding sites of transcriptional activators was cloned in front of an E1b basal promotor initiating the expression of firefly luciferase (Figure 21). Binding sites of a variety of transcriptional activators of prominent signal transduction cascades were cloned into this construct backbone.

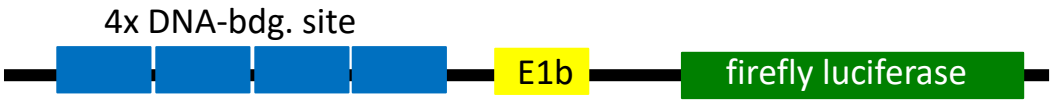

Figure 21: Schematic overview of reporter construct design containing 4x tandems of transcriptional activators. The consensus binding site construct backbone contains a 4 times repeat of already known DNA binding sites cloned in front of an E1b promotor which initiates expression of firefly luciferase.

It was shown up to now, that erinacine C is able to induce *ngf* and *bdnf* expression in astroglial cells, but it is not known, how in astroglial cells respond on the transcriptional level to erinacine C incubation. STAT3 is among the transcriptional activators known to be culpable of inducing *ngf* expression. The consensus binding sites of STAT3 have been identified (Langlais *et al*., 2008; Vallania *et al*., 2009). STAT3 belongs to the family signal transducer and activator of transcription (STAT) proteins. This group mediates many facets of cellular immunity, proliferation, apoptosis and differentiation (Vinkemeier *et al*.,1998; Tkach *et al*., 2013). STAT3

initiates the expression of a variety of genes, and by that it plays a key role in many cellular processes, such as cell growth and apoptosis (Yuan *et al*., 2004).

Another known binding site is recognized by NFkappaB (Kuri *et al*., 2017). NFkappaB is implicated in cellular responses to stimuli such as stress, cytokines, free radicals, and bacterial or viral antigens (Gilmore, 2006; Brasier, 2006; Perkins, 2007; Gilmore, 1999; Tian and Brasier, 2003). NFkappaB plays a key role in regulating the immune response to infection. NF-κB has also been involved in processes of synaptic plasticity and memory (Albensi and Mattson, 2000; Meffert *et al*., 2003; Freudenthal *et al*., 1998; Merlo *et al*., 2002; Park and Youn, 2013).

Also, different ETS binding sites were cloned (Webb *et al*., 2016; Boros *et al*., 2009; Odrowaz and Sharrocks, 2012; Brown *et al*., 1999). ETS belongs to the E26 transformation-specific or E-twenty-six family, the largest family of transcriptional activators, containing of highly conserved DNA binding domain (ETS domain). By binding to DNA and it is involved in regulation of cellular differentiation, cell cycle control, cell migration, cell proliferation, apoptosis and angiogenesis.

Another consensus binding site was used that is recognized by NFAT (Zhang *et al*., 2018; Chen *et al*., 1998). NFAT stands for Nuclear factor of activated T-cells. The NFAT transcription factor family is important for the immune response, but is also involved in development of cardiac, skeletal muscle, and nervous systems. Calcium signaling is critical to NFAT activation because Calmodulin, a calcium sensor protein, activates the serine/threonine phosphatase Calcineurin. Activated Calcineurin dephosphorylates NFAT proteins, which results in a conformational change that exposes a nuclear localization signal, resulting in NFAT nuclear import.

Another binding site which was used in the luciferase reporter is BRE (Morikawa *et al*., 2011). BMP responsive element (BRE) is a bone morphogenetic protein (BMP) signaling cascade which is recognized by Smad proteins, which are part of the transforming growth factor ß (TGFß) family. These proteins are involved in proliferation, differentiation and apoptosis of several types of cells (Wozney and Rosen, 1998; Reddi, 2001).

In this thesis also the estrogen responsive element (ERE) binding site was used for analysis (Gorelick and Halper, 2011). This represents a DNA consensus sequence to which the estrogene receptors can bind. The estrogene receptor is a ligand-activated cytoplasmic enhancer protein,

a member of the steroid nuclear receptor family. It transactivates gene expression in response to estradiol.

Another DNA consensus binding site which was used in this thesis is HIF1 (Greenald *et al*., 2015; Kulkarni *et al*., 2010). HIF stands for hypoxia inducible factor that respond to decreases in available oxygen in the cellular environment, and it is responsible for the cellular adaptation response to oxygen availability (Smith *et al*., 2008; Wilkins *et al*., 2016).

Also, the function of Dyrk1A binding to DNA was analyzed (Di Vona *et al*., 2015). The dual specificity tyrosine-phosphorylation-regulated kinase 1A (Dyrk1A) is usually known as a catalysator for autophosphorylation on serine/threonine and tyrosine residues and by that it plays a important role in signaling pathways regulating cell proliferation and is involved in brain development. In addition to that it was shown that the kinase is also recruited to promoters of genes which are transcribed by RNA polymerase II. By that, this transcriptional activator is associated with translation, RNA processing, and cell cycle (Di Vona *et al*., 2015).

Additional to the already introduced binding sites, the consensus binding sequence of FOXO was also employed (Webb *et al*., 2016). Forkhead-Box-Protein O is involved in cell growth, proliferation, differentiation, and longevity (Tuteja and Kaestner, 2007).

Also, the binding site of Gli1 transcription factor was analyzed (Kinzler and Vogelstein, 1990). Gli is a zinc finger protein, which is an effector of the Hedgehog signaling cascade. It was shown to be involved in cell fate determination, proliferation and patterning in several different cell types.

RBP binding sites, which are mediating Notch signaling, were used (Tun *et al*., 1994; Minoguchi *et al*., 1997; Parsons *et al*., 2009; Schiavone *et al*., 2014). Recombination signal binding protein (RBP) is part of the Notch signaling pathway (Artavanis-Tsakonas *et al*., 1999). Notch signaling promotes proliferation during neurogenesis, and when its activity is inhibited by Numb this leads to neural differentiation. It plays also an important role in the regulation of embryonic development. Apart from that it is also involved in neuronal development and function (Gaiano and Fishell, 2002; Bolós *et al*., 2007; Aguirre *et al*., 2010; Hitoshi *et al*., 2002).

The FGF mediated signaling was also analyzed using a Pea3b DNA binding site (Znosko *et al*., 2010). The fibroblast growth factors (FGF) are a group of cell signaling proteins which are involved in a wide variety of processes, like neural stem cell proliferation, neurogenesis, axon

growth, differentiation and neuronal survival (Reuss *et al*., 2003). Surprisingly, the binding site included sequences highly conserved to ETS sites.

CREB mediated signaling was also analyzed in this thesis using CREB specific DNA binding sites (Moore *et al*., 2016; Bobinet *et al*., 2013). CREB is a cAMP response element-binding protein, which is a cellular transcriptional activator. CREB is known to be involved in mediating neuronal plasticity as well as in promoting long-term memory (Silva *et al*., 1998).

The activity of Wnt signaling can be analyzed by using the DNA binding sites of TCF/LEF (Shimizu *et al*., 2012; Moro *et al*., 2012). It was shown that Wnt is involved after binding to its receptor Frizzled in activation of Dishevelled which subsequently inhibits constructive ß Catenin degradation. The stabilized accumulating ß catenin moves into the cellular nucleus, where it directly binds to TCF/LEF binding sites. By that the signaling has an influence on cell fate determination, cell proliferation and migration (Nusse and Varmus, 1992; Nusse, 2005).

In this thesis also TGFß signaling was addressed using SBE binding sites (Dennler *et al*., 1998; Schiavone *et al*., 2014). Smad-binding elements (SBE) are Transforming Growth Factor-β (TGFβ) responsive elements. TGFβ belongs to the group of growth factors including Activins, Bone morphogenic proteins (BMP) and Glial Derived Neurotrophic Factors (GDNF) (Attisano and Wrana, 2002). TGFβ is widely expressed in the embryonic and adult organism and takes over function in regulating cell-proliferation and differentiation, extracellular matrix production, wound healing, immune function, apoptosis, angiogenesis, chemotaxis and hematopoiesis.

The thesis deals also with NBRE binding site activity (Wilson *et al*., 1993; Callard *et al*., 2001). Nerve growth factor inducible-B protein (NBRE) is also known as nuclear receptor subfamily 4 group A member 1 (NR4A1) with a known DNA consensus binding site. NR4A1 is involved in cell cycle mediation, inflammation and apoptosis (Pei *et al*., 2006). But one has to mention that NR4A1 is itself an activator of TGF-β/SMAD signaling (Zhou *et al*., 2014).

Also, Krüppel like factor 5 (KLF5) was characterized in this work exporting the known KLF5 DNA consensus binding site (Webb *et al*., 2016). The family of KLFs are zinc finger DNA binding proteins, which are able to regulate protein expression, and by that they are able to

influence proliferation, differentiation, and apoptosis, as well as the development and homeostasis of several types of tissue.

The NFY binding site for analyzing the CCAAT/enhancer-binding protein beta (CEBP) signaling was also cloned in this work (Webb *et al*., 2016). Proteins which are expressed after CEBP binding and activation of transcription are involved in immune and inflammatory responses.

Also, the binding site for early response factor (Egr1) also known as nerve growth factor inducible protein A (NGFI-A) was analyzed in this thesis (Wolfe and Call, 1999). EGR1 can activate the transcription of several hundred genes. Depending on the cell type and the stimulus, EGR1 induces the expression of growth factors, growth factor receptors, extracellular matrix proteins, proteins involved in the regulation of cell growth or differentiation, and proteins involved in apoptosis, growth arrest, and stress responses.

Binding sites which are recognized by Single-minded homolog 2 (Sim2) were also characterized in this work (Letourneau *et al*., 2015). Sim2 is a basic helix-loop-helix (bHLH) protein which is important for neurogenesis (Shamblott *et al*., 2002).

E2F which belongs to a group of eukaryotic transcription factors was also analyzed regarding their activity (Webb *et al*., 2016). These transcriptional activators are involved in the cell cycle regulation and synthesis of DNA in mammalian cells.

With such experiments it should be characterized, whether signaling cascades become stimulated in astrocytoma cells when they are exposed to erinacine C and before NGF is expressed. To answer this question 38 different constructs were established using the already introduced firefly reporter plasmid. These firefly luciferase constructs were co-transfected with an ubiquitously expressed renilla luciferase and in addition to that, a transfection of an ubiquitously expressed firefly luciferase together with the renilla luciferase construct was used, as a reference, to make the independent experiments comparable with respect to different transfection efficiencies. The transfected constructs were allowed to express for 48h in serum-reduced media as control, with 0.5% ethanol as solvent control. Alternatively, erinacine C was added to the transfected cells which were incubated for another 24h. After this incubation time the cells were lysed and the luciferase activity of the firefly and the renilla luciferases were measured independently by different luminescence substrates. Binding sites recognized by the yeast transcription factor Gal4 were the transcription factors which were used to detect the background activity of this approach. Therefore, a construct with 4x UAS sites was used. This

DNA binding site is specific for galactose-responsive transcription factor (GAL4). GAL4 is a yeast specific transcription factor and is not expressed in other model organisms (Kakidani and Ptashne, 1988).

First, the basic level of the different signaling cascade activity in 1321N1 astrocytoma cells was characterized. Therefore, 1321N1 cells were transfected with the different constructs together with a renilla standard expression vector as a reference for the different transfection efficiencies. The transfected cells were incubated with serum-reduced media, to make the results comparable to the experiments of neurotrophin induction in astrocytoma cells before, since fetal calf serum contains a high amount of growth factors, which can change the results, for another 24h. After this incubation time the cells were lysed and the luciferase activity of the firefly and the renilla luciferase activity was measured. The results were quantified as the quotient of firefly luciferase activity to renilla luciferase activity to normalize the firefly luciferase values to the respective transfection efficiency. The background activity was quantified by using a UAS construct. The background level was deducted from the quotient and the obtained results are shown in Figure 22. Some transcription factor consensus binding sites generated relatively high firefly luciferase activity values in 1321N1 cells, for example NRF (nuclear respiratory factor; reactive oxygen species (ROS) signaling; 217.6 ±53.3), ARE (antioxidant response element; antioxidant signaling; 217.6 ±20.3), Elk1 (ETS like protein 1; E-twenty six (ETS) signaling; 164.6 ±11.6), ETS (87 ±5) and KLF5 (Krueppel-like factor 5; epidermal growth factor (EGF) signaling; 62.9 ±23.6). This indicates that these transcription factors are endogenously expressed by 1321N1 cells. It was suggested that some cascades are more active, like ETS or KLF5, since these cascades are involved in proliferation and cell cycle. In addition, there were a number of transcription factor binding sites, which had moderate activity firefly luciferase, such as: NFAT/AP1 (nuclear factor of activated T cells co-binding site with the activator protein 1; NFAT signaling; 42.8 ±7.9), Dyrk1A (binding site for Dual-specificity tyrosine phosphorylation-regulated kinase 1A; Dyrk1A mediated signaling; 39.5 ±5.8), Pea3b (fibroblast growth factor (FGF) signaling; 36.7 ±3.6), HRE (hypoxia responding element; hypoxia; 26.8 ±3.3), SP1/KLF (Sp1-like/Kruppel-like factors; 25.8 ±5.5); CREB (cAMP response element-binding protein; 21.1 ±2.1), NFkappaB (nuclear factor 'kappa-light-chain-enhancer' of activated B-cells; 17.9 ±2.4), bZIP (basic leucine zipper; 17.5 ±2.2), SRE (serum-respond element; 8.4 ±0.4), NFY (nuclear transcription factor Y; 6.3 ±0.6), Egr1 (early growth response protein 1; 4.7 ±0.6) and Sim2 (Single-minded homolog 2; 3.7 ±0.6) suggesting a low endogenous expression of these transcription factors in astrocytic cells. Furthermore, the majority of the analyzed binding sites were not producing any significant firefly luciferase

activity showing that these signaling cascades are inactive in 1321N1 cells, among them: NBRE (nuclear receptor binding respond element; 1.1 ±0.2), TEAD (TEA domain family member; Yes-associated protein (YAP) and transcriptional coactivator with PDZ-binding motif (TAZ) signaling; 1 ±0.4), STAT3 (signal transducer and activator of transcription 3; 0.8 ±0.3), HSE (heat shock element; 0.8 ±0.1), Lhx2-Sox2 (LIM homeobox gene and SoxB1 related family members; 0.6 ±0.3), bHLH (basic helix-loop-helix motif; 0.6 ±0.2), FOXO (forkhead-Box-Protein O; 0.6 ±0.2) , SF1 (steroidogenic factor 1; 0.6 ±0.3), Gli1 (Zinc finger protein GLI1, hedgehog signaling; 0.6 ±0.05), ERE (estrogene responding element, estrogene signaling; 0.4 ±0.06), E2F (0.4 ±0.1), TCF/LEF (transcription factor/lymphoid enhancer-binding factor 1; Wnt signaling; 0.4 ±0.1), NFAT (nuclear factor of activated T-cells; 0.3 ±0.03), a1ACT (alpha-1-antichymotrypsin; 0.2 ±0.1), Runx (runt-related transcription factor 1; 0.2 ±0.09), Sox-Pou (0.2 ±0.07), BRE (BMP responsive element; BMP signaling; 0.2 ±0.03), RBP7 (retinol binding protein 7; Notch signaling; 0.2 ±0.09) and Fexf2 (Fez signaling; 0.08 ±0.05).

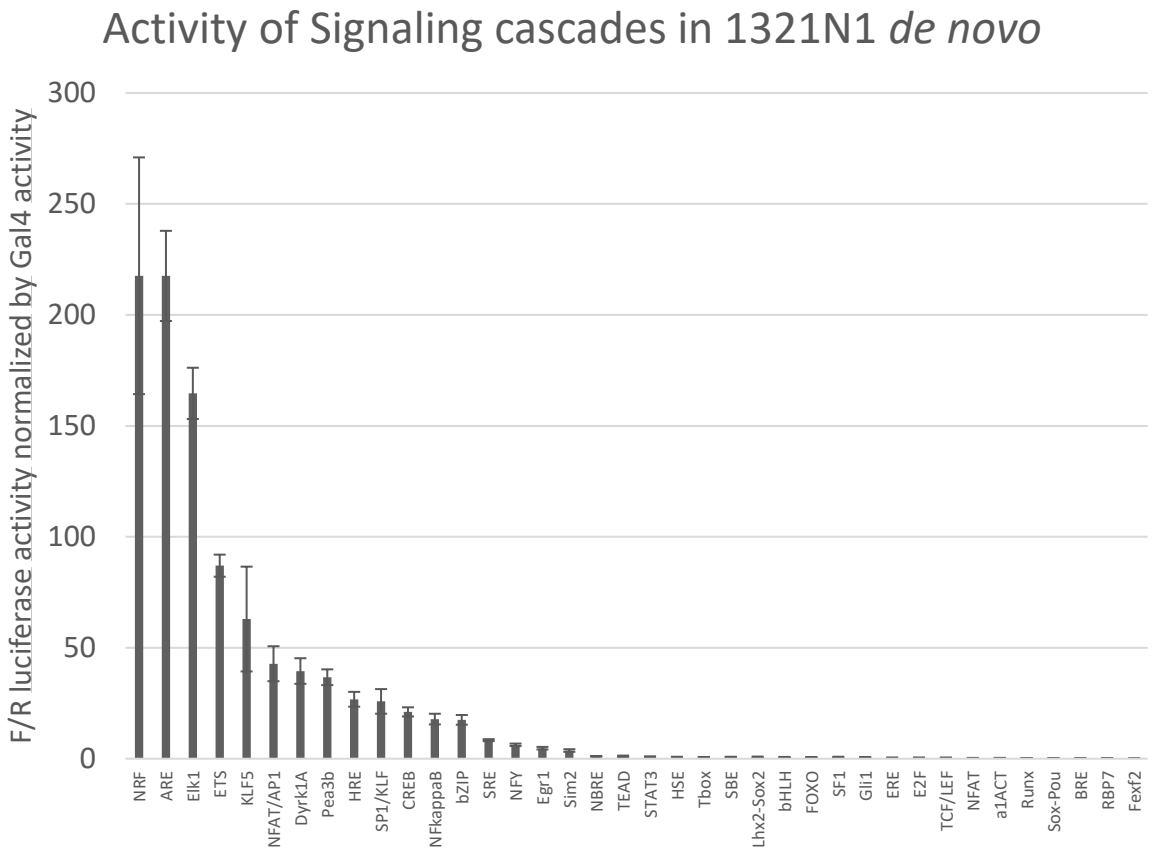

Figure 22: Activity of signaling cascades in 1321N1 *de novo*. The graph shows the activity of different signaling cascades in 1321N1 astrocytoma cells incubated with serum-reduced media. The values were shown as the absolute firefly activity divided by the renilla activity values. The UAS level was used as background. All values were normalized for the background activity by deducting the UAS value from the respective activity values. (n = 4; ± SEM)

After the basic luciferase activity for the different transcription factor binding sites in the reporter construct were evaluated, the effect of ethanol on the reporter gene expression was quantified, since ethanol was used as the solvent for erinacine C. 1321N1 astrocytoma cells were transfected as described before with the different reporter constructs and the renilla luciferase plasmid. The cells were incubated for 48h. After transfection serum-reduced media only or supplemented with 0.5% ethanol as additive was added. The cells were incubated for another 24h. After this time the luciferase activity was determined to quantify the expression strength mediated by the different transcription factor binding sites. In Figure 23 the x fold upregulation in comparison to the serum-reduced media incubated control cells. This showed that ethanol treatment has an influence on several transcription factor recognizing their respective binding site on the reporter construct. One expression level was significant increased, the E2F (5.3 ±1.1) binding site reporter. Others were significantly decreased, like for Pea3B (Fibroblast growth factor (FGF) signaling; 0.7 ±0.1), BRE (BMP responsive element; BMP signaling; 0.5 ±0.2), Egr1 (early growth response protein 1; 0.5 ±0.07), FOXO (forkhead-Box-Protein O; 0.4 ±0.09), SRE (serum-respond element; 0.1 ±0.02), NBRE (nuclear receptor binding respond element; 0.09 ±0.03) and Tbox (0.05 ±0.02). This influence of ethanol has to be taken into account, when analyzing the effect of erinacine C.

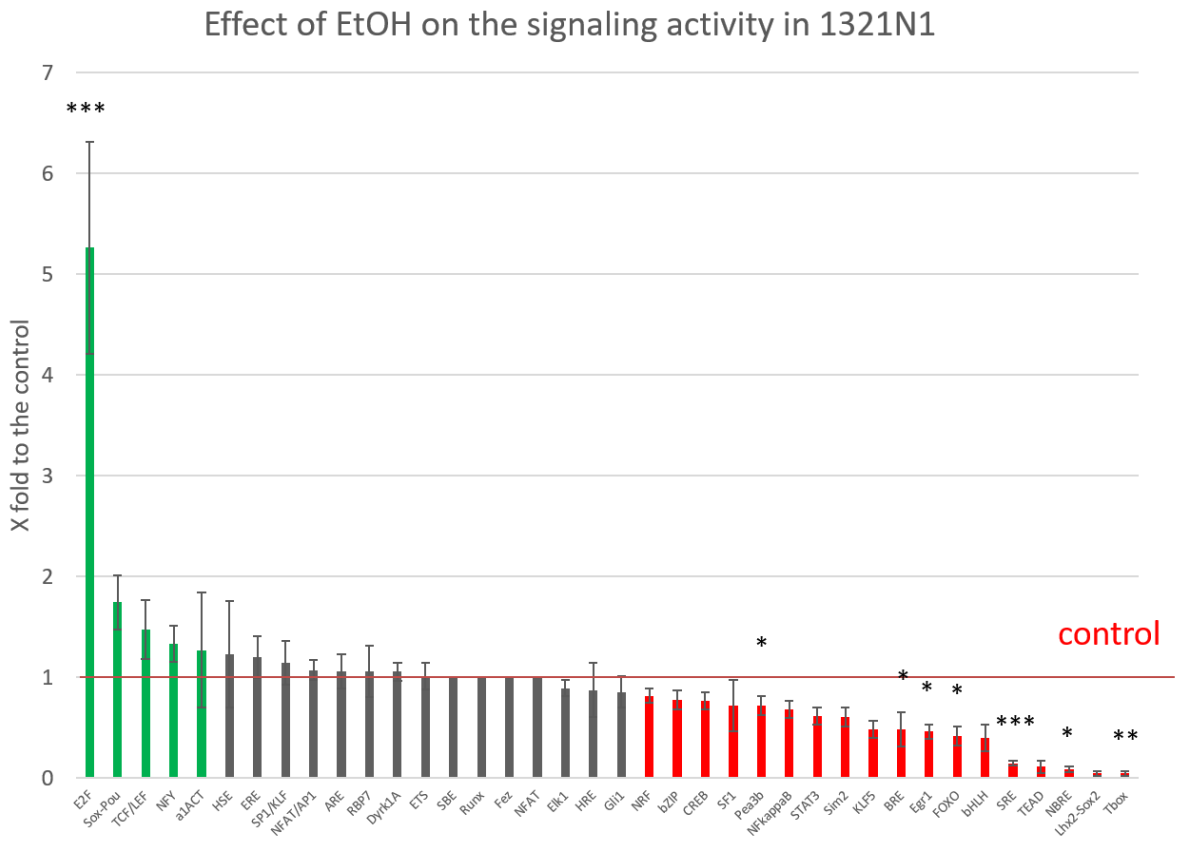

Figure 23: Effect of 0.5% EtOH on the signaling activity in 1321N1. The graph shows the activity of different signaling cascade reporter constructs in 1321N1 astrocytoma cells incubated with serum-reduced media compared to 0.5% ethanol treated cells. The values are shown as x time upregulation compared to the control cells. (n = 4; ± SEM; One-way-Anova: * $p \leq 0.05$; ** $p \leq 0.001$; *** $p \leq 0.001$; **** $p \leq 0.0001$)

After the basic activity level and the effect of 0.5% ethanol was analyzed, the effect of erinacine C on the reporter construct activity was classified to elucidate the response of the astrocytoma cells to erinacine C on the transcriptional level followed by incubation in serum-reduced media as control, with 0.5% ethanol as additive to include a solvent control and erinacine C for 24h. After this incubation time the cells were lysed and the luciferase activity was determined. Figure 24 shows the x fold increase compared to the ethanol control. Clearly, activated firefly luciferase expression compared to the ethanol control were visible, such as: ERE (estrogene responsive element; 2.7 ±0.8), FOXO (forkhead-Box-Protein O; 2.3 ±0.7), NFY (nuclear transcription factor Y; 2.2 ±0.7), NBRE (nuclear receptor binding respond element; 2.2 ±0.5), ETS (E-twenty six (ETS) signaling; 2.1 ±0.5), Tbox (2 ±0.7), Gli1 (Zinc finger protein GLI1, hedgehog signaling; 1.9 ±0.4), NFkappaB (nuclear factor 'kappa-light-chain-enhancer' of activated B-cells; 1.8 ±0.4), STAT3 (signal transducer and activator of transcription 3; 1.8 ±0.3), BRE (BMP responsive element; BMP signaling; 1.7 ±0.5), HRE (hypoxia responding element; hypoxia; 1.6 ±0.7), Elk1 (ETS like protein 1; E-twenty six (ETS) signaling; 1.5 ±0.2), bHLH (basic helix-loop-helix motif; 1.4 ±0.3), Pea3b (fibroblast growth factor (FGF) signaling;

1.4 ±0.2) and KLF5 (Krueppel-like factor 5; epidermal growth factor (EGF) signaling; 1.3 ±0.4). A significant increase in the firefly luciferase activity was detected for: ERE, ETS, Gli, STAT3, Elk1 and Pea3B.

On the other hand some transcription factor binding sites did not respond with alteration in luciferase expression levels, such as: Dyrk1A (binding site for Dual-specificity tyrosine phosphorylation-regulated kinase 1A; Dyrk1A mediated signaling; 1.3 ±0.2), CREB (cAMP response element-binding protein; 1.2 ±0.3), Sim2 (Single-minded homolog 2; 1.2 ±0.2), TEAD (TEA domain family member; Yes-associated protein (YAP) and transcriptional coactivator with PDZ-binding motif (TAZ) signaling; 1.2 ±0.5), SRE (serum-respond element; 1.2 ±0.3), Lhx2-Sox2 (LIM homeobox gene and SoxB1 related family members; 1.18 ±0.5), a1ACT (alpha-1-antichymotrypsin; 1.1 0.4), Egr1 (early growth response protein 1; 1.1 ±0.1), bZIP (basic leucine zipper; 1.0 ±0.2), HSE (heat shock element; 1.0 ±0.3), NRF (nuclear respiratory factor; reactive oxygen species (ROS) signaling; 1.0 ±0.1), SP1/KLF (Sp1-like/Kruppel-like factors; 1.0 ±0.2), NFAT/AP1 (nuclear factor of activated T cells co-binding site with the activator protein 1; NFAT signaling; 1.0 ±0.1), ARE (antioxidant response element; antioxidant signaling; 0.9 ±0.2) and E2F (0.9 ±0.2). In addition a number of transcription factor binding sites mediated a downregulation of firefly expression upon erinacine C exposure like: Sox-Pou (0.7 ±0.1), SF1 (steroidogenic factor 1; 0.7 ±0.3), RBP7 (retinol binding protein 7; Notch signaling; 0.6 ±0.3) and TCF/LEF (transcription factor/lymphoid enhancer-binding factor 1; Wnt signaling; 0.5 ±0.1). It has be to mentioned at this timepoint, that some bindings site did not result in any expression of firefly luciferase, even after erinacine C incubation, like: SBE (Smad-binding elements), Runx (runt-related transcription factor 1), Fexf2 (Fez signaling) and NFAT (nuclear factor of activated T-cells).

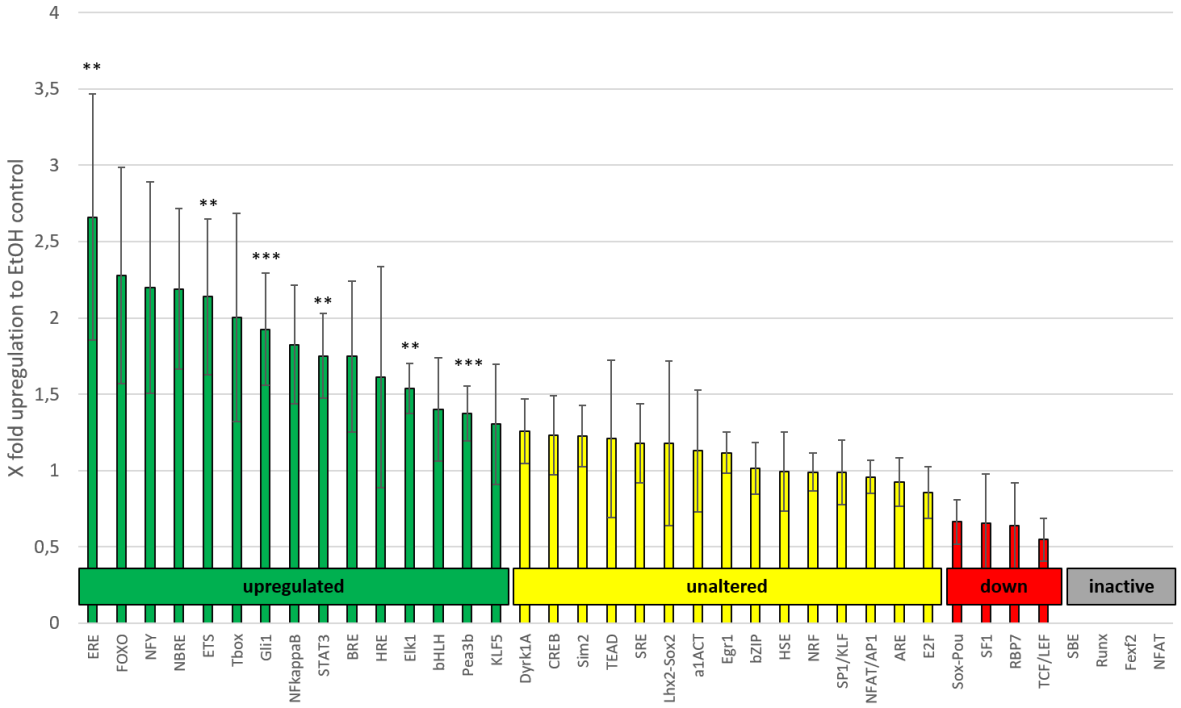

Figure 24: Effect of erinacine C on the activity of reporter constructs with transcription factor binding sites driving firefly luciferase expression in 1321N1. The graph shows the activity of different reporter constructs in 1321N1 astrocytoma cells incubated with 0.5% ethanol onto serum-reduced media compared to erinacine C treated cells. The values are shown as x fold upregulation compared to the 0.5% ethanol treated cell. (n = 4; ± SEM; One-way-Anova: * $p \leq 0.05$; ** $p \leq 0.001$; *** $p \leq 0.001$; **** $p \leq 0.0001$)

The results suggest that treatment of astrocytoma cells with erinacine C causes a profound change in their transcriptional activity. Several constructs for transcriptional activation were significantly increased in their firefly luciferase expression, like ETS, Gli1, STAT3, Elk1 and Pea3B. Since several times the conserved sequence of ETS is highly activated upon erinacine C treatment (in ETS, Elk1 and Pea3B), a prominent member to analyze was the ETS-mediated signaling cascades. In order to characterize the ETS signaling more in detail further analysis will be done.

3.2.2 Analysis of ETS signaling

The ETS transcription factor family is a highly conserved group of helix-turn-helix DNA binding factors (Lee *et al.*, 2005). These transcription factors are the major downstream effectors of the Ras-MAPK signaling cascades (Tetsu and McCormick, 2017). Their transcription is regulated by MAPK. In this thesis the effect of erinacine C on ETS mediated expression in 1321N1 astrocytoma cells was analyzed in more detail.

To establish a constitutive activator and repressor of the transcription factor the ETS DNA binding domain was established from cDNA of 1321N1 cells (Figure 25). ETS1 is a prominent member of the ETS transcription family and is constructed by two protein parts: the DNA

binding domain and the transcriptional activation domain. The cDNA of the DNA binding domain was cloned in front and in frame of two different strong transcriptional activator domains derived from the Herpes simplex viral protein VP16 (TA4 and TA2) (Baron *et al*., 1997). These two constructs were used as constitutively active transcriptional activators of ETS downstream signaling. To construct a constitutive repressor plasmid, the cDNA of the ETS1 DNA binding domain was cloned in front and in frame of a strong transcriptional inhibitor domain from NFkappaB termed KRAB, which is thought to mediate its inhibitory activity by DNA methylation. Expression of the transgenes was driven by the CMV promotor included in the pCS2+ expression vector (Rupp *et al*., 1994).

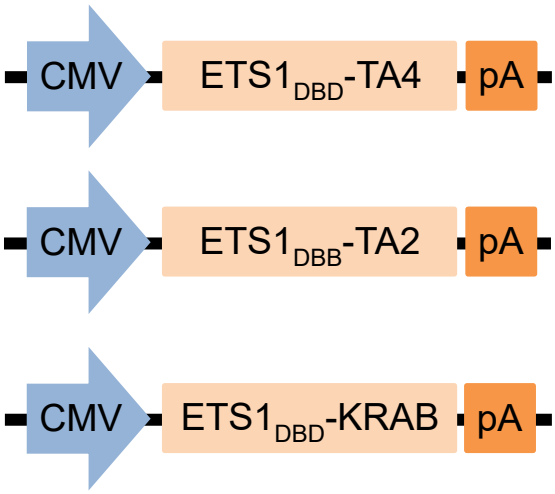

Figure 25: Overview of the different constructs for analysis of the ETS signaling. The constructs contains the cDNA of the DNA binding domain of the transcription factor ETS1 including a nuclear localization signal. This binding site was cloned in front of two transcriptional activator domains of different strength (TA4 and TA2) as well as in front of a KRAB DNA methylating domain. The transgenes are expressed by a CMV promotor.

These constructs were co-transfected with an expression construct containing an 8 times repeat of the ETS binding sites followed by the basal promotor E1b driving firefly luciferase as reporter in 1321N1 astroglial cells. After transfection, the cells co-transfected with the two activators ($ETS1_{DBD}$-TA4 and $ETS1_{DBD}$-TA2) as well as with only the 8xETS luciferase expression vector were treated with serum-reduced media, the cells transfected with only the 8xETS luciferase construct and co-transfected with the KRAB construct were incubated afterwards with 0.5% ethanol and erinacine C and incubated for another 24h. After that, the luciferase expression was measured as described before. When the ETS binding site reporter construct was transfected in astroglial cells, which were afterwards incubated with normal serum-reduced media, ethanol and erinacine C the already described upregulation of ETS mediated transcription was visible (Figure 26A). The control showed an average quotient of luciferase activity of 111 ±15, whereas the ethanol control showed 101 ±7.5. When cells were treated with erinacine C the activity was increased up to 235 ±14.7, which means that there was

a significant average upregulation of 1.9 ±0.2 times compared to the control incubated with serum-reduced media only (Figure 26B). The two activator constructs were co-transfected together with the 8 times ETS binding site luciferase reporter construct in two different ratios of vectors (1:1 and 1:5). When the ETS luciferase reporter construct was transfected with the two activator constructs ($ETS1_{DBD}$-TA4 and $ETS1_{DBD}$-TA2) an increase in the activation of luciferase was observed: TA4 (1:1) 154 ±7.3; TA4 (1:5) 305 ±21; TA2 (1:1) 201 ±6.9; TA2 (1:5) 353 ±30.1 (Figure 26A). The findings lead to the suggestion that TA4 was a weaker transcriptional activator domain, whereas TA2 was a stronger transcriptional activator domain, which has been described before (Baron *et al*., 1997). The above values translate into a fold-activation of (Figure 26B): TA4 (1:1) 1.4 ±0.1, TA4 (1:5) 2.6 ±0.3, TA2 (1:1) 1.9 ±0.2 and TA2 (1:5) 3.1 ±0.5. When different ratios (1:1 and 1:5) of the construct $ETS1_{DBD}$-KRAB were co-transfected and afterwards incubated with serum-reduced media, ethanol and erinacine C, a strong decrease in the activation of the reporter construct was visible (Figure 26A). Once the ETS reporter construct was co-transfected with the $ETS1_{DBD}$-KRAB inhibitor construct using a ratio of 1:1, the luciferase activity in cells incubated with serum-reduced media was decreased down to 5 ±0.1, which was 20 times weaker than in the control cells, which expressed the luciferase reporter construct with 8xETS binding site only (Figure 26B). The activity of the co-transfected cells being incubated with ethanol was 7 ±0.5 and for erinacine C incubated cells 11 ±1.2. The results of the co-transfection with a high amount of ETS inhibitor construct demonstrated the same as for the lower value, which shows that the KRAB domain exhibits a strong transcriptional inhibition activity. These findings suggest that the binding site indeed

responds to ETS binding and transcriptional activation and erinacine C is not able to increase ETS signaling when the ETS dependent transcription is inactivated.

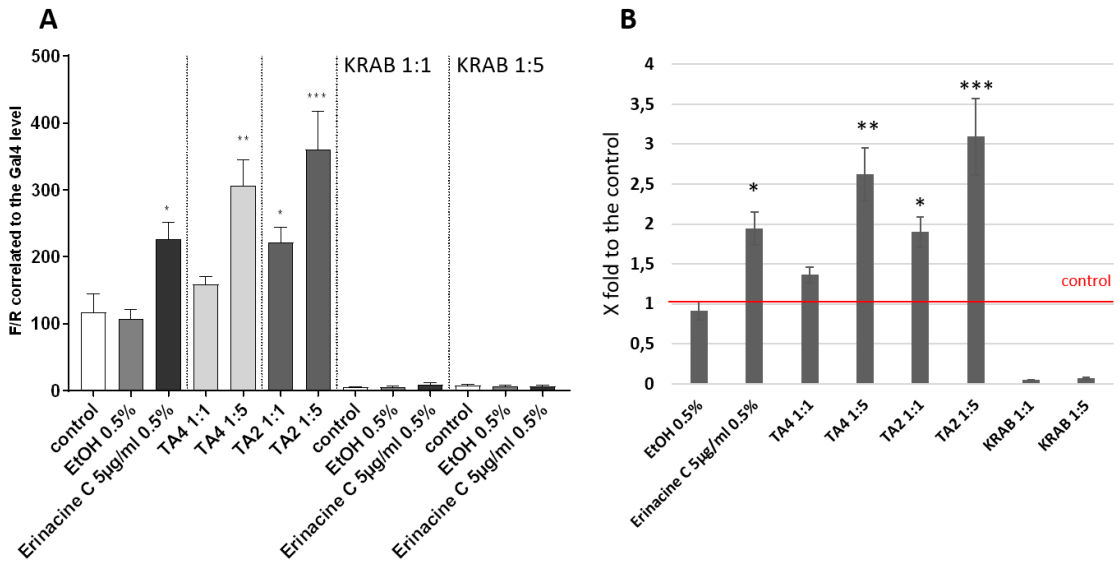

Figure 26: Effect of constitutive ETS activator and inactivator expression on ETS luciferase reporter. A) The graph shows the quotient of the firefly luciferase activity, which was calculated to the standard quotient of ubiquitous expressed firefly luciferase activity to the renilla luciferase activity. Later on, the values were correlated to the background level of the luciferase activity elicited by UAS binding site reporter. The first three bars show 1321N1 astrocytoma cells transfected only with an 8 times repeat ETS binding site firefly luciferase reporter construct. These cells were incubated with control (serum-reduced media), ethanol (0.5% ethanol) and erinacine C. An increase of the activity when these cells were incubated with erinacine C (5 µg/ml) is visible. The bars four and five show a co-transfection with the first activator construct ($ETS1_{DBD}$-TA4) in two different ratios (1:1 binding site reporter to activator and 1:5). With the 1:5 ratio a significant upregulation of 2.5 times can be seen. The bars six and seven relate to a co-transfection with the second activator ($ETS1_{DBD}$-TA2) in the same two ratios. A significant upregulation is visible for both ratios. The bars eight, nine and ten and the three bars afterwards demonstrate two values of the repressor of ETS both incubated with serum-reduced media (control), ethanol (0.5%) and erinacine C. A strong activity decrease is noticable. The second graph shows a x fold upregulation compared to the control, which are cells transfected with the 8xETS luciferase construct and incubated afterwards with serum-reduced media only. Incubation with erinacine C (5 µg/ml) causes a significant upregulation as well as with the two activators constructs (as described before). With the $ETS1_{DBD}$-KRAB repressor the activity is decreased instead. (n = 4; ± SEM; One-way-Anova: * $p \leq 0.05$; ** $p \leq 0.001$; *** $p \leq 0.001$; **** $p \leq 0.0001$)

The next step was the quantification of the upregulation of ETS signaling upon erinacine C incubation. First, the time-dependent upregulation of ETS-binding site mediated luciferase activity and this ETS-mediated transcriptional activation upon erinacine C exposure was analyzed (Figure 27). Consequently, 1321N1 astrocytoma cell were transfected with 8 times repeat of the ETS binding sites construct driving firefly luciferase expression. 48 h after the transfection the cells were incubated with 0.5% ethanol and erinacine C (5 µg/ml). The luciferase activity was measured after 3, 6, 10, 16 and 24h of erinacine exposure. There was no significant upregulation in the luciferase activity after 3h (1.5 ±0.2 times compared to the ethanol control), 6h (1.1 ±0.2), 10h (1.2 ±0.2) and 16h (1.4 ±0.4) of incubation with erinacine C but a trend forwards increasing luciferase activity was observed. Yet, after 24h of incubation with erinacine C the luciferase activity was significantly increased by 2.7 ±0.6 fold compared to the ethanol control. These results showed that erinacine C induced upregulation of ETS

mediated transcription was time-dependent and started after about 24h of incubation with the compound.

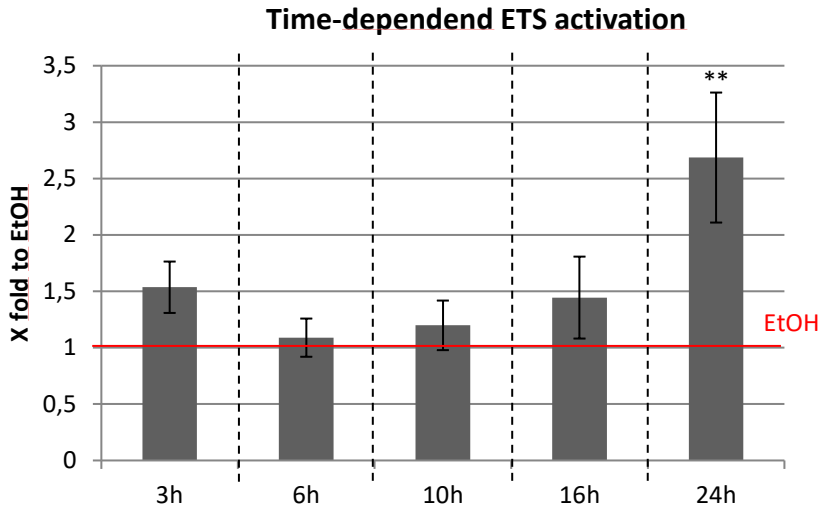

Figure 27: Time-dependent activation of ETS-mediated transcription by erinacine C. The graph shows 1321N1 astrocytoma cells, which were transfected with the 8 time repeat of ETS DNA binding sites driving firefly luciferase expression and incubated after transfection with either 0.5% ethanol or erinacine C (5 µg/ml). The bars display an x fold upregulation compared to the ethanol control (0.5%). (n = 4; ± SEM; One-way-Anova: * $p \leq 0.05$; ** $p \leq 0.001$; *** $p \leq 0.001$; **** $p \leq 0.0001$)

After analysis of the time-dependent upregulation of ETS-mediated firefly luciferase reporter expression, the concentration dependence of erinacine C induced ETS-mediated firefly luciferase transcription was analyzed (Figure 28). Hence, the 8 times repeat of ETS DNA binding site luciferase construct was transfected into 1321N1 astrocytoma cells, which were subsequently incubated either with ethanol or erinacine C in different concentrations (1 µg/ml – 15 µg/ml) (Figure 28A). At this timepoint it has to be mentioned that a new batch of purified erinacine C was used containing a higher amount of erinacine C, which was diluted in ethanol. The highest non-toxic concentration was measured again using a MTT-assay. The non-toxic concentration changed in its value up to 20 µg/ml. Possibly, cytotoxicity was reduced because of the increased purity of the compound. At this timepoint a higher amount of erinacine C was added on the cells (now up to 15 µg/ml). Therefore, it was shown that with increasing concentrations of erinacine C the ETS-mediated luciferase expression and thus the resulting luciferase activity was also increased compared to the ethanol control (1 µg/ml 1.2 ±0.2; 2 µg/ml 1.3 ±0.3; 3 µg/ml 1.7 ±0.3; 4 µg/ml 1.9 ±0.3) up to a significant average upregulation of 2.9 ±0.9 fold. Using concentration higher than 5µg/ml the luciferase activity decreased down to an average value of 0 (10 µg/ml 1.6 ±0.5; 15 µg/ml 0.005 ±0.001), probably caused by an adverse effect of erinacine C. To analyze if the concentration dependence was also responsive to increasing amounts of ETS-DNA binding sites, different constructs containing an increasing

amount of ETS binding sites (2 – 8x) followed by a basal promotor driving firefly luciferase as reporter were transfected into 1321N1 astrocytoma cells. After the transfection the media was exchanged by media containing either 0.5% ethanol or erinacine C at two different concentrations 3 and 5 µg/ml respectively. With an increasing amount of ETS binding sites the luciferase activity of this enzyme increased indicating elevated expression levels of luciferase as shown in Figure 28B. Also, increasing concentrations of erinacine C, raised the activity of luciferase of constructs containing the same number of ETS binding sites in front of the luciferase. In detail, when a 2 times ETS binding site reporter plasmid was transfected the quotient of firefly to renilla luciferase activity was 1.2 ±0.2 for 3µg/ml and 1.6 ±0.2 for 5µg/ml. With the double amount of binding sites (4x) the luciferase activity increased further (3 µg/ml 1.7 ±0.3; 5 µg/ml 2.1 ±0.2). With 6 and 8 repeats of the ETS consensus binding site the luciferase activity was increased even further (6 times: 3 µg/ml 2.1 ±0.2, 5 µg/ml 2.1 ±0.4; 8 times: 3 µg/ml 2.6 ±0.1, 5 µg/ml 3.3 ±0.7). This allows one to conclude that with rising concentrations of erinacine C the ETS-mediated transcription was enhanced similarly to an increasing amount of ETS consensus binding sites.

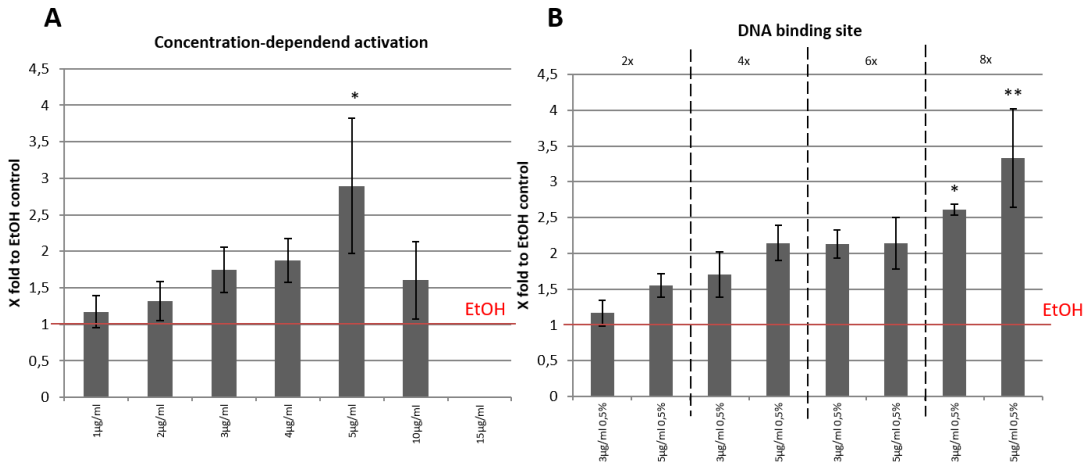

Figure 28: Concentration-dependent activation of ETS signaling by erinacine C. A) The graph shows the concentration dependence of the ETS mediated luciferase activity when increasing concentrations of erinacine C were added to 8x ETS reporter transfected astroglial cells, shown here as x fold upregulation compared to the ethanol control. The ethanol concentration in all experiments was 0.5%. With increasing concentrations of erinacine C the ETS-mediated expression increased as well. The highest activity was recognized with erinacine C concentrations of 5µg/ml leading to a significant upregulation of around 3-fold in expression and thus enzymatic activity of luciferase. B) The graph shows the dependence of luciferase expression in respect to increasing numbers of ETS DNA binding sites in the firefly luciferase reporter construct. In all experiments the same concentration of erinacine C (3 µg/ml and 5 µg/ml) was added. With an increasing amount of ETS DNA binding sites, the activity increased as well. (n = 4; ± SEM; One-way-Anova: * $p \leq 0.05$; ** $p \leq 0.001$; *** $p \leq 0.001$; **** $p \leq 0.0001$)

It was shown that the ETS mediated luciferase activity increased upon erinacine C incubation suggesting that the upregulation of this reporter is indeed mediated by ETS transcription factor

binding and activation of expression. Using constitutive ETS activator and repressor variants it was possible to activate and inactivate ETS dependent luciferase activity. With increasing concentrations of erinacine C it was possible to increase the luciferase activity mediated by ETS signaling as well. This consistently argues for endogenous ETS mediated transcription activation of gene expression induced in astrocytoma cells by erinacine C. And with increasing numbers of ETS DNA binding sites the luciferase activity could also be increased.

3.2.3 Analysis of the connection between neurotrophin upregulation and ETS signaling

All findings shown until now, lead to the idea that ETS-mediated transcriptional activation and neurotrophin upregulation by erinacine C were connected. The two possibility was characterized now: The first possibility is that ETS transcriptional activation is connected to the shown *ngf* and *bdnf* induction of expression. The other possibility is that the activation of *ets* transcription is completely independent to the activation of the expression of the two neurotrophins. To quantify the potential connection between induced ETS signaling and *ngf* or *bdnf* upregulation upon erinacine C incubation, first the temporal relation between both processes were analyzed.

Thus, time-dependent mRNA upregulation was examined by semiquantitative RT-PCR. Therefore, 1321N1 astrocytoma cells were incubated with serum-reduced media, ethanol or erinacine C and after 3, 6, 10, 16, 24, 32 and 48h the RNA of these cells was isolated to perform a RT-PCR for *gapdh* (as control), *ngf* and *bdnf* mRNA. The results for each time point and each treatment were correlated to the mRNA level of the housekeeping gene *gapdh*. The control, which were cells incubated with serum-reduced media for 48h, was set to 1. The amplified cDNA amounts were shown as x-fold upregulation compared to this control (Figure 29). The *ngf* mRNA level of cells being incubated with 0.5% ethanol as additive did not show a major difference compared to the control cells, being incubated with serum-reduced media (1.1 ±0.1). When the cells were incubated with erinacine C, the *ngf* mRNA levels were increased during the incubation periods (3h 1.9 ±0.1, 6h 2.5 ±0.2, 10h 2.3 ±0.3, 16h 2.3 ±0.3, 24h 3.2 ±0.5, 32h 3.6 ±0.5, 48h 9.8 ±3.8), starting with a significant upregulation after 6h and the highest peak after 48h of erinacine C incubation. A significant upregulation of *bdnf* mRNA was observed only after 48h of erinacine C incubation with an increase of 5.8 ±2.5 fold compared to the control. At shorter incubation periods a trend towards *bdnf* mRNA upregulation was seen, yet it was statistically not significant until 48h of incubation times was reached (3h 1.1 ±0.005, 6h 1.2 ±0.004, 10h 0.9 ±0.005, 16h 0.9 ±0.004, 24h 1 ±0.003, 32h 1.3 ±0.005). Changes in *ets1*

mRNA levels differed a bit from these results shown for *ngf* and *bdnf* mRNA. During the first 6h there was an increase of *ets1* mRNA starting at 3h (1.3 ±0.2) until a significant peak was visible after 6h of erinacine C incubation with a 7.1 ±1.6 times upregulation compared to the control. After this peak the *ets1* mRNA level dropped down again (10h 2.7 ±0.5, 16h 1.6 ±0.3, 24h 1.8 ±0.4), followed by a weaker increase starting at 32h with a 2.5 ±0.2 fold upregulation. The *ets1* mRNA upregulation remained consistent until 48h (2.3 ±0.2). In summary the results, showed that *ngf* mRNA was significantly upregulated starting 6h after onset of incubation with erinacine C. The mRNA amount increased steadily until 48h of incubation. The first significant *ngf* mRNA upregulation was seen at the same time, when *ets1* mRNA reached its highest elevation. The influence of erinacine C on *bdnf* mRNA production was not so drastic. The first significant upregulation of *bdnf* mRNA was visible after 48h of incubation. The highest rise in the *ets1* mRNA production was seen already after 6h of erinacine C incubation. Afterwards, the ETS production decreased, but stayed significantly upregulated until 10h of incubation. In addition, a second smaller, but also significant upregulation in the *ets1* mRNA expression occurred after 32h of erinacine C incubation and remained stable until 48h of incubation (Figure 29).

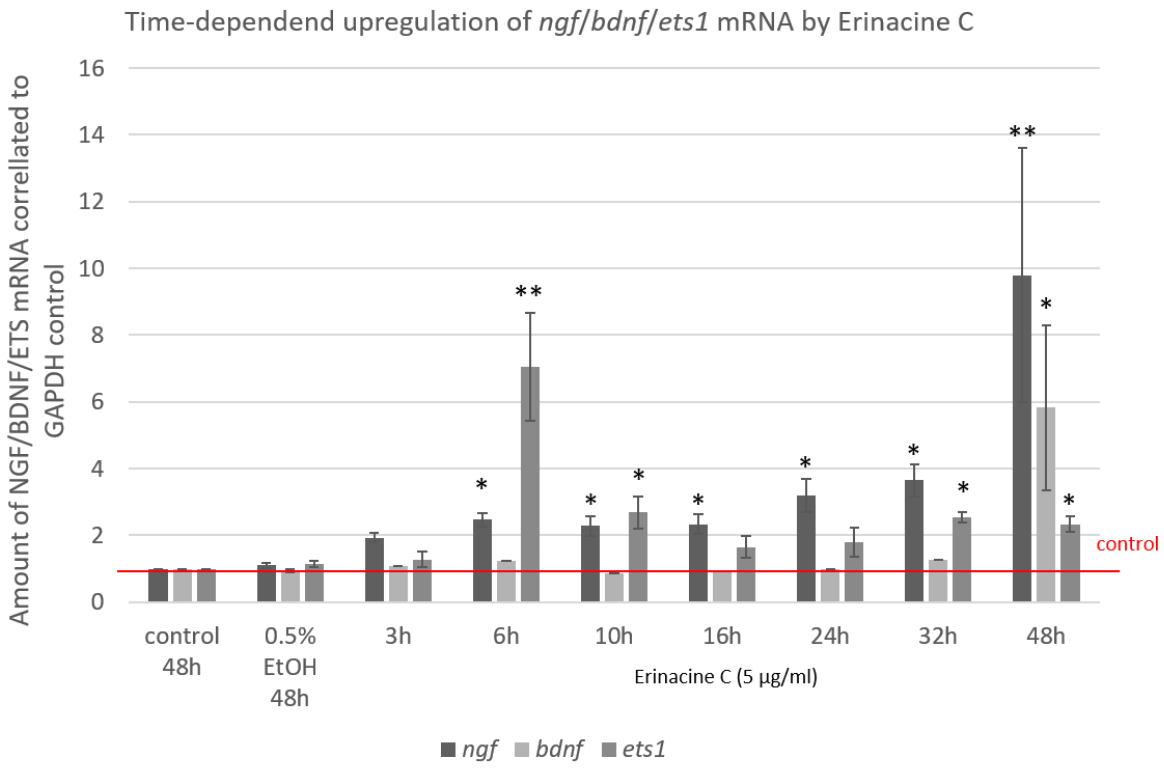

Figure 29: Time-dependent upregulation of *ngf*, *bdnf* and *ets1* mRNA by erinacine C. 1321N1 astrocytoma cells were incubated with normal serum-reduced media, ethanol or erinacine C. After 3h, 6h, 10h, 16h, 24h, 32h and 48h incubation periods the mRNA was isolated, and the mRNA levels were quantified using semiquanitative RT-PCR. The graph shows the respective mRNA levels correlated to the *gapdh* (loading control) control. The amount for serum-reduced media incubated cells is set to 1 as reference. The dark bars represent the *ngf* mRNA levels. Control and ethanol show no difference. The first

significant increase of *ngf* mRNA levels are visible after 6h of erinacine C incubation with around 2.3 times upregulation. The *ngf* mRNA amounts increase until 48h when erinacine C mediated mRNA upregulation is significant increase of around 10 fold is recognized. The bright bars show the *bdnf* mRNA levels. A significant increase is only visible after 48h of erinacine C incubation compared to the control. The bars to the right show the *ets1* mRNA levels which display two peaks of increase. The first peak becomes visible at 6h of incubation until 10h, the second peak occurs at 32h until 48h. (n = 4; ± SEM; One-way-Anova: * $p \leq 0.05$; ** $p \leq 0.001$; *** $p \leq 0.001$; **** $p \leq 0.0001$)

In comparison, *ets1* mRNA levels in 1321N1 cells rise before an upregulation of *ngf* and *bdnf* mRNA occurs in response to erinacine C exposure. To ask whether the activity of ETS signaling was sufficient for neurotrophin production, like NGF and BDNF, the already introduced constructs of constitutively active ETS signaling ($ETS1_{DBD}$-TA4 and $ETS1_{DBD}$-TA2) were used and transfected using electroporation in 1321N1 astrocytoma cells. Electroporation was used to obtain a high percentage of transfected astroglial cells up to 85%. After transfection, the media was changed to serum-reduced media and the cells were incubated for another 48h. After this incubation period the supernatant conditioned by the transfected astrocytoma cells was added to PC12 cells, to analyze the ability of this medium to induce PC12 cell differentiation. As control, PC12 cells were also incubated with serum-reduced media (negative control), and with 200 ng/ml recombinant NGF (positive control). The PC12 cells were then incubated for 48h. The results are shown as brightfield pictures (Figure 30). The control picture shows PC12 cells in their normal round shape of undifferentiated cells. When NGF was added to these cells, the cells got protrusions showing initiation of differentiation. The PC12 cells, which were incubated with the conditioned media of astroglial cells transfected with the ETS activator constructs, $ETS1_{DBD}$-TA4 and $ETS1_{DBD}$-TA2, showed no sign of neurite outgrowth, suggesting that both constructs were not able to induce *ngf* transcription and thus NGF synthesis and secretion in astroglial cells and thereby were not able to induce PC12 cell differentiation.

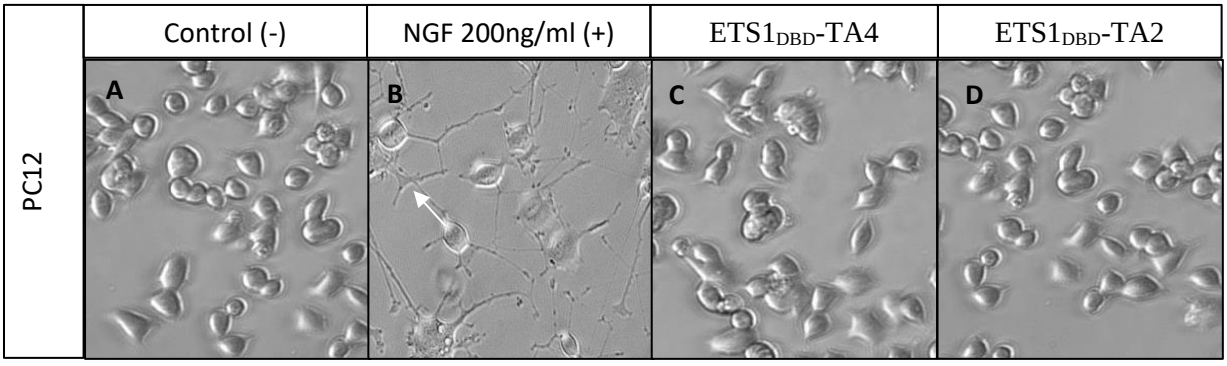

Figure 30: Effect of supernatant conditioned by 1321N1 cells transfected with elevated ETS transcriptional activators. The images show PC12 cell differentiation upon addition of conditioned media of $ETS1_{DBD}$-TA4 and $ETS1_{DBD}$TA2 transfected 1321N1 astrocytoma cells. A) The first picture control cells represent PC12 cells incubated with normal serum-reduced media. B) PC12 cells incubated with the positive control of recombinant human NGF (200 ng/ml). Here, PC12 cells show the characteristic sign of differentiation (white arrow). C) and D) PC12 cells are incubated with conditioned media of 1321N1 astrocytoma cells transfected with C) $ETS1_{DBD}$-TA4 and D) $ETS1_{DBD}$TA2 respectively. In both approaches no sign of differentiation are visible.

To investigate whether ETS-mediated transcriptional activation is necessary for ngf and bdnf expression or if erinacine C activates ets1 transcription independently of inducing neurotrophin expression, different inhibitors for signaling cascades acting upstream of ETS were employed. 1321N1 astrocytoma cells were incubated with serum-reduced media supplemented with either 0.5% ethanol, erinacine C (5 µg/ml), or with erinacine C in addition to different inhibitors prohibiting MAPK signaling (PD98059) or Erk1/2 (U0126) signaling (Figure 31). These inhibitors were chosen because MAPK and Erk1/2 usually work upstream of the ETS transcription factor (Liu *et al*., 2018). After treatment for 48h, the RNA was isolated and semiquantitative RT-PCR for *gapdh* (as control), *ngf* and *bdnf* mRNA was performed. The value of amplified cDNA from 1321N1 astrocytoma cells that were incubated with 0.5% ethanol only was set to 1 as reference. The results are shown as x fold upregulation to the ethanol control. When the 1321N1 astrocytoma cells were incubated with erinacine C a significant upregulation of the *ngf* mRNA of 3.7 ±0.7 and *bdnf* mRNA of 1.5 ±0.2 was observed. When different inhibitors, for MAPK signaling (PD98059) and Erk1/2 signaling (U0126), were added, the amounts of *ngf* mRNA were weakly but not significantly decreased compared to erinacine C only treatment (+PD98059 3 ±0.4; +U0126 2.8 ±0.08; +PD98059+U0126 2.7 ±0.3). This is also true *bdnf* mRNA levels (+PD98059 1.6 ±0.6; +U0126 1.8 ±0.5; +PD98059+U0126 1.5 ±0.5). In conclusion, erinacine C induced an upregulation of *ngf* and *bdnf* mRNA levels, as described before; and this increase was not affected whether by inhibiting MAPK nor Erk1/2 activity. The same was observed when both inhibitors were applied together. This suggested that erinacine C induces neurotrophin expression independently of increasing *ets1* transcription.

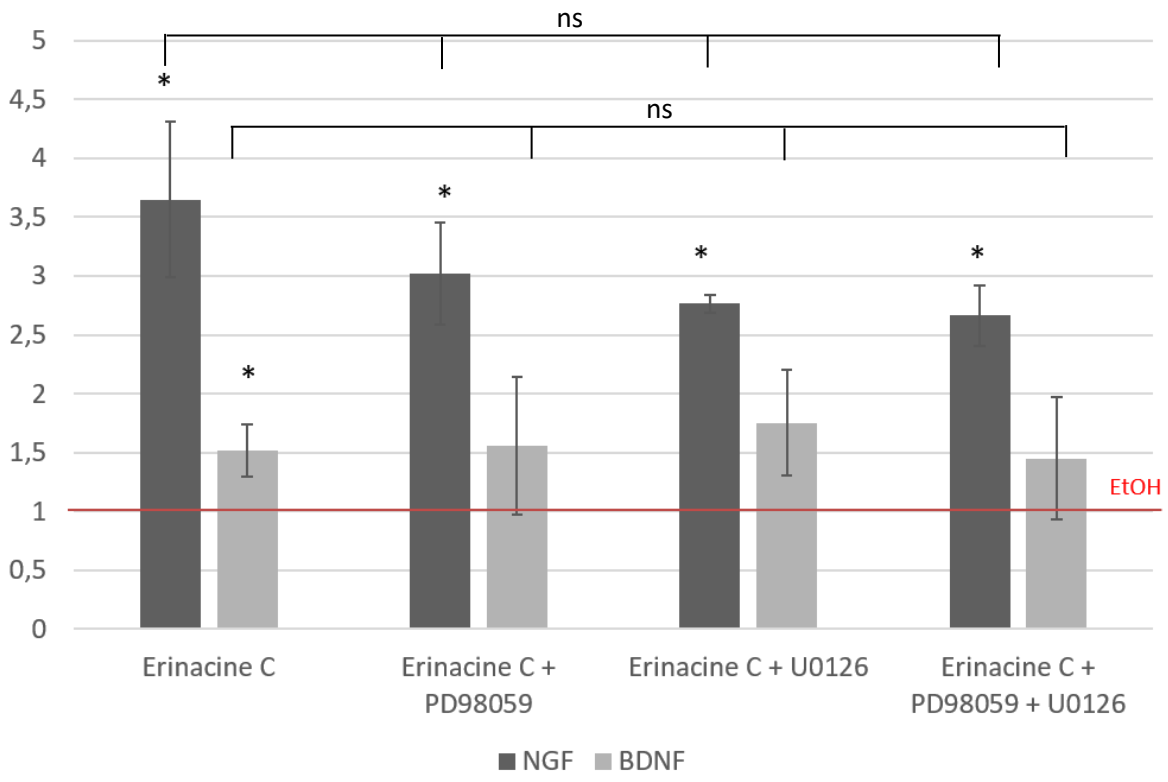

Figure 31: Pharmacological inhibition of MAPK signaling and Erk1/2 signaling does not affect erinacine C mediated induction of *ngf* and *bdnf* transcription. 1321N1 astrocytoma cells were incubated with ethanol, erinacine C or erinacine C with different inhibitors in addition. After incubation for 48h semiquantitative RT-PCR was performed for *ngf* or *bdnf* mRNA and correlated to *gapdh* mRNA amounts as reference. The solvent control where cells were incubated with ethanol was set to 1. Here the x times upregulation compared to the solvent control is shown. When incubated with erinacine C (5µg/ml in 0.5% ethanol) the average *ngf* mRNA was upregulated 3.5-fold and the average *bdnf* level was upregulated by 1.5 fold. When incubated with different inhibitors like PD98059 for MAPK and U0126 to impair Erk1/2 activity there was no significant difference to erinacine C only upregulation of neurotrophin transcription. (n = 4; ± SEM; One-way-Anova: * $p \leq 0.05$; ** $p \leq 0.001$; *** $p \leq 0.001$; **** $p \leq 0.0001$)

To further corroborate this finding, 1321N1 astrocytoma cells were transfected with the different activator and repressor constructs ($ETS1_{DBD}$-TA4, $ETS1_{DBD}$-TA2, $ETS1_{DBD}$-KRAB and as control vector the plasmid pBluescriptII SK (pSK)) using electroporation. In comparison to the transfection method, which was used before, electroporation yielded a higher transfection efficiency of 80-85% cells, versus 20-25% of transfected cells obtained by lipofection. After transfection, the media was exchanged to serum-reduced media for the $ETS1_{DBD}$-TA4 and $ETS1_{DBD}$-TA2 construct, and to serum-reduced media, ethanol or erinacine C for the control and the $ETS1_{DBD}$-KRAB transfected cells. The cells were incubated for another 48h. After this period the RNA was isolated and semiquantitative RT-PCR for *gapdh* (as control), *ngf* and *bdnf* cDNA was performed. In Figure 32A, values for RNA isolated from ethanol treated cells was used as reference and were set to 1. The values are displays as x fold upregulation compared to the ethanol control. When cells were transfected with the vehicle (pSK) and afterwards treated with erinacine C the already described significant upregulation of *ngf* (2.8 ±0.5 fold compared to the ethanol control) and *bdnf* mRNA (1.5 ±0.3 fold compared to the ethanol control) was

visible. When the cells were transfected with the ETS1$_{DBD}$-KRAB construct, the DNA downstream of ETS1 binding site are supposed to be methylated (Ma et al., 2014). The semiquantitative RT-PCR showed that the *ngf* (3 ±0.2 fold compared to the ethanol control) and *bdnf* mRNA levels (1.6 ±0.2 fold compared to the ethanol control) were not downregulated upon erinacine C incubation in the presence or absence of ETS1$_{DBD}$-KRAB inhibitor. In Figure 32B, RNA isolated from cells incubated with serum-reduced media was used in semiquantitative RT-PCR reactions as reference and set to 1. When the cells were transfected with a vehicle (pSK) and afterwards incubated with erinacine C, the cDNA levels for *ngf* (2.8 ±0.5 times) and *bdnf* (1.5 ±0.3 times) were upregulated compared to the control. Once, the cells were transfected with either one or both of the activator constructs (ETS1$_{DBD}$-TA4 and ETS1$_{DBD}$-TA2), there was no significant upregulation of *ngf* (TA4: 1.4 ±0.4 times; TA2: 1.5 ±0.5 times) or transcription of *bdnf* mRNA (TA4: 0.7 ±0.2 fold; TA2: 0.5 ±0.2 fold) compared to the control. Surprisingly, the *bdnf* mRNA level seemed to be slightly but not significantly downregulated. This led to the proposal that inhibition of ETS activity by using the ETS1$_{DBD}$-KRAB construct is not sufficient to decrease the neurotrophin expression upregulation upon erinacine C treatment, suggesting that *ets1* transcription upregulation is not causing the upregulation of the neurotrophin expression. The results shown for the two activators support this idea was supported.

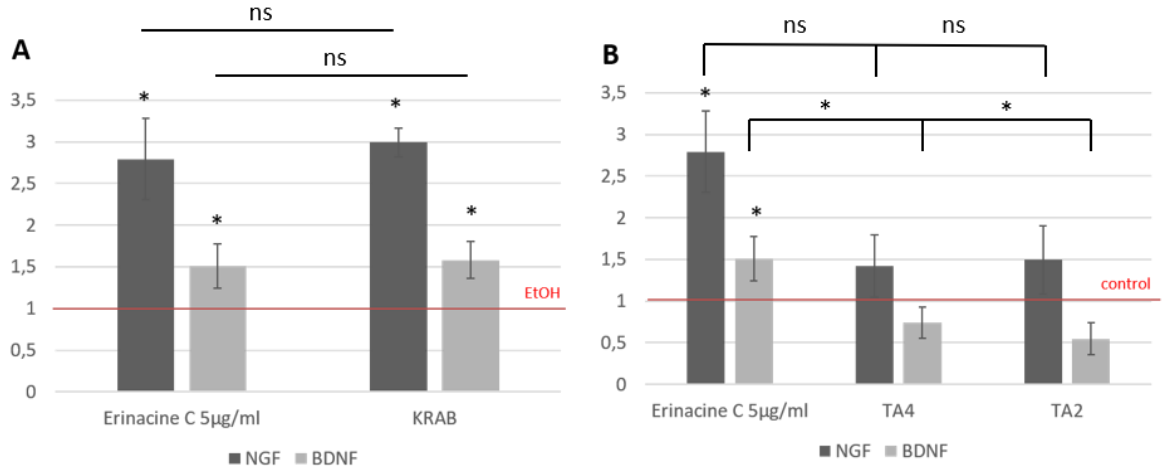

Figure 32: Effect of constitutive ETS1 activation or inhibition in 1321N1 on *ngf* and *bdnf* transcription. 1321N1 astrocytoma cells were transfected with a control plasmid or with the already introduced constructs for constitutive ETS1 transcriptional activation or inhibition. The cells which were transfected with the control were incubated with serum-reduced media as control, ethanol or erinacine C. A) The first graph shows the x times upregulation of *ngf* or *bdnf* compared to the ethanol control whereas the second graph (B) shows the x times upregulation of these neurotrophin mRNAs compared to control cells, which were only incubated with serum-reduced media. An upregulation in the *ngf* and *bdnf* mRNA levels was observed upon incubation with erinacine C. When cells were incubated with the ETS1 inhibitor construct (A) no difference in the upregulation of *ngf* and *bdnf* mRNAs compared to the control transfected cells was obtained. B) After transfection with the different ETS signaling activator constructs (ETS1$_{DBD}$-TA4 and ETS1$_{DBD}$-TA2) the *ngf* and *bdnf* mRNA level were not significantly induced. (n = 4; ± SEM; One-way-Anova: * $p \leq 0.05$; ** $p \leq 0.001$; *** $p \leq 0.001$; **** $p \leq 0.0001$)

Summarizing the results shown in this chapter, it was shown that the mRNA levels, during erinacine C treatment in astroglial cells, of *ngf* mRNA were upregulated within 6h of incubation and reached their highest levels at 48h, whereas the *bdnf* mRNA was upregulated only after 48h erinacine C of treatment. When characterizing a possible dependence of neurotrophin transcription on ETS1 activity, the first mRNA peak of *ets1* mRNA was significantly upregulated after 6h, suggesting that this upregulation had no connection to the first significant upregulation of *ngf* after 6h of erinacine C treatment. Since the mRNA has to be translated and folded until it is active. But it was that the *ets1* upregulation is involved in the highest level of *ngf* mRNA upregulation after 48h of incubation. On the other hand, it is possible that the *ets1* upregulation was involved in *bdnf* mRNA transcription upregulation, since there was the highest level after 48h of erinacine C incubation. But it was suggested that ETS1 is not sufficient to induce neurotrophin transcription, since the transfected activators ($ETS1_{DBD}$-TA4 and $ETS1_{DBD}$-TA2) in 1321N1 cells, were not able to initiate PC12 cells differentiation as well as inducing transcription of the both neurotrophins. When ETS signaling was impaired by different pharmacological inhibitors of regulators of ETS1 activity the transcription of neurotrophins was induced by erinacine C could not be impaired, suggesting that ETS activity has no influence on the *ngf* transcription, but maybe a slight yet not significant influence on *bdnf* transcription. Furthermore, this led to the suggestion that ETS signaling is not necessary for *ngf* transcription, since *ngf* induction by erinacine C could not be inhibited by the constitutive ETS1 inhibitor $ETS1_{DBD}$-KRAB construct. As *ngf* transcription could also not be increased by the different ETS1 activator constructs. ETS1 activity is also not sufficient to induce *ngf* transcription. Therefore, erinacine C induces *ets1* as well as *ngf* and *bdnf* transcription independently from one another.

3.3 Analysis of predicted NGF enhancer region

Another approach, when answering the question about the effect of astrocytoma cells incubation with erinacine C and how the NGF production is upregulated was the analysis of the putative enhancer region of *ngf*. The potential enhancer region of *ngf* in humans or mouse is very complex, as the 5' region contains a large intron. In contrast, the *Tetraodon nigrovirdis* coding region of *ngf* contains only a single exon, suggesting that regulatory elements of *ngf* are possibly located upstream of the coding sequence. The *Tetraodon ngf* region is 88% conserved (shown in Figure 33).

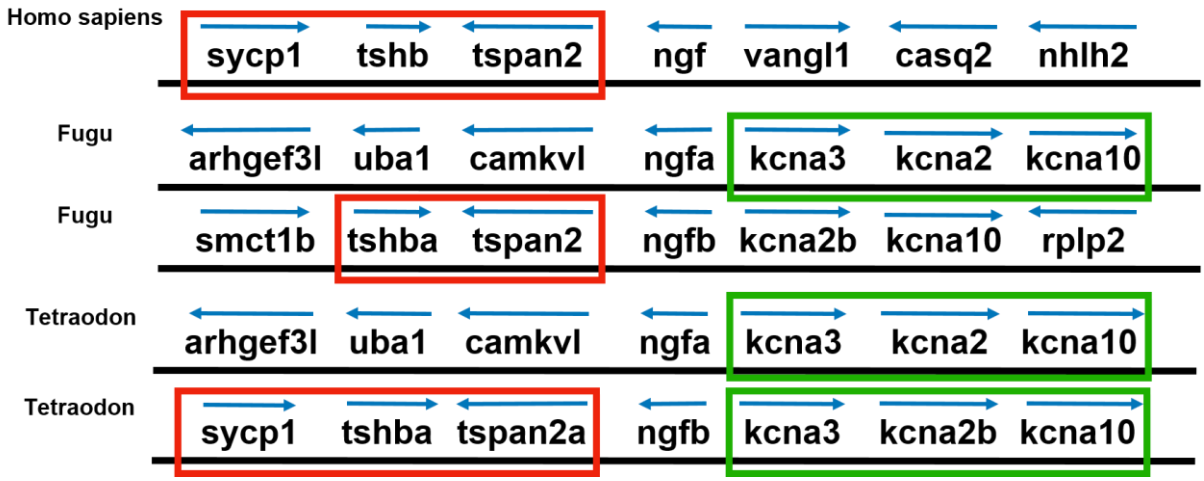

Figure 33: Comparison of the 5' region of humans, *Fugu* and *Tetraodon*. The 5' region of the *ngf* genes are relatively conserved from human to *Tetraodon*, more than to the *Fugu*.

About 2.1kb of genomic DNA directly upstream of the *ngfß* coding sequence from *Tetraodon nigrovirdis* were cloned into a reporter construct containing the open reading frame of firefly luciferase (Figure 34). Successive deletions at the 5' end of this Tetraodon genomic DNA were generated to establish a series of related constructs. In addition, similar several deletions were generated at the 3' end of this genomic DNA fragment. As these deletions likely destroyed the endogenous basal promotor of *ngfß*, the basal promotor E1b was inserted in front of the luciferase encoding cDNA fragment.

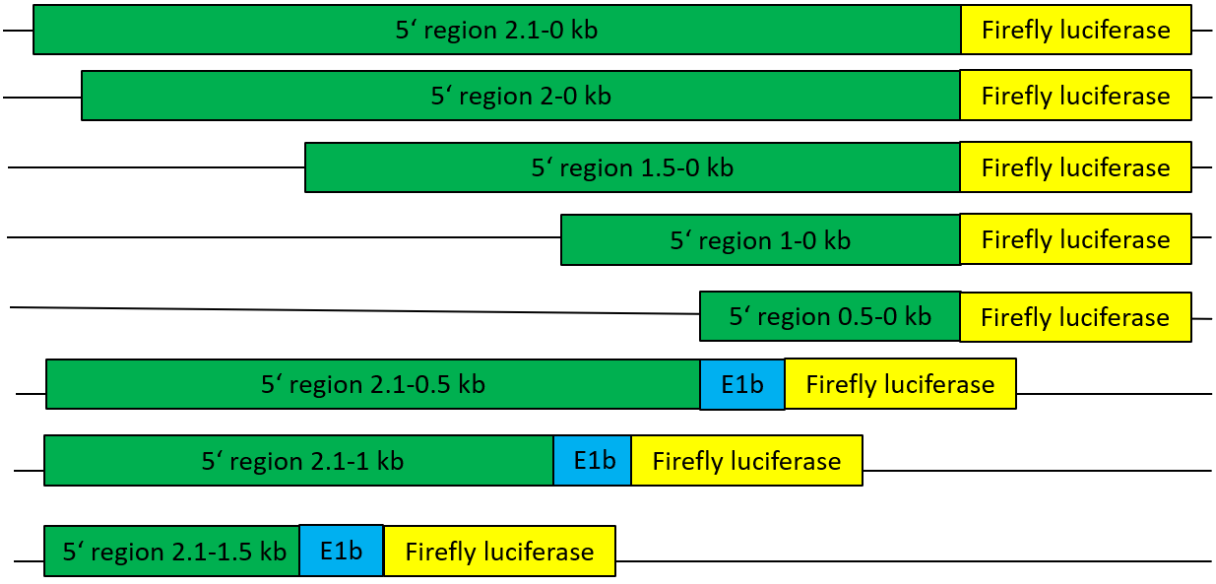

Figure 34: Schematic drawing of serial deletion constructs of the potential *ngfß* enhancer sequence from *Tetraodon nigrovirdis*. The drawing shows different constructs for deleting potential regulatory elements in the 5' region of *ngfß* from *Tetraodon nigrovirdis*. In green the 5' genomic region is marked; the firefly region is depicted in yellow while the E1b basal promotors drown in blue. Constructs are not drawn to scale.

To characterize, if the 5' upstream region of the *Tetraodon ngf* coding sequence was erinacine C responsive and which region would mediate this response luciferase assays were performed.

First, the different reporter constructs were transfected into 1321N1 astrocytoma cells together with the reference vector expressing renilla luciferase. After transfection, cells were incubated with normal serum-reduced media, 0.5% ethanol, or erinacine C (5 µg/ml). After 24h of incubation the expression of the luciferase was quantified by analyzing the respective luciferase activity which is correlated to the induction of luciferase expression (Figure 35). The first graph shows the activity of the firefly luciferase divided by the reference of activated renilla luciferase to correct for different transfection efficiencies. Next, the obtained luciferase activity from an unrelated Gal4-dependent luciferase reporter were deducted to subtract background activity from the ngf reporter value. Finally, the values of the different *ngf* reporter constructs were compared.

The 2.1 kb genomic fragment induced luciferase expression was activated in an erinacine C dependent manner by about 1.7 ±0.2 fold (serum-reduced media 0.71 ±0.05; 0.5% ethanol 0.75 ±0.04; erinacine C 1.31 ±0.2). Upon removal of the first 5' 500bp, the genomic fragment (1.5-0kb) lost its activity to levels of the control, which was drastically reduced (serum-reduced media 0.42 ±0.02; ethanol 0.37 ± 0.2; erinacine C 0.49 ±0.02). When another 500bp of genomic DNA was removed (1-0kb) activity raised again upon erinacine C treatment to 1.6 ±0.2 fold (serum-reduced media 1.1 ±0.2; ethanol 1 ±0.1; erinacine C 1.7 ±0.3). Further reducing the elements from the 5' end down to 500bp no increase upon erinacine C stimulation was observed (serum-reduced media 0.7 ±0.05; ethanol 0.65 ±0.04; erinacine C 0.75 ±0.06).

Next, the reporters were analyzed in which the *ngfß* genomic fragment was stepwise deleted from its 3' ends. When 500bp were removed from the 3' end, the region 2-0.5kb was activated by erinacine C yet to non-significant values (serum-reduced media 0.48 ±0.08; ethanol 0.5 ±0.09; erinacine C 0.63 ±0.1). Similar results were obtained when the 1000bp were removed (serum-reduced media 0.64 ±0.11; ethanol 0.68 ±0.12; erinacine C 1.1 ±0.15). When only the fragment 2-1.5kb was used in the reporter construct, the luciferase activity did not at all respond to erinacine C (serum-reduced media 0.2 ±0.001; ethanol 0.18 ±0.001; erinacine C 0.1 ±0.001). No response to erinacine C was obtained, suggesting that this genomic part does not contain an activator region. This hints of the 1.0kb-500bp fragment to contain an erinacine C responsive element. The second graph displays the respective luciferase activity as fold upregulation compared to the cells being incubated with 0.5% ethanol control (ethanol was set to 1). The highest and significant upregulation was visible for the 2.1-0kb (1.7 ±0.2 fold). Compared to the respective ethanol control the next upregulation was 1.5-0kb (1.6 ±0.2 fold), but as shown before, the activity was drastically lower. The next significant upregulation was 1-0kb (1.7 ±0.2

fold). This was followed by a lack of activation from the 0.5-0kb fragment (1.2 ±0.1 fold), 2-0.5kb (1.5 ±0.4 fold) and 2-1kb (1.4 ±0.3 fold). The last tested fragment 2-1.5kb showed no upregulated activity at all (0.6 ±0.3). This suggest that the both regions 2.0-1.5kb and 1.0-0.5kb contained no elements responsive to erinacine C treatment, while the 1.5-1.0kb fragment harbors a repressive element. Alternatively, the 2.1-1.5kb region contains a repressive function of the 1.5-1.0kb repressor. Apart from that, the constructs containing not the endogenous *ngfß* promotor region, but instead the basal E1b promotor, seemed to be weaker than the constructs, which did not lack the endogenous promotor, suggesting that the endogenous promotor was stronger than the basal E1b promotor. This would lead to a drastically weaker induction of the firefly luciferase expression and activity.

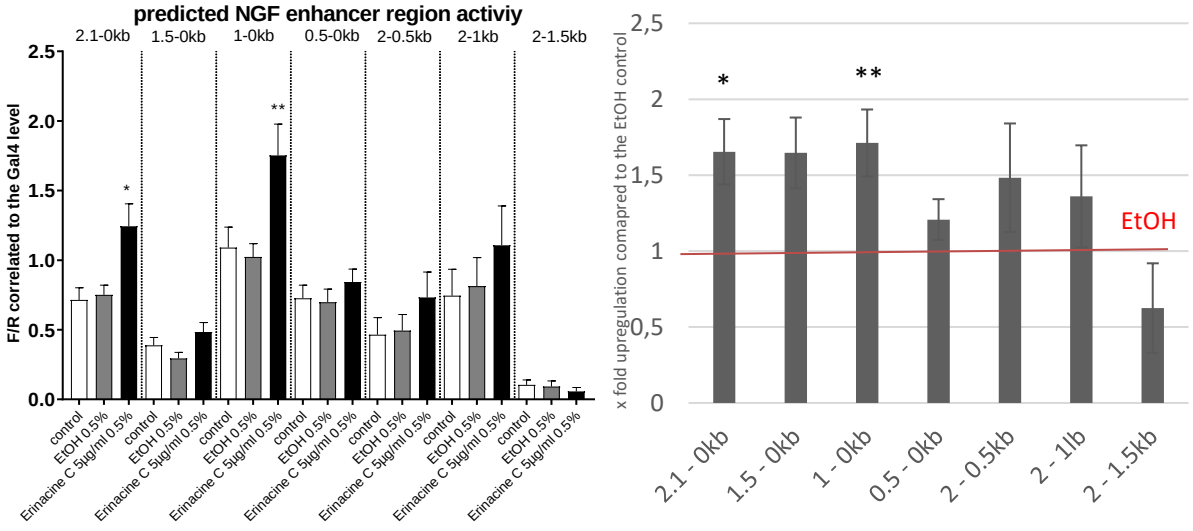

Figure 35: erinacine C induced luciferase activity of reporter constructs containing genomic DNA of different length 5' to *Tetraodon ngfß*. The first graph shows the activity of the firefly luciferase divided by renilla luciferase activity and connected for to background expression constructs with Gal4 level. Seven different genomic DNA fragments of the 5' region of the *Tetraodon ngf* gene driving firefly luciferase were transfected into 1321N1 astrocytoma cells and incubated with normal serum-reduced media (control, white bars), supplemented with ethanol (EtOH, gray bars) or erinacine C (black bars). The two fragments 1.5 – 0kb and 2 – 1.5kb showed the lowest luciferase activity. Only the 2.1 – 0kb and the 1 – 0kb fragments were able to be significantly stimulated by erinacine C. The second graph shows the x fold upregulation compared to the ethanol control. Only two fragments were able to be significantly stimulated by erinacine C. These are the 2.1-0kb and 1.0-0kb fragments. The fragments 0.5 – 0kb and 2 – 1.5kb did not mediate an upregulation of the reporter activity when erinacine C is added compared to the ethanol control. (n = 4; ± SEM; One-way-Anova: * $p \leq 0.05$; ** $p \leq 0.001$; *** $p \leq 0.001$; **** $p \leq 0.0001$)

In order to determine whether ETS signaling has an influence on the activity of the *Tetraodon* sequence 2.1 kb large fragment of the *Tetraodon ngf* 5' upstream region, the respective reporter construct was co-transfected with the different already introduced constructs for constitutive ETS activation ($ETS1_{DBD}$-TA4 and $ETS1_{DBD}$-TA2) as well as repression ($ETS1_{DBD}$-KRAB) in 1321N1 astrocytoma cells (Figure 36). After transfection, the media was exchanged for the 2.1kb fragment transfection and for the co-transfection with the ETS repressor construct (KRAB) to serum-reduced media supplemented with ethanol (0.5%) or erinacine C (5 µg/ml).

For the ETS activator constructs ($ETS1_{DBD}$-TA4 and $ETS1_{DBD}$-TA2) the media was exchanged to serum-reduced media. After incubation for 24h the luciferase expression was measured by analyzing the luciferase activity. In this assay the ratio of firefly luciferase construct to the activator/repressor constructs was chosen as 1:1, because the activity for the putative *ngf* regulatory region was very low. In Figure 36A the results are shown as the quotient of firefly luciferase activity to the renilla luciferase and as reference level. The results were corrected for background level activity with the luciferase activity of Gal4 mediated luciferase activity (which was set as the background with transfecting the 4xUAS binding site). When the 2.1kb fragment alone was transfected and incubated afterwards with serum-reduced media supplemented with ethanol or erinacine C, a significant upregulation at the activity was visible, as shown before (serum-reduced media 1.1 ±0.1; ethanol 1.2 ±0.1; erinacine C 1.8 ±0.25). Once, the activators of ETS were transfected together with the 2.1kb fragment of the putative *ngf* regulatory element and treated with only serum-reduced media after that, the luciferase activity was also upregulated, but weakly and only significantly for the $ETS1_{DBD}$-TA2 construct, which is the stronger transcriptional activator (TA4 1.5 ±0.4; TA2 1.6 ±0.3). Using instead the ETS repressor construct ($ETS1_{DBD}$-KRAB), the activity of the putative 2.1kb *ngf* regulatory fragment was significantly decreased compared to the control, but an upregulation caused by erinacine C was still visible (serum-reduced media 0.5 ±0.1; ethanol 0.5 ±0.1; erinacine C 0.9 ±0.2). Figure 36B shows the representation of luciferase activities displays as x fold upregulation compared to the control, which was only transfected with the 2.1kb fragment and incubated with serum-reduced media. When incubated with erinacine C only a significant upregulation by 1.7 ±0.2 fold was visible. When the 2.1kb fragment was co-transfected with the activator TA4 the activity was also upregulated (1.4 ±0.2 fold), but not significantly, like it was seen for TA2 (1.6 ±0.2 fold). When the signaling activity of ETS was inhibited, the activity of the 2.1kb fragment was also downregulated (1 ±0.1 fold). This led to the suggestion that ETS activity is involved in the erinacine C dependent upregulation of the 2.1kb fragment, but it was seen that this was not alone involved in the upregulation, since there was an erinacine C dependent upregulation visible in the presence of the ETS repressor ($ETS1_{DBD}$-KRAB) in astroglial cells.

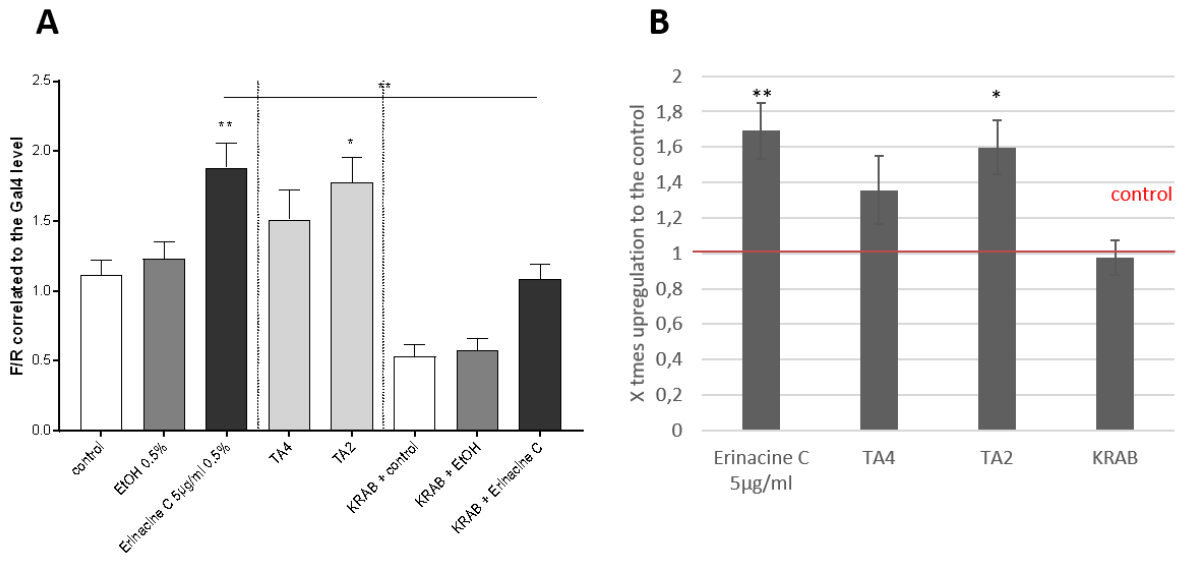

Figure 36: Effect of the different ETS constructs on the predicted enhancer region. 1321N1 astrocytoma cells were transfected with the 2.1 kb NGF enhancer fragment together with the different ETS inducing constructs. When the fragment is transfected alone and afterwards incubated with serum-reduced media as control, ethanol and erinacine C, the activity of the luciferase is significantly increased with erinacine C. When the fragment is cotransfected with the different ETS inducing constructs TA4 and TA2 the signaling is induced but only significant with the stronger TA2 construct. When cotransfected with the methylation inducing KRAB construct and afterwards incubation with the different additives the signaling at all is significantly increased but compared to the control after KRAB transfection the erinacine C incubation cause also significantly increase in the activation.

These results showed that the predicted *ngf* regulatory region was able to respond to erinacine C incubation. The last 500bp did not appear to contribute to this response, suggesting that these parts were not responsible for erinacine C dependent NGF regulation. The last experiment showed also that the NGF regulation seem to be ETS mediated, but not alone.

3.4 Effect of erinacine C and other substances isolated from *Hericium* sp. *in vivo*

So far, the effect of erinacine C was only shown *in vitro*, where the effect was characterized in cells within a single culture of cell line. But in an organism, cells are normally surrounded by several cell types. In addition, organs are often protected by barriers, like the blood-brain barrier (BBB), where the central nervous system is separated from the blood flow. Therefore, it remains questionable, whether pharmacological substances are able to reach a certain cell type of choice. Therefore, the possibility of erinacine C to reach the vertebrate brain should be investigated.

3.4.1 Is erinacine C able to cross the blood-brain barrier?

When thinking about using erinacine C as medication, the compound should be able to cross the blood-brain barrier (BBB). To analyze the ability of erinacine C to cross the BBB, an already established assay was used, were the BBB was mimic as a co-culture of the cell types involved in BBB formation. The BBB consists of three different cell types: the astrocytes, pericytes and

endothelial cells (Daneman and Prat, 2015). Such three cell types were isolated by Verena Ledwig, a member of the Institute of pharmaceutical technology (Technical University Braunschweig), from pig primary cell culture and cultivated to obtain purified single cell types. With specific markers, the purity of each cell type was validated (Figure 37). Endothelial cells were identified by the expression of the Van-Willebrand-factor that was detected by immunohistochemistry. The von Willebrand factor (vWF) is a glycoprotein, which is a useful marker for endothelial cells. This protein performs as both an antihemophilic factor carrier and a platelet-vessel wall mediator in the blood coagulation system (Ginsburg *et al*., 1985). In endothelial cells that produce vWF, the factor is stored in the so-called Weibel-Palade bodies (Berriman *et al*., 2009). Pericytes was identified using an antibody against alpha-smooth muscle Actin. Actins are a family of globular multi-functional proteins that form microfilaments. It was shown that smooth muscle alpha-actin mRNA and smooth muscle alpha-actin contractile protein elements were present within the renal medullary pericytes (Park *et al*., 1997). Astrocytes were identified by their expression of Glial Fibrillary Acidic Protein (GFAP). This protein represents the main component of the intermediate filaments in the cytoplasm of glial cells and especially in astrocytes in the central nervous system (Zhang *et al*., 2017). The three different cell types, endothelial cells, pericytes and astrocytes, were cocultivated in a specific chamber, schematic shown in the drawing (Figure 37). These culture conditions allowed the cells to form a strong barrier resembling the blood-brain barrier (Figure 37).

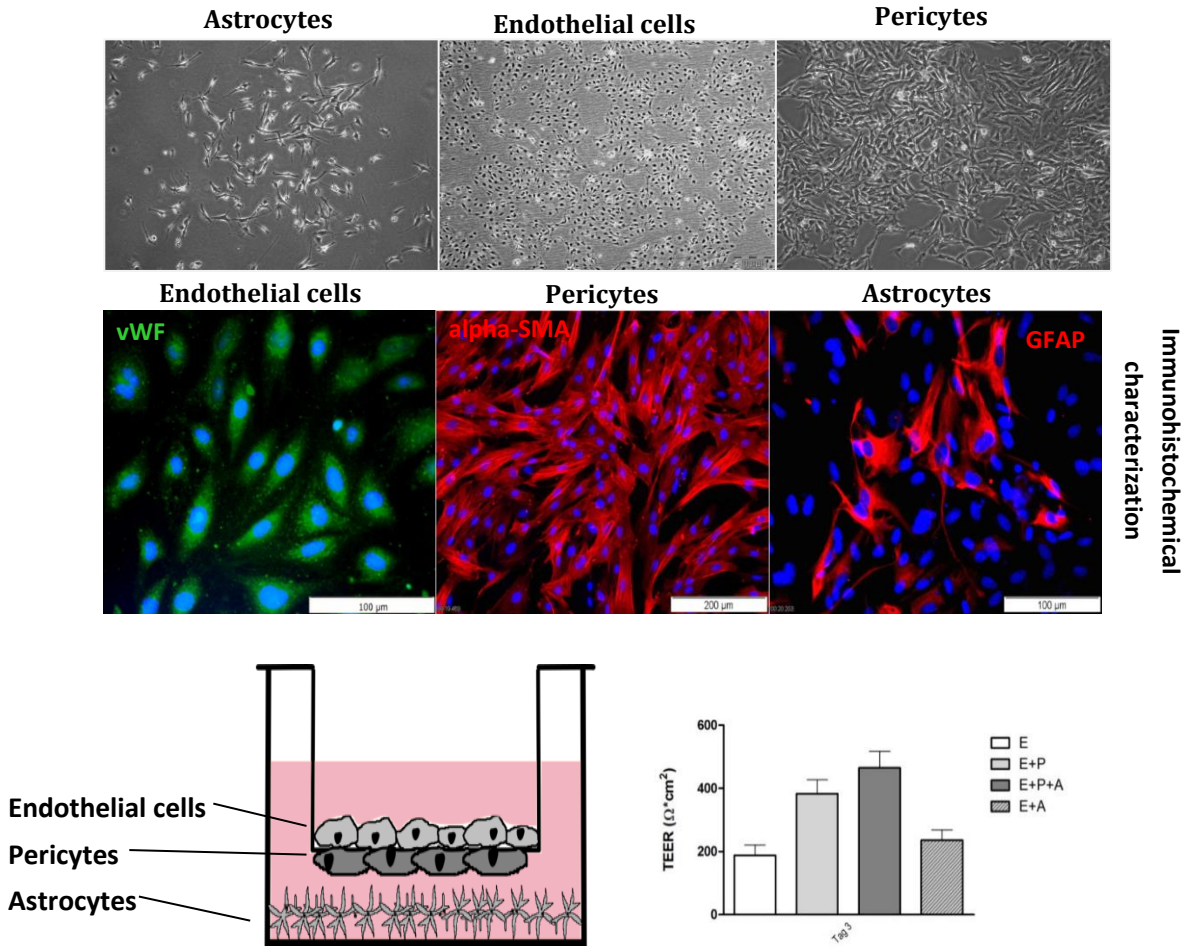

Figure 37: Structure of the Experiment performed by Verena Ledwig. The blood-brain barrier consists of three different cell types: astrocytes (A), endothelial cells (E), and pericytes (P). The cells were isolated from pig primary cell culture and purified to obtain individual cell types. The picture for a pure single cell type is shown in the upper row and their characterization by immunohistochemistry displays expression of different markers in the lower row. The nuclei war counter stained using DAPI. The first picture for the endothelial cells displays expression of the van-Willebrand-Factor specifically identify endothelial cells. The picture for pericytes reveals immunofluorescence staining of the alpha-smooth muscle actin antibody to specifically validate immunohistochemical pericytes. And the picture for astrocytes shows a staining against GFAP marking specifically glial fibrillary acidic protein in the astrocytes. The lower row depicts the cocultivation of these three cell types on a costumer-made chamber. By that, a strong barrier can be established by the cells shown in the diagram on the lower right site. The graph shows the TEER value in Ω per cm2. Only a cocultivation of E (endothelial cells), P (pericytes) and A (astrocytes) can establish a strong barrier of high TEER values, nearly comparable to the natural blood-brain barrier (normally around 1200 Ωxcm2. (Experiments, pictures, and graphs performed by Verena Ledwig)

Using erinacine C in the brain barrier like co-cultivation method, established by Verena Ledwig, the penetration of erinacine C through this barrier was analyzed (Figure 38). The time course of permeabilization was characterized by an analysis of erinacine C (10 µg/ml) paasing through a mono-culture of endothelial cells (left graph, dark line Figure 38) compared to the passage through a triple-cell culture (left graph, bright line, Figure 38). There was no difference visible in the time course of metabolite penetration. When the time course of barrier penetration for erinacine C was compared between a mono-culture of endothelial cells (without strong barrier) only and the triple-culture of endothelial cells, astrocytic cells and pericytes building the strong barrier no differences was observed (Figure 38). This suggests that erinacine C was

able to pass through different cell barrier and by that should be able to also cross the blood-brain barrier.

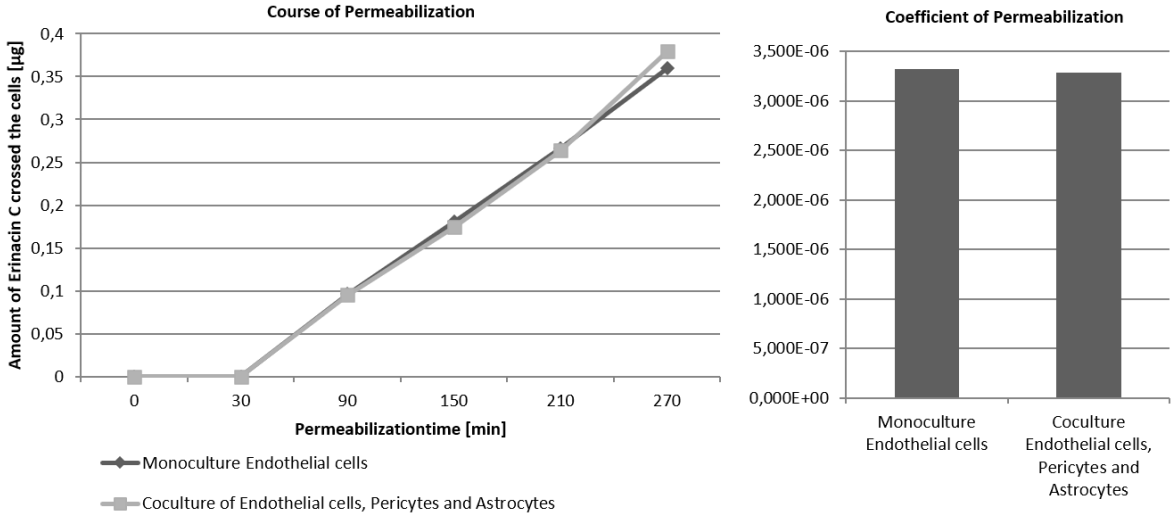

Figure 38: Course of Permeabilization of erinacine C performed by Verena Ledwig and Dr. Kathrin Wittstein. To establish a strong blood-brain barrier like structure astrocytes, pericytes and endothelial cells isolated from pig primary cell culture are cocultivated and erinacine C is added to the donor site. The amount of erinacine C is measured using HPLC after a permeabilization time starting at 30 min of incubation until 270 min of incubation. The amount of erinacine C increases over time in the component across the endothelial cell monoculture (dark gray) or in the coculture (bright gray). There is no difference in the amount of erinacine C in the monoculture in comparison to the cocultivation visible. With the incubation time and the amount of erinacine C, the coefficient of the permeabilization can be quantified as shown in the second graph. Also here it is visible that there is no difference for the cocultivation compared to the monoculture. (Experiment was performed by Verena Ledwig, quantification with HPLC performed by Dr. Kathrin Wittstein, n = 2)

In cells, the efflux transporter is important to transport ions and other molecules from the inside of a cell to the outer extracellularly space. For medications, it is important to clarify, if substances are recognized by these transporters. erinacine C was able to cross the blood-brain barrier. But in case it was recognized by an efflux transporter its amount would decline again. Therefore, the apical to the basolateral (A>B) transport through the *in vitro* BBB was analyzed as defined before and this was compared to the basolateral to apical (B>A) transport with and without an inhibitor for the P-gp efflux transporter (Figure 39). P-glycoprotein (P-gp) is a primarily active efflux transporter that transports its substrates from the cell membrane into the extracellular space. It is expressed in the intestine, liver, blood-brain barrier, placenta, and kidney, among others, and acts as a transport barrier against foreign substances. On the one hand, P-gp inhibits the absorption of these substances in the organism and sensitive organs and on the other hand it promotes their excretion. The substrates include numerous active pharmaceutical compounds, the pharmacokinetics of which are determined by P-glycoprotein. P-gp inhibitors can increase the bioavailability and the distribution of the active substances inside the target tissue. Conversely, inductors increase the barrier function of the transporter and promote the elimination of the medication. As explained before the permeabilization

coefficient for erinacine C was quantified. The graph showed that there was no difference in the directional transport coefficient when comparing the apical to basolateral to the basolateral to apical transport of erinacine C in the presence or absence of the P-gp inhibitor suggesting that erinacine C is not a target of the P-gp efflux transporter. This suggests that erinacine C once it has crossed the blood-brain barrier will not be returned to the blood vessels in the brain.

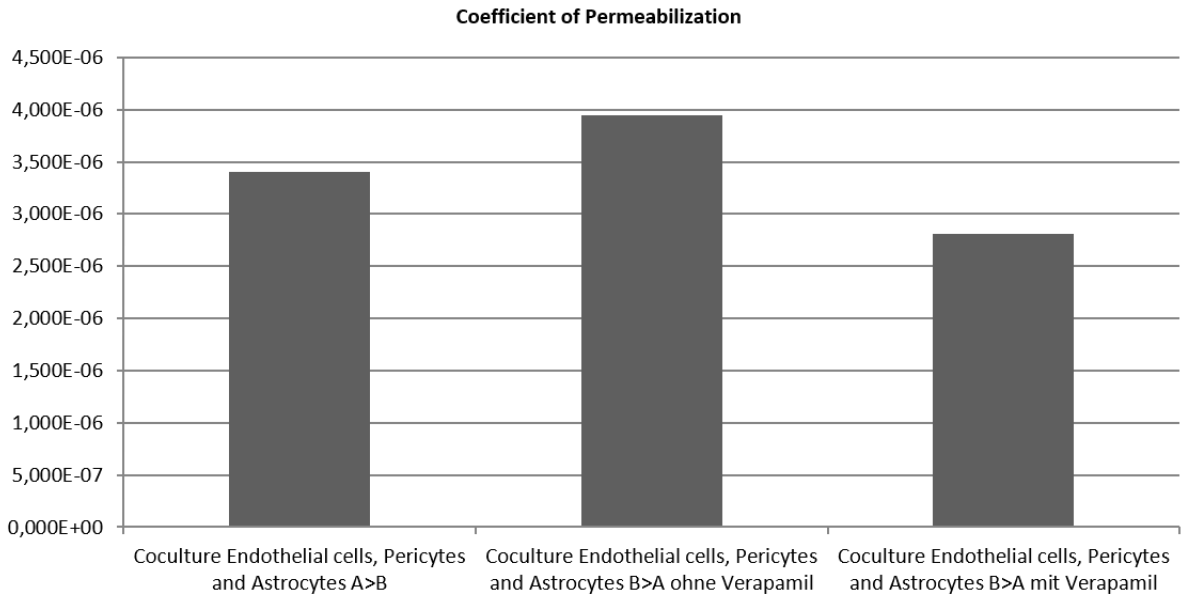

Figure 39: Coefficient of Permeabilization with and without an inhibitor of the efflux transporter performed by Verena Ledwig. The efflux transporter is a transport protein which can transport chemicals from the inside of the brain to the outside and into the blood system. The first bar shows the coefficient when measured the erinacine C amount which passed from the apical to basolateral side of the epithelial barrier, as described before. The second bar is the amount of erinacine C that passed from the basolateral to the apical side of the epithelium in the absence of verapamil (which is an inhibitor for a P-gp efflux transporter). The third bar shows the coefficient for the amount of erinacine C which had passed from the basolateral to the apical side of the epithelium in the presence of verapamil. No difference between these conditions is visible indicating that erinacine C is not a target of the P-gp efflux transport system. (Experiment was performed by Verena Ledwig, quantification with HPLC was performed by Dr. Kathrin Wittstein, n = 1)

With the *in vitro* model it can be seen that erinacine C should be able to cross the BBB. But these data still have to award their validation *in vivo*. Therefore, the zebrafish was used as a model system, being a small vertebrate model with a functional BBB and an endothelial cell-based vasculature (Eliceiri *et al*., 2011). The BBB is established in zebrafish larvae between 4dpf and 10dpf (Eliceiri *et al*., 2011). To characterize the ability of erinacine C to cross the BBB, 4dpf old larvae were incubated with 5µg/ml erinacine C for 48h in normal zebrafish media. After this incubation time, 50 heads and 50 brains were isolated. Using HPLC (performed by Dr. Kathrin Wittstein and Dr. Zeljka Rupcic) the amount of erinacine C was measured and quantified with the help of the erinacine C specific retention time. Figure 40 shows the chromatogram of the suspensions obtained from isolated heads and brains. The yellow box marks the erinacine C specific peak. Erinacine C was clearly visible in the suspension obtained from the head after an incubation period for 48h, as well as in the isolated brains. Of note these suspensions also contained cells from the vasculature of the brain and in case of the heads also gills and other cranial tissue.

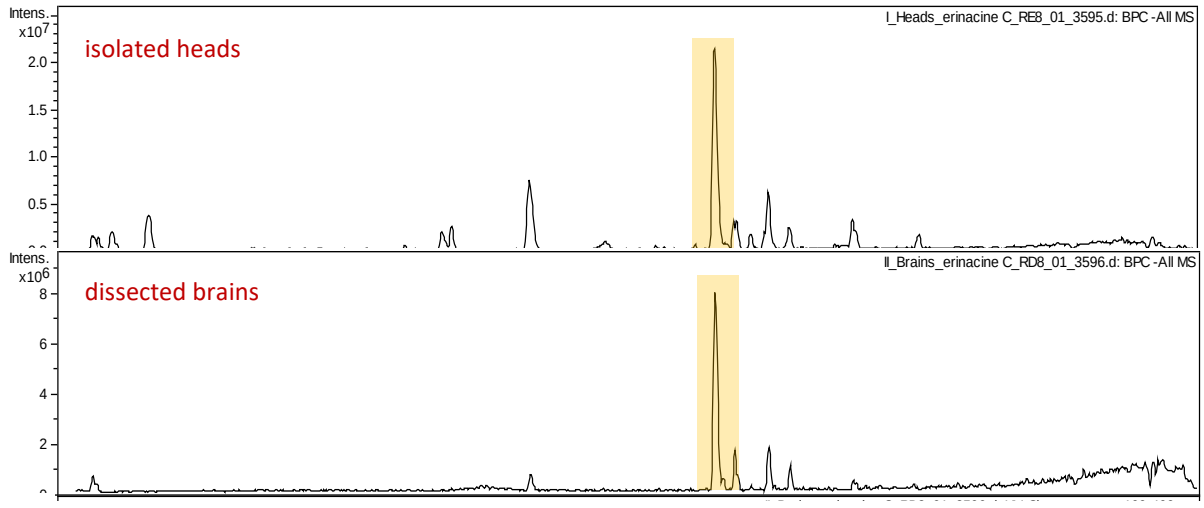

Figure 40: HPLC chromatogram of a suspension of an erinacine C treated zebrafish larvae brain. 4dpf old larvae were incubated with erinacine C (5µg/ml) for 48h. After the incubation time, 50 heads and 50 brains are isolated, suspended and measured for the content of erinacine C using HPLC. The peak of erinacine C is visible in both samples (yellow bar).

Since the BBB is established between 4dpf and 10dpf in the zebrafish, different developmental stages during the formation of the BBB were chosen. To quantify the ability of erinacine C to pass the BBB, zebrafish larvae were incubated with erinacine C (5µg/ml) at different ages (Figure 41). The incubation with erinacine C was started at 4dpf, 7dpf, and 10dpf, for periods of 24h, 48h, and 72h. After this incubation, 50 brains of each time point and treatment were isolated. The selected brains were taken up in methanol and extracted in an ultrasonic bath. After evaporation of the supernatant, the residues were dissolved in methanol. The amount of erinacine C was measured by HPLC by Dr. Kathrin Wittstein (Helmholtz Centre for Infection Research). The peak area occurring at the retention time of erinacine C was quantified and correlated to a calibration line. With a progressing time of incubation of the zebrafish, the amount of erinacine C increased over time in the extracts (4dpf: 24h 11.9 ±4 area units, 48h 30.4 ±9 area units, 72h 105.4 ±36.5 area units; 7dpf: 24h 39.1 ±21.3 area units, 48h 63.3 ±30.2 area units, 72h 196.8 ±87.4 area units; 10dpf: 24h 8.6 ±4 area units, 48h 18.6 ±6 area units, 72h 51.6 ±19.1 area units). These data revealed that initially from 4dpf to 7dpf the uptake of erinacine C in the brain increased. Yet, with a mature BBB at 10dpf the amount of erinacine C taken up by the brain was reduced again. Nevertheless, with increasing incubation time, the amount of erinacine C in the brain accumulated constantly at all ages. Of note, the values for this experiment vary, since during the experiment some of the larvae died and thus, a high standard derivation was visible. The amount of erinacine C was calculated to the amount per brain and here the increase over time and the differences for the different starting points were equivalent (4dpf: 24h 4.5 ±0.4 ng per brain, 48h 37.9 ±20.7 ng, 72h 229 ±146.1 ng; 7dpf: 24h 15.3 ±6.1 ng, 48h 41.4 ±13.9 ng, 72h 284 ±134.9 ng; 10dpf: 24h 3.6 ±1 ng, 48h 42.3 ±25.5 ng,

72h 155.3 ±57.9 ng). With the increasing incubation time, the amount of erinacine C, deduced from the peak area and also the amount of erinacine C per brain in all three stages of development (4 dpf, 7 dpf, 10 dpf). The variance during the experiments was relatively high due to the variation in egg quality and their maintenance. Nevertheless, at all developmental time points erinacine C could be detected in the head and brain of the specimens, showing that erinacine C was able to enter into the brain of a zebrafish.

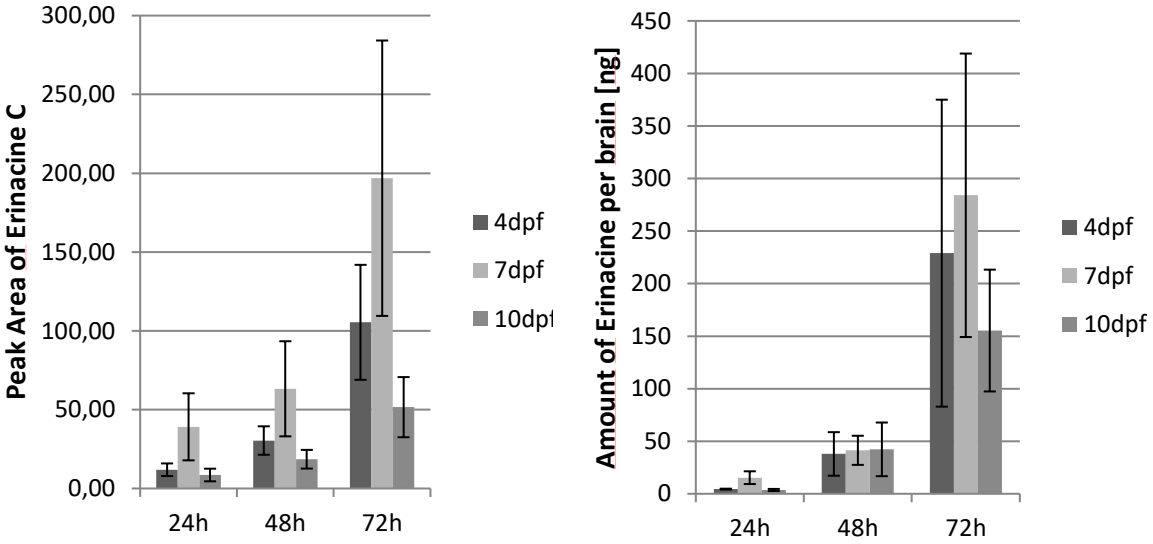

Figure 41: Ability of erinacine C to enter the zebrafish brain. Zebrafish from different stages (4dpf, 7dpf, 10dpf) were incubated with erinacine C (5µg/ml) for 24h, 48h, and 72h. After the incubation time, the larvae were washed with 10% methanol in fish water and the brains were isolated. The washing supernatant was not free from erinacine C and contained a small amount of erinacine C yet smaller than the measured sample. The samples were measured by HPLC (performed by Dr. Kathrin Wittstein, Helmholtz Centre for Infection Research). The peak area or the amount of erinacine C per brain can be analyzed. This data revealed that with progressing time an increasing amount of erinacine C is taken up by the fish. At all stages, erinacine C can be detected.

These findings show that erinacine C was detected *in vitro* after penetrating through the blood-brain barrier model or *in vivo* after diffusion into the zebrafish brain, suggesting that erinacine C is able to cross the blood-brain barrier.

3.4.2 Effect of substances isolated from *Hericium* sp. *in vivo*

Secondary metabolites were isolated from an edible mushroom. This leads to the suggestion, that all isolated substances should not have a toxic effect. But keeping high concentration can cause multiple side effects. Thinking about the effects *in vitro*, this leads to the conclusion, that starting at a specific concentration, these metabolites can cause toxic effects in cells.

Since the zebrafish is a suitable model system, for analyzing side effects *in vivo*, the zebrafish was used to analyze these side effects. To highlight one metabolite, which was used regarding its side effects *in vivo*, corallocin A was used (Figure 42). A 24hpf old larvae was dechorionated

with forceps and incubated for 48h with corallocin A (15µg/ml). This incubation caused aggregation of blood in the head, especially in the hindbrain region. This leads to the suggestion, that corallocin A is able to destroy the blood vessels and leads to an aggregation of blood in the head.

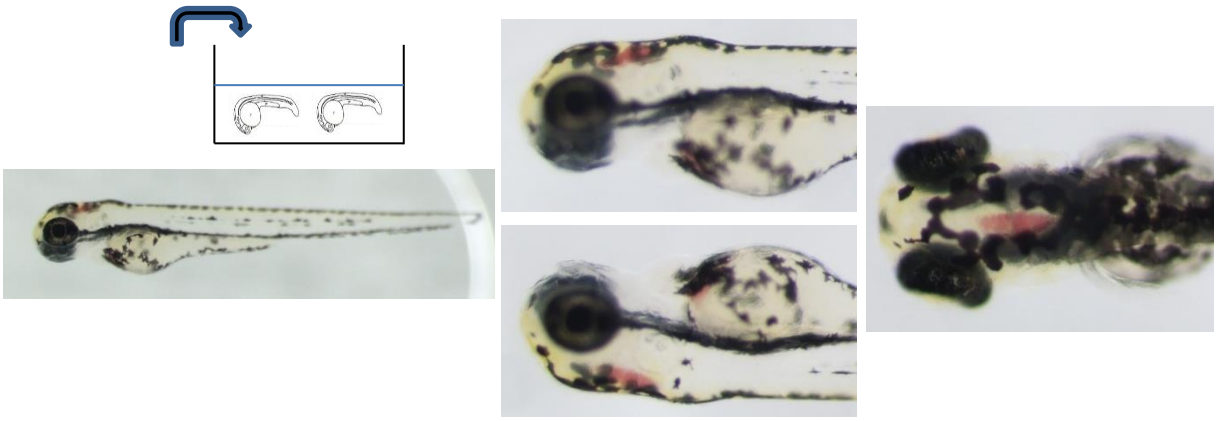

Figure 42: Effect of corallocin A *in vivo*. 24 hpf old zebrafish embryos are incubated with corallocin A (15µg/ml). After 48h of incubation, a red color in the brain is visible in the hindbrain. (n = 2)

It was shown, that corallocin A is able to cause accumulation of blood in the head, especially in the hind brain region, since there is a ventricle, making space to accumulate blood.

3.5 Establishment of different assays to analyze the effect of erinacine C and other substances isolated from *Hericium* spp. in vivo.

Erinacine C has been identified as an NGF inducing secondary metabolite from the fungus *Hericium erinaceus*. Moreover, this substance was shown to be able to pass the blood-brain barrier and could thus likely induce NGF expression in the brain. To identify cell populations that may be affected by an increased presence of this neurotrophin, the expression of its high affinity receptor TrkA needs to be analyzed. Thus, mRNA *in situ* hybridization an adult brain section against the expression of the ligand *ngf* and its cognate receptor *trkA* was performed.

3.5.1 Analysis of expression of NGF and its high-affinity receptor TrkA.

To analyze the expression pattern for *ngf* and *bdnf* mRNA adult zebrafish brains were isolated and cut by a vibratome in 50µm thick sagittal sections. Using these sections fluorescent *in situ* hybridization for *ngf* and *bdnf* was performed and analyzed using a laser scanning microscope. Figure 43 shows the expression pattern of *ngf* mRNA costained with DAPI to mark the nucleus of individual cells. There was a widespread expression of *ngf* noticeable. Expression was observable in the forebrain, in the medial zone of the diencephalon (Dm) and the diencephalon (D) itself, as well as in the midbrain, in the optic tectum (TeO), the periventricular gray zone

(PGZ), the central and dorsal posterior thalamic nucleus (CP/DP), periventricular nucleus of posterior tuberculum (TPp) and intermediate reticular formation (IMRF), and also in the hindbrain, especially in the valvula of Cerebelli (Val), medial division of valvula cerebelli (Vam), the corpus cerebelli (CCe) and the crista cerebellaris (CC).

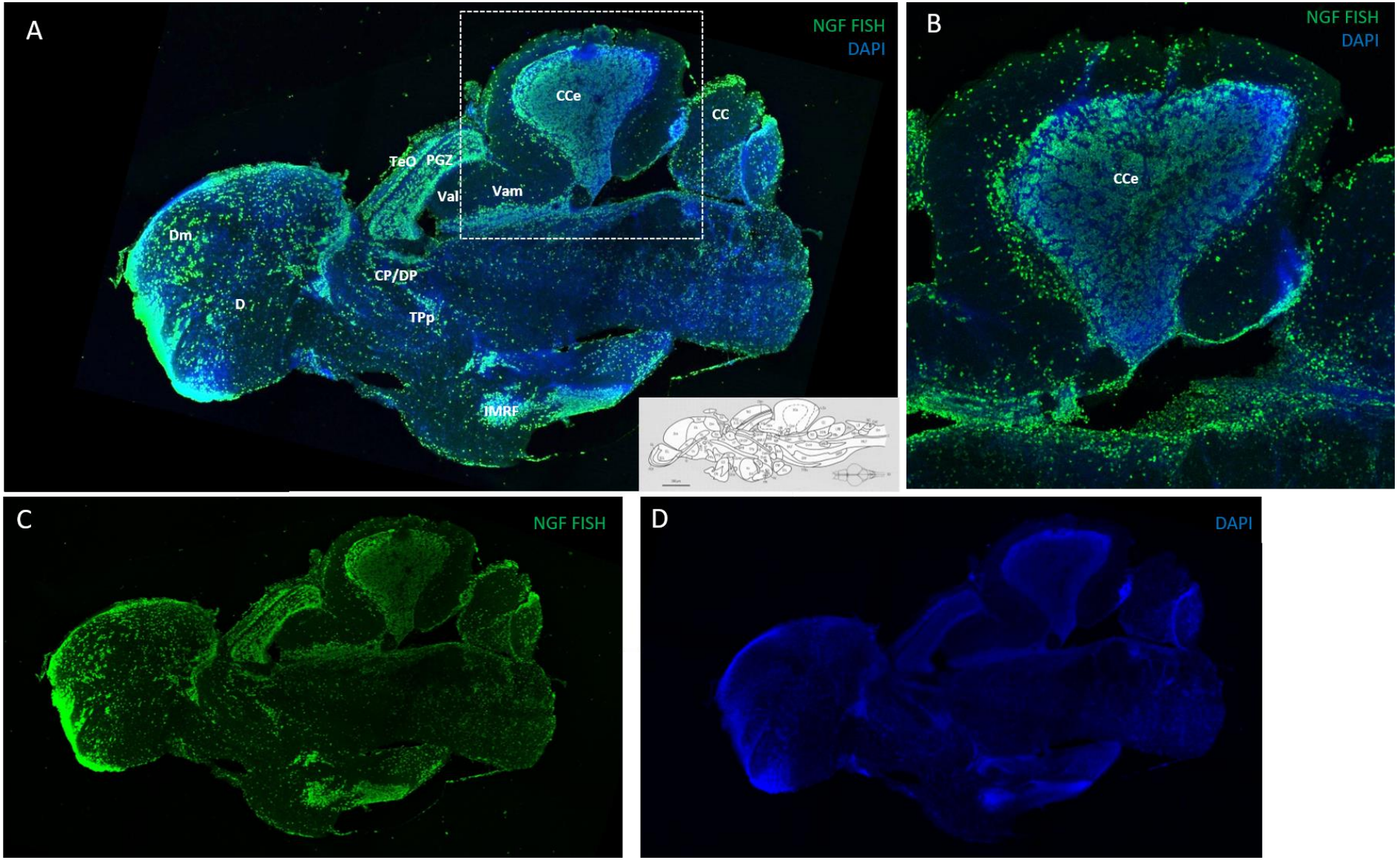
A
NGF FISH
DAPI
CCe
CC
TeO
PGZ
Val
Vam
Dm
CP/DP
D
TPp
IMRF
B
NGF FISH
DAPI
CCe
C
NGF FISH
D
DAPI

Figure 43: Expression pattern of *ngf* in the adult zebrafish brain. The pictures show the expression pattern of *ngf* mRNA. To mark specifically *ngf* mRNA *in situ* hybridization for *ngf* was performed (green fluorescence; picture A, B, C). In blue the nuclei are marked by flouresent DAPI staining (picture A, B, D). A schematic drawing of the adult zebrafish brain in sagittal view is shown in gray (taken from Wullimann *et al*., 1996). A higher magnification of the cerebellum is shown in picture B. Expression is visible in: medial zone of diencephalon (Dm), diencephalon (D), optic tectum (TeO), periventricular gray zone (PGZ), central and dorsal posterior thalamic nucleus (CP/DP), periventricular nucleus of posterior tuberculum (TPp), intermediate reticular formation (IMRF), valvula of Cerebelli (Val), medial division of valvula cerebelli (Vam), corpus cerebelli (CCe), crista cerebellaris (CC).

The cerebellum is an important part of the central nervous system. The structure of the cerebellum is highly conserved through evolution, the mammalian and teleost cerebelli show the same cell types, containing three different layers: the molecular layer, the Purkinje cell layer, and the granular cell layer (Hibi and Shimizu, 2012). In the granular cell layer, mossy fiber afferents arrive and contact granule cells and Golgi cells. Below the granular layer is the white matter, formed by the input and output nerve-fiber systems of this cortex (Lackey *et al*., 2018). The Purkinje cell layer is a simple cell layer, containing the Purkinje cell somata as well as Bergmann glia. This layer is positioned above the granule cell layer. The level peripheral to the Purkinje cell layer, containing the molecular layer interneurons (baskets and stellate cells), Purkinje cell dendritic arbors and parallel fibers and the axons of the granule cells (Bae *et al*., 2009). The cerebellum performs important tasks in controlling motor skills: It is responsible for coordination, fine-tuning, unconscious planning and learning of movement sequences (Manto *et al*., 2012). It has also recently been assigned a role in numerous higher cognitive processes. If the cerebellum is damaged or dysfunctions, several characteristic symptoms can occur depending on the location and extent of the affected area. The common term for most cerebellar symptoms is ataxia (Walter *et al*., 2006). Ataxia is the failure of proper motor coordination. This is the most common symptom in case the function of the cerebellum is impaired. In this thesis, the cerebellum was the main brain compartment in focus, because of its high evolutionary conservation. To analyze the expression of *ngf* in the cerebellum, an adult zebrafish brain was cut in sagittal sections and these were costained in addition to the *in situ* hybridization against *ngf* with an antibody against ZebrinII (Aldolase C) to mark specifically Purkinje cells (Figure 44). Purkinje cells are the characteristic large multipolar nerve cells with a highly branched dendrite tree in the cerebellar cortex, the axons of which represent the efferent

of the cerebellar cortex. Green fluorescence of ngf mRNA was visible in the granular cell layer of the cerebellum, but also in Purkinje cells (Figure 44, white arrow).

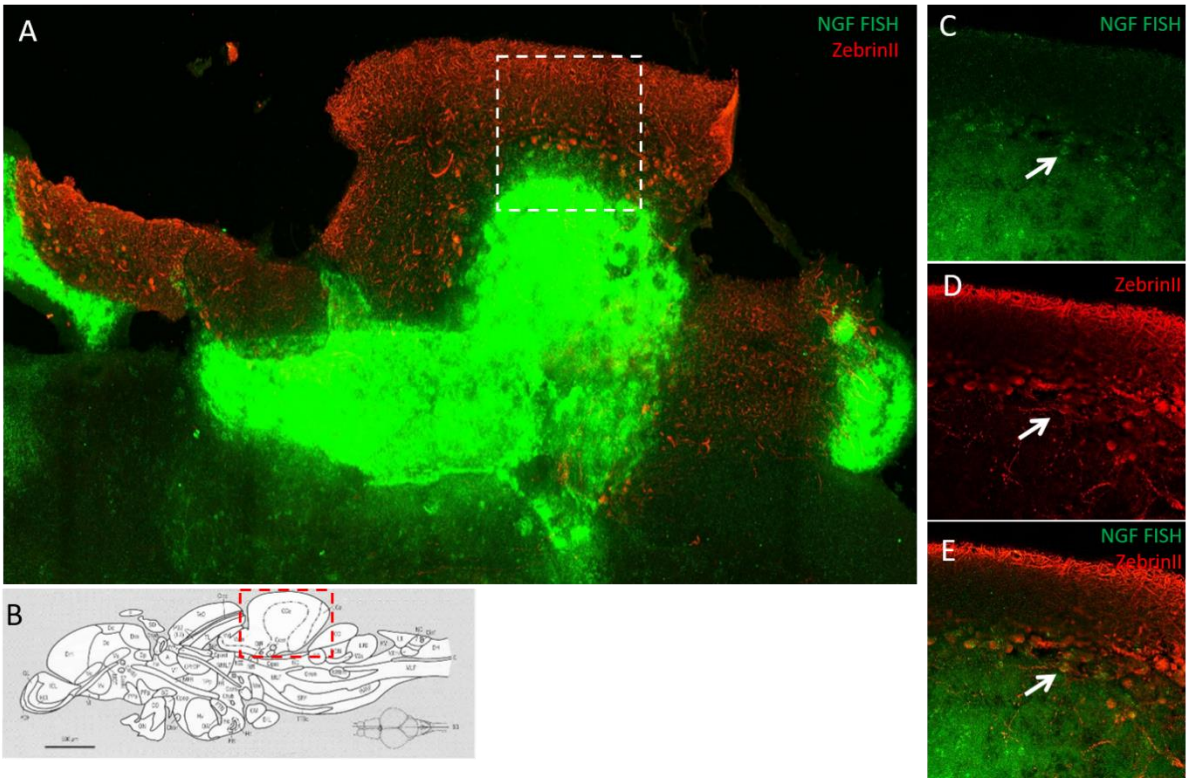

Figure 44: Expression pattern of *ngf* in the adult zebrafish cerebellum. The pictures show the expression pattern of *ngf* in the adult zebrafish cerebellum detected by fluorescent mRNA *in situ* hybridization (A, C, E) costained with an antibody against ZebrinII (red fluorescence; A, D, E) marking Aldolase C in Purkinje cells. To mark specifically *ngf* mRNA *in situ* hybridization against *ngf* was performed (green fluorescence; A, C, E). The pictures C, D and E show a higher magnification of the box in the left picture (A). The white arrow points out a double fluorescent Purkinje cell. The lower picture (B) shows a drawing of the adult zebrafish brain in sagittal view (taken from Wullimann *et al*., 1996).

Since *ngf* mRNA was widely expressed in the brain as shown before, the expression of the high-affinity receptor TrkA, to characterize the NGF responding cells, needed to be analyzed. Therefore, the *in situ* hybridization against *trkA* was performed in the adult zebrafish brain (Figure 45). The expression pattern of *trkA* was widespread like shown for *ngf* through the adult zebrafish brain. Expression was visible in the forebrain regions like the medial zone of the diencephalon (Dm) and the diencephalon (D), but also in midbrain regions, like in the optic tectum (TeO) and in the periventricular gray zone (PGZ) and in the caudal zone of periventricular hypothalamus (HC). The expression of *trkA* was also found in hindbrain regions, like the valvula of the cerebellum (Val) and the medial division of the valvula cerebelli (Vam), and the corpus cerebelli (Cce) and the crista cerebellaris (CC). Flourescence of the *trkA* in situ hybridization was clearly seen in the cytoplasm.

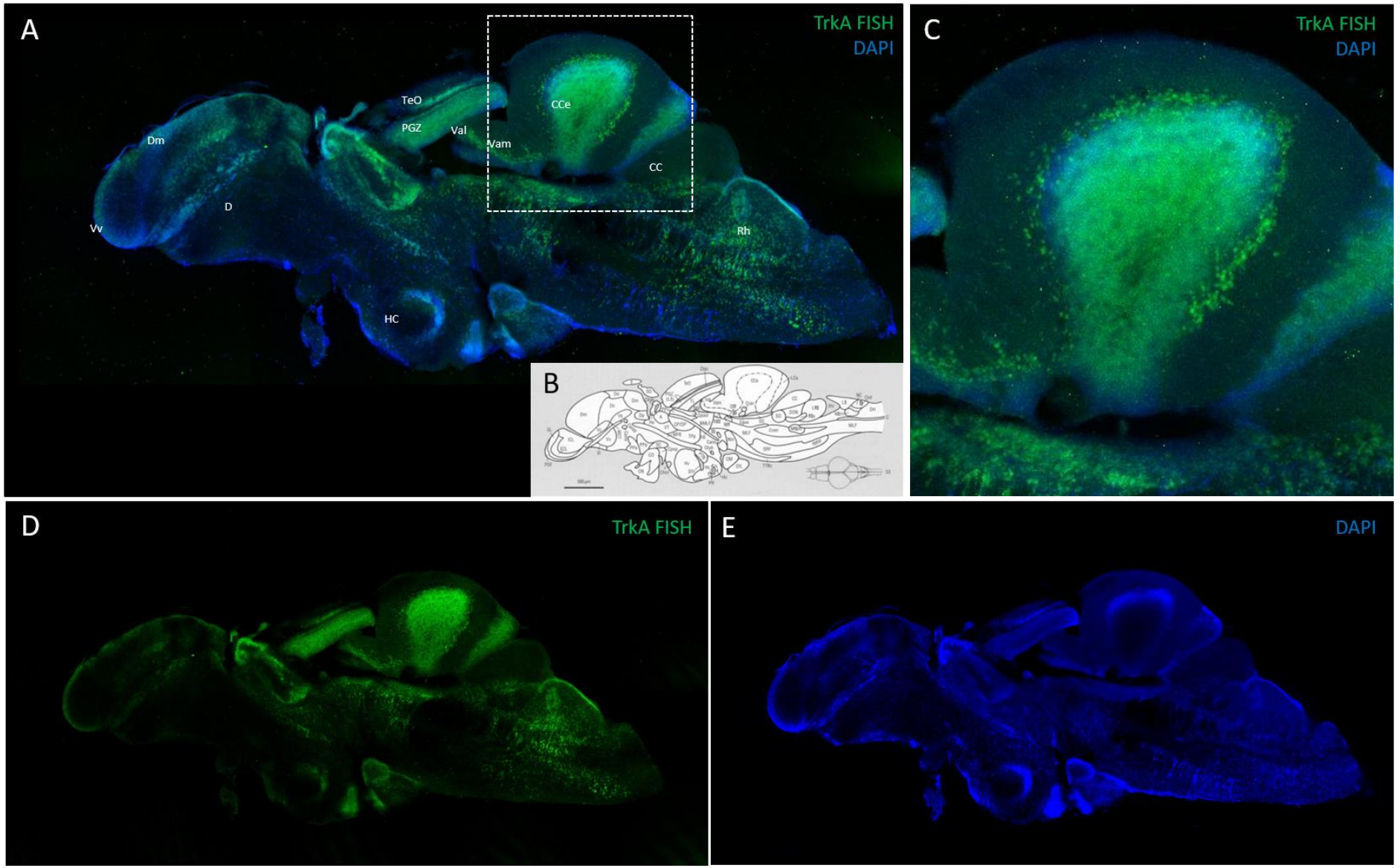
A
TrkA FISH
DAPI
TeO
PGZ
Val
Vam
CCe
CC
Dm
D
Vv
Rh
HC
B
C
TrkA FISH
DAPI
D
TrkA FISH
E
DAPI

Figure 45:Expression pattern of *trkA* mRNA in the adult zebrafish brain. The pictures A, C, D and E show the expression pattern of *trkA* mRNA. To mark specifically *trkA* mRNA, *in situ* hybridization against *trkA* mRNA was performed (green fluorescence; A, C, D). In blue the nuclei were marked by DAPI staining (A, C, E). The lower picture (B) shows a drawing of the adult zebrafish brain in sagittal (taken from Wullimann *et al*., 1996). Expression of *trkA* mRNA is visible in: ventral nucleus of the ventral telencephalic area (Vv), medial zone of diencephalon (Dm), diencephalon (D), optic tectum (TeO), periventricular gray zone (PGZ), caudal zone of periventricular hypothalamus (HC), valvular of cerebellum (Val), medial division of valvula cerebelli (Vam), corpus cerebelli (Cce), crista cerebellaris (CC), rhombencephalus (Rh).

The expression pattern in the cerebellum was characterized in more detail by using the anti-ZebrinII antibody to detect Purkinje cells (Figure 46). Surprisingly, apart from the expression of *trkA* in the granular cell layer, *trkA* was expressed not in all Purkinje cells. It seemed that there are two different populations of Purkinje cells: one expressing *trkA* and one not expressing *trkA*.

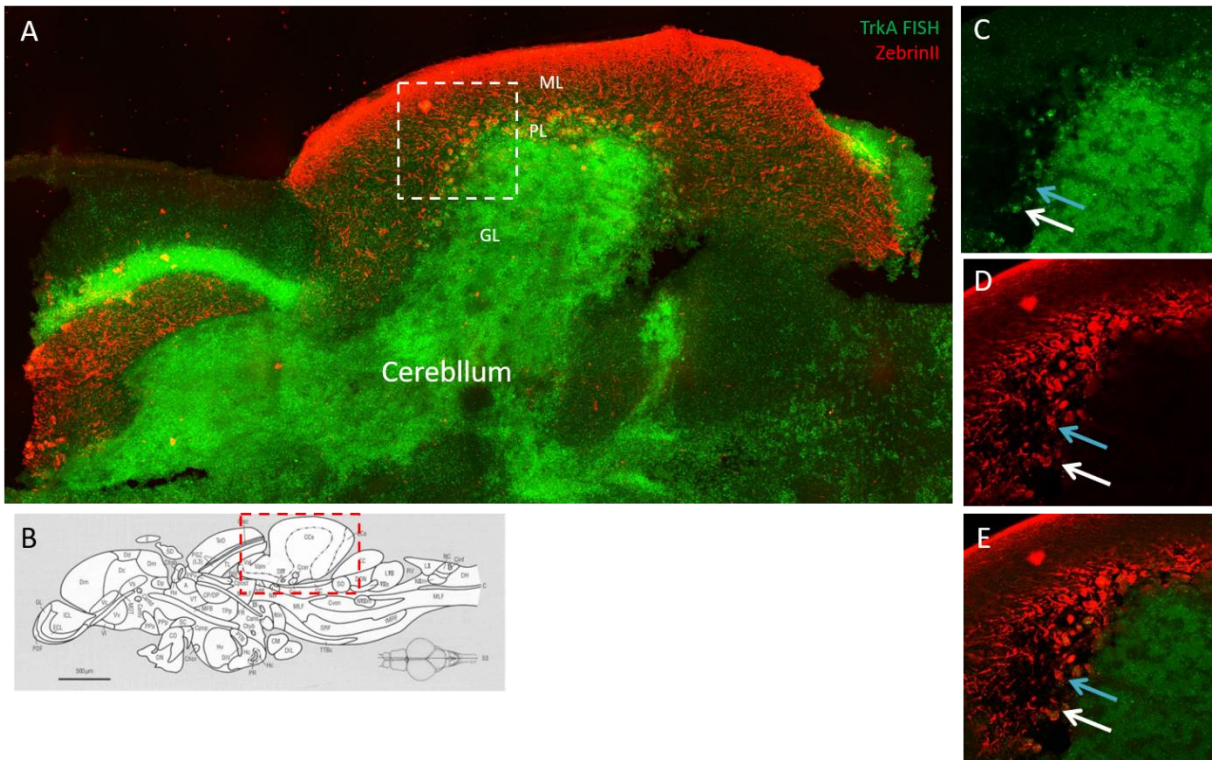

Figure 46: Expression pattern of *trkA* mRNA in the adult zebrafish cerebellum. The pictures A, C, D and E show the expression pattern of *trkA* mRNA (green flourscence; A, C, E) in the adult zebrafish cerebellum costained with an antibody against ZebrinII (red fluorescence; A, D, E) marking Aldolase C in Purkinje cells. To mark specifically *trkA* mRNA, *in situ* hybridization against *trkA* was performed (green fluorescence; A, C, E). The right pictures (C, D, E) show a higher magnification of the boxed area in the left picture. The white arrow marks a double fluorescent Purkinje cell whereas the blue arrow marks a Purkinje cell without *trkA* expression. The lower picture (B) shows a drawing of the adult zebrafish brain in sagittal view (taken from Wullimann *et al*., 1996).

Expression of *ngf* and *trkA* were widespread in the adult zebrafish brain. It can be suggested that expression of *ngf* and *trkA* were visible in neurogenic regions, like it was also shown by Kaslin *et al*. (2008; Figure 47). In this publication it was shown that neurogenic regions are found in the telencephalon, optic tectum, cerebellum and hypothalamus. In this thesis it can be suggested, when analyzing the whole brain using *in situ* hybridization, that *ngf* and *trkA* mRNA were also expressed in these regions. However, this should be investigated in the future using specific proliferation markers.

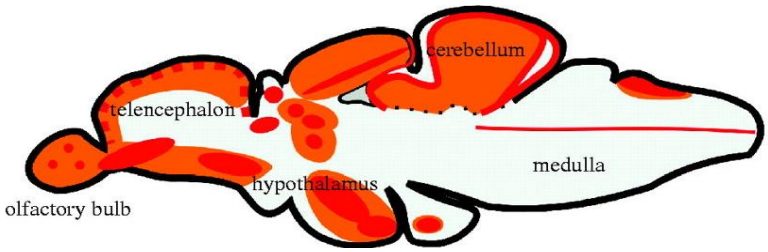

Figure 47: Neurogenic region in the adult zebrafish brain. Neurogenic regions are visible in the telencephalon, optic tectum, hypothalamus, cerebellum and hindbrain. In orange the neurogenic areas are marked and in red the adult stem cell niches (Kaslin *et al*., 2008)

3.5.2 Characterization of a transgenic *trkA*:mClover zebrafish line.

The cells, which are able to respond to NGF secretion by expressing the high affinity receptor *trkA* were analyzed before. However, it would be suitable, to have a stable transgenic reporter fish line, to characterize *trkA* expressing cells over time and to also characterize their possible reaction on erinacine C treatment. Therefore, a stable line expressing a reporter gene in all *trkA* expressing cells should be established. Since the zebrafish is an organism suitable for screening approaches, because the zebrafish has a small size and develops completely outside of the mother, it is a water living organism, so substances, which need to be analyzed, can be diluted directly into the surrounding water. First of all, an enhancer fragment driving expression in *trkA*-expressing cells would be useful, and such a regulatory element has been described previously by Palanca *et al*. (2013).

A transgenic zebrafish line was introduced by me previously, expressing the fluorescent protein mClover under control of this *trkA* regulatory element. This fish line was analyzed in this thesis in more detail (Figure 48). First expression of mClover was visible after 24h in sensory neurons, such as the lateral line nerve, the motoneurons (Figure 48 D) and the trigeminal neurons (Figure 48 C). After 48 to 72h expression started in the central nervous system; in the optic tectum, the rhombencephalon, and in the cerebellum region (Figure 48 I). To characterize the expression in the cerebellum in more detail and to compare the results with the *in situ* hybridization data, the transgenic line was crossed with a specific Purkinje cell marking zebrafish line where a Purkinje cell specific enhancer was used, called ca8 – a Purkinje cell specific regulatory element derived from the carbonic anhydrase related protein 8 gene of zebrafish (Namikawa *et al*.,

2019a). In this fish strain the ca8 enhancer drives expression of the red fluorescence protein tagRFP-T specifically in cerebellar Purkinje cells. In the double transgenic embryos and larvae expression in the cerebellum of Purkinje cells was comparable to the expression pattern of the *in situ* hybridization of *trkA*. Some Purkinje cells revealed expression of mClover in tagRFP-T positive Purkinje cells, but not all red fluorescent Purine cells expressed mClover. In addition, other cells of the cerebellum located in the molecular layer above the Purkinje cell layer as well as some located below in the granular cell layer also expressed the green fluorescent mClover. The *trkA*-mClover strain therefore expresses the green fluorescent mClover protein in a subset of Purkinje cells as shown in the *trkA* fluorescent mRNA *in situ* hybridization results.

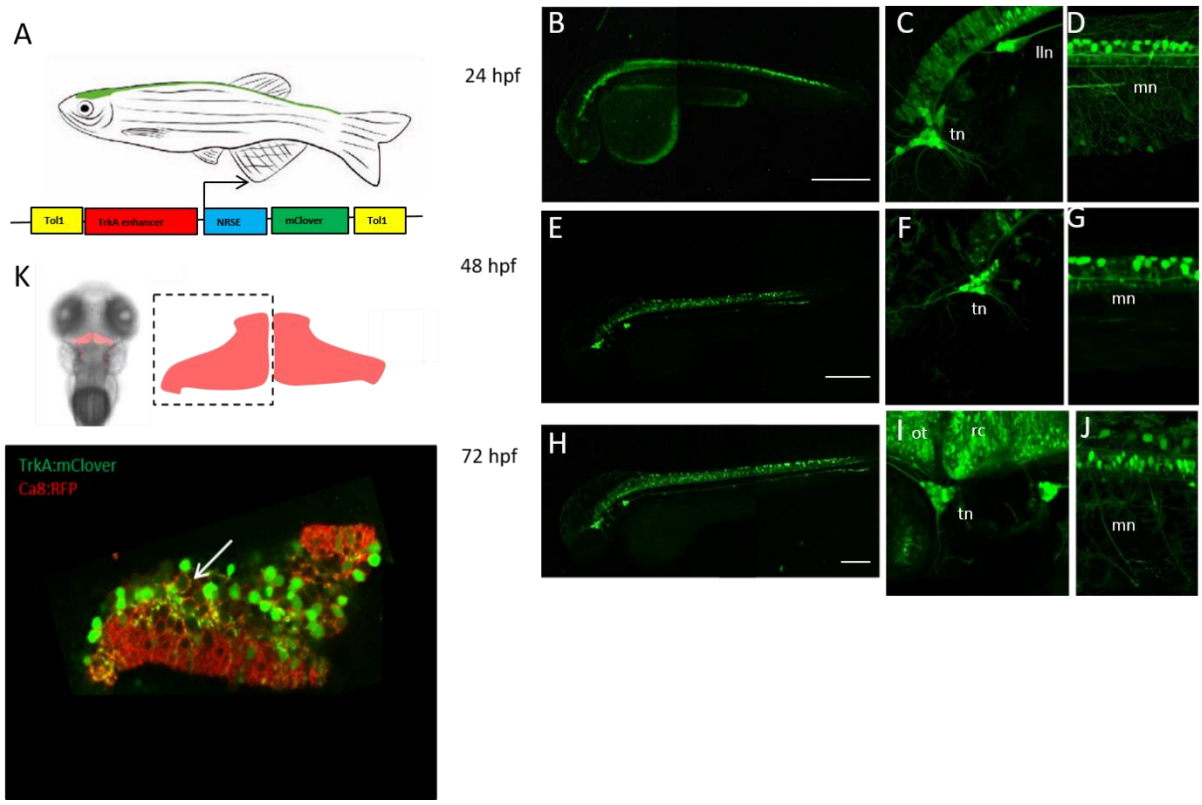

Figure 48: Analysis of a transgenic zebrafish line showing mClover fluorescence under control of a *trkA* regulatory element. The picture A shows a schematic drawing of an adult zebrafish and of the construct used to establish a stable transgenic *trkA*-mClover reporter line. The construct consists of the promotor/enhancer region of *trkA* in front of the coding region of the fluorescence protein mClover. To target the expression only to neurons a NRSE (neuron specific silencer element) was cloned in between of the enhancer and mClover. The construct was cloned in between two Tol1 transposon sites to introduce the DNA easily into the genome by injecting the construct together with a Tol1 transposase. In pictures on the right (B, C, D, E, F, G, H, I and J) the development of the transgenic line is shown after 24 (B, C, D), 48 (E, F, G) and 72h (H, I, J) of development recorded by confocal laser scanning microscopy. The head is to the left. Expression is visible in sensory neurons, like the trigeminal neurons (tn), the lateral line nerve (lln) and the motoneurons (mn). The shown scale bar indicates 500 µm. The picture K shows an analysis of the cerebellum after crossing the transgenic line with another transgenic line ca8:RFP expressing the red fluorescent protein tagRFP-T specifically in Purkinje cells of the cerebellum. Expression of the green fluorescence of mClover is visible in Purkinje cells (white arrow) but also some other cells show mClover expression. However, there is a heterogeneity of Purkinje cells, since some Purkinje cells show no mClover expression.

A stable transgenic zebrafish line was established, showing green fluorescence in dependence of a regulatory element derived from the *Fugu rubripes trkA* enhancer, especially in

motoneurons, lateral line nerve and the trigeminal neurons, but also in cells of the central nervous system, shown exemplary by analysis of the expression in Purkinje cells. The results, which were shown in this chapter support also the results, which were shown for the expression of *trkA* by *in situ* hybridization.

3.5.3 Establishment of different screening assay for analysis of different neurotrophin stimulating metabolites

The zebrafish is able to generate new neurons in all stages of life. Because of that, the zebrafish is a suitable model for analysis of regeneration *in vivo*. Neurotrophins are possible candidates to promote regeneration, since they have an influence on neurodegeneration as well as neuroregeneration. Secondary metabolites, like erinacine C, which are able to stimulate neurotrophin production, could be used in regeneration assays and the possible regeneration-promoting activity can be characterized.

Since the introduced transgenic line should mark *trkA* expressing cells and by that cells, which should be able to respond to NGF stimulating substances, this transgenic line was used as a model. As already explained, neurotrophins are involved in maintenance, differentiation and regeneration of neurons. The effect of regeneration inducing capacity of secondary metabolites being able to induce neurotrophin expression should be analyzed during the regeneration process. Therefore, a regeneration system needed to be established.

The spinal cord is an optimal region to induce regeneration. The spinal cord region can be easily destroyed with a needle trying to only touch this region and not the blood vessel underneath of the spinal cord (Figure 49). At 3dpf the spinal cord is completely established in the zebrafish larvae (Lewis and Eisen, 2003). At this time point the lesion was performed in a *trkA*:mClover transgenic line, where it was shown, that the spinal cord including motoneurons are marked with the fluorescence protein mClover, using a needle in a region above and behind the end of the yolk. The regeneration curve was analyzed using the confocal laser scanning microscope. Directly after lesion the gap was visible (Figure 49). After 48h the gap was closed by axons passing through the wound region (shown in the last picture, Figure 49). All in all, it can be suggested, that regeneration of the spinal cord occurred within 48h.

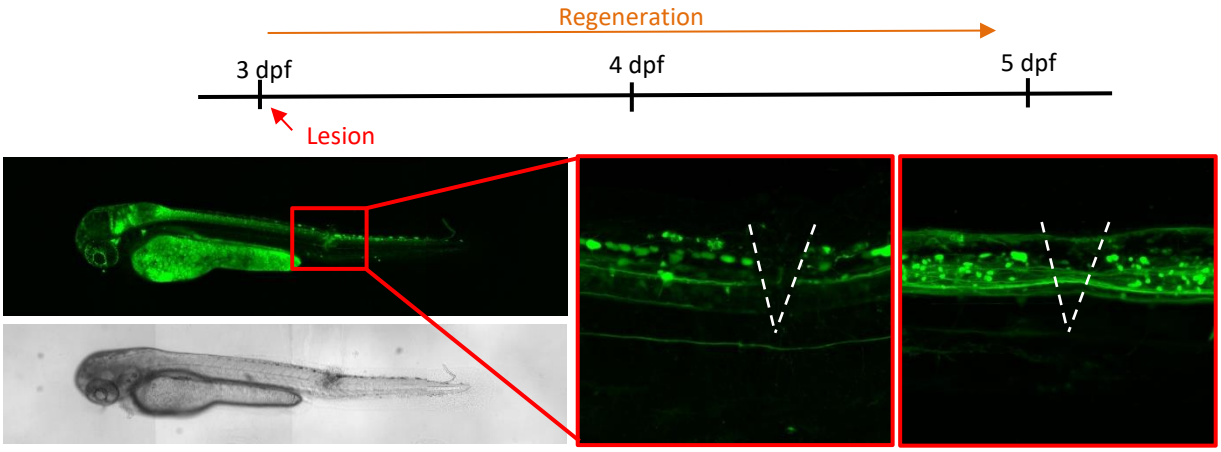

Figure 49: Overview of the spinal cord lesion in *trkA*:mClover transgene zebrafish and regeneration afterwards. 3dpf old larvae were lesioned in the spinal cord using a needle to destroy the spinal cord including motoneurons and axons in a region above and behind the end on the yolk. Important is to avoid inflammation or bleeding out by taking care to not destroy the blood vessel which is located underneath the spinal cord. The transection through the spinal cord is imaged afterwards with the confocal laser scanning microscope. After 48h the lesioned spinal cord region is completely regenerated by axons crossing the lesion side.

The next step was to classify if *trkA* expression was involved in the regeneration of the spinal cord lesion. Therefore, an *in situ* hybridization against *trkA* was performed during spinal cord regeneration (Figure 50). After 6, 10, 24, 32 and 48h of transsectioned larvae were fixed and the *in situ* hybridization to detect *trkA* mRNA was conducted. As control the *in situ* hybridization against *trkA* was performed with unlesioned embryos. To characterize the specificity of the *trkA* signal in the lesion other probes were used as control. The first was the sense probe, which should not give any signal. The second control was a probe, which is not involved in regeneration, called parvalbumin (*parv*). Parvalbumin is related to Calmodulin and Troponin C and has 3 EF hand motifs that serve to bind calcium. It is found in the fast-contracting muscles, in the brain and in endocrine-active tissue. It is known to mark in the zebrafish larvae muscle tissue in the head especially in the masticatory muscles and also in the cerebellum of the zebrafish especially in the Purkinje cells. This specific expression was also seen in this experiment. Expression of *trkA* mRNA in the lesioned region was visible starting at 10h post lesion and decreased until 48h post lesion. Unlesioned embryos that served as control did not show the expression of *trkA* in this region. Also, the lesioned embryos showed a specific pattern of *trkA* mRNA expression, where the sense probe and also another probe (used as negative control), were not expressed during the regeneration period (*parv* – parvalbumin) showed no pattern in the lesion area. With that it can be suggested, that *trkA* expression is involved in the spinal cord region.

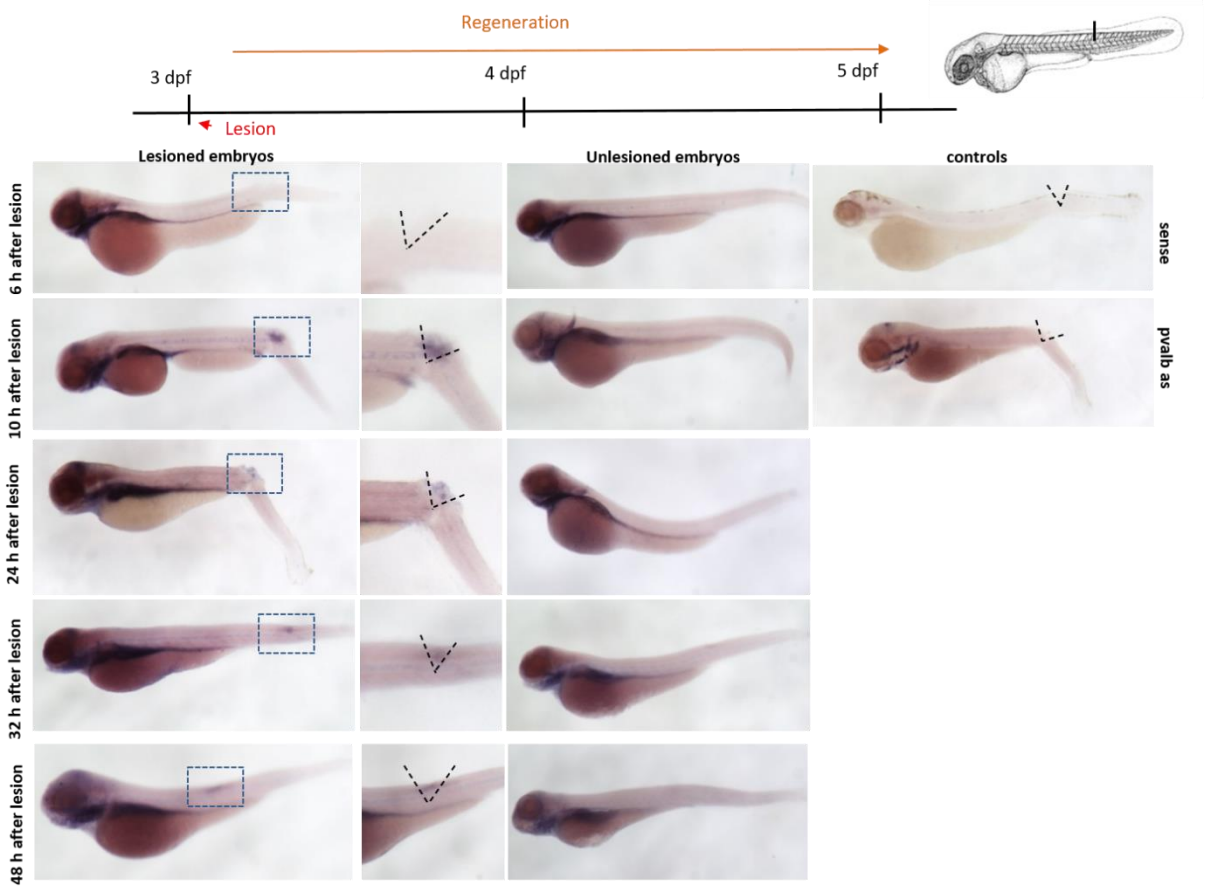

Figure 50: Expression pattern of *trkA* mRNA during spinal cord regeneration. Transsection through the spinal cord was performed at 3dpf and larvae 6, 10, 24, 32 and 48h after lesion were fixed and *in situ* hybridization against *trkA* was performed afterwards. Expression of *trkA* mRNA in the lesion side was visible starting at 10h after the lesion, where the unlesioned larvae (first row, lesioned embryos) show no *trkA* expression. The expression pattern of *trkA* mRNA stayed there until 48h after the lesion. To proof the specificity of the *trkA* mRNA pattern the *in situ* hybridization was performed for the *trkA* mRNA sense probe as well as for a probe unrelated to regeneration (*parv*) marking parvalbumin. (n = 4)

A quantification was performed after the *in situ* hybridization, since not all larvae showed *trkA* mRNA expression at the lesion side at the specific time points, the number of larvae showing *trkA* mRNA expression in the lesion side was quantified and calculated against the larvae which showed no expression of *trkA* mRNA in the lesion (Figure 51). The expression pattern of *trkA* mRNA in the lesion side increased significantly at 10h after the lesion was performed and was maintained until 24h post lesion. At 48h after the lesion there was again a significant increase in the amount of embryos showing the *trkA* mRNA expression. This lead to the suggestion that NGF/TrkA signaling was involved in the region of spinal cord lesion in the zebrafish.

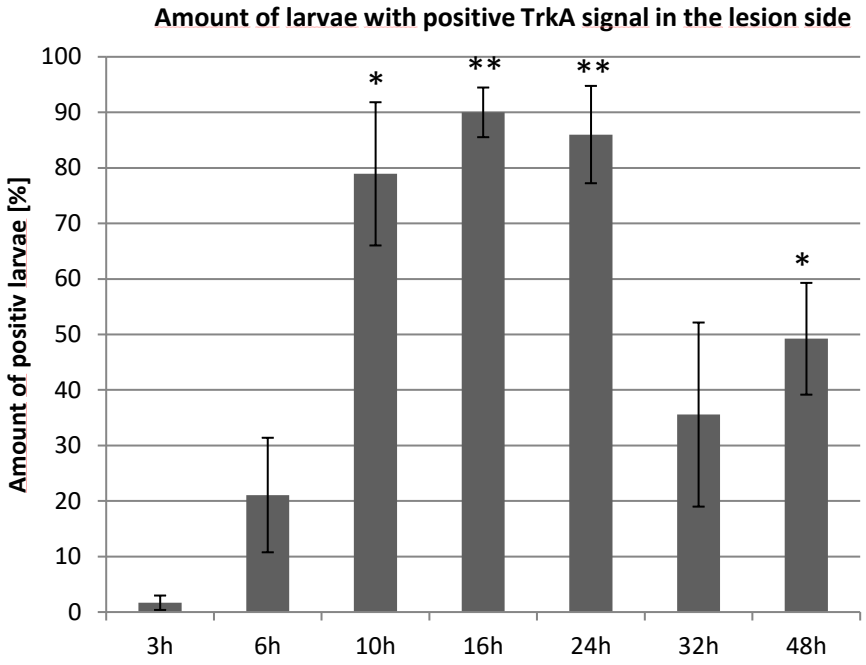

Figure 51: Quantification of *trkA* mRNA expressing embryos which show a signal in the lesion side. The number of fishes showing the *trkA* mRNA expression in the lesion side was analyzed and calculated against the number showing no expression in the side. The expression in the lesion side becomes significantly increase at 10h post lesion and stay significant until 24h. At 32h the number of fishes decreased. At 48h after lesion the expression is significantly increased again. (n = 4)

The lesion in the spinal cord was performed to study the regeneration in the central nervous system. To analyzed now the peripheral nervous system, which is more selected by NGF/TrkA signaling, since NGF/TrkA is more located in the peripheral nervous system (Manni *et al*., 2011; Hudson *et al*., 2000; Cao *et al*., 2011), lesion in the lateral line nerve will be established. Therefore, the already introduced fish line marking sensory neurons by the *trkA*:mClover system was used (Figure 52). At 3dpf the lesion was performed. Therefore, a cut in the region of the lateral line nerve (as shown in Figure 52, upper picture) was conducted by using a needle. It is important to not destroy the blood vessel, which is located underneath the lateral line nerve. Directly after lesion a clear cut is visible (Figure 52, second picture) It can be seen that the lesion side was closed within 24h (Figure 52, third picture).

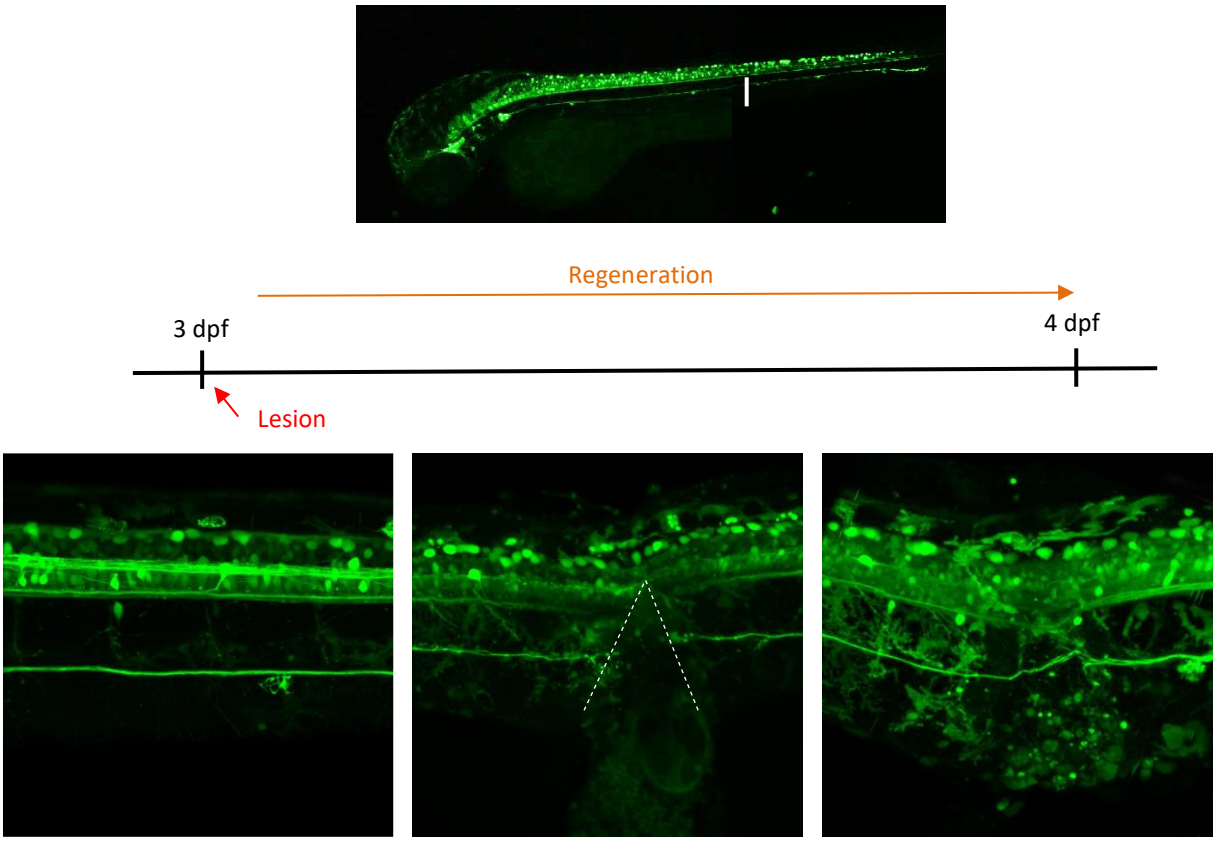

Figure 52: Overview of the lateral line nerve transsection in *trkA*:mCLover transgenic zebrafish and regeneration afterwards. The lesion was performed at 3dpf in larvae from *trkA*:mClover strain. The lesion was analyzed directly after the lesion was performed and after 24h with laser scanning microscope. After 24h the lesion site was closed again. (n = 4)

These two different wounding assays were established to analyze the effect of the different *Hericium* secondary metabolites in possibly promoting regeneration. Since the introduced compounds isolated from *Hericium spec*. were able to stimulate neurotrophin production, like it was shown for NGF and BDNF, these substances are the best compounds to study the effect of cyathane diterpenoids in a model organism especially during regeneration. The both established regeneration models are efficient models, to perform compound screening for regeneration stimulating substances, since a larger number of animals can be challenged easily and with that a high number can be analyzed. But for high throughput assays, another way to challenge neurons should be found than microsurgery.

4. Discussion

Neurotrophins, like NGF and BDNF, have increasingly attracted attention for the treatment of neurodegenerative diseases. The common feature for all neurodegenerative diseases are characterized by a loss of neurons that leads to impairment of neural functions (Bredesen *et al*., 2006). Neurotrophins can act as survival factors to support the maintenance and differentiation of neurons, as well as the proliferation of neuronal precursors (Reichardt, 2006). Neurotrophins cannot be used as external therapeutic factors, because they are unable to cross the blood-brain barrier, which is an important barrier that separates the blood flow from the neuronal system (Pardridge, 2002b). Therefore, smaller metabolites with lower molecular weights become increasingly important in research. Compounds that can cross the blood brain barrier to stimulate the neurotrophin production are in the focus of this thesis.

4.1 Secondary metabolites of *Hericium* spp. are able to stimulate neurotrophin production

Different metabolites isolated from *Hericium* spp. were characterized in this thesis. A new group of compounds called corallocins was identified that have an influence on neurotrophin production. Corallocins are related to hericenones, which can be isolated from the fruiting body of *Hericium erinaceus*. These substances are known to promote neurotrophin expression Kawagishi *et al*., 1992; Ma *et al*., 2010). In this thesis it was shown that corallocins have an influence not only on *ngf* expression, but also on *bdnf* transcription. There two of three corallocins were able to induce PC12 cell differentiation after the incubation with a supernatant that was conditioned by astrocytoma cells. In this thesis there was shown that corallocin A is able to induce PC12 cell differentiation by upregulation of the *ngf* mRNA level in astrocytoma cells, while a *bdnf* upregulation could not be observed. Corallocin B failed to induce PC12 cell differentiation, but it was able to induce the *ngf* mRNA expression, yet at a lower amount than corallocin A. This suggests a threshold for PC12 cell differentiation requiring higher levels of NGF in the media. Mori and coworkers showed that the amount of NGF protein, secreted by 1321N1 cells after incubation with ethanol extracts of *Hericium erinaceus,* is too low to induce PC12 cell differentiation. The authors conclude that other neurotrophic factors were become activated by these extracts (Mori *et al*., 2008). An alternative explanation could be that extracts contains lower amounts of specific corallocins leading to lower amounts of neurotrophin expression below a threshold required for PC12 cell differentiation. Corallocin C can induce PC12 cell differentiation by treatment with the conditioned media of corallocin C treated

astrocytoma cells. It was shown that corallocin C is able to induce *ngf* mRNA and *bdnf* mRNA expression. Surprisingly, corallocin B and C, which share an isoindolinone backbone, have different biological properties. Corallocin B stimulates *ngf* expression weakly, whereas corallocin C can increase both, *ngf* and *bdnf* expression. Corallocin A, which possesses a benzofuranone structure, is only able to stimulate *ngf* production. These findings provide first hints for a structure-activity-relationship analysis.

In addition, a group of already known derivates, called erinacines, was analyzed and two new structures were found. Erinacines are cyathans. To this subclass Striatoides also belong. These compounds are known to enhance NGF-mediated neurite outgrowth in PC12 cells (Bai *et al.*, 2015). All erinacines were able to stimulate *ngf* expression, even the new ones, but at weaker levels. It was shown for the first time that erinacine C stimulates *bdnf* transcription. Remarkably, erinacine B and C differ only by one residue: Erinacine B has an aldehyde group at the position where erinacine C has a hydroxyl group (Figure 53). Erinacine C is the corresponding allyl alcohol to the reactive vicinal unsaturated aldehyde erinacine B. The latter compound is a Michael acceptor and therefore exerts a much high toxicity than erinacine C. A Michael acceptor is a carbonyl group, by which the Michael donator, e.g. other carbonyl groups, can be added.

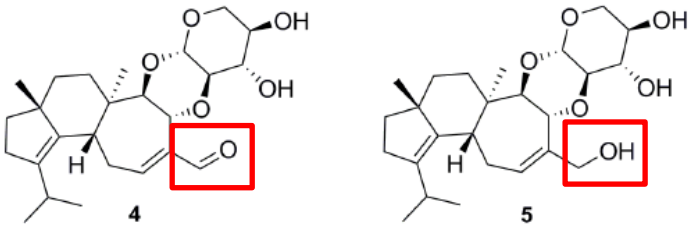

Figure 53: Nearly identical structure of erinacine B and C. The structure of erinacine B and C is nearly identical, the only difference is the aldehyde group for erinacine B, where erinacine C has a hydroxyl group as residue (shown with the red boxes).

The precise structure by which the stimulation of neurotrophin expression takes place is still unknown. Further analysis needs to be performed, starting with *de-novo* synthesis and changing of different residues, followed by analysis of the activity and ability to induce neurotrophin expression and secretion.

We assume that more growth factors could become stimulated by these compounds than the two neurotrophins that were tested so far. For example, EGF and FGF can cause differentiation of PC12 cells (Tyson *et al.*, 2003). Their differentiation is not exclusively induced by TrkA signaling, because other factors like FGF, EGF or PDGF was involved. This cannot be excluded

by our experiments with dnTrkA or inhibitor analysis. In case of the dnTrkA receptor experiments not all cells could become transfected and hence differentiation of PC12 cells induced by NGF and or by the conditioned media was never completely abolished. There was never a complete absence of differentiated cells after the incubation with the different inhibitors. Especially, the Erk1/2 and MAPK are downstream of the EGF signaling cascades or the FGF and PDGF mediated signaling. Further analysis should focus also on these growth factors.

4.2 Different signaling cascades are activated by erinacine C

Different transcription factor binding site activities in cells are increased upon erinacine C incubation. ETS was the binding site, which was analyzed in more detail in this thesis. The analysis included positive and negative controls (activating and inactivating ETS). ETS activity is not necessary for *ngf* transcription. Some results suggest that ETS mediated signaling could have a minor influence on the *bdnf* expression, because *ets1* transcription had a high level after 6h of erinacine C incubation whereas the *bdnf* expression took 48h to a reach a significant peak. With the ETS1 transcriptional activators, no upregulation of the *bdnf* levels was shown, suggesting that ETS1 activity is not sufficient to induce *bdnf* expression.

There are more binding sites showing increased activities after erinacine C incubation, like ERE, NFkappaB, Gli1 or STAT3. It is known that the predicted *ngf* enhancer element isolated from *Tetraodon* contains also binding sites for NFkappaB, suggesting, that NFkappaB is probably involved in the erinacine C dependent upregulation of *ngf*.

ERE is the downstream DNA binding site of the nuclear estrogen signaling. Estrogen signaling has a neuroprotective function in brain injury models (McCullough and Hurn, 2003) and increases the neurogenesis after stroke (Li *et al*., 2011). This factor was important, when searching for a treatment against neuronal death or for regeneration. It was shown that *bdnf* levels are increased after treatment with estrogen (Li *et al*., 2011; Sohrabji *et al*., 1995). NFkappaB was an interesting factor, too. NFkappaB plays an important role in inflammation, immunity, cancer and neuronal plasticity (Häcker and Karin, 2006; Perkins, 2007). Furthermore, NFkappaB is involved in embryonic and adult neurogenesis (Wang and Bordey, 2008; Young *et al*., 2009). Gli proteins are essentially involved in development, homeostasis and disease, including neurogenesis and tumorigenesis. Gli1 is the binding site for the Hedgehog pathway. In embryonic development Hedgehog proteins control the patterning of neuronal precursors, and their neuronal and glial progenitors. It was also shown that Hedgehog is involved in the formation and plasticity of neuronal circuits (Yao *et al*., 2016). Among others,

Hedgehog is able to increase the *bdnf* expression levels in regenerating cavernous nerve (Bond *et al*., 2013). In addition, STAT3 would be a very interesting candidate, since it was shown that there is a connection between brain inflammation and STAT3 activation (Chen *et al*., 2013). STAT3 has an influence on cytokine- and growth factor induced signals and by that it has an influence on cell proliferation, differentiation and apoptosis (Ihle, 2001).

These growth factors which are involved in PC12 cell differentiation, was affected by Erinacine C mediated by ETS signaling.

4.3 The predicted *ngf* enhancer fragment is erinacine C responsive

The 5' regulatory region of the human *ngf* gene has a very complex structure, it is hard to predict the enhancer region of this gene. Luckily, the *Tetraodon nigrovirdis* genome is highly conserved. The *ngf* gene consists of only one exon, and the regulatory region could be in the 5' upstream region. A 2.1 kb fragment upstream of the *ngf* exon, isolated from *T. nigrovirdis*, was cloned in front of a luciferase reporter. It was shown, that the predicted *ngf* enhancer fragment, responds to erinacine C incubation. This was analyzed in more detail on four subcloned fragments (500 bp fragments of the 2.1kb enhancer region; 1, 2, 3, 4). It seemed, when using the endogenous promotor, which is probably located in the 500bp nearest to the start codon (Figure 54; 4), is necessary for a strong activation of the luciferase expression. The construct, where a basal E1b promotor was used, are weaker in the activation of luciferase expression. For further analysis this has to be kept in mind, since no significant upregulation upon erinacine C treatment with the basal promotor was observed.

Our results indicate that the first 500bp region of the enhancer fragment (Figure 54; 1) is required to activate the luciferase expression. Interestingly, also the third element (Figure 54; 3) contains regions that are involved in the process of luciferase activation by erinacine C, while the second region (Figure 54; 2) that lies in between has no, or an inhibitory function. The fourth most distant part of the 2.1kb fragment containing the 5' most 500bp region (Figure 54; 4) shows no inducible luciferase activity by erinacine C. Hence, this element is very likely not involved in the erinacine C dependent upregulation, but this part probably contains the endogenous promotor (Figure 54).

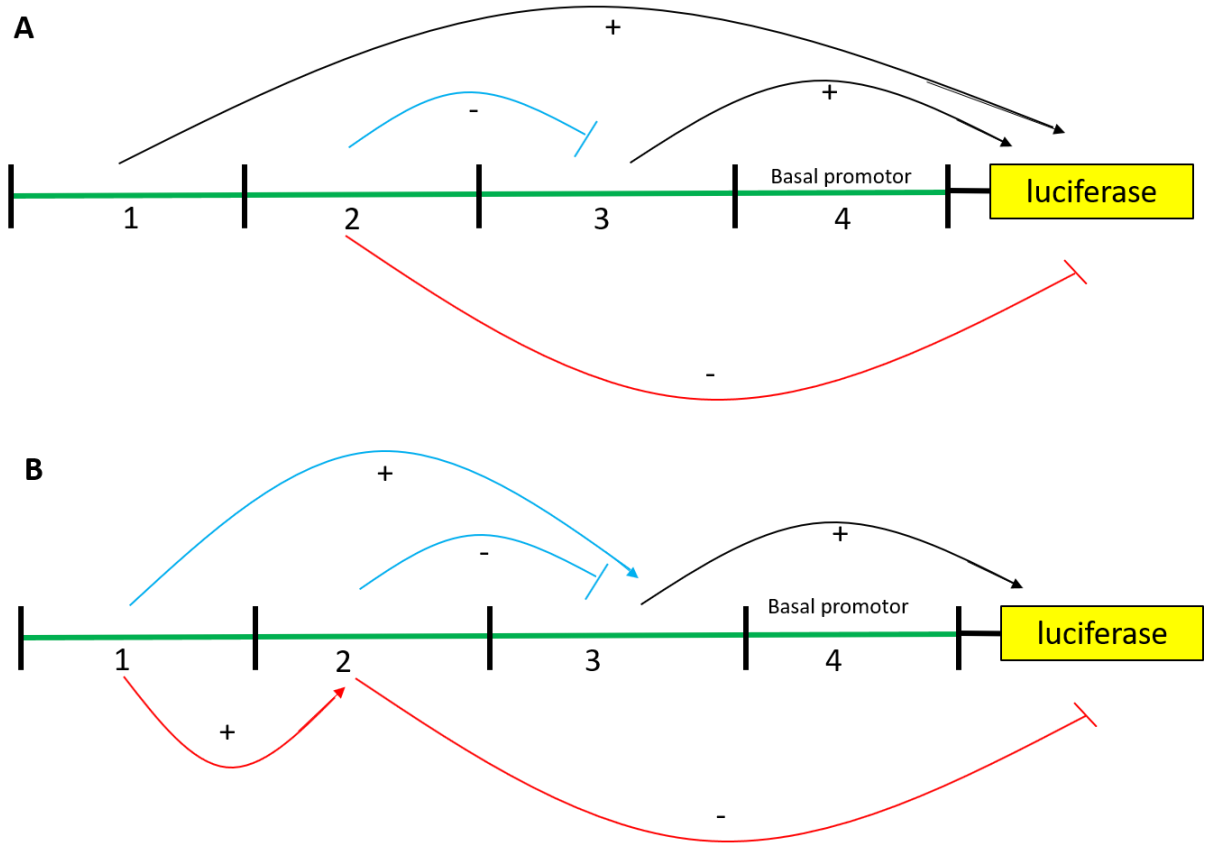

Figure 54: Assumption of effects of the regulatory elements in the putative *ngf* regulatory 5' region of *Tetraodon*. There are two of the several possible variants of activating or inhibiting elements contained in the 2.1 kb 5' fragment (A, B, green fragment). Elements of the first 500bp (1) seem to act as an activator: it could directly activate the expression of luciferase as shown in Figure A, or it could activate the second 500bp (2) laying elements (B, red) or the third 500bp (3) containing elements (B, blue). On the other side elements of the second 500bp (2) seem to work as repressor, for the third 500bp (A, B; blue; 3) or directly for the luciferase expression (A, B; red). The third 500bp (3) could act as activator, directly activate the luciferase expression (A, B). In the experiments, the last 500bp (4) seem to be not responsive to erinacine C incubation, but probably contain the basal promotor.

Apart from that, our results lead to the suggestion that a 2.1kb *ngf* enhancer fragment is responding to ETS activation and repression. These binding sites should become identified in future experiments. Interestingly, the use of a KRAB construct to repress ETS signaling did not completely inhibit the luciferase activity after erinacine C treatment. This suggests that additional factors are involved in the erinacine C dependent activation within the predicted *ngf* enhancer fragment.

4.4 Erinacine C can cross the blood-brain barrier

In this thesis it was shown that erinacine C is likely able to cross the blood brain barrier. This was proven *in vitro* and *in vivo*. For the *in vitro* approach, a triple culture of endothelial cells, pericytes and astrocytes was used to establish a strong barrier. Using this approach, it was also shown, that erinacine C is able to pass this barrier and is not a target of the P-gp efflux transporter. For the *in vivo* approach we used the zebrafish as a vertebrate model to test whether

erinacine C is able to cross the blood-brain barrier. In zebrafish larvae the blood-brain barrier is established between day 4 - 10 post fertilization (Leeuwen *et al*., 2018). We treated different larval stages with erinacine C. After 3 days of incubation, the brains of the larvae were dissected and the amount of erinacine C was measured using HPLC. Erinacine C was detected in varying amounts, but in all zebrafish brains at all developmental stages. But it is not clear yet, if erinacine C was isolated from the nervous system or from the blood vessels.

Future experiments should clarify in which brain regions erinacine C is active. Different approaches were applied: erinacine C was coupled to a fluorescent marker to make it visible in the zebrafish larvae. Another approach could generate a split fluorescent protein, which can become active only, when the two components are co-localized in the same region. Neurotrophin is upregulated by erinacine C and NGF is widely expressed in the zebrafish brain. The suggestion is to express one part of the split fluorescent protein under control of an enhancer that activates expression specifically in one cell type. The second part can be expressed under the control of the binding sites that can become activated by erinacine C, as shown in this thesis. Then, fluorescence should indicate if a certain signaling cascade becomes activated in a specific cell type.

In this thesis it has been shown that erinacine C is likely able to cross the blood-brain barrier. Based on this finding, further analysis was performed using the zebrafish model. The zebrafish is a very suitable organism and needs little space. Embryos, larvae and even adults can be kept temporarily in small volumes of conditioned media, which is beneficial for compound screenings. Because the zebrafish is able to regenerate neuronal cells, different regeneration models was used to screen the effect of erinacine C *in vivo*.

4.5 Analysis of possible effects of erinacine C *in vivo*

Some compounds of edible fungi could have side effects *in vivo*. Pure substances in higher concentrations can induce toxicity. The zebrafish is a perfect screening system, to analyze side effects of substances.

Neurotrophin stimulating compounds could influence different signaling pathways: In this thesis it was shown that the zebrafish *ngf* gene as well as the high affinity receptor *trkA*, are seemed to be expressed in neurogenic niches of the brain (D'Angelo *et al*., 2014). In future experiments compounds was used that are able to induce neurotrophin expression like NGF, to test their regenerative potencies. Successful compound treatments were verified by an increase

of neurogenic marker expression in corresponding niches. However, a double fluorescent *in situ* hybridization for both mRNA together would be very interesting, since some regions, like the cerebellum show both expressions, *ngf* and *trkA*. Purkinje cells, for example, seemed to show expression of *ngf* as well as *trkA*, suggesting, that there are autocrine pathways being activated.

In a previous master thesis (Monique Rascher), a transgenic zebrafish line was established to analyze the effect of neurotrophin inducing compounds. This line was used to induce neurodegeneration and regeneration and to quantify late effects of compounds *in vivo*. In this context, also other factors like FGF was analyzed regarding their upregulated activity upon erinacine C incubation. FGF is known to be involved in glial cell bridges during spinal cord regeneration (Goldsmit *et al*., 2012). FGF8 was upregulated after erinacine C treatment in astrocytoma cell *in vitro* (Figure 24). This activity could also be important for spinal cord regeneration. It is known that zebrafish are able to regenerate spinal cord injuries within 48h (Goldshmit et al., 2012; Becker et al., 2004; Mokalled et al., 2017; Becker et al., 1997). The connective tissue growth factor a (ctgfa) is another trophic factor involved in spinal cord regeneration (Mokalled *et al*., 2017) that was tested for activation by erinacine C.

In this thesis another regeneration model was established. The lateral line nerve belongs to the peripheral nervous system and substances, which are diluted in the surrounding media, are immediately accessible for the lateral line. This neuronal region has an easier access to compounds than neuronal cells of the central nervous system that are protected by the BBB. It was shown in this thesis that a regeneration of the lateral line nerve occurs 24h after lesion. Several signaling pathways including Notch, Wnt (canonical and non-canonical), FGF, BMP and Hedgehog play a role during regeneration of the lateral line nerve (Kelley, 2006, Fritzsch *et al*., 2011, Wu and Kelley, 2012, Munnamalai and Fekete, 2013). FGF, BMP and Hedgehog binding sites were activated by erinacine C treatment in astroglial cells and it was shown that NGF/TrkA signaling is involved in spinal cord regeneration.

The *bdnf* expression pattern, as well as the high affinity receptor of BDNF, TrkB, should be analyzed and quantified regarding their expression during the regenerative processes of cells. In addition, zebrafish models for cerebellar Purkinje cell degeneration have been established in the lab of Prof. Dr. Reinhard W. Köster, modelling genetically induced ataxia in the zebrafish (Namikawa *et al*., 2019b) or by pharmacological induction of Purkinje cell degeneration (Weber *et al*., 2016). These two models could also be useful in future experiments to study the effect of neurotrophin inducing compounds during degeneration and regeneration.

The results shown in this thesis provide the first insights of direct cell responses upon natural product incubation. Using this approach, the effects of erinacine C treatment can be analyzed also *in vivo*, but also other substances isolated from fungi and plants can be analyzed.

5. Literature

Acheson A, Conover JC, Fandl JP, DeChiara TM, Russell M, Thadani A, Squinto SP, Yancopoulos GD and Lindsay RM (1995)
A BDNF autocrine loop in adult sensory neurons prevents cell death.
Nature. **374**, Nr. 6521, März 1995, S. 450–3.

Aguirre A, Rubio ME and Gallo V. (2010)
Notch and EGFR pathway interaction regulates neural stem cell number and self-renewal.
Nature. **467** (7313): 323–7.

Albensi BC and Mattson MP. (2000)
Evidence for the involvement of TNF and NF-κB in hippocampal synaptic plasticity.
Synapse. **35** (2): 151–9.

Alberts B, Bray D, Hopkin K, Johnson AD, Lewis J, Raff M, Roberts K and Walter P. (2001)
Lehrbuch der molekularen Zellbiologie. 2., korrigierte Auflage. Wiley-VCH, Weinheim u. a. 2001, ISBN 3-527-30493-2.

Amaya E, Musci TJ and Kirschner MW. (1991)
Expression of a dominant negative mutant of the FGF receptor disrupts mesoderm formation in *Xenopus* embryos.
Cell. 1991 Jul 26;**66**(2):257-70.

Arakawa T1, Haniu M, Narhi LO, Miller JA, Talvenheimo J, Philo JS, Chute HT, Matheson C, Carnahan J and Louis JC (1994)
Formation of heterodimers from three neurotrophins, nerve growth factor, neurotrophin-3, and brain-derived neurotrophic factor.
J Biol Chem. 1994 Nov 11;**269**(45):27833-9.

Arsenijevic Y ad Weiss S. (1998)
Insulin-like growth factor-I is a differentiation factor for postmitotic CNS stem cell-derived neuronal precursors: Distinct actions from those of brain-derived neurotrophic factor.
J Neurosci **18**: 2118-2128

Artavanis-Tsakonas S, Rand MD and Lake RJ. (1999)
Notch signaling: cell fate control and signal integration in development.
Science. **284** (5415): 770–6.

Attisano L and Wrana JL. (2002)
Signal transduction by the TGF-b superfamily.
Science. 2002;**296**:1646–1647.

Bai R, Zhang CC, Yin X, Wei J and Gao JM. (2015)
Striatoids A-F, Cyathane Diterpenoids with Neurotrophic Activity from Cultures of the Fungus *Cyathus striatus*.
J Nat Prod. 2015 Apr 24;**78**(4):783-8.

Bae YK, Kani S, Shimizu T, Tanabe K, Nojima H, Kimura Y, Higashijima S and Hibi M. (2009)
Anatomy of zebrafish cerebellum and screen for mutations affecting its development.
Dev Biol. 2009 Jun 15;**330**(2):406-26.

Bandmann O and Burton EA. (2010)
Genetic zebrafish models of neurodegenerative diseases.
Neurobiol Dis. 2010 Oct;**40**(1):58-65.

Barbacid M (1994)
The Trk family of neurotrophin receptors.
J. Neurobiol. **25**, 1386-1403

Barde YA, Edgar D and Thoenen H. (1982)
Purification of a new neurotrophic factor from mammalian brain.
EMBO J., **1**, 549 – 553

Baron U, Gossen M and Bujard H. (1997)
Tetracycline-controlled transcription in eurokrayotes: Novel transactivators with graded transactivation potential.
Nucleic Acids Res **25**:2723-2729

Becker CG, Lieberoth BC, Morellini F, Feldner J, Becker T and Schachner M. (2004)
L1.1 is involved in spinal cord regeneration in adult zebrafish.
J Neurosci. 2004 Sep 8;**24**(36):7837-42.#

Becker T, Wullimann MF, Becker CG, Bernhardt RR and Schachner M. (1997)
Axonal regrowth after spinal cord transection in adult zebrafish.
J Comp Neurol. 1997 Jan 27;**377**(4):577-95.

Bekinschtein P, Cammarota M, Katche C, Slipczuk L, Rossato JI, Goldin A, Izquierdo I and Medina JH (2008)
BDNF is essential to promote persistence of long-term memory storage.
Proc. Natl. Acad. Sci. U.S.A. **105**, Nr. 7, Februar 2008, S. 2711–6.

Berkemeier LR, Winslow JW, Kaplan DR, Nikolics K, Goeddel DV, Rosenthal A (1991)
Neurotrophin-5: a novel neurotrophic factor that activates trk and trkB.
Neuron. 1991 Nov;**7**(5):857-66.

Berkemeier LR, Ozcelik T, Frncke U and Rosenthal A (1992)
Human chromosome 19 contains the neurotrophin-5 gene locus and three related genes that may encode novel acidic neurotrophins.
Somat Cell Mol Genet. 1992 May;**18**(3):233-45.

Berriman JA, Li S, Hewlett LJ, Wasilewski S, Kiskin FN, Carter T, Hannah MJ and Rosenthal BP. (2009)
Structural organization of Weibel-Palade bodies revealed by cryo-EM of vitrified endothelial cells
Proc Natl Acad Sci U S A. 2009 Oct 13; **106**(41): 17407–17412.

Besnard A, Galan-Rodriguez B, Vanhoutte P and Caboche J. (2011)
Elk-1 a transcription factor with multiple facets in the brain.
Front Neurosci. 2011 Mar 16;**5**:35.

Binder DK and Scharfman HE. (2004)
Brain-derived neurotrophic factor.
Growth Factors. **22**, Nr. 3, September 2004, 123–31.

Bobinet M, Vignard V, Florenceau L, Lang F, Labarriere N and Moreau-Aubry A. (2013)
Overexpression of *meloe* gene in melanomas is controlled both by specific transcription factors and hypomethylation.
PLoS One. 2013 Sep 25;**8**(9):e75421.

Bolós V, Grego-Bessa J and de la Pompa JL. (2007)
Notch signaling in development and cancer.
Endocrine Reviews. **28** (3): 339–63.

Bond CW, Angeloni N, Harrington D, Stupp S and Podlasek CA. (2013)
Sonic Hedgehog regulates brain-derived neurotrophic factor in normal and regenerating cavernous nerves.
J Sex Med. 2013 Mar;**10**(3):730-7.

Boros J, Donaldson IJ, O'Donnell A, Odrowaz ZA, Zeef L, Lupien M, Meyer CA, Liu XS, Brown M and Sharrocks AD. (2009)
Elucidation of the ELK1 target gene network reveals a role in the coordinate regulation of core components of the gene regulation machinery.
Genome Res. 2009 Nov;**19**(11):1963-73.

Brasier AR. (2006)
The NF-κB regulatory network.
Cardiovascular Toxicology. **6** (2): 111–30.

Bredesen DE, Rao RV and Mehlen P. (2006)
Cell death in the nervous system.
Nature. 2006 Oct 19; **443**(7113): 796–802.

Brown LA, Yang SH, Hair A, Galanis A and Sharrocks AD. (1999)
Molecular characterization of a zebrafish TCF ETS-domain transcription factor.
Oncogene. 1999 Dec 23;**18**(56):7985-93.

Brunner D, Oellers N, Szabad J, Biggs WHR, Zipursky SL and Hafen E. (1994)
A gain-of-function mutation in Drosophila MAP kinase activates multiple receptor tyrosine kinase signaling pathways
Cell, **76** (1994), pp. 875-888

Cacialli P and Lucini C. (2019)
Adult neurogenesis and regeneration in zebrafish brain: are the neurotrophins involved in?
Neural Regen Res. 2019 Dec; **14**(12): 2067–2068.

Callard GV, Tchoudakova AV, Kishida M and Wood E. (2001)
Differential tissue distribution, developmental programming, estrogen regulation and promoter characteristics of cyp19 genes in teleost fish.
J Steroid Biochem Mol Biol. 2001 Dec;**79**(1-5):305-14.

Cao J, Sun C, Zhao H, Xiao Z, Chen B, Gao J, Zheng T, Wu W, Wu S, Wang J and Dai J. (2011)
The use of laminin modified linear ordered collagen scaffolds loaded with laminin-binding ciliary neurotrophic factor for sciatic nerve regeneration in rats.
Biomaterials. 2011;**32**(16):3939–3948.

Cao CY, Zhang CC, Shi XW, Li D, Cao W, Yin X and Gao JM. (2018)
Sarcodonin G derivated exhibit distinctive effects on neurite outgrowth by modulating NGF signaling in PC12 cells.
ACS Chem Neurosci **9** (7): 1607-1615

Casaccia-Bonnefil P, Carter BD, Dobrowsky RT and Chao MV (1996)
Death of oligodendrocytes mediated by the interaction of nerve growth factor with its receptor p75.
Nature. 1996 Oct 24;**383**(6602):716-9.

Cauchy P, Maqbool MA, Zacarias-Cabeza J, Vanhille L, Koch F, Fenouil R, Gut M, Gut I, Santana MA, Griffon A, Imbert J, Moraes-Cabé C, Bories JC, Ferrier P, Spicuglia S and Andrau JC. (2016)
Dynamic recruitment of Ets1 to both nucleosome-occupied and -depleted enhancer regions mediates a transcriptional program switch during early T-cell differentiation.
Nucleic Acids Res. 2016 May 5;**44**(8):3567-85.

Chao MV and Hempstead BL (1995)
p75 and Trk: a two-receptor system.
Trends Neurosci. 1995 Jul;**18**(7):321-6.

Chen E, Xu D, Lan X, Jia B, Sun L, Zheng JC and Peng H. (2013)
A novel role of the STAT3 pathway in brain inflammation-induced human neural progenitor cell differentiation.
Curr Mol Med. 2013 Nov;**13**(9):1474-84.

Chen L, Glover JN, Hogan PG, Rao A and Harrison SC. (1998)
Structure of the DNA-binding domains from NFAT, Fos and Jun bound specifically to DNA.
Nature. 1998 Mar 5;**392**(6671):42-8.

Cordon-Cardo C, Tapley P, Jing S, Nanduri V, O`Rocke E, Lamballe F, Kovary K, Klein R, Jones KR, Reichardt LF and Barbacid M (1991)
The *trk* tyrosine protein kinase mediates the mitotic properties of nerve growth factor and neurotrophin-3.
Cell *66*: 173-183.

Cowley DO and Graves BJ. (2000)
Phosphorylation represses Ets-1 DNA binding by reinforcing autoinhibition
Genes Dev. 2000 Feb 1; **14**(3): 366–376.

Cunningham ME and Greene LA. (1998)
A function–structure model for NGF-activated TRK.
EMBO J (1998)**17**:7282-7293

Daneman R and Prat A. (2015)
The Blood–Brain Barrier
Cold Spring Harb Perspect Biol. 2015 Jan; **7**(1): a020412.

Datta SR, Brunet A and Greenberg ME. (1999)
Cellular survival: a play in three Akts.
Genes Dev. 1999 Nov 15;**13**(22):2905-27.

D'Angelo L, Castaldo L, Cellerino A, de Girolamo P and Lucini C. (2014)
Nerve growth factor in the adult brain of a teleostean model for aging research: *Nothobranchius furzeri*.
Ann Anat. 2014 Jul;**196**(4):183-91.

Dechant G and Barde YA (2002)
The neurotrophin receptor p75(NTR): novel functions and implications for diseases of the nervous system.
Nat Neurosci. 2002 Nov;**5**(11):1131-6.

Dekkers MPJ, Nikoletopoulou V and Barde YA. (2013)
Death of developing neurons: New insights and implications for connectivity
J Cell Biol. 2013 Nov 11; **203**(3): 385–393.

Dennler S, Itoh S, Vivien D, ten Dijke P, Huet S and Gauthier JM. (1998).
Direct binding of Smad3 and Smad4 to critical TGF beta-inducible elements in the promoter of human plasminogen activator inhibitor-type 1 gene.
EMBO J. **17**, 3091–3100.

Di Vona C, Bezdan D, Islam AB, Salichs E, López-Bigas N, Ossowski S and de la Luna S. (2015) Chromatin-wide profiling of DYRK1A reveals a role as a gene-specific RNA polymerase II CTD kinase.
Mol Cell. 2015 Feb 5;**57**(3):506-20.

Ebendal T, Larhammar D and Persson H (1986)
Structure and expression of the chicken beta nerve growth factor gene.
EMBO J. 1986 Jul;**5**(7):1483-7.

Edwards RH, Selby MJ and Rutter WJ (1986)
Differential RNA splicing predicts two distinct nerve growth factor precursors.
Nature. 1986 Feb 27-Mar 5;**319**(6056):784-7.

Eik LF, Naidu M, David P and Wong KH. (2012)
Lignosus rhinoceros (Cooke) Ryvarden: a medicinal mushroom, that stimulated neurite outgrowth in PC-12 cells.
Evid Based Complement Alternat Med 2012:320308

Eliceiri BP, Gonzalez AM and Baird A. (2011)
Zebrafish model of the blood-brain barrier: morphological and permeability studies.
Methods Mol Biol. 2011;**686**:371-8.

Flames N and Hobert O. (2009)
Gene regulatory logic of dopamine neuron differentiation.
Nature. 2009 Apr 16;**458**(7240):885-9.

Francke U, de Martinville B, Coussens L and Ullrch A (1983)
The human gene for the beta subunit of nerve growth factor is located on the proximal short arm of chromosome 1.
Science, 1983, **222**(4629), 1248-1251

Freudenthal R, Locatelli F, Hermitte G, Maldonado H, Lafourcade C, Delorenzi A and Romano A. (1998)
κ-B like DNA-binding activity is enhanced after spaced training that induces long-term memory in the crab *Chasmagnathus*.
Neuroscience Letters. **242** (3): 143–6.

Fritzsch B, Jahan I, Pan N, Kersigo J, Duncan J and Kopecky B. (2011)
Dissecting the molecular basis of organ of Corti development: Where are we now?
Hearing research. 2011;**276**:16–26.

Gaiano N and Fishell G. (2002)
The role of notch in promoting glial and neural stem cell fates.
Annual Review of Neuroscience. **25** (1): 471–90.

Gilmore TD. (1999)
The Rel/NF-κB signal transduction pathway: introduction.
Oncogene. **18** (49): 6842–4.

Gilmore TD. (2006)
Introduction to NF-κB: players, pathways, perspectives.
Oncogene. **25** (51): 6680–4.

Ginsburg D, Handin RI, Bonthron DT, Donlon TA, Bruns GA, Latt SA and Orkin SH. (1985)
Human von Willebrand factor (vWF): isolation of complementary DNA (cDNA) clones and chromosomal localization.
Science. 1985 Jun 21;**228**(4706):1401-6.

Goldshmit Y, Sztal TE, Jusuf PR, Hall TE, Nguyen-Chi M and Currie PD. (2012)
Fgf-dependent glial cell bridges facilitate spinal cord regeneration in zebrafish.
J Neurosci. 2012 May 30;**32**(22):7477-92.

Gorelick DA and Halper ME. (2011)
Visualization of estrogen receptor transcriptional activation in zebrafish.
Endocrinology **152**: 2690-2703.

Götz R, Köster R, Winkler C, Raulf F, Lottspeich F, Schartl M and Thoenen H. (1994)
Neurotrophin-6 is a new member of the nerve growth factor family.
Nature. 1994 Nov 17;**372**(6503):266-9.

Greenald D, Jeyakani J, Pelster B, Sealy I, Mathavan S and van Eeden FJ. (2015)
Genome-wide mapping of Hif-1α binding sites in zebrafish.
BMC Genomics. 2015 Nov 11;**16**:923.

Greene LA and Tischler AS (1976)
Establishment of a noradrenergic clonal line of rat adrenal pheochromocytoma cells which respond to nerve growth factor.
Proc. Natl. Acad. Sci. USA, Vol. 73, No. 7, pp. 2424 – 2428, July 1976; Cell Biology.

Hallbrook F, Ibanez CF and Persson H (1991)
Evolutionary studies of the nerve growth factor family reveal a novel member abundantly expressed in *Xenopus* ovary.
Neuron, 1991, **6**(5), 845-858

Harrington AW and Ginty DD. (2013)
Long-distance retrograde neurotrophic factor signaling in neurons.
Nat Rev Neurosci. 2013 Mar;**14**(3):177-87.

Häcker H and Karin M. (2006)
Regulation and function of IKK and IKK-related kinases.
Sci STKE. 2006 Oct 17;**2006**(357):re13.

Hefti F. (1994)
Neurotrophic factor therapy for nervous system degenerative diseases.
J Neurobiol. 1994 Nov;**25**(11):1418-35.

Heinrich G and Lum T. (2000)
Fish neurotrophins and Trk receptors.
Int J dev Neurosci. **18**(1):1-27.

Hennigan A, O'Callaghan RM and Kelly AM. (2007)
Neurotrophins and their receptors: roles in plasticity, neurodegeneration and neuroprotection.
Biochem Soc Trans. 2007 Apr;**35**(Pt 2):424-7.

Hetman M, Cavanaugh JE, Kimelman D, Xia Z. (2000)
Role of glycogen synthase kinase-3beta in neuronal apoptosis induced by trophic withdrawal.
J Neurosci. 2000 Apr 1;**20**(7):2567-74.

Hibi M and Shimizu T. (2012)
Development of the cerebellum and cerebellar neural circuits.
Dev Neurobiol. 2012 Mar;**72**(3):282-301.

Hipskind RA, Büscher D, Nordheim A and Baccarini M. (1994)
Ras/MAP kinase-dependent and -independent signaling pathways target distinct ternary complex factors.
Genes Dev. 1994 Aug 1;**8**(15):1803-16.

Hitoshi S, Alexson T, Tropepe V, Donoviel D, Elia AJ, Nye JS, Conlon RA, Mak TW, Bernstein A and van der Kooy D. (2002)
Notch pathway molecules are essential for the maintenance, but not the generation, of mammalian neural stem cells.
Genes & Development. **16** (7): 846–58.

Hoke KL and Fernald RD (1998)
Cell death precedes rod neurogenesis in embryonic teleost retinal development.
Brain Res Dev Brain Res. 1998 Nov 1;**111(**1):143-6.

Hollenhorst PC, McIntosh LP and Graves BJ. (2011)
Genomic and Biochemical Insights into the Specificity of ETS Transcription Factors
Annu Rev Biochem. 2011; **80**: 437–471.

Hopman AH, Ramaekers FC and Speel EJ. (1998)
Rapid synthesis of biotin-, digoxigenin-, trinitrophenyl-, and fluorochrome-labeled tyramides and their application for *In situ* hybridization using CARD amplification.
The journal of histochemistry and cytochemistry: official journal of the Histochemistry Society **46**, 771–777.

Howe DG, Bradford YM, Conlin T, Eagle AE, Fashena D, Frazer K, Knight J, Mani P, Martin R, Taylor Moxon SA, Paddock H, Pich C, Ramachandran S, Ruef BJ, Ruzicka L, Schaper K, Shao X, Singer A, Sprunger B, Van Slyke CE and Westerfield M. (2013)
ZFIN, the Zebrafish Model Organism Database: increased support for mutants and transgenics
Nucleic Acids Res. 2013 Jan; **41**(Database issue): D854–D860.

Huang EJ and Reichardt LF (2001)
Neurotrophins: roles in neuronal development and function.
Annu. Rev. Neurosci. **24**, 2001, S. 677–736.

Hudson TW, Evans GR and Schmidt CE. (2000)
Engineering strategies for peripheral nerve repair.
Orthop Clin North Am. 2000;**31**(3):485–498.

Ihle JN. (2001)
The Stat family in cytokine signaling.
Curr Opin Cell Biol. 2001 Apr;**13**(2):211-7.

Ip NY, Ibanez CF, Nye SH, McClain J, Jones PF, Gies DR, Belluscio L, Le Beau MM, Espinosa R and Squinto SP (1992)
Mammalian neurotrophin-4: structure, chromosomal localization, tissue distribution, and receptor specificity.
Proc Natl Acad Sci U S A. 1992 Apr 1; **89**(7): 3060–3064.

Janning W and Knust E. (2008)
Genetik: Allgemeine Genetik - Molekulare Genetik – Entwicklungsgenetik
Thieme; Auflage: 2 (24. September 2008)

Jing S, Tapley P and Barbacid M (1992)
Nerve growth factor mediates signal transduction through trk homodimer receptors.
Neuron *9*: 1067-1079.

Johnson EM and Gorin PG (1980)
Dorsal root ganglion neurons are destroyed by exposure *in utero* to maternal antibody to nerve growth factor.
Science *210*: 916-918.

Kakidani H and Ptashne M. (1988)
GAL4 activates gene expression in mammalian cells.
Cell. **52** (2): 161–167.

Kaplan DR, Martin-Zanca D and Parada LF (1991)
Tyrosine phosphorylation and tyrosine kinase activation of the trk proto-oncogene product induced by NGF.
Nature *350*: 158-160.

Kaplan DR and Miller FD. (2000)
Neurotrophin signal transduction in the nervous system.
Curr Opin Neurobiol. 2000 Jun;**10**(3):381-91.

Kaslin J, Ganz J and Brand M. (2008)
Proliferation, neurogenesis and regeneration in the non-mammalian vertebrate brain.
Philos Trans R Soc Lond B Biol Sci. 2008 Jan 12;**363**(1489):101-22.

Kawagishi H, Ando M, Shinba K, Sakamoto H, Yoshida S, Ojima F, Ishiguro Y, Ukai N and Furukawa S. (1992)
Chromans, hericenones F, G and H from the mushroom *Hericium erinaceum*.
Phytochemistry. **32**: 175–178.

Kawagishi H, Mori H, Uno A, Kimura A and Chiba S. (1994)
A sialic acid-binding lectin from the mushroom *Hericium erinaceum*.
FEBS Lett. 1994 Feb 28;**340**(1-2):56-8.

Kawagishi H, Murakami H, Sakai S and Inoue S. (2006)
Carnitine-esters from the mushroom *Suillus laricinus*.
Phytochemistry. 2006 Dec;**67**(24):2676-80.

Kawagishi H, Nomura A, Mizuno T, Kimura A and Chiba S. (1990)
Isolation and characterization of a lectin from *Grifola frondosa* fruiting bodies.
Biochim Biophys Acta. 1990 Jun 20;**1034**(3):247-52.

Kim YO, Lee SW, Oh CH and Rhee YH. (2012)
Hericium erinaceus suppresses LPS-induced pro-inflammation gene activation in RAW264.7 macrophages.
Immunopharmacol Immunotoxicol **34**:504–512

Kim JY, Woo EE, Lee IK and Yun BS. (2018)
New antioxidants from the culture broth of *Hericium coralloides*.
J Antibiot (Tokyo). 2018 Sep;**71**(9):822-825.

Kimmel CB, Ballard WW, Kimmel AR, Ullmann B and Schilling TF (1995)
Stages of Embryonic Development of the Zebrafish.
Developmental Dynamic **203**:253-310 (1995).

Kinzler KW and Vogelstein B. (1990)
The GLI gene encodes a nuclear protein which binds specific sequences in the human genome. *Molecular and Cellular Biology* **10**: 634-642.

Kelley MW. (2006)
Regulation of cell fate in the sensory epithelia of the inner ear.
Nature reviews. Neuroscience. 2006;**7**:837–849.

Klein R (1994)
Role of neurotrophins in mouse neuronal development.
FASEB J. **8**, 738-744

Klein R, Conway D, Parada LF and Barbacid M (1990)
The trkB tyrosine protein kinase gene codes for a second neurogenic receptor that lacks the catalytic kinase domain.
Cell. 1990 May 18;**61**(4):647-56.

Klein R, Jing SQ, Nanduri V, O'Rourke E and Barbacid M (1991)
The trk proto-oncogene encodes a receptor for nerve growth factor.
Cell. 1991 Apr 5;**65**(1):189-97.

Knippers R. (2006)
Molekulare Genetik. 9., komplett überarbeitete Auflage. Thieme, Stuttgart u. a. 2006, ISBN 3-13-477009-1.

Kulkarni RP, Tohari S, Ho A, Brenner S and Venkatesh B. (2010)
Characterization of a hypoxia-response element in the Epo locus of the pufferfish, *Takifugu rubripes*.
Mar Genomics. 2010 Jun;**3**(2):63-70.

Kuri P, Ellwanger K, Kufer TA, Leptin M and Bajoghli B. (2017).
A high-sensitivity bi-directional reporter to monitor NF-κB activity in cell culture and zebrafish in real time.
J. Cell Sci. **130**, 648 LP – 657.

Lackey EP, Heck DH and Sillitoe RV. (2018)
Recent advances in understanding the mechanisms of cerebellar granule cell development and function and their contribution to behavior
F1000Res. 2018; **7**: F1000 Faculty Rev-1142.

Lai PL, Naidu M, Sabaratnam V, Wong KH, David RP, Kuppusamy UR, Abdullah N and Malek SN. (2013)
Neurotrophic properties of the Lion's mane medicinal mushroom, *Hericium erinaceus* (Higher Basidiomycetes) from Malaysia.
Int J Med Mushrooms. 2013;**15**(6):539-54.

Lamballe F, Klein R and Barbacid M (1991)
trkC, a new member of the trk family of tyrosine protein kinases, is a receptor for neurotrophin-3.
Cell. 1991 September 6; **66**(5): 967-979.

Langlais D, Couture C, Balsalobre A and Drouin J. (2008)
Regulatory network analyses reveal genome-wide potentiation of LIF signaling by glucocorticoids and define an innate cell defense response.
PLoS Genet. 2008 Oct;**4**(10):e1000224.

Lauter G, Söll I and Hauptmann G. (2011)
Multicolor fluorescent in situ hybridization to define abutting and overlapping gene expression in the embryonic zebrafish brain.
Neural development **6**, 10.

Leibrock J, Lottspeich F, Hohn A, Hofer M, Hengerer B, Masiakowski P, Thoenen H and Barde YA (1989)
Molecular cloning and expression of brain-derived neurotrophic factor.
Nature, 1989, **341**(6238), 149-152

Leingärtner A and Lindholm D (1994)
Two promoters direct transcription of the mouse NT-3 gene.
Eur J Neurosci. 1994 Jul 1;**6**(7):1149-59.

Lee GM, Donaldson LW, Pufall MA, Kang HS, Pot I, Graves BJ and McIntosh LP. (2005)
The structural and dynamic basis of Ets-1 DNA binding autoinhibition.
J Biol Chem. 2005 Feb 25;**280**(8):7088-99.

van Leeuwen LM, Evans RJ, Jim KK, Verboom T, Fang X, Bojarczuk A, Malicki J, Johnston SA and van der Sar AM. (2018)
A transgenic zebrafish model for the in vivo study of the blood and choroid plexus brain barriers using claudin 5.
Biol Open. 2018 Feb 2;**7**(2).

Leprince D, Gegonne A, Coll J, de Taisne C, Schneeberger A, Lagrou C and Stehelin D. (1983)
A putative second cell-derived oncogene of the avian leukaemia retrovirus E26.
Nature. 1983 Nov 24-30;**306**(5941):395-7.

Letourneau A, Cobellis G, Fort A, Santoni F, Garieri M, Falconnet E, Ribaux P, Vannier A, Guipponi M, Carninci P, Borel C and Antonarakis SE. (2015)
HSA21 Single-Minded 2 (Sim2) Binding Sites Co-Localize with Super-Enhancers and Pioneer Transcription Factors in Pluripotent Mouse ES Cells.
PLoS One. 2015 May 8;**10**(5):e0126475

Levi-Montalcini R (1987)
The nerve growth factor 35 years later.
Science *237*: 1154-1161.

Levi-Montalcini R and Hamburger V (1951)
Selective growth-stimulating effects of mouse sarcoma on the sensory and sympathetic nervous system of the chick embryo.
J. Exp. Zool., **116**, 321 – 361.

Lewis KE and Eisen JS. (2003)
From cells to circuits: development of the zebrafish spinal cord.
Prog Neurobiol. 2003 Apr;**69**(6):419-49.

Li J, Siegel M, Yuan M, Zeng Z, Finnucan L, Persky R, Hurn PD and McCullough LD. (2011)
Estrogen enhances neurogenesis and behavioral recovery after stroke.
J Cereb Blood Flow Metab. 2011 Feb;**31**(2):413-25.

Lindholm D, Castren E, Berzaghi M, Blöchl A and Thoenen H (1994)
Activity-dependent and hormonal regulation of neurotrophin mRNA levels in the brain-implications for neuronal plasticity.
J. Neurobiol. **25**, 1362-1372

Liu F, Yang X, Geng M and Min Huang M. (2018)
Targeting ERK, an Achilles' Heel of the MAPK pathway, in cancer therapy
Acta Pharm Sin B. 2018 Jul; **8**(4): 552–562.

Loeb DM, Maragos J, Martin-Zanca D, Chao MV, Parada LF and Greene LA (1991)
The trk proto-oncogene rescues NGF responsiveness in mutant NGF-nonresponsive PC12 cell lines.
Cell *66*: 961-966.

Lotto RB, Asavaritikrai P, Vali L and Price DJ. (2001)
Target-derived neurotrophic factors regulate the death of developing forebrain neurons after a change in their trophic requirements.
J Neurosci. 2001 Jun 1;**21**(11):3904-10.

Loughlin SE and Fallon JH. (1993)
Neurotrophic factors.
Academic, SanDiego

Longo FM, Holtzman DM, Grimes ML and Mobley WC (1992)
Nerve growth factor: actions in the peripheral and central nervous systems.
Neurotrophic factors (Fallon J, Loughlin S, eds), pp 209-256. New York: Academic.

Lu Z and Xu S. (2006)
ERK1/2 MAP kinases in cell survival and apoptosis.
IUBMB Life. 2006 Nov;**58**(11):621-31.

Ma BJ, Shen JW, Yu HY, Ruan Y, Wu TT and Zhao X (2010)
Hericenones and erinacines: stimulators of nerve growth factor (NGF) biosynthesis in *Hericium erinaceus*.
Taylor&Francis Group, Volume 1, Issue 2, 92-98 (2010)

Ma AN, Wang H, Guo R, Wang YX, Li W, Cui J, Wang G, Hoffman AR and Hu JF. (2014)
Targeted gene suppression by inducing de novo DNA methylation in the gene promoter.
Epigenetics Chromatin. 2014 Aug 18;**7**:20.

Maisonpierre PC, Belluscio L, Squinto S, Ip NY, Furth ME, Lindsay RM and Yancopoulos GD (1990)
Neurotrophin-3: a neurotrophic factor related to NGF and BDNF.
Science, 1990, **247**(4949 Pt 1), 1446-1451

Manni L, Rocco ML, Barbaro Paparo S and Guaragna M. (2011)
Electroacupucture and nerve growth factor: potential clinical applications.
Arch Ital Biol. 2011;**149**(2):247–255.

Manto M, Bower JM, Conforto AB, Delgado-García JM, Farias da Guarda SN, Gerwig M, Habas C, Hagura N, Ivry RB, Mariën P, Molinari M, Naito E, Nowak DA, Ben Taib NO, Pelisson D, Tesche CD, Tilikete C and Timmann D. (2012)
Roles of the Cerebellum in Motor Control—The Diversity of Ideas on Cerebellar Involvement in Movement
Cerebellum. 2012 Jun; **11**(2): 457–487.

McCracken DA and Dodd JL. (1971)
Molecular structure of starch-type polysaccharides from *Hericium ramosum* and *Hericium coralloides*.
Science. 1971 Oct 22;**174**(4007):419.

McCullough LD and Hurn PD. (2003)
Estrogen and ischemic neuroprotection: an integrated view.
Trends Endocrinol Metab. 2003 Jul;**14**(5):228-35.

Meffert MK, Chang JM, Wiltgen BJ, Fanselow MS and Baltimore D. (2003)
NF-κB functions in synaptic signaling and behavior.
Nature Neuroscience. **6** (10): 1072–8.

Meier R, Becker-André M, Götz R, Heumann R, Shaw A and Thoenen H (1986)
Molecular cloning of bovine and chick nerve growth factor (NGF): delineation of conserved and unconserved domains and their relationship to the biological activity and antigenicity of NGF.
EMBO J. 1986 Jul;**5**(7):1489-93.

Merlo E, Freudenthal R and Romano A. (2002)
The IκB kinase inhibitor sulfasalazine impairs long-term memory in the crab *Chasmagnathus*. *Neuroscience*. **112** (1): 161–72.

Metcalfe WK, Myers PZ, Trevarrow B, Bass MB and Kimmel CB (1990)
Primary neurons that express the L2/HNK-1 carbohydrate during early development in the zebrafish.
Development. 1990 Oct;**110**(2):491-504.

Minoguchi S, Taniguchi Y, Kato H, Okazaki T, Strobl LJ, Zimber-Strobl U, Bornkamm GW and Honjo T. (1997)
RBP-L, a transcription factor related to RBP-Jkappa.
Mol Cell Biol. 1997 May;**17**(5):2679-87.

Mitschke N. (2017)
Isolation and charactierzation of secondary metabolites from basidiomycete *Dentipellis fragilis*.
Master thesis, University of Bremen

Mokalled MH, Patra C, Dickson AL, Endo T, Stainier DYR, and Poss KD. (2016)
Injury-induced ctgfa directs glial bridging and spinal cord regeneration in zebrafish
Science. 2016 Nov 4; **354**(6312): 630–634.

Moore SP, Kruchten J, Toomire KJ and Strauss PR. (2016)
Transcription Factors and DNA Repair Enzymes Compete for Damaged Promoter Sites.
J Biol Chem. 2016 Mar 11;**291**(11):5452-60.

Mori K, Obara Y, Hirota M, Azumi Y, Kinugasa S, Inatomi S and Nakahata N (2008)
Nerve Growth Factor-Inducing Activity of Hericium erinaceus in 1321N1 Human Astrocytoma cells.
Bio. Pharm. Bull. **31**(9) 1727-1732 (2008)

Morikawa M, Koinuma D, Tsutsumi S, Vasilaki E, Kanki Y, Heldin CH, Aburatani H and Miyazono K. (2011)
ChIP-seq reveals cell type-specific binding patterns of BMP-specific Smads and a novel binding motif.
Nucleic Acids Res. 2011 Nov 1;**39**(20):8712-27.

Moro E, Ozhan-Kizil G, Mongera A, Beis D, Wierzbicki C, Young RM, Bournele D, Domenichini A, Valdivia LE, Lum L, Chen C, Amatruda JF, Tiso N, Weidinger G and Argenton F. (2012)
In vivo Wnt signaling tracing through a transgenic biosensor fish reveals novel activity domains.
Dev Biol. 2012 Jun 15;**366**(2):327-40.

Munnamalai V and Fekete DM. (2013)
Wnt signaling during cochlear development.
Seminars in cell & developmental biology. 2013;**24**:480–489.

Naidu M, Kuan CY, Lo WL, Raza M, Tolkovsky A, Mak NK, Wong RN and Keynes R. (2007)
Analysis of the action of euxanthone, a plant-derived compound that stimulates neurite outgrowth.
Neuroscience. 2007 Sep 21;**148**(4):915-24.

Namikawa K, Dorigo A and Köster RW. (2019a)
Neurological Disease Modelling for Spinocerebellar Ataxia Using Zebrafish
J Exp Neurosci. 2019; **13**: 1179069519880515.

Namikawa K, Dorigo A, Zagrebelsky M, Russo G, Kirmann T, Fahr W, Dübel S, Korte M, Köster RW. (2019b)
Modeling Neurodegenerative Spinocerebellar Ataxia Type 13 in Zebrafish Using a Purkinje Neuron Specific Tunable Coexpression System.
J Neurosci. 2019 May 15;**39**(20):3948-3969.

Nilsson AS, Fainzilber M, Falck P, Ibáñez CF (1998)
Neurotrophin-7: a novel member of the neurotrophin family from the zebrafish.
FEBS Lett. 1998 Mar 13;**424**(3):285-90.

Nunn MF, Seeburg PH, Moscovici C and Duesberg PH. (1983)
Tripartite structure of the avian erythroblastosis virus E26 transforming gene.
Nature. 1983 Nov 24-30;**306**(5941):391-5.

Nusse R. (2005)
Wnt signaling in disease and in development.
Cell Research. **15** (1): 28–32.

Nusse R and Varmus HE. (1992)
Wnt genes.
Cell. **69** (7): 1073–87.

Nüsslein-Volhard C. (1996)
The Identification of Genes Controlling Development in Flies and Fishes (Nobel Lecture)
The Nobel Foundation 1996. We thank the Nobel Foundation, Stockholm, for permission to print this lecture.

Obara Y and Nakahata N (2002)
The signaling pathway of neurotrophic factor.
Drug News Perspect. *15*: 290-298.

Obermeier A, Lammers R, Wiesmüller KH, Jung G, Schlessinger J, Ullrich A. (1993)
Identification of Trk binding sites for SHC and phosphatidylinositol 3'-kinase and formation of a multimeric signaling complex.
J Biol Chem. 1993 Nov 5;**268**(31):22963-6.

Odrowaz Z and Sharrocks AD. (2012)
ELK1 uses different DNA binding modes to regulate functionally distinct classes of target genes.
PLoS Genet. 2012;**8**(5):e1002694.

Palanca AM, Lee SL, Yee LE, Joe-Wong C, Trinh le A, Hiroyasu E, Husain M, Fraser SE, Pellegrini M and Sagasti A. (2013)
New transgenic reporters identify somatosensory neuron subtypes in larval zebrafish.
Dev Neurobiol. 2013 Feb;**73**(2):152-67.

Panula P, Chen YC, Priyadarshini M, Kudo H, Semenova S, Sundvik M and Sallinen V. (2010)
The comparative neuroanatomy and neurochemistry of zebrafish CNS systems of relevance to human neuropsychiatric diseases.
Neurobiol Dis. 2010 Oct;**40**(1):46-57.

Pardridge WM. (2002a)
Drug and gene delivery to the brain: the vascular route.
Neuron. 2002 Nov 14;**36**(4):555-8.

Pardridge WM. (2002b)
Blood-brain barrier drug targeting enables neuroprotection in brain ischemia following delayed intravenous administration of neurotrophins.
Adv Exp Med Biol. 2002;**513**:397-430.

Park HJ and Youn HS. (2013)
Mercury induces the expression of cyclooxygenase-2 and inducible nitric oxide synthase.
Toxicology and Industrial Health. **29** (2): 169–74.

Park F, Mattson DL, Roberts LA and Cowley AW Jr. (1997)
Evidence for the presence of smooth muscle alpha-actin within pericytes of the renal medulla.
Am J Physiol. 1997 Nov;**273**(5):R1742-8.

Parsons MJ, Pisharath H, Yusuff S, Moore JC, Siekmann AF, Lawson N and Leach SD. (2009)
Notch-responsive cells initiate the secondary transition in larval zebrafish pancreas.
Mech Dev. 2009 Oct;**126**(10):898-912

Paves H and Saarma M (1997)
Neurotrophins as in vitro growth cone guidance molecules for embryonic sensory neurons.
Cell Tissue Res., 1997 Nov., **290** (2), 285-97.

Pearson G, Robinson F, Beers Gibson T, Xu BE, Karandikar M, Berman K, Cobb MH. (2001)
Mitogen-activated protein (MAP) kinase pathways: regulation and physiological functions.
Endocr Rev. 2001 Apr;**22**(2):153-83.

Pei L, Castrillo A and Tontonoz P. (2006)
Regulation of macrophage inflammatory gene expression by the orphan nuclear receptor Nur77.
Mol. Endocrinol. **20** (4): 786–94.

Perkins ND. (2007)
Integrating cell-signalling pathways with NF-κB and IKK function.
Nature Reviews Molecular Cell Biology. **8** (1): 49–62.

Persson H and Ibanez CF (1993)
Role and expression of neurotrophins and the *trk* family of tyrosine kinase receptors in neural growth and rescue after injury.
Curr. Opin. Neurol. Neurosurg. **6**, 11-18

Phan CW and Sabaratnam V. (2012)
Potential uses of spent mushroom substrate and its associated lignocellulosic enzymes.
Appl Microbiol Biotechnol **96**:863-873

Pontén J and Macintyre EH. (1968)
Long term culture of normal and neoplastic human glia.
Acta Pathol Microbiol Scand. 1968;**74**(4):465-86.

Reddi AH. (2001)
Bone morphogenetic proteins: from basic science to clinical applications.
J Bone Joint Surg Am. 2001;**83**-A Suppl 1(Pt 1):S1-6.

Reichardt LF. (2006)
Neurotrophin-regulated signalling pathways
Philos Trans R Soc Lond B Biol Sci. 2006 Sep 29; **361**(1473): 1545–1564.

Reuss B, von Bohlen and Halbach O. (2003)
Fibroblast growth factors and their receptors in the central nervous system.
Cell and Tissue Research. **313** (2): 139–157.

Riccio A, Ahn S, Davenport CM, Blendy JA, Ginty DD. (1999)
Mediation by a CREB family transcription factor of NGF-dependent survival of sympathetic neurons.
Science. 1999 Dec 17;**286**(5448):2358-61.

Rupcic Z and Rascher M, Kanaki S, Köster RW, Stadler M and Wittstein K. (2018)
Two New Cyathane Diterpenoids from Mycelial Cultures of the Medicinal Mushroom *Hericium erinaceus* and the Rare Species, *Hericium flagellum*.
Int. J. Mol. Sci.,**19** (2018)

Rupp RA, Snider L and Weintraub H. (1994)
Xenopus embryos regulate the nuclear localization of XMyoD.
Genes Dev. 1994 Jun 1;**8**(11):1311-23.

Saito T, Aoki F, Hirai H, Inagaki T, Matsunaga Y, Sakakibara T, Sakemi S, Suzuki Y, Watanabe S, Suga O, Sujaku T, Smogowicz AA, Truesdell SJ, Wong JW, Nagahisa A, Kojima Y and Kojima N. (1998)
Erinacine E as a kappa opioid receptor agonist and its new analogs from a basidiomycete, *Hericium ramosum.*
J Antibiot (Tokyo). 1998 Nov;**51**(11):983-90.

Salin T, Timmusk T, Lendahl U and Metsis M (1997)
Structural and functional characterization of the rat neurotrophin-4 gene.
Mol Cell Neurosci. 1997;**9**(4):264-75.

Sambrook JF and Russell DW. (2001)
Molecular Cloning: A Laboratory Manual (3rd ed.).
Cold Spring Harbor Laboratory Press. ISBN 978-0-87969-577-4.

Samorodnitsky D, Szyjka C and Koudelka GB. (2015)
A Role for Autoinhibition in Preventing Dimerization of the Transcription Factor ETS1
J Biol Chem. 2015 Sep 4; **290**(36): 22101–22110.

Schiavone M, Rampazzo E, Casari A, Battilana G, Persano L, Moro E, Liu S, Leach SD, Tiso N and Argenton F. (2014)
Zebrafish reporter lines reveal in vivo signaling pathway activities involved in pancreatic cancer.
Dis Model Mech. 2014 Jul;**7**(7):883-94.

Sekimoto M, Fukamachi K, Nemoto F, Miyata S, Degawa M, Senba E, Ueyama T and Nemoto K (1998)
Novel alternative splicing in the 5' exon of the neurotrophin-3 gene.
Neuroreport. 1998 Nov 16;**9**(16):3675-9.

Seow SL, Naidu M, David P, Wong KH and Sabaratnam V. (2013)
Potentiation of neuritogenic activity of medicinal mushrooms in rat pheochromocytoma cells.
BMC Compl Alt Med **13**:157

Server AC, Herrup K, Shooter EM, Hogue-Angeletti RA, Frazier WA and Bradshaw RA (1976)
Comparison of the nerve growth factor proteins from cobra venom (*Naja naja*) and mouse submaxillary gland.
Biochemistry. 1976 Jan 13;**15**(1):35-9.

Shamblott MJ, Bugg EM, Lawler AM and Gearhart JD. (2002)
Craniofacial abnormalities resulting from targeted disruption of the murine Sim2 gene.
*Developmental Dynamics***. 224** (4): 373–380.

Shimizu N, Kawakami K and Ishitani T. (2012)
Visualization and exploration of Tcf/Lef function using a highly responsive Wnt/β-catenin signaling-reporter transgenic zebrafish.
Dev Biol. 2012 Oct 1;**370**(1):71-85.

Silva AJ, Kogan JH, Frankland PW and Kida S. (1998)
CREB and memory.
Annu Rev Neurosci. 1998;**21**:127-48.

Smith TG, Robbins PA and Ratcliffe PJ. (2008)
The human side of hypoxia-inducible factor.
British Journal of Haematology. **141** (3): 325–34.

Squinto SP, Stitt TN, Aldrich TH, Davis S, Bianco SM, Radziejewski C, Glass DJ, Masiakowski P, Furth ME, Valenzuela DM, *et al*. (1991)
trkB encodes a functional receptor for brain-derived neurotrophic factor and neurotrophin-3 but not nerve growth factor.
Cell. 1991 May 31;**65**(5):885-93.

Sohrabji F, Miranda RC, and Toran-Allerand CD. (1995)
Identification of a putative estrogen response element in the gene encoding brain-derived neurotrophic factor.
Proc Natl Acad Sci U S A. 1995 Nov 21; **92**(24): 11110–11114.

Soutschek J and Zupanc GKH (1996)
Apoptosis in the cerebellum of adult teleost fish, *Apteronotus leptorhynchus.*
Developmental Brain Research, Volume **97**, Issue 2, 23 December 1996, Pages 279–286.

Stephens L, Smrcka A, Cooke FT, Jackson TR, Sternweis PC and Hawkins PT. (1994)
A novel phosphoinositide 3 kinase activity in myeloid-derived cells is activated by G protein βγ subunits.
Cell. 1994 Apr 8;**77**(1):83-93.

Streisinger G, Walker C, Dower N, Knauber D and Singer F. (1981)
Production of clones of homozygous diploid zebra fish (Brachydanio rerio).
Nature. 1981 May 28;**291**(5813):293-6.

Sucher NJ, Brose N, Deitcher DL, Awobuluyi M, Gasic GP, Bading H, Cepko CL, Greenberg ME, Jahn R, Heinemann SF, et al. (1993)
Expression of endogenous NMDAR1 transcripts without receptor protein suggests post-transcriptional control in PC12 cells.
J Biol Chem. 1993 Oct 25;**268**(30):22299-304.

Sugita S, Khvochtev M and Sudhof TC. (1999)
Neurexins are functional alpha-latrotoxin receptors.
Neuron **22**: 489-496.

Tetsu O and McCormick F. (2017)
ETS-targeted therapy: can it substitute for MEK inhibitors?
Clin Transl Med. 2017 Dec;**6**(1):16.

Thongbai B, Rapior S, Hyde KD, Wittstein K and Stadler M. (2015)
Hericium erinaceus, an amazing medicinal mushroom.
Mycol Progress (2015) **14**: 91.

Tian B and Brasier AR. (2003)
Identification of a nuclear factor κB-dependent gene network.
Recent Progress in Hormone Research. **58**: 95–130.

Tkach M, Rosemblit C, Rivas MA, Proietti CJ, Díaz Flaqué MC, Mercogliano MF, Beguelin W, Maronna E, Guzmán P, Gercovich FG, Deza EG, Elizalde PV and Schillaci R. (2013)
p42/p44 MAPK-mediated Stat3Ser727 phosphorylation is required for progestin-induced full activation of Stat3 and breast cancer growth.
Endocrine-Related Cancer. **20** (2): 197–212.

Treisman R. (1994)
Ternary complex factors: growth factor regulated transcriptional activators.
Curr Opin Genet Dev. 1994 Feb;**4**(1):96-101.

Tun T, Hamaguchi Y, Matsunami N, Furukawa T, Honjo T and Kawaichi M. (1994)
Recognition sequence of a highly conserved DNA binding protein RBP-J kappa.
Nucleic Acids Res. 1994 Mar 25;**22**(6):965-71.

Tuteja G and Kaestner KH. (2007)
Forkhead transcription factors II.
Cell. **131** (1): 192–192

Turner JE, Blair JR and Chappel ET. (1987)
Peripheral nerve implant effects on survival of retinal ganglion layer cells after axotomy initiated by a penetrating lesion.
Brain Research.1987 Sep 1; **419**: 46-54

Tyson DR, Lakin S, Hamai Y and Bradshaw RA. (2003)
PC12 cell activation by epidermal growth factor receptor: Role of autophosphorylation sites.
Int J Dev Neurosci **21**: 63-74

Vallania F, Schiavone D, Dewilde S, Pupo E, Garbay S, Calogero R, Pontoglio M, Provero P and Poli V. (2009)
Genome-wide discovery of functional transcription factor binding sites by comparative genomics: the case of Stat3.
Proc Natl Acad Sci U S A. 2009 Mar 31;**106**(13):5117-22.

Vinkemeier U, Moarefi I, Darnell JE and Kuriyan J. (1998)
Structure of the amino-terminal protein interaction domain of STAT-4.
Science. **279** (5353): 1048–52. doi:10.1126/science.279.5353.1048

Walter JT, Alviña K, Womack MD, Chevez C and Khodakhah K. (2006)
Decreases in the precision of Purkinje cell pacemaking cause cerebellar dysfunction and ataxia.
Nat Neurosci. 2006 Mar;**9**(3):389-97.

Wang DD and Bordey A. (2008)
The astrocyte odyssey.
Prog Neurobiol. 2008 Dec 11;**86**(4):342-67.

Wang T, Xie K and Lu B (1995)
Neurotrophins promote maturation of developing neuromuscular synapses.
J. Neurosci. **15**, 4796-4805

Wang G, Zhang X, Maier SE, Zhang L and Maier RJ. (2019)
In Vitro and *In Vivo* Inhibition of *Helicobacter pylori* by Ethanolic Extracts of Lion's Mane Medicinal Mushroom, *Hericium erinaceus* (Agaricomycetes).
Int J Med Mushrooms. 2019;**21**(1):1-11.

Wasylyk B, Hagman J and Gutierrez-Hartmann A. (1998)
Ets transcription factors: nuclear effectors of the Ras-MAP-kinase signaling pathway.
Trends Biochem Sci. 1998 Jun;**23**(6):213-6.

Wasylyk C, Bradford AP, Gutierrez-Hartmann A and Wasylyk B. (1997)
Conserved mechanisms of Ras regulation of evolutionary related transcription factors, Ets1 and Pointed P2.
Oncogene. 1997 Feb 27;**14**(8):899-913.

Webb AE, Kndaje A and Brunet A. (2016)
Characterization of the direct targets of FOXO transcription factors throughout evolution.
Aging Cell. 2016 Aug;**15**(4):673-85.

Weber T, Namikawa K, Winter B, Müller-Brown K, Kühn R, Wurst W and Köster RW. (2016)
Caspase-mediated apoptosis induction in zebrafish cerebellar Purkinje neurons.
Development (2016) **143**, 4279-4287

Weis JS (1968)
Analysis of the development of the nervous system of the zebrafish, *Brachydanio rerio*.
J. Embryol. Exp. Morphol., 1968, **19** (2), 109-119.

Weis, JS (1972)
The effect of nerve growth factor on fin regeneration in the goldfish, *Carassius auratus*.
Growth, 1972, **36**(2), 155-161

Westerfield M (1993)
The Zebrafish Book: A Guide for the Laboratory Use of Zebrafish (*Brachydanio rerio*)
Eugene: University of Oregon Press.

Wilkins SE, Abboud MI, Hancock RL and Schofield CJ. (2016)
Targeting Protein-Protein Interactions in the HIF System.
ChemMedChem. **11** (8): 773–86.

Wilson TE, Fahrner TJ and Milbrandt J. (1993)
The orphan receptors NGFI-B and steroidogenic factor 1 establish monomer binding as a third paradigm of nuclear receptor-DNA interaction.
Mol Cell Biol. 1993 Sep;**13**(9):5794-804.

Wittstein K and Rascher M, Rupcic Z, Löwen E, Winter B, Köster RW, Stadler M. (2016)
corallocins A-C, Nerve Growth and Brain-Derived Neurotrophic Factor Inducing Metabolites from the Mushroom *Hericium coralloides*.
J Nat Prod.; **79**(9):2264-9 (2016)

Wolfe MW and Call GB. (1999).
Early growth response protein 1 binds to the luteinizing hormone- beta promoter and mediates gonadotropin-releasing hormone-stimulated gene expression.
Mol Endocrinol. 1999 May;**13**(5):752-63.

Wozney JM and Rosen V. (1998)
Bone morphogenetic protein and bone morphogenetic protein gene family in bone formation and repair.
Clin Orthop Relat Res. 1998 Jan;(**346**):26-37.

Wu DK and Kelley MW. (2012)
Molecular mechanisms of inner ear development.
Cold Spring Harbor perspectives in biology. 2012;**4**:a008409.

Wulliman MF, Rupp B and Reichert H. (1996)
Neuroanatomy of the Zebrafish Brain: A Topological Atlas.
Birkhäuser

Xiao N and Le QT. (2016)
Neurotrophic Factors and Their Potential Applications in Tissue Regeneration.
Arch Immunol Ther Exp (Warsz). 2016 Apr;**64**(2):89-99.

Yamada K and Nabeshima T (2003)
Brain-derived neurotrophic factor/TrkB signaling in memory processes.
J Pharmacol Sci. **91**, Nr. 4, April 2003, S. 267–70.

Yang S, Huang S, Gaertig MA, Li X-J and Li S (2014)
Age-dependent decrease in Chaperone activity impairs MANF expression, leading to Purkinje Cell degeneration in inducible SCA17 Mice.
Neuron **81**, 349-365, January 22, 2014.

Yao PJ, Petralia RS and Mattson MP. (2016)
Sonic Hedgehog Signaling and Hippocampal Neuroplasticity.
Trends Neurosci. 2016 Dec;**39**(12):840-850.

Ying J, Mao X, Ma Q, Zong Y and Wen H. (1987)
Icones of medicinal fungi from China (translated, Yuehan X).
Science Press, Beijing, p 575

Yong HY, Koh MS and Moon A. (2009)
The p38 MAPK inhibitors for the treatment of inflammatory diseases and cancer.
Expert Opin Investig Drugs. 2009 Dec;**18**(12):1893-905.

Yuan ZL, Guan YJ, Wang L, Wei W, Kane AB and Chin YE. (2004)
Central role of the threonine residue within the p+1 loop of receptor tyrosine kinase in STAT3 constitutive phosphorylation in metastatic cancer cells.
Molecular and Cellular Biology. **24** (21): 9390–400.

Zhang W, Takahara T, Achiha T, Shibata H and Maki M. (2018)
Nanoluciferase Reporter Gene System Directed by Tandemly Repeated Pseudo-Palindromic NFAT-Response Elements Facilitates Analysis of Biological Endpoint Effects of Cellular Ca2+ Mobilization.
Int J Mol Sci. 2018 Feb 18;**19**(2). pii: E605.

Zhang S, Wu M, Peng C, Zhao G and Gu R. (2017)
GFAP expression in injured astrocytes in rats
Exp Ther Med. 2017 Sep; **14**(3): 1905–1908.

Zhou J, Holtzman DM, Weiner R and Mobley WC (1994)
TrkA confers neuronal-like NGF response to imoortalized hypothalamic neurons.
Proc Natl Acad Sci USA *91*: 3824-3828.

Znosko WA, Yu S, Thomas K, Molina GA, Li C, Tsang W, Dawid IB, Moon AM and Tsang M. (2010)
Overlapping functions of Pea3 ETS transcription factors in FGF signaling during zebrafish development.
Dev Biol. 2010 Jun 1;**342**(1):11-25.

Zou YJ, Wang HX, Ng TB, Huang CY and Zhang JX. (2012)
Purification and characterization of a novel laccase from the edible mushroom *Hericium coralloides*.
J Microbiol. 2012 Feb;**50**(1):72-8.

6. Supplement

6.1 Figure Directory

6.2 Table Directory

6.3 Maps of used plasmids

6.3.1 pCS-rat dnTrkA-CitrineERex

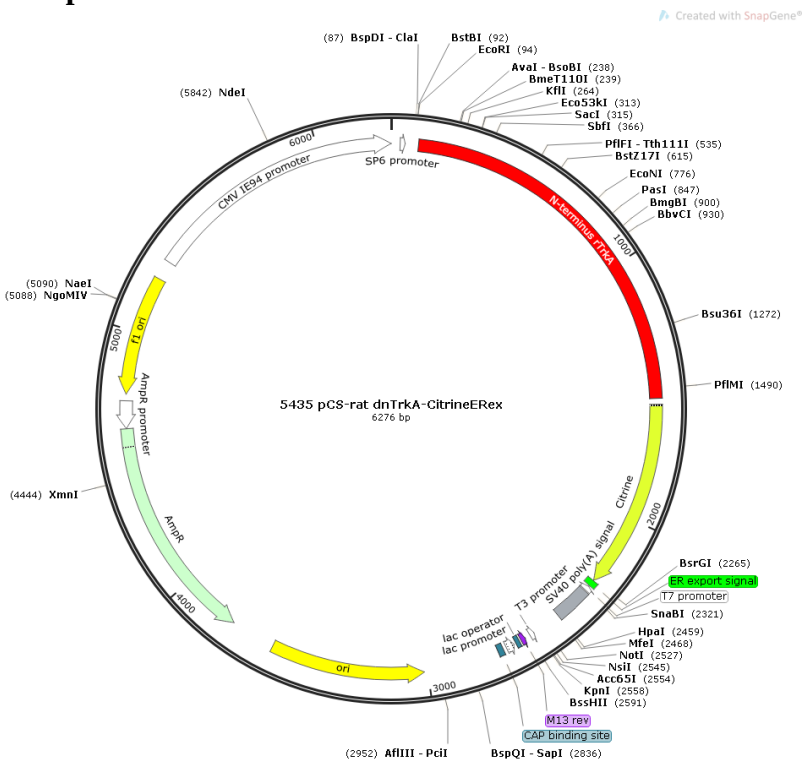

Figure 54: Plasmid Map of Plasmid #5435 pCS-rat dnTrkA-CitrineERex. Map was generated with SnapGene®.

6.3.2 pBSII-Tol2-4xNFkb-EIb-Luc2

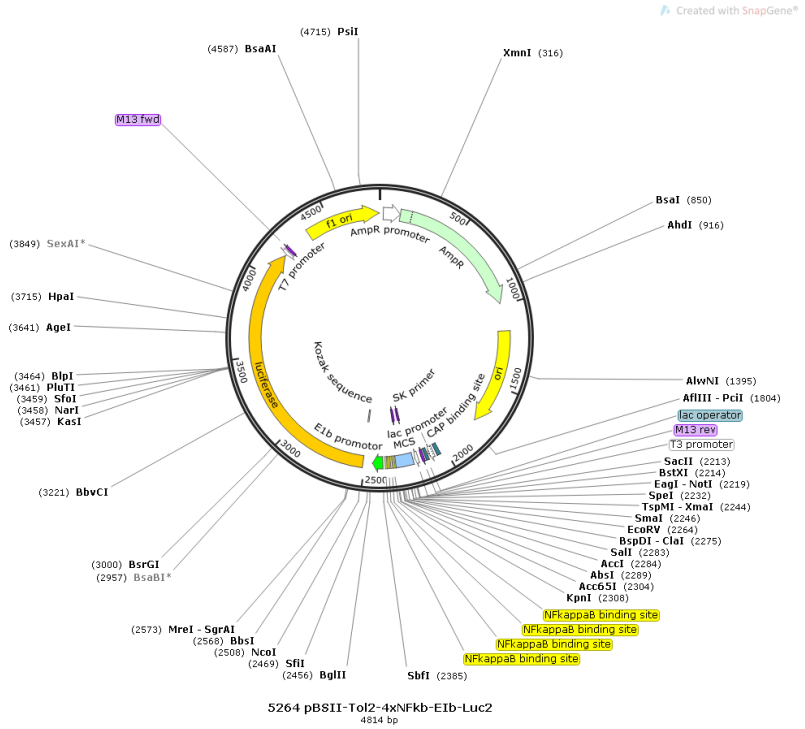

Figure 55: Plasmid Map of Plasmid #5264 pBSII-Tol2-4xNFkb-EIb-Luc2. Map was generated with SnapGene®.

6.3.3 pBSII-Tol2-4xGli-E1b-Luc2

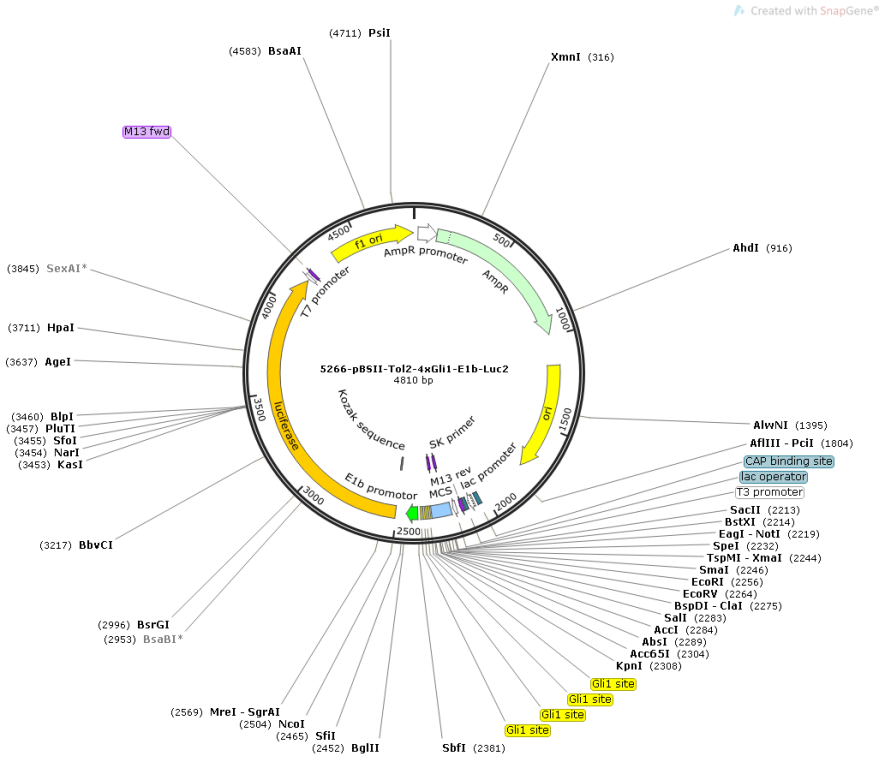

Figure 56: Plasmid Map of Plasmid #5264 pBSII-Tol2-4xGli-EIb-Luc2. Map was generated with SnapGene®.

6.3.4 pBSII-Tol2-4xNotch-E1b-Luc2

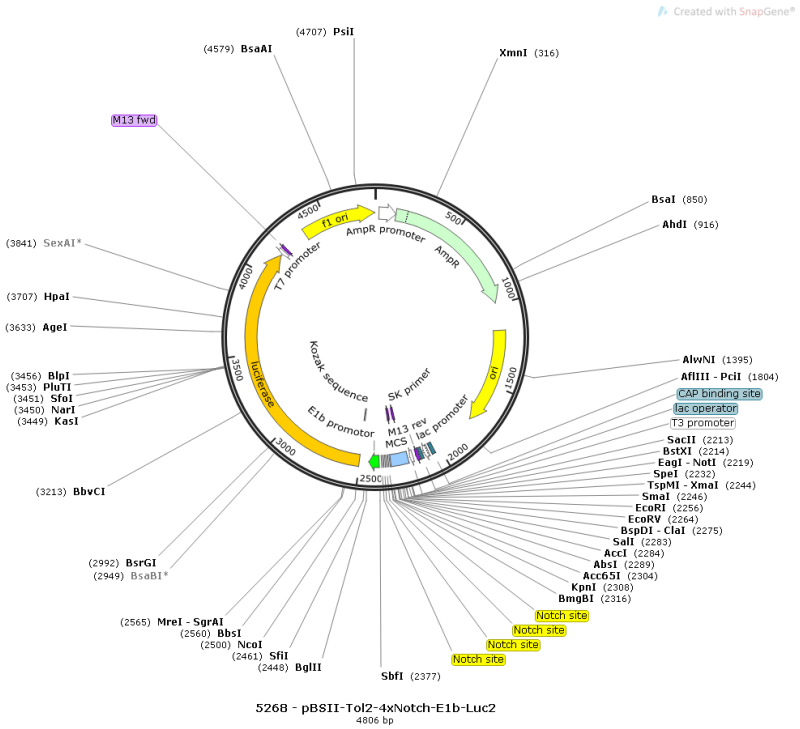

Figure 57: Plasmid Map of Plasmid #5268 pBSII-Tol2-4xNotch-EIb-Luc2. Map was generated with SnapGene®.

6.3.5 pBSII-Tol2-4xDyrk1A-E1b-Luc2

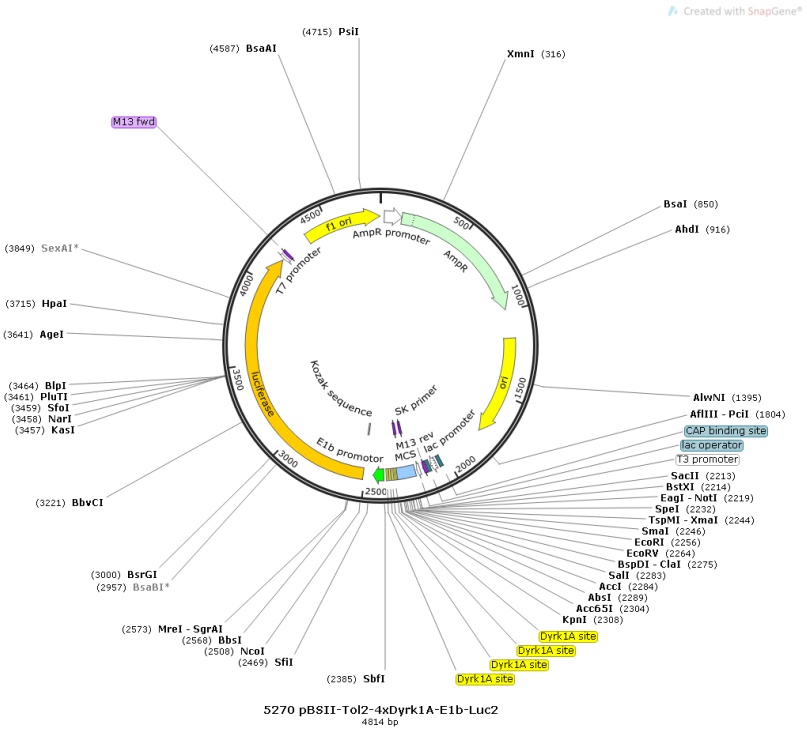

Figure 58: Plasmid Map of Plasmid #5270 pBSII-Tol2-4xDyrk1A-EIb-Luc2. Map was generated with SnapGene®.

6.3.6 pBSII-Tol2-4xPea3B-E1b-Luc2

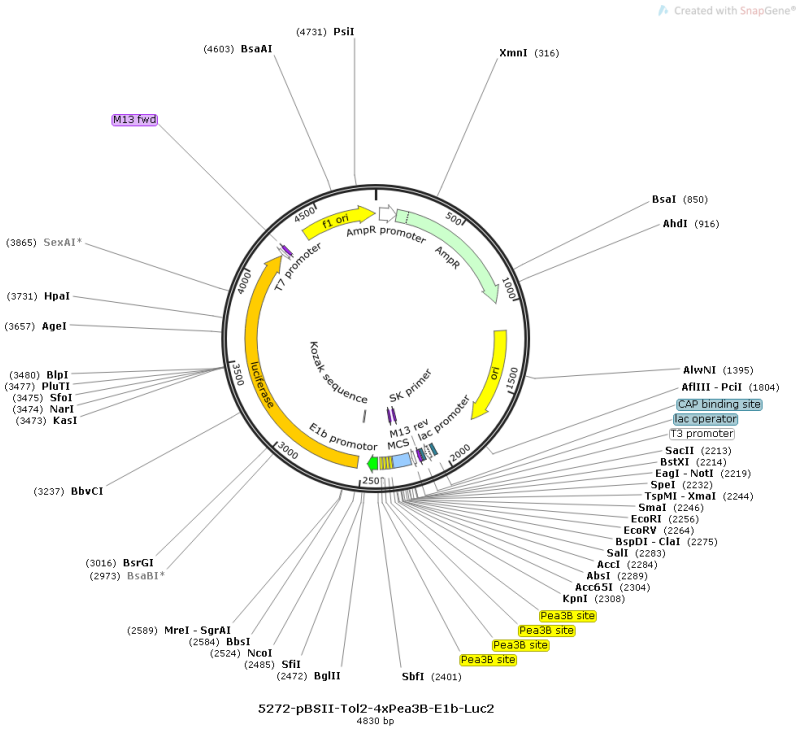

Figure 59: Plasmid Map of Plasmid #5272 pBSII-Tol2-4xPea3B-EIb-Luc2. Map was generated with SnapGene®.

6.3.7 pBSII-Tol2-4xCREB1-E1b-Luc2

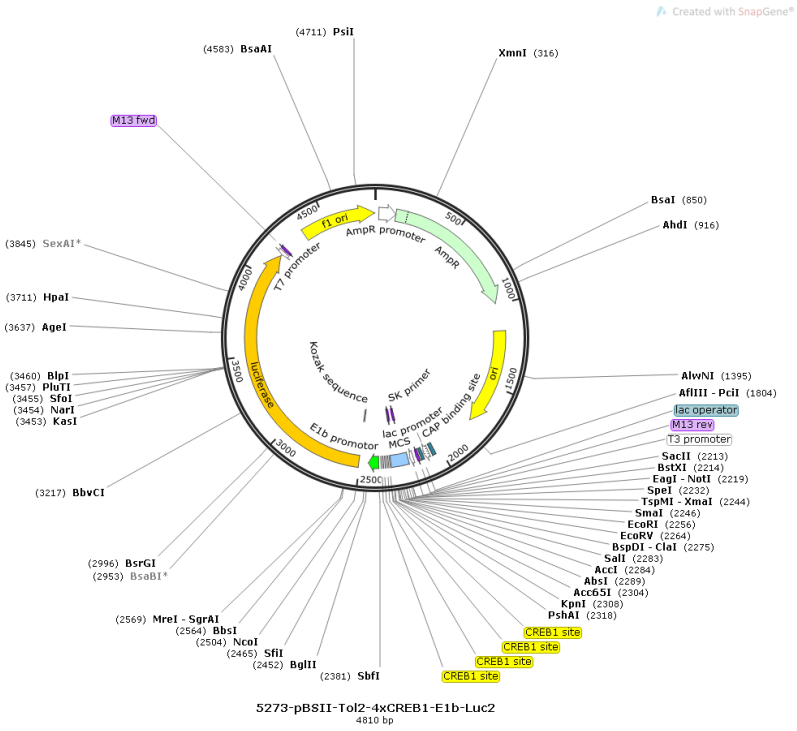

Figure 60: Plasmid Map of Plasmid #5273 pBSII-Tol2-4xCREB1-EIb-Luc2. Map was generated with SnapGene®.

6.3.8 pBSII-Tol2-4xTCF/LEF-E1b-Luc2

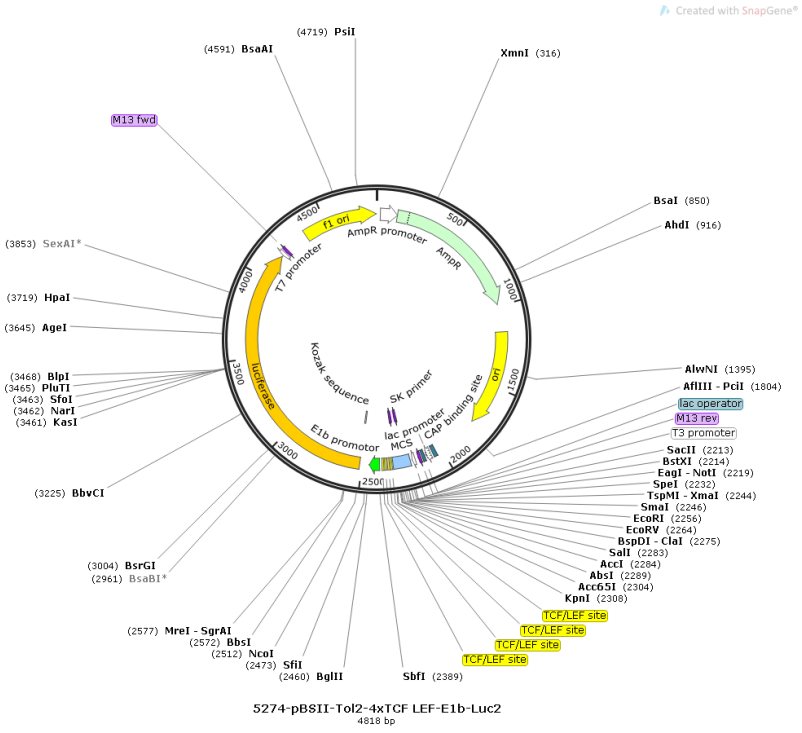

Figure 61: Plasmid Map of Plasmid #5274 pBSII-Tol2-4xTCF/LEF-EIb-Luc2. Map was generated with SnapGene®.

6.3.9 pBSII-Tol2-4xLhx2-Sox2-E1b-Luc2

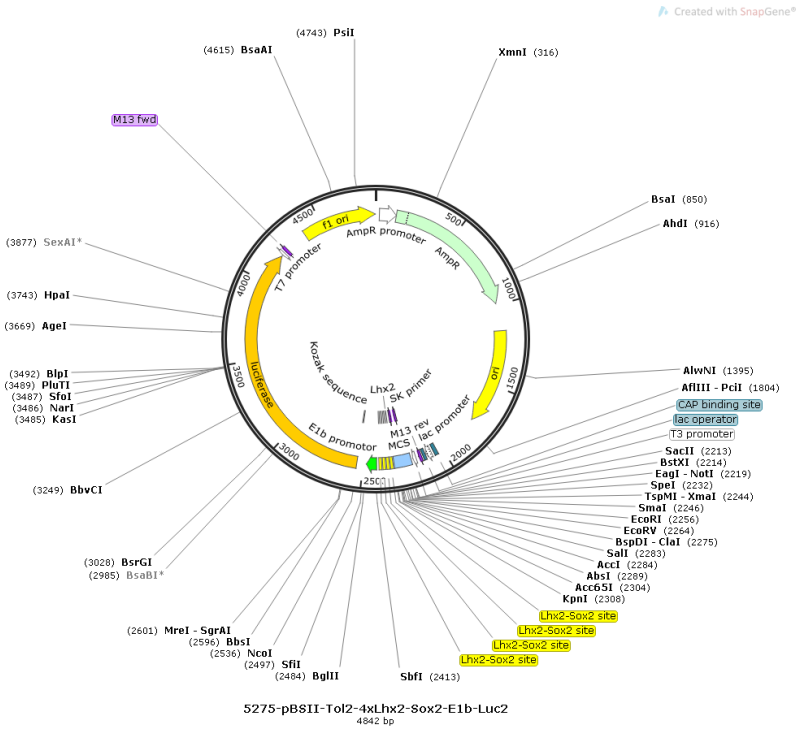

Figure 62: Plasmid Map of Plasmid #5275 pBSII-Tol2-4xLhx2-Sox2-EIb-Luc2. Map was generated with SnapGene®.

6.3.10 pBSII-Tol2-4xSBE-E1b-Luc2

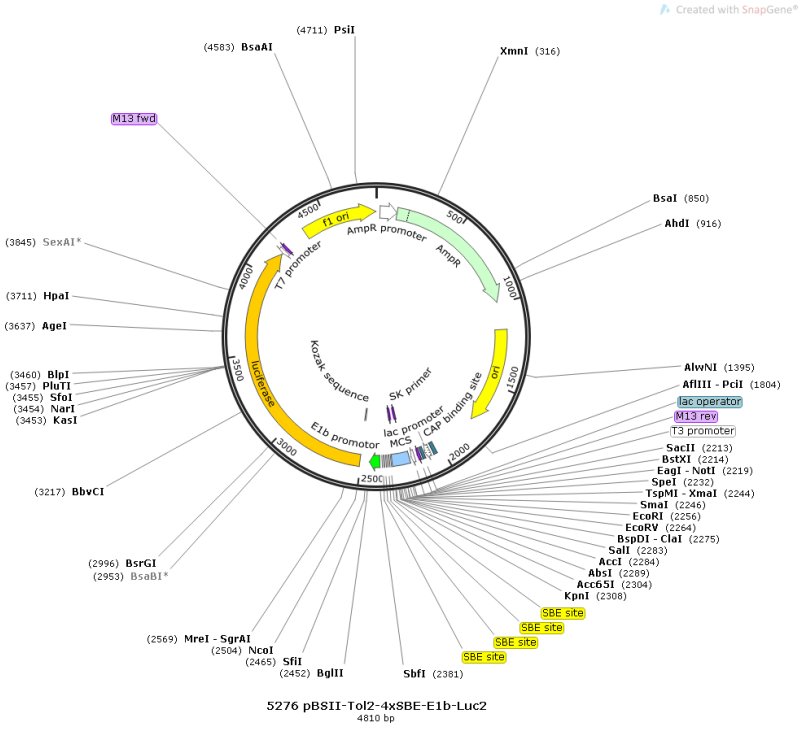

Figure 63: Plasmid Map of Plasmid #5276 pBSII-Tol2-4xSBE-EIb-Luc2. Map was generated with SnapGene®.

6.3.11 pBSII-Tol2-4xHRE-E1b-Luc2

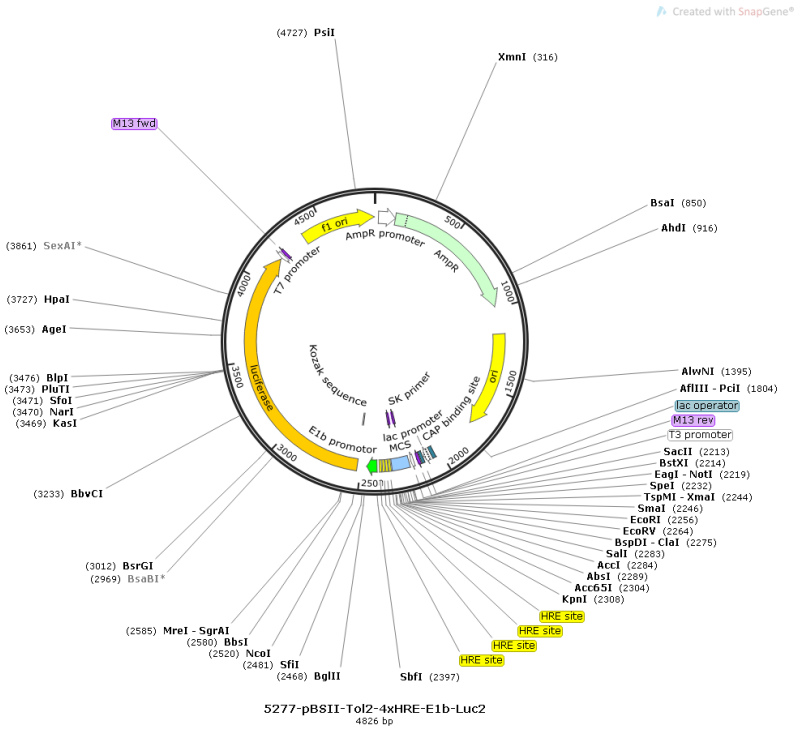

Figure 64: Plasmid Map of Plasmid #5277 pBSII-Tol2-4xHRE-EIb-Luc2. Map was generated with SnapGene®.

6.3.12 pBSII-Tol2-4xNBRE-E1b-Luc2

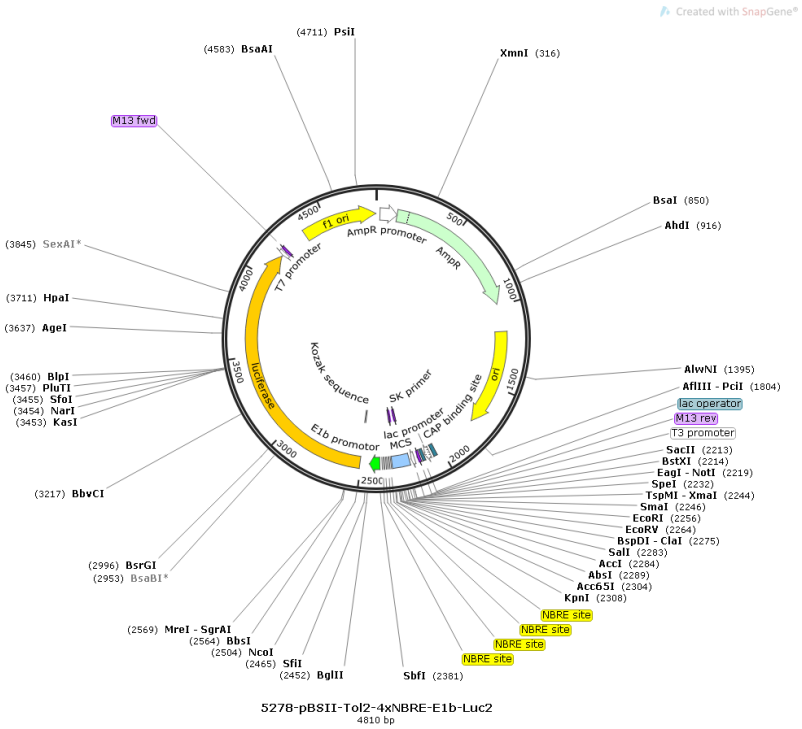

Figure 65: Plasmid Map of Plasmid #5278 pBSII-Tol2-4xNBRE-EIb-Luc2. Map was generated with SnapGene®.

6.3.13 pBSII-Tol2-4xSF1-E1b-Luc2

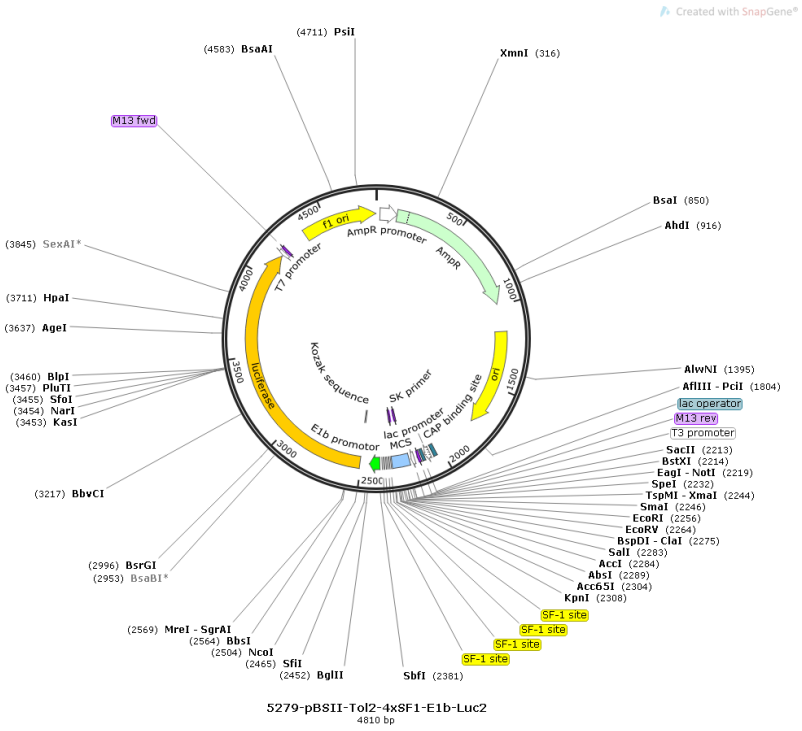

Figure 66: Plasmid Map of Plasmid #5279 pBSII-Tol2-4xSF1-EIb-Luc2. Map was generated with SnapGene®.

6.3.14 pBSII-Tol2-4xSRE-E1b-Luc2

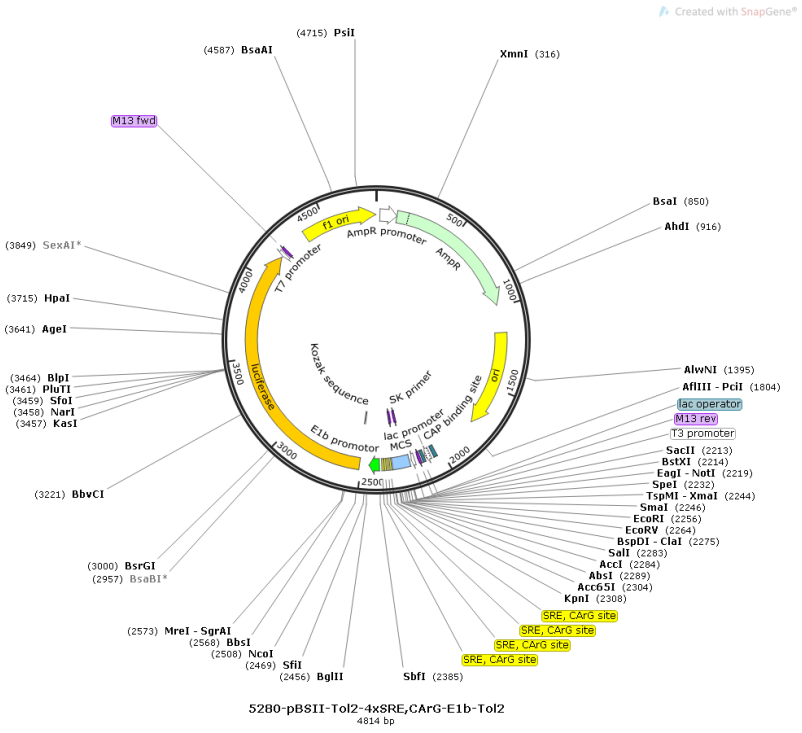

Figure 67: Plasmid Map of Plasmid #5280 pBSII-Tol2-4xSRE-EIb-Luc2. Map was generated with SnapGene®.

6.3.15 pBSII-Tol2-4xHSE-E1b-Luc2

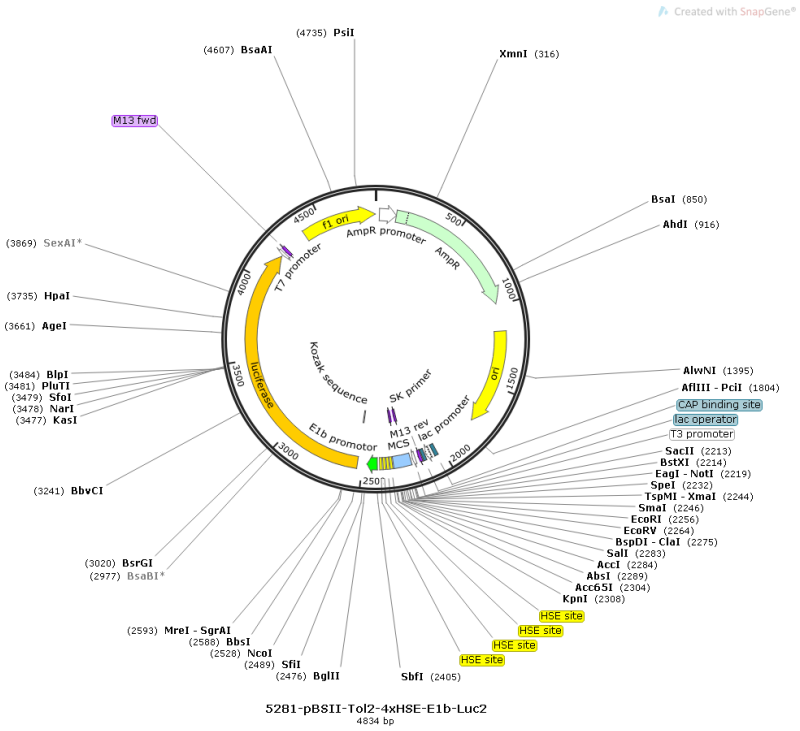

Figure 68: Plasmid Map of Plasmid #5281 pBSII-Tol2-4xHSE-EIb-Luc2. Map was generated with SnapGene®.

6.3.16 pBSII-Tol2-4xUAS-E1b-Luc2

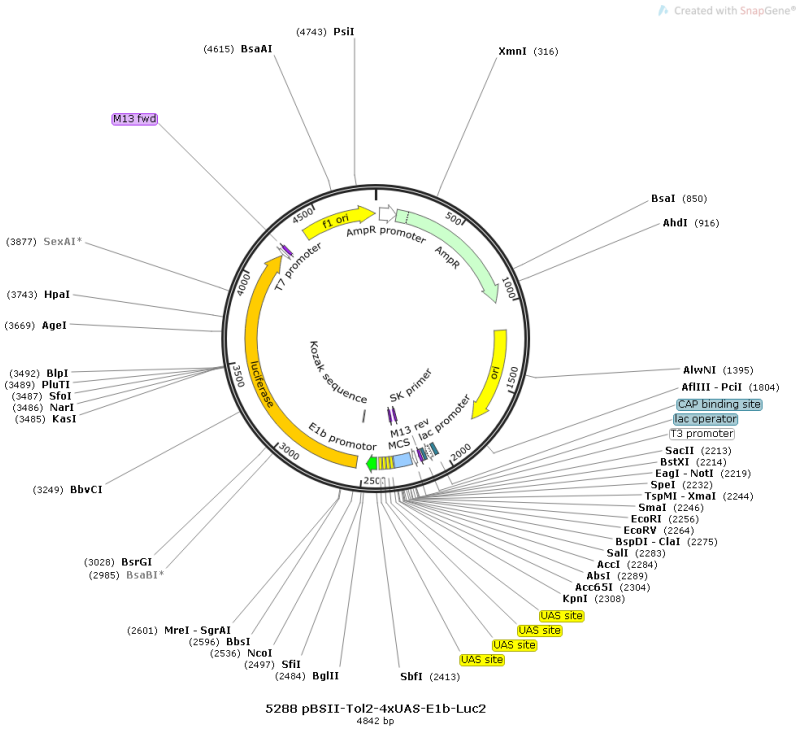

Figure 69: Plasmid Map of Plasmid #5288 pBSII-Tol2-4xUAS-EIb-Luc2. Map was generated with SnapGene®.

6.3.17 pBSII-Tol2-4xSTAT3-E1b-Luc2

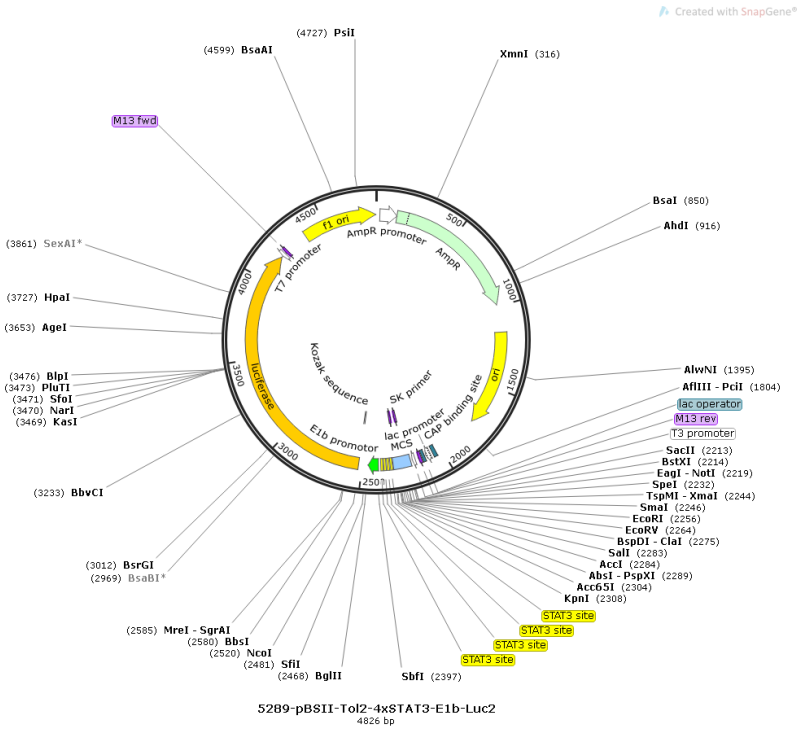

Figure 70: Plasmid Map of Plasmid #5289 pBSII-Tol2-4xSTAT3-EIb-Luc2. Map was generated with SnapGene®.

6.3.18 pBSII-Tol2-4xARE-E1b-Luc2

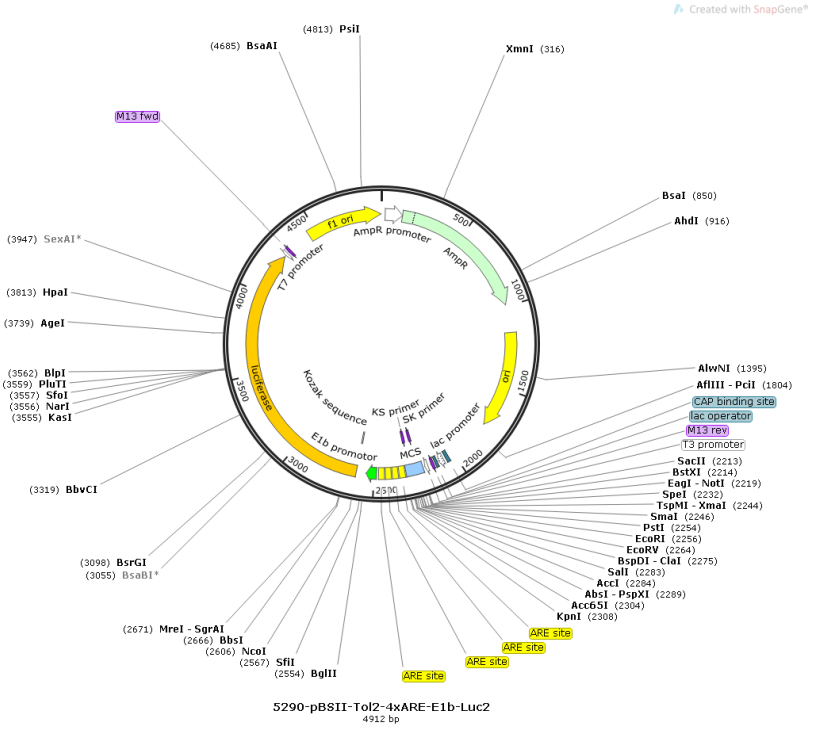

Figure 71: Plasmid Map of Plasmid #5290 pBSII-Tol2-4xARE-EIb-Luc2. Map was generated with SnapGene®.

6.3.19 pBSII-Tol2-4xElk1-E1b-Luc2

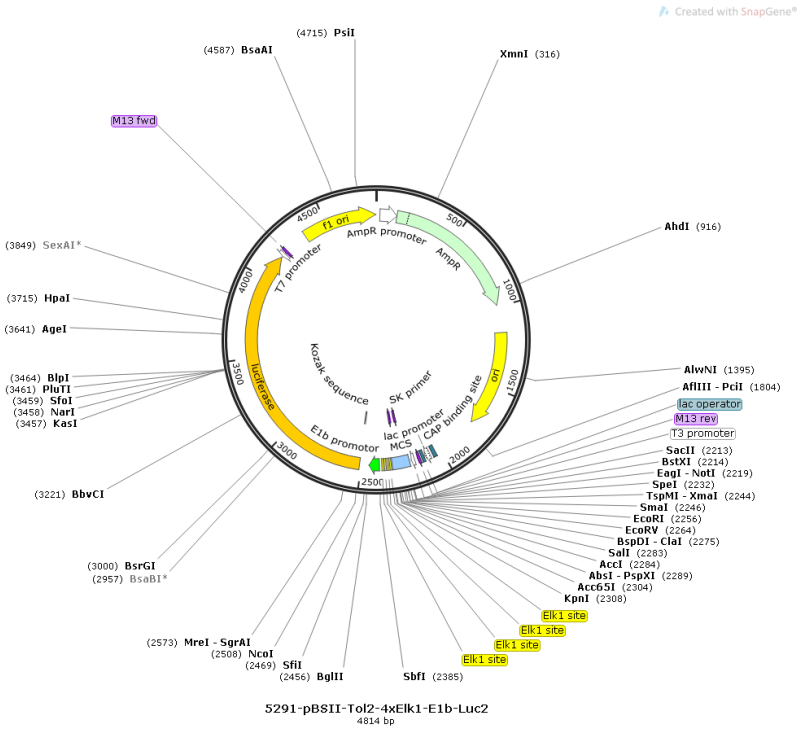

Figure 72: Plasmid Map of Plasmid #5291 pBSII-Tol2-4xElk1-EIb-Luc2. Map was generated with SnapGene®.

6.3.20 pBSII-Tol2-4xnfy-E1b-Luc2

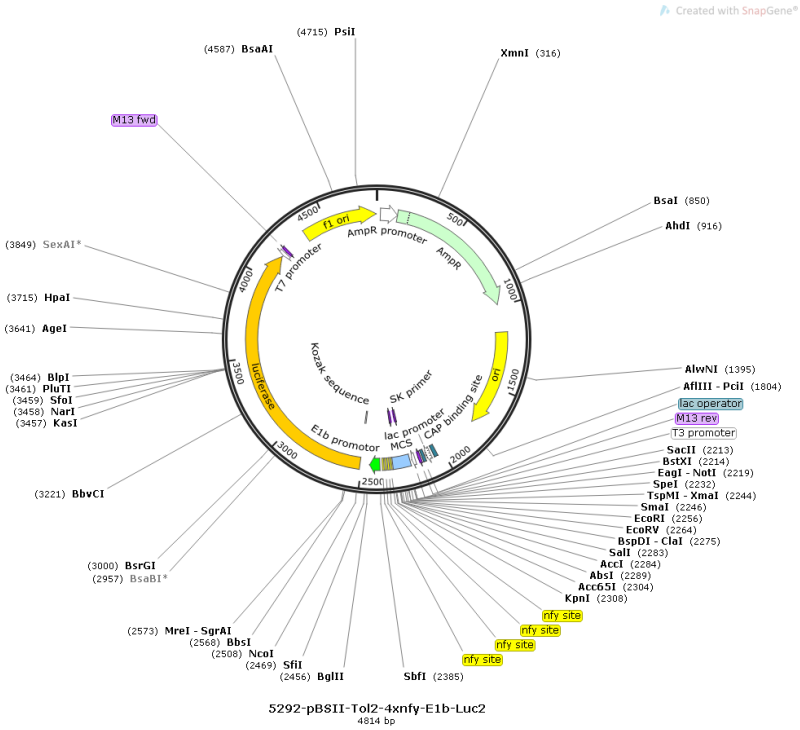

Figure 73: Plasmid Map of Plasmid #5292 pBSII-Tol2-4xnfy-EIb-Luc2. Map was generated with SnapGene®.

6.3.21 pBSII-Tol2-4xSP1/KLF-E1b-Luc2

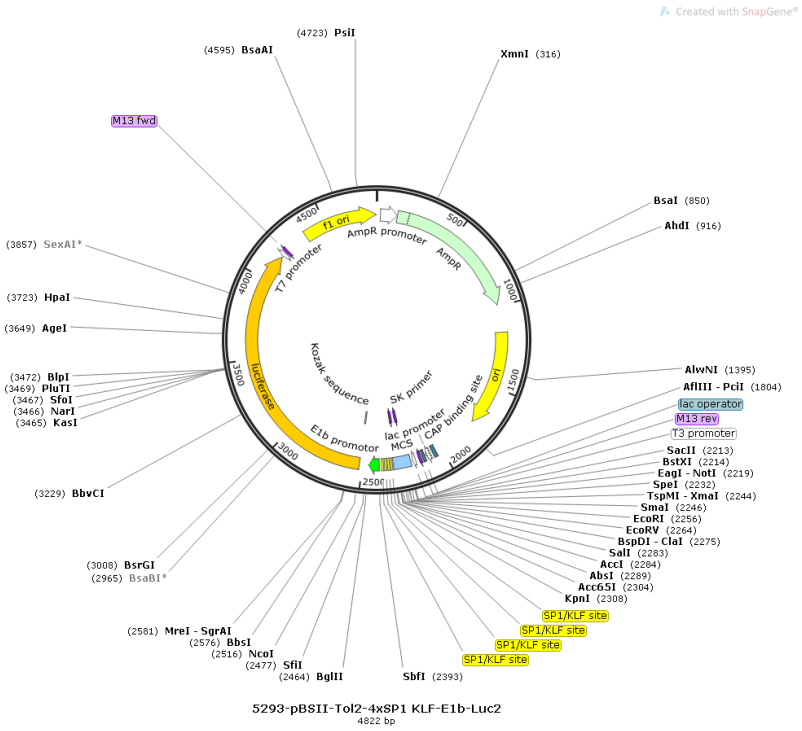

Figure 74: Plasmid Map of Plasmid #5293 pBSII-Tol2-4xSP1/KLF-EIb-Luc2. Map was generated with SnapGene®.

6.3.22 pBSII-Tol2-4xNRF-E1b-Luc2

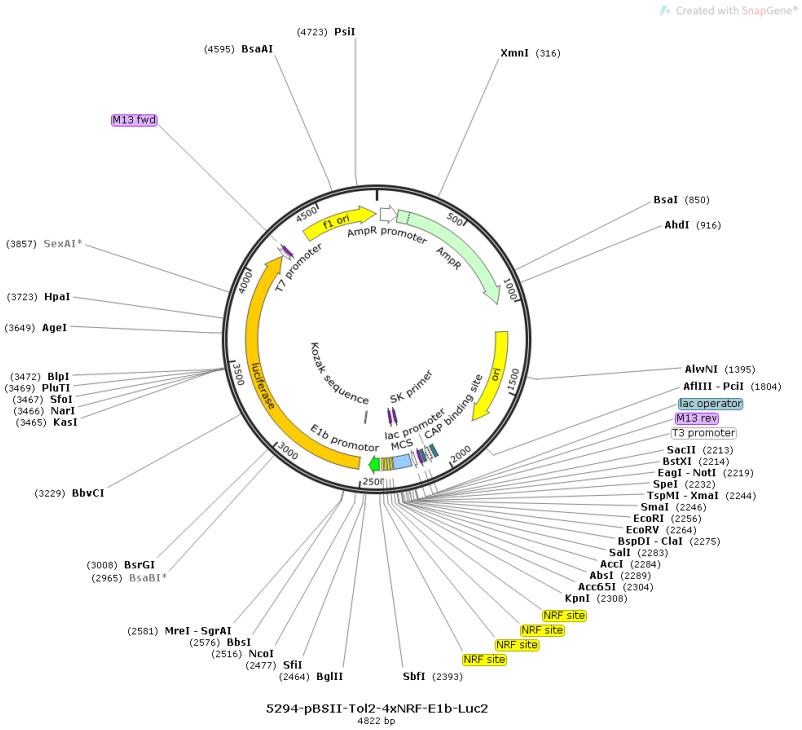

Figure 75: Plasmid Map of Plasmid #5294 pBSII-Tol2-4xNRF-EIb-Luc2. Map was generated with SnapGene®.

6.3.23 pBSII-Tol2-4xE2F-E1b-Luc2

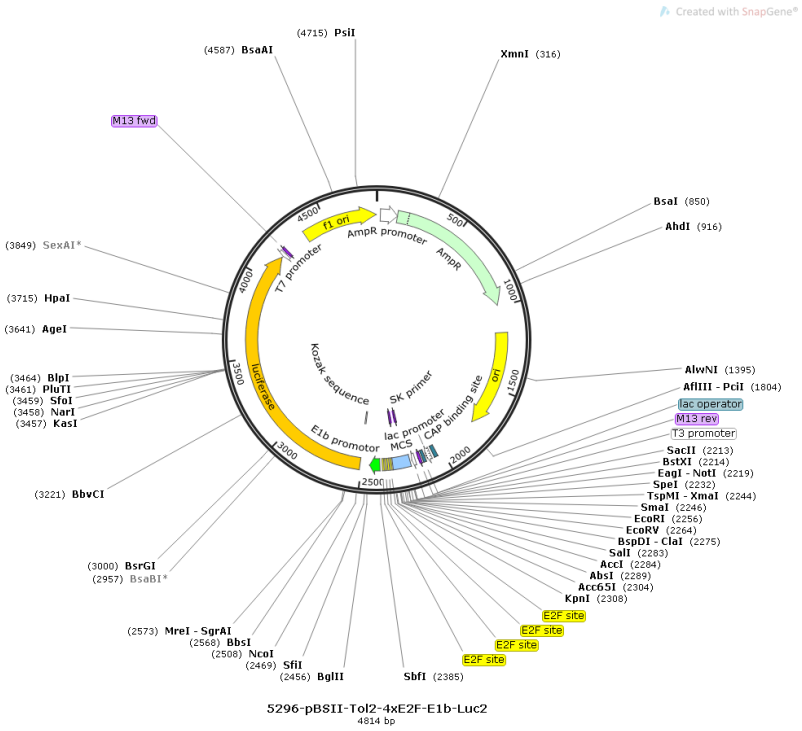

Figure 76: Plasmid Map of Plasmid #5296 pBSII-Tol2-4xE2F-EIb-Luc2. Map was generated with SnapGene®.

6.3.24 pBSII-Tol2-4xbHLH-E1b-Luc2

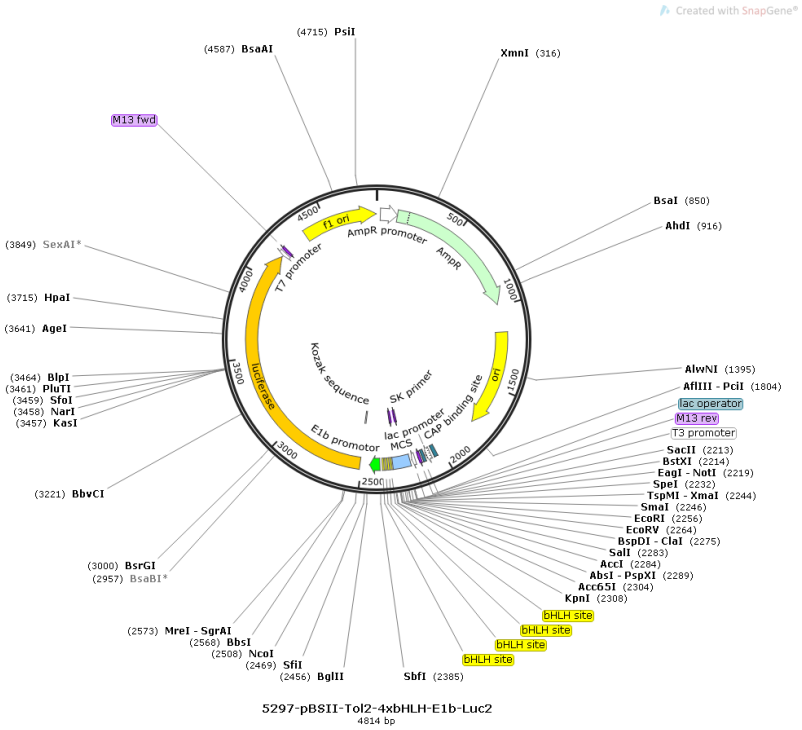

Figure 77: Plasmid Map of Plasmid #5297 pBSII-Tol2-4xbHLH-EIb-Luc2. Map was generated with SnapGene®.

6.3.25 pBSII-Tol2-4xbZIP-E1b-Luc2

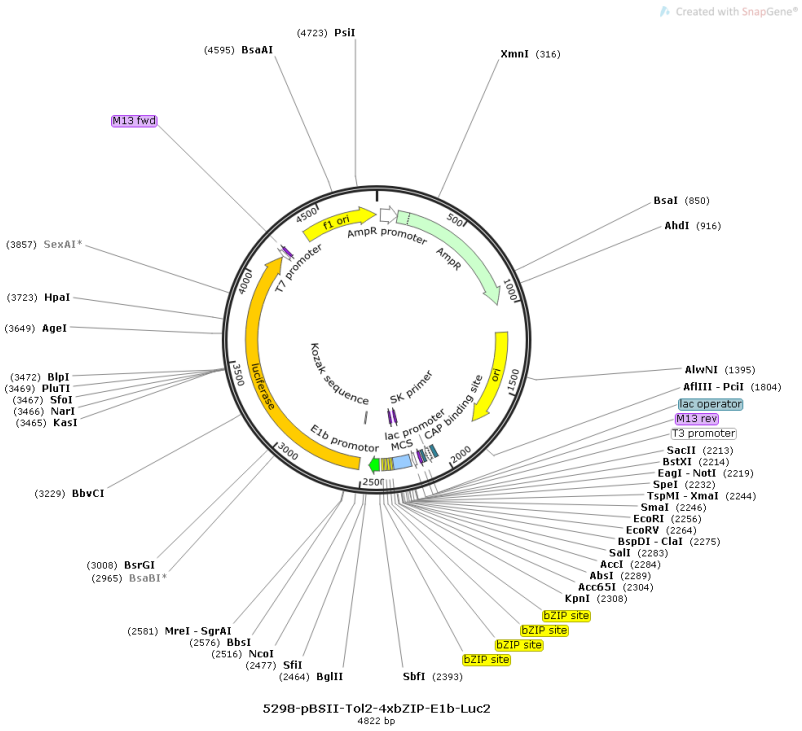

Figure 78: Plasmid Map of Plasmid #5298 pBSII-Tol2-4xbZIP-EIb-Luc2. Map was generated with SnapGene®.

6.3.26 pBSII-Tol2-4xSox/Pou-E1b-Luc2

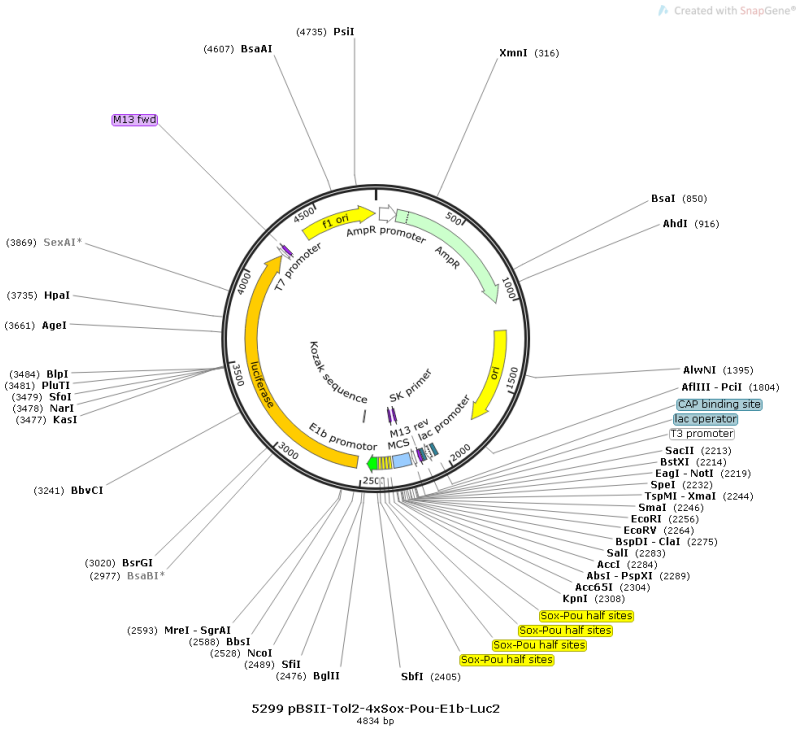

Figure 79: Plasmid Map of Plasmid #5299 pBSII-Tol2-4xSox/Pou-EIb-Luc2. Map was generated with SnapGene®.

6.3.27 pBSII-Tol2-4xKLF5-E1b-Luc2

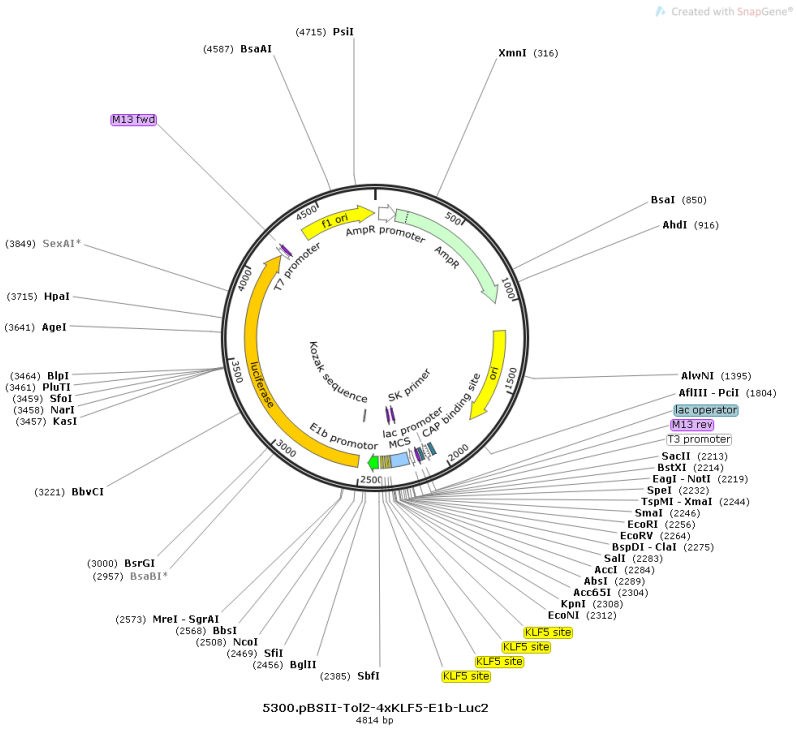

Figure 80: Plasmid Map of Plasmid #5300 pBSII-Tol2-4xKLF5-EIb-Luc2. Map was generated with SnapGene®.

6.3.28 pBSII-Tol2-4xETS-E1b-Luc2

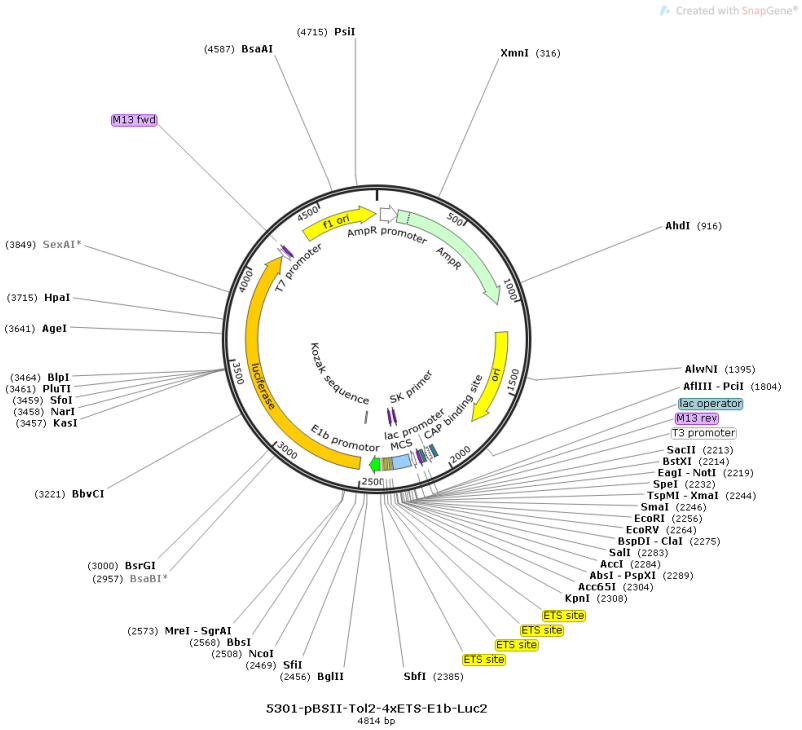

Figure 81: Plasmid Map of Plasmid #5301 pBSII-Tol2-4xETS-EIb-Luc2. Map was generated with SnapGene®.

6.3.29 pBSII-Tol2-4xNGF1A-RE-E1b-Luc2

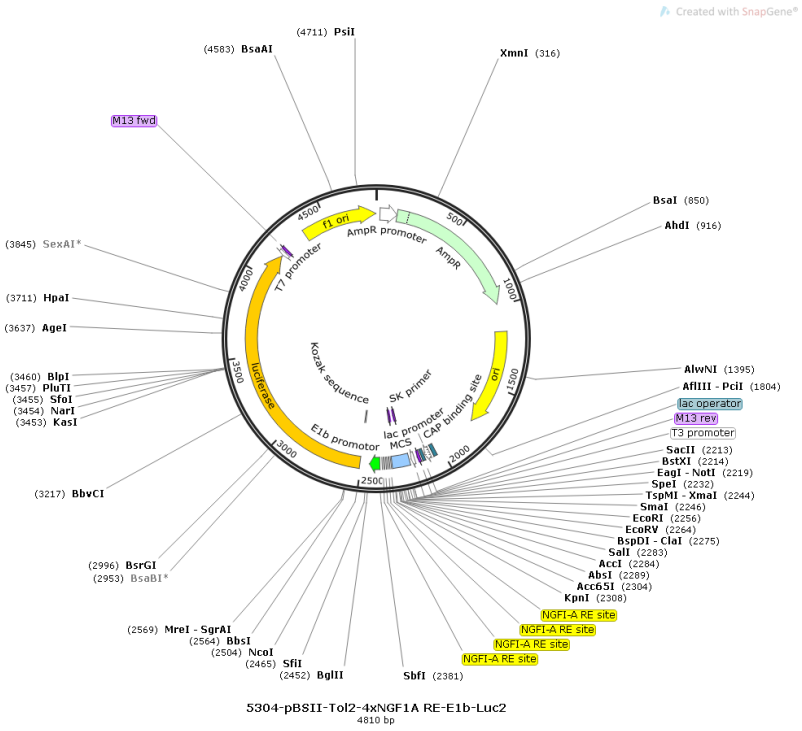

Figure 82: Plasmid Map of Plasmid #5304 pBSII-Tol2-4xNGF1A-RE-EIb-Luc2. Map was generated with SnapGene®.

6.3.30 pBSII-Tol2-4xNFAT/AP1-E1b-Luc2

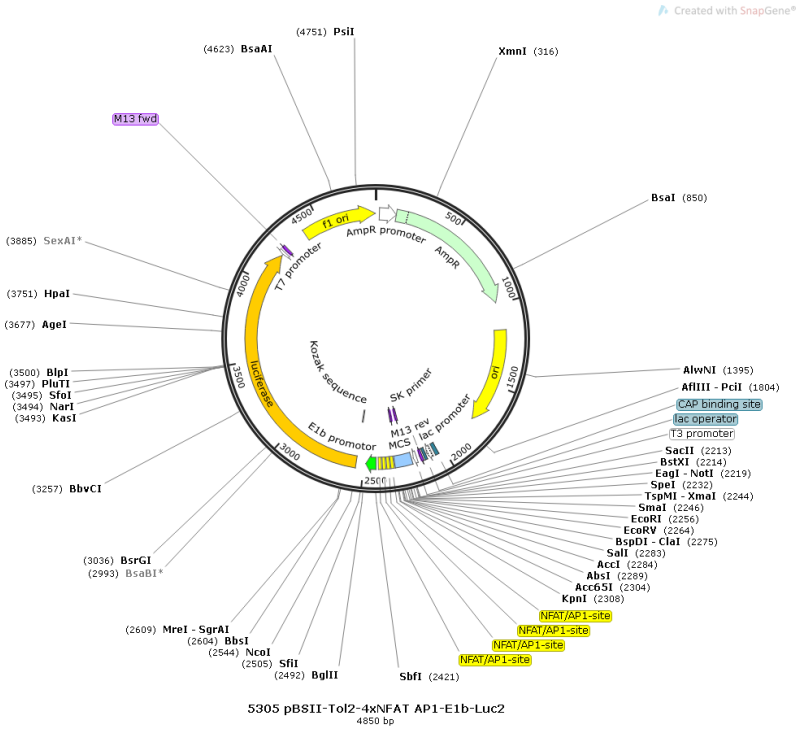

Figure 83: Plasmid Map of Plasmid #5305 pBSII-Tol2-4xNFAT/AP1-EIb-Luc2. Map was generated with SnapGene®.

6.3.31 pBSII-Tol2-4xERE-E1b-Luc2

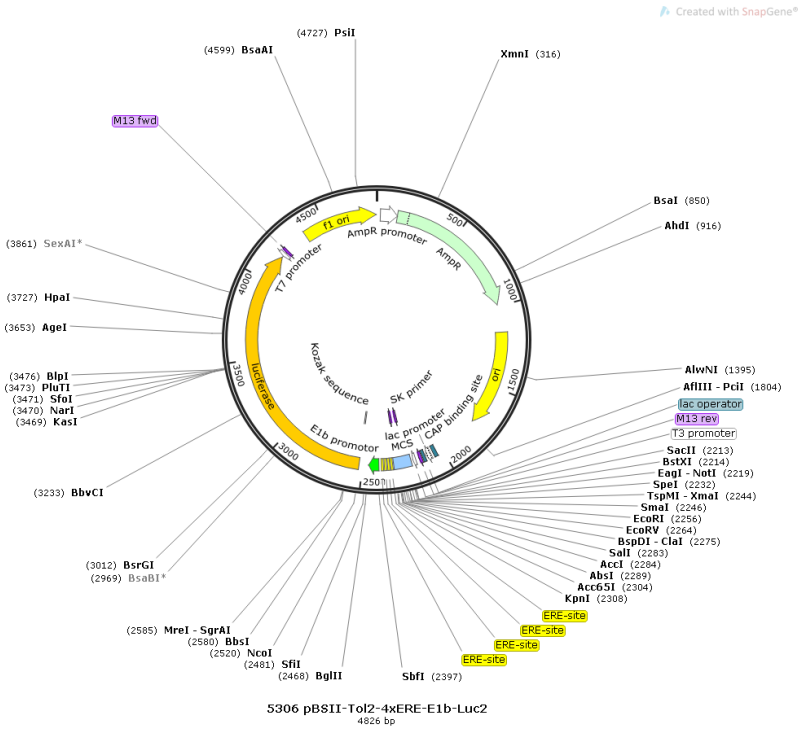

Figure 84: Plasmid Map of Plasmid #5306 pBSII-Tol2-4xERE-EIb-Luc2. Map was generated with SnapGene®.

6.3.32 pBSII-Tol2-4xRunt-E1b-Luc2

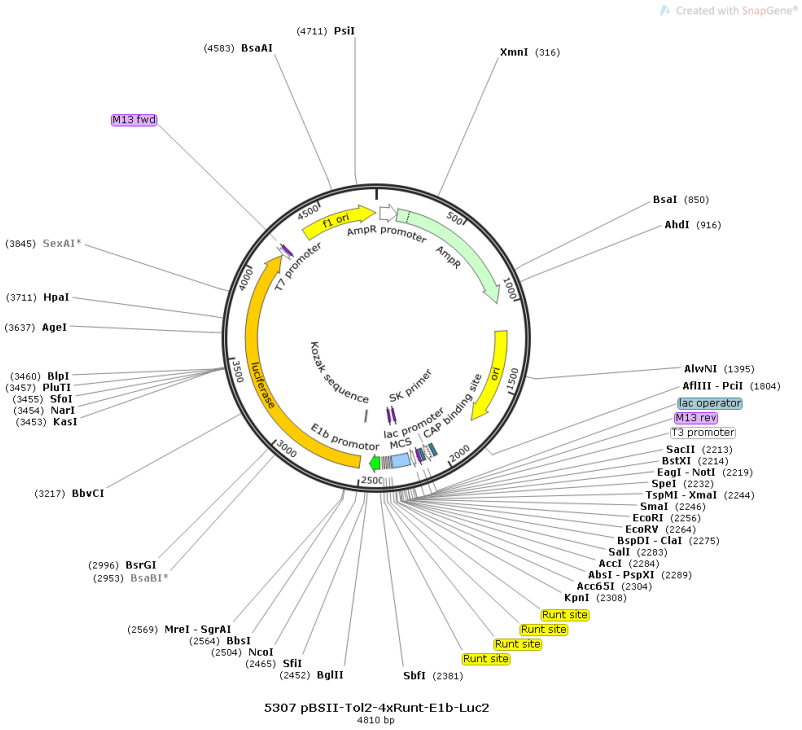

Figure 85: Plasmid Map of Plasmid #5307 pBSII-Tol2-4xRunt-EIb-Luc2. Map was generated with SnapGene®.

6.3.33 pBSII-Tol2-4xFexf2-E1b-Luc2

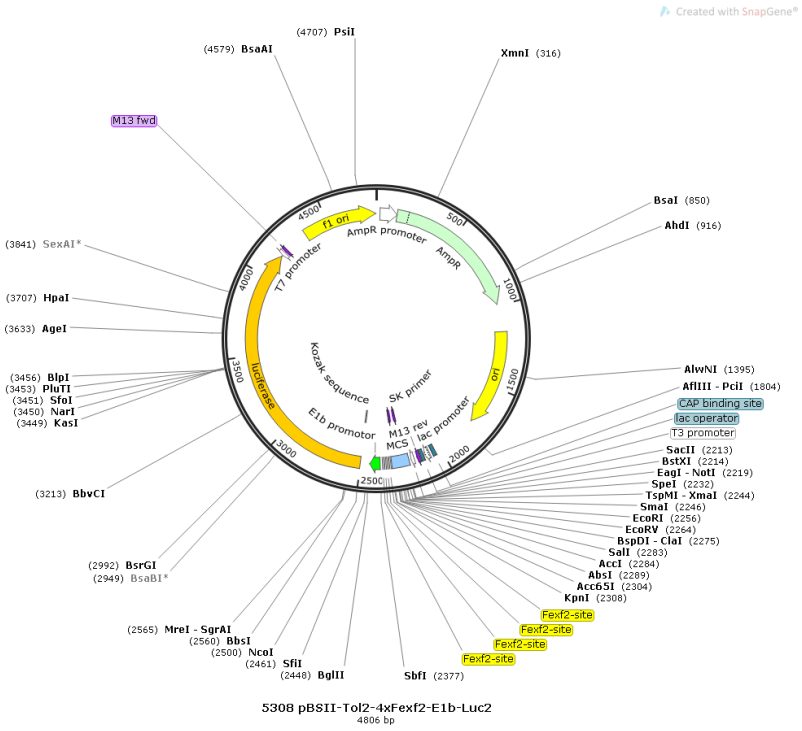

Figure 86: Plasmid Map of Plasmid #5308 pBSII-Tol2-4xFexf2-EIb-Luc2. Map was generated with SnapGene®.

6.3.34 pBSII-Tol2-4xLexA-E1b-Luc2

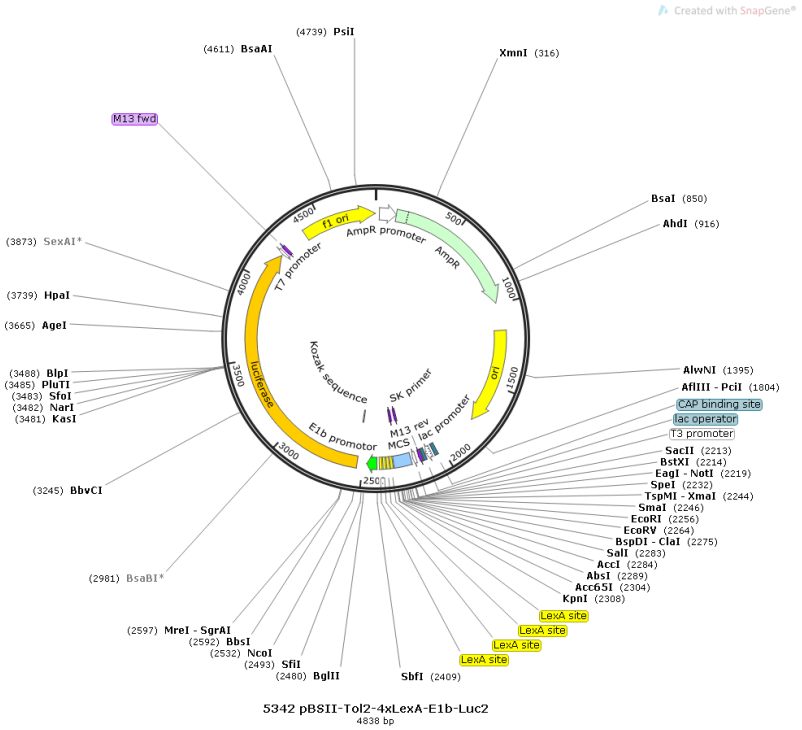

Figure 87: Plasmid Map of Plasmid #5342 pBSII-Tol2-4xLexA-EIb-Luc2. Map was generated with SnapGene®.

6.3.35 pBSII-Tol2-4xNFAT-E1b-Luc2

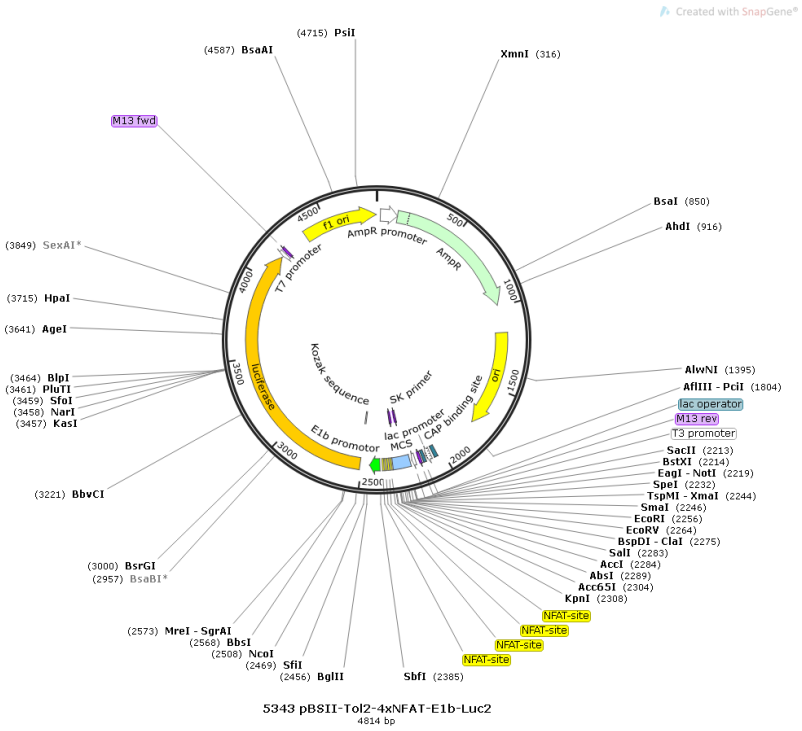

Figure 88: Plasmid Map of Plasmid #5343 pBSII-Tol2-4xNFAT-EIb-Luc2. Map was generated with SnapGene®.

6.3.36 pBSII-Tol2-4xSim2-E1b-Luc2

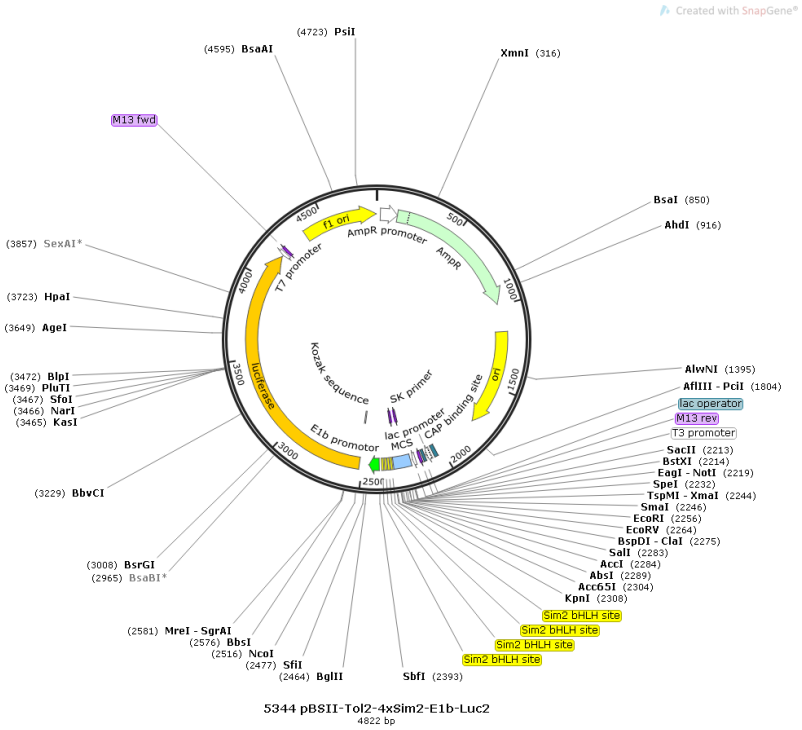

Figure 89: Plasmid Map of Plasmid #5344 pBSII-Tol2-4xSim2-EIb-Luc2. Map was generated with SnapGene®.

6.3.37 pBSII-Tol2-4xTbox-E1b-Luc2

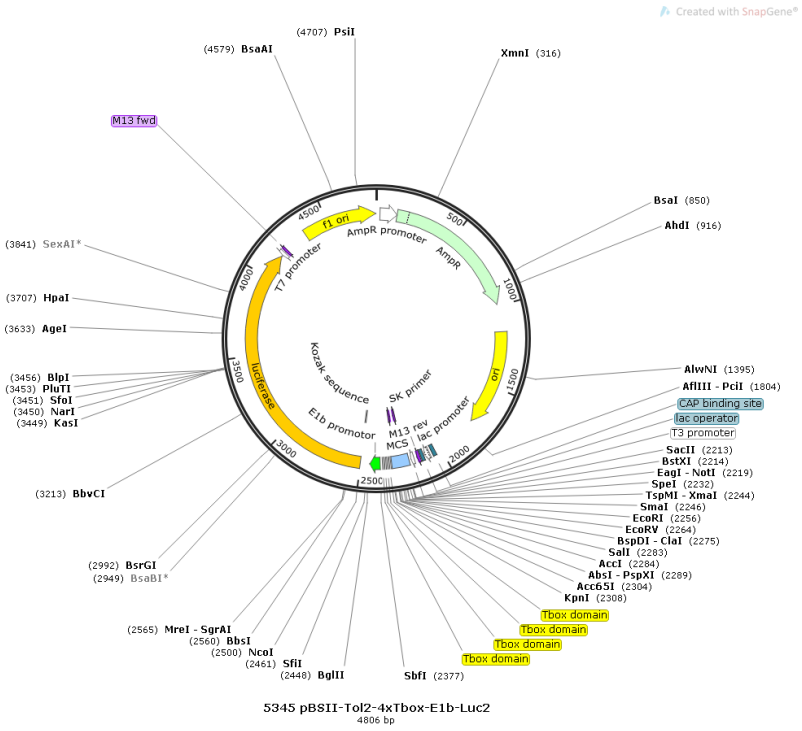

Figure 90: Plasmid Map of Plasmid #5345 pBSII-Tol2-4xTbox-EIb-Luc2. Map was generated with SnapGene®.

6.3.38 pBSII-Tol2-4xFOXO-E1b-Luc2

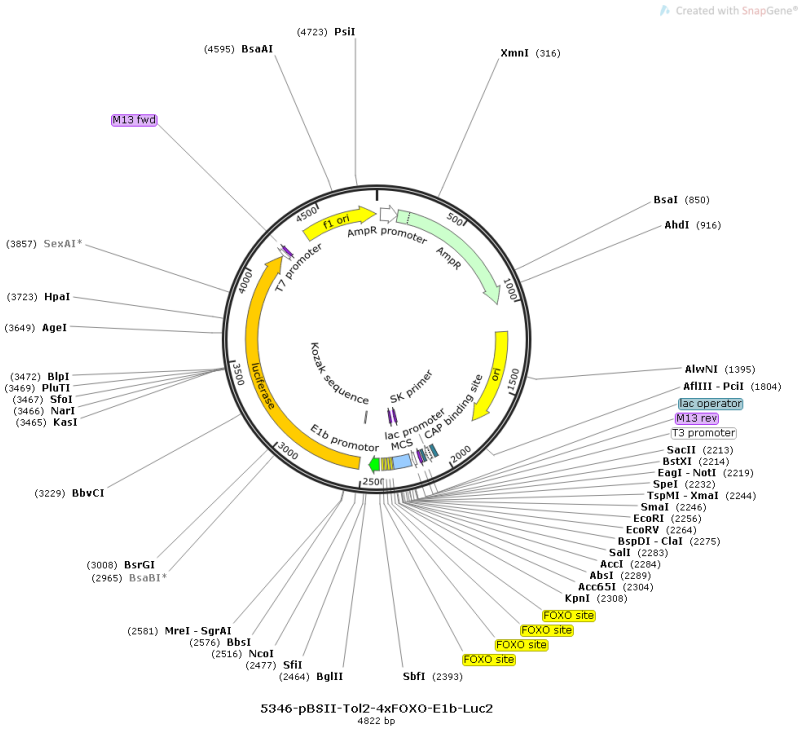

Figure 91: Plasmid Map of Plasmid #5346 pBSII-Tol2-4xFOXO-EIb-Luc2. Map was generated with SnapGene®.

6.3.39 pBSII-Tol2-4xBRE-E1b-Luc2

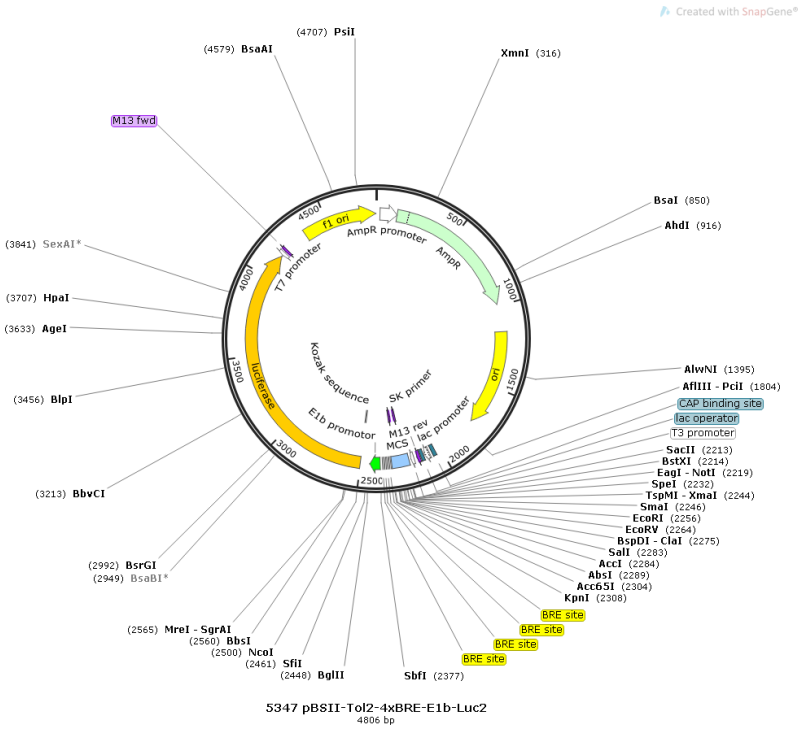

Figure 92: Plasmid Map of Plasmid #5347 pBSII-Tol2-4xBRE-EIb-Luc2. Map was generated with SnapGene®.

6.3.40 pBSII-Tol2-4xTEAD-E1b-Luc2

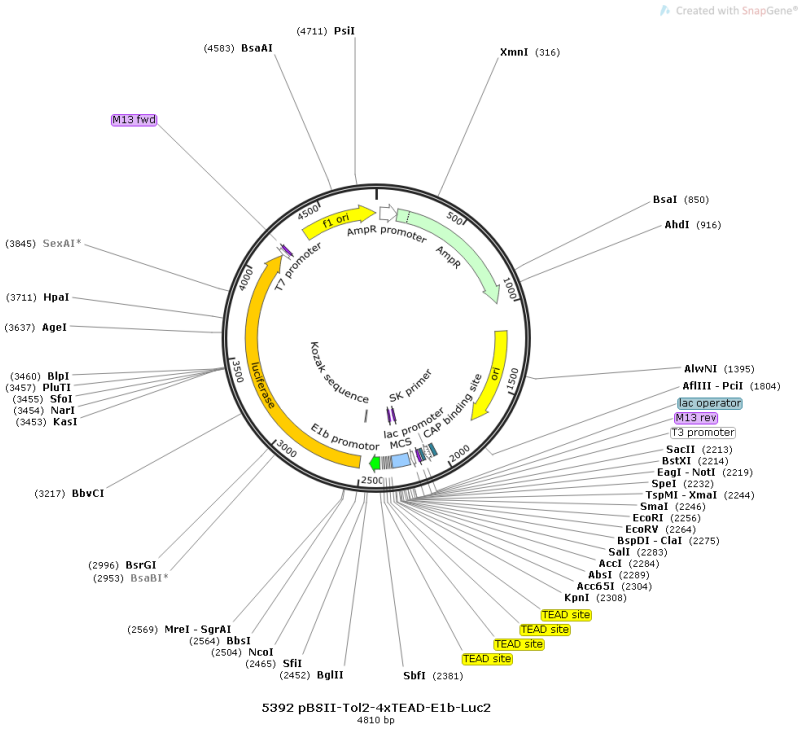

Figure 93: Plasmid Map of Plasmid #5392 pBSII-Tol2-4xTEAD-EIb-Luc2. Map was generated with SnapGene®.

6.3.41 pTol2-2xUAS-E1b-Luc2

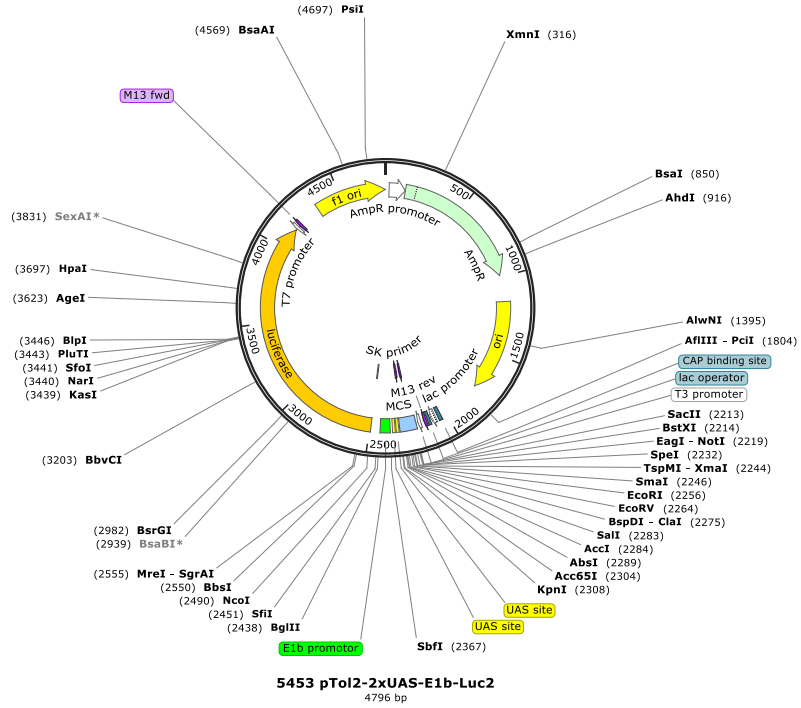

Figure 94: Plasmid Map of Plasmid #5453 pTol2-2xUAS-E1b-Luc2. Map was generated with SnapGene®.

6.3.42 pTol2-6xUAS-E1b-Luc2

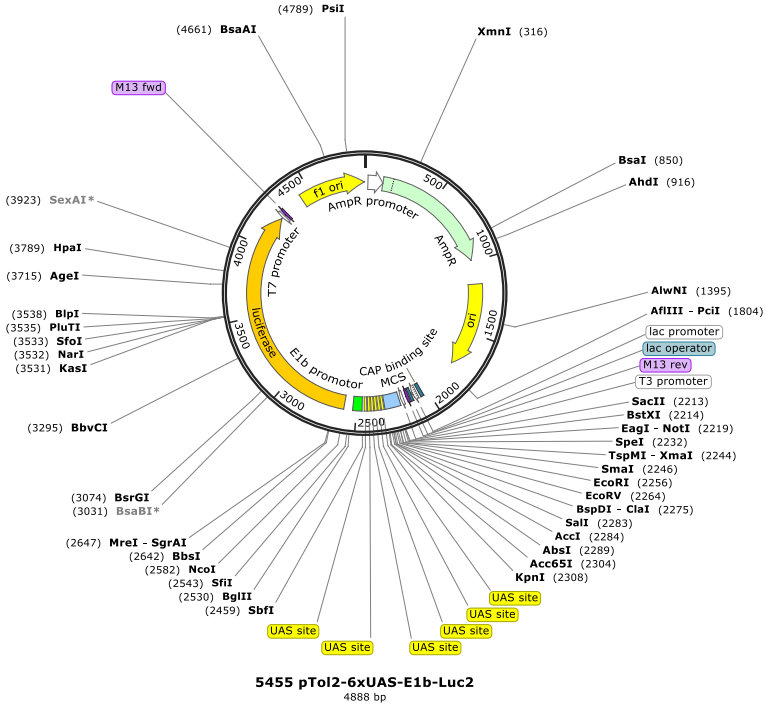

Figure 95: Plasmid Map of Plasmid #5455 pTol2-6xUAS-E1b-Luc2. Map was generated with SnapGene®.

6.3.43 pTol2-8xUAS-E1b-Luc2

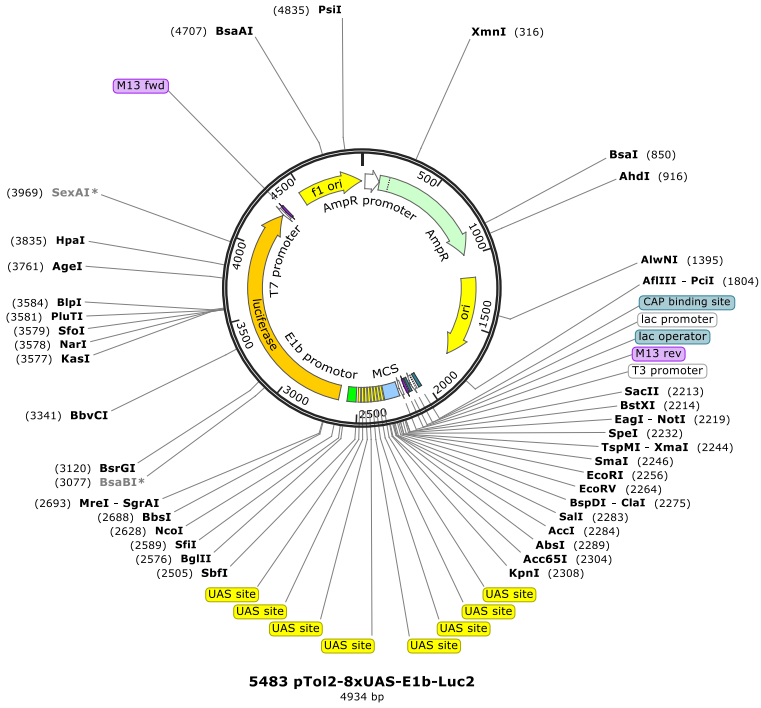

Figure 96: Plasmid Map of Plasmid #5483 pTol2-8xUAS-E1b-Luc2. Map was generated with SnapGene®.

6.3.44 pTol2-2xETS-E1b-Luc2

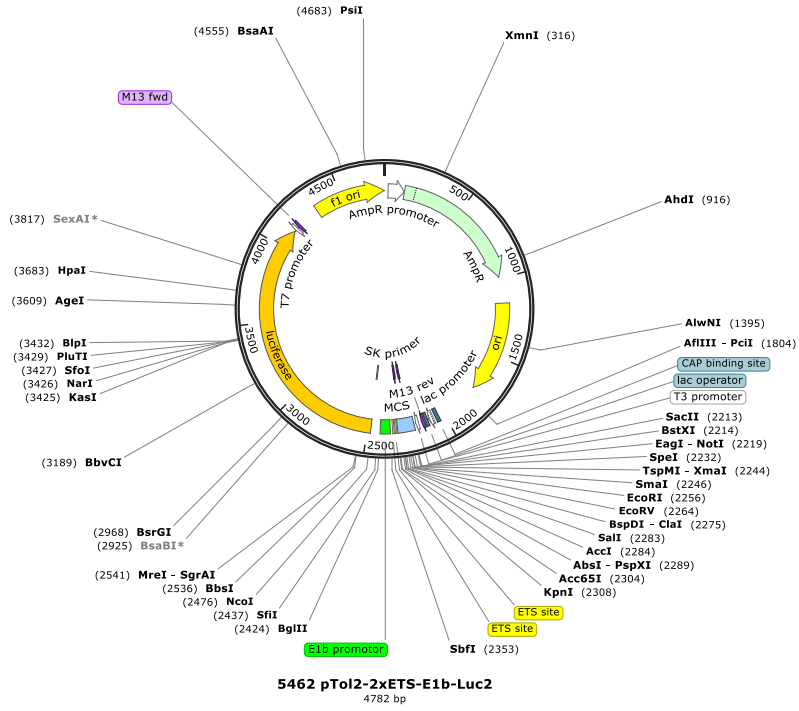

Figure 97: Plasmid Map of Plasmid #5462 pTol2-2xETS-E1b-Luc2. Map was generated with SnapGene®.

6.3.45 pTol2-6xETS-E1b-Luc2

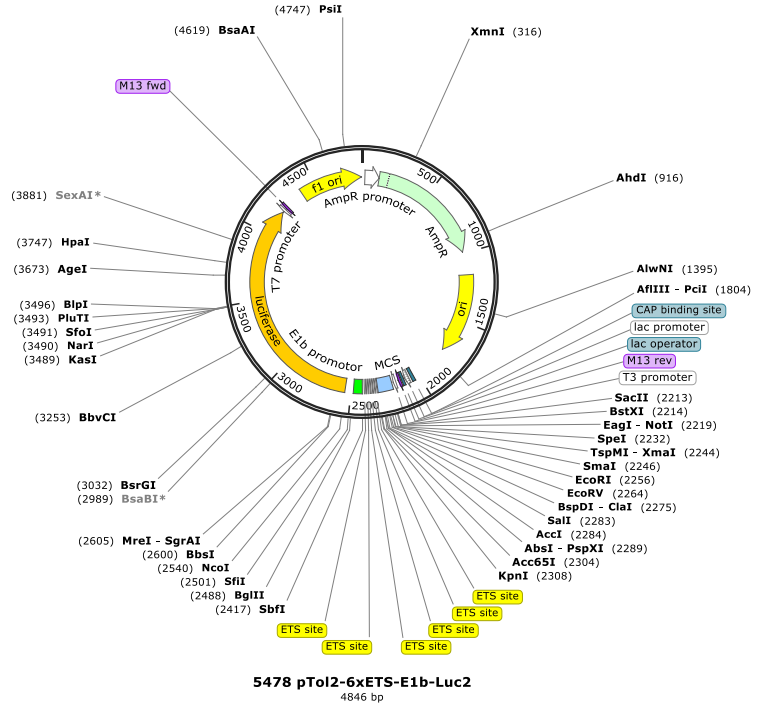

Figure 98: Plasmid Map of Plasmid #5478 pTol2-6xETS-E1b-Luc2. Map was generated with SnapGene®.

6.3.46 pTol2-8xETS-E1b-Luc2

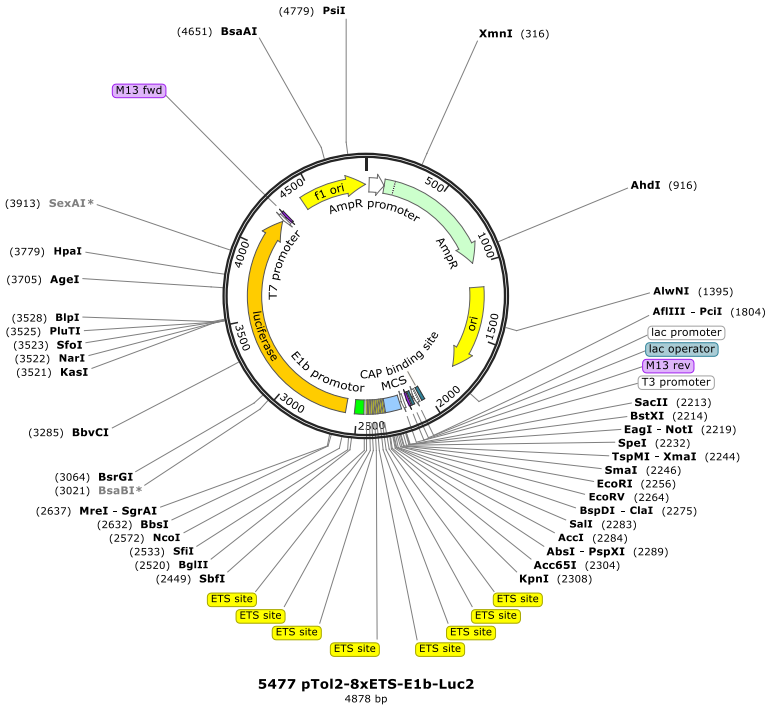

Figure 99: Plasmid Map of Plasmid #5477 pTol2-8xETS-E1b-Luc2. Map was generated with SnapGene®.

6.5 Abbreviation

ATP	Adenosine triphosphate
BDNF	brain-derived neurotrophic factor
cDNA	complementary DNA
CO_2	carbon dioxide
CREB	cAMP response element-binding protein
DMEM	Dulbecco's Modified Eagle's Medium
DMSO	Dimethylsulfoxid
dn	dominant negative
DNA	deoxyribonucleic acid
DTT	Dithiothreitol
Dyrk1A	Dual specificity tyrosine-phosphorylation-regulated kinase 1A
ER	Endoplasmic reticulum
ERex	ER export signal
Erk	Extracellular-signal Regulated Kinases
EtOH	Ethanol
ex	export
FIJI	FIJI is just ImageJ
GAP	Growth Associated Protein
GAPDH	Glycerinaldehyd-3-phosphat-Dehydrogenase
Gli	glioma-associated oncogene
HCl	hydrochloric acid
LEF	Lymphoid enhancer-binding factor
Lhx	LIM homeobox
MAPK	Mitogen-activated protein kinase
MAPKK	Mitogen-activated protein kinase kinase
mRNA	messenger RNA
MTT	3-(4,5-Dimethylthiazol-2-yl)-2,5-diphenyltetrazoliumbromid
NFkB	nuclear factor 'kappa-light-chain-enhancer' of activated B-cells
NGF	nerve growth factor
SBE	Smad binding element
Sox	SRY-related HMG-box genes
PBS	Phosphate buffered saline
PC12	pheochromocytoma cells
PCR	polymerase chain reaction
PLCγ	Phosphoinositid-Phospholipase C
RNA	ribonucleic acid
RPMI	Roswell Park Memorial Institute
RT	room temperature
RT-PCR	reverse transcriptase PCR
TCF	transcriptionfactor
TrkA	Tropomyosin receptor kinase A
UV	ultraviolet light